THE UNIVERSITY OF SYDNEY

COPYRIGHT AND USE OF THIS THESIS

This thesis must be used in accordance with the provisions of the Copyright Act 1968.

Reproduction of material protected by copyright may be an infringement of copyright and copyright owners may be entitled to take legal action against persons who infringe their copyright.

Section 51 (2) of the Copyright Act permits an authorized officer of a university library or archives to provide a copy (by communication or otherwise) of an unpublished thesis kept in the library or archives, to a person who satisfies the authorized officer that he or she requires the reproduction for the purposes of research or study.

The Copyright Act grants the creator of a work a number of moral rights, specifically the right of attribution, the right against false attribution and the right of integrity.

You may infringe the author's moral rights if you:

- fail to acknowledge the author of this thesis if you quote sections from the work
- attribute this thesis to another author
- subject this thesis to derogatory treatment which may prejudice the author's reputation

For further information contact the University's Director of Copyright Services

sydney.edu.au/copyright

MANY-BODY MODELS FOR TOPOLOGICAL QUANTUM INFORMATION

Courtney G. Brell

THE UNIVERSITY OF SYDNEY

FACULTY OF SCIENCE

A thesis submitted in fulfilment of the requirements
for the degree of Doctor of Philosophy
2015

To the wee baby Hamish on the occasion of his first birthday.

Abstract

We develop and investigate several quantum many-body spin models of use for topological quantum information processing and storage. These models fall into two rough categories: those that are designed to be more realistic than alternative models with similar phenomenology, and those that are designed to have richer phenomenology than related models.

In the first category, we present a procedure to obtain the Hamiltonians of the toric code and Kitaev quantum double models as the low-energy limits of entirely two-body Hamiltonians. Our construction makes use of a new type of perturbation gadget based on error-detecting subsystem codes. The procedure is motivated by a PEPS description of the target models, and reproduces the target models' behavior using only couplings which are natural in terms of the original Hamiltonians. This allows our construction to capture the symmetries of the target models.

As an extension of this work, we construct parent Hamiltonians involving only local 2-body interactions for a broad class of Projected Entangled Pair States (PEPS). Again making use of perturbation gadget techniques, we define a perturbative Hamiltonian acting on the virtual PEPS space with a finite order low energy effective Hamiltonian that is a gapped, frustration-free parent Hamiltonian for an encoded version of a desired PEPS. For topologically ordered PEPS, the ground space of the low energy effective Hamiltonian is shown to be in the same phase as the desired state to all orders of perturbation theory.

We then move on to define models that generalize the phenomenology of several well-known systems. We first define generalized cluster states based on finite group algebras in analogy to the generalization of the toric code to the Kitaev quantum double models. We do this by showing a general correspondence between systems with CSS structure and finite group algebras, and applying this to the cluster states to derive their generalization. We then investigate properties of these states including their PEPS representations, global symmetries, and relationship to the Kitaev quantum double models. We also comment on possible applications of the generalized cluster states, including a protocol for universal adiabatic topological cluster state quantum computation.

Continuing this programme, we finally propose a generalization of the color codes based on finite groups algebras. For non-Abelian groups, the resulting model supports non-Abelian anyonic quasiparticles and topological order. We examine the properties of these models such as their relationship to Kitaev quantum double models, quasiparticle spectrum, and boundary structure.

Statement of Contribution

The main body of this thesis is comprised of four research papers, presented as Chapters 2-5. For the first two of these papers, I was primary (first) author as well as the only student author, and the last two papers were written as sole author papers.

Chapter 2: Toric Codes and Quantum Doubles from Two-Body Hamiltonians
This chapter contains the published paper [BFBD11] with minor corrections and clarifications. This project was suggested by SDB, and the bulk of the technical analysis was carried out by myself under the supervision of SDB, with the exception of Sec. 2.5 which was based in part on the work of ACD and STF. The paper was written by me with edits by the other authors.

Chapter 3: Perturbative Two-body Parent Hamiltonians for Projected Entangled Pair States
This chapter contains the published paper [BBD14a] with minor corrections and clarifications. The research, calculations, and write-up for this project were completed by me with supervision from SDB and ACD.

Chapter 4: Generalized Cluster States Based on Finite Groups
This chapter contains the published paper [Bre15a] with minor corrections and clarifications. This was a sole author paper, devised and completed by myself.

Chapter 5: Generalized Color Codes Supporting Non-Abelian Anyons
This chapter contains the published paper [Bre15b] with minor corrections and clarifications. This was a sole author paper, devised and completed by myself.

Acknowledgements

Many people have been invaluable aids to the long preparation of this thesis. Most prominent among them is of course my thesis supervisor Stephen Bartlett for introducing me to the world of quantum information, for endless assistance and patience, and generally for embodying the ideal of a teacher. Along with him, I must also thank Steve Flammia and my associate supervisor Andrew Doherty for always having time and enthusiasm for any question I might have.

All members of the quantum group at USyd deserve thanks for maintaining such a lively and supportive atmosphere. Special mentions go to Rafael "Ralph" Alexander, Jacob "Jackie" Bridgeman, Simon "Simmo" Burton, Andrew "Shamwow" Darmawan, Natasha "Tash" Gabay, Dominic "Vladimir" Williamson, Nicolas "D.C." Menicucci, and Leanne Price.

I am also grateful to the greater quantum information community that make it such an exciting and enjoyable field. In particular for helpful discussions and comments on the various works that have formed this thesis, I thank Jonas Anderson, Stephen Bartlett, Gavin Brennan, Ben Brown, Hector Bombin, Chris Cesare, Andrew Doherty, Dominic Else, Leander Fiedler, Steve Flammia, Jeongwan Haah, Robert Koenig, Spyridon Michalakis, Pieter Naaijkens, David Poulin, Ilai Schwarz, and Guifre Vidal. For their hospitality I also thank Hector Bombin, Claudio Castelnovo, Ignacio Cirac, Jens Eisert, Ville Lahtinen, Daniel Loss, Tobias Osborne, Jiannis Pachos, David Perez-Garcia, John Preskill, Robert Raussendorf, Terry Rudolph, and Norbert Schuch.

Of course, I thank my family and friends for their support over the years, especially Erin Bubb, together with my brother and parents.

Finally, my most deeply heartfelt gratitude to Natasha Gabay and Stephen Bartlett, for helping keep my head above water when I felt like I was drowning.

Sydney, August 29, 2014 C. G. B.

Contents

1 Introduction

Quantum information science is the study of the methods and mechanisms of quantum information storage and processing. This burgeoning field has produced many significant results pointing to the practical applications of these procedures, as well as their theoretical scope. A key cornerstone in quantum information science is the theory of quantum error correction and fault tolerance [NC10]. Without this, quantum information theory would largely be a theoretical curiosity without real-world application in the inherently noisy laboratory (though like classical analog computation, may still find application that does not require asymptotic guarantees of correctness).

Several paradigms for considering quantum information processing protocols have been proposed. Each of these protocols has a basis in an idealised physical realization of a quantum computer, which may have relative practical advantages and/or drawbacks. Significantly they each also offer a different theoretical vantage point from which to view problems in quantum information. Most notably, these paradigms include the standard quantum circuit model [Deu89, NC10], adiabatic quantum computation [FGGS00, AvDK$^+$07], measurement-based quantum computation [RB01], and topological quantum computation [Kit03, NSS$^+$08]. In this thesis we will focus most closely on systems of interest for topological quantum computation.

Topological quantum computation typically considers systems with some underlying geometry in space that limits the available interactions. This is motivated by analogy to realistic condensed matter systems whose interactions are typically local in $\mathbb{R}^2$ or $\mathbb{R}^3$. Although this might seem like a disadvantageous constraint, locality also allows topologically ordered systems to achieve certain robustness to physical noise processes [WOP99, DKLP02], which are generally considered to respect spatial locality in the same sense. Topological systems derive their name from the fact that typically the quantum information they encode or process is delocalized over global degrees of freedom, often related to topological features of a manifold [DKLP02]. This delocalization is exactly the quality that allows them robustness to local noise sources - like topology itself, the information is invariant under local deformations (suitably defined). In this sense, topological quantum computation builds in to its framework

some inherent features of quantum error correction and fault tolerance that must be added by hand to protocols in other implementations such as a circuit-based scheme.

A further advantage of topological quantum information protocols is that the global nature of the encoded information often means that the precise microscopic details of the implementation are less important than the emergent macroscopic features [NSS+08]. This often allows us to define protocols in the continuum, making use of quantum field theory techniques when convenient, and port the results to more realistic physical implementations in condensed matter systems. Alternatively, we can make use of toy models of interacting bosons, fermions, or spins on lattices to study phenomena of interest before relating the main results to more complicated experimental systems. In this thesis we will mainly study models of interacting spins on a lattice, and their topological properties or ability to perform interesting computational tasks in the topological quantum computing paradigm.

Quantum many-body spin models

Quantum many-body models are useful tools for describing or modelling many systems of interest, particularly for condensed matter physics [Aue94], but also more broadly for example in high energy physics [KS75, Kog79] or quantum gravity [Rov08, KMS06]. The fundamental degrees of freedom in a quantum many-body model are typically arranged in a lattice (as in solid-state systems) and may be either fermionic or bosonic in nature. Such systems can describe many interesting materials such as integer or fractional quantum hall liquids, topological insulators, Bose-Einstein condensates, quantum magnets, quantum spin liquids, and high temperature superconductors.

Many-body spin models correspond to hard-core bosonic systems, in the sense that there are only finitely many available states corresponding to each site of the lattice, and operations at one lattice site commute with those at all other lattice sites. Since finite-dimensional spins are the building blocks of most quantum information protocols, it is natural to look for many-body spin models for use in quantum information as opposed to fermionic or soft-core bosonic lattice models. These kinds of spin models, and their application to quantum information science, are the focus of this thesis.

Many-body spin systems are ubiquitous in condensed matter physics, being a natural description of many solid-state systems. As well as being representative of models for natural physical systems, spin models are also amenable to engineering in the laboratory, for example with arrays of Josephson junctions [DIV04] or interacting neutral atoms in optical lattices [Blo05]. Many-body fermionic systems are also equivalent to certain spin models. Most straightforwardly, the Jordan-Wigner transformation [JW28] can be used to relate fermionic and spin models in 1 dimension, and in higher dimensions similar analogues can be found [BK02, Bal05, VC05] (though they are usually less natural). Additionally, fermions themselves can be found as emergent quasi-particle excitations of spin models in two dimensions or higher [LW03].

Rules of the many-body spin game: A quantum many-body spin model has a Hilbert space formed by the tensor product of d_i-dimensional spins at each site i of a finite valency lattice or graph Λ. Λ is typically a discretization of $\mathbb{R}^D$ for some spatial dimension D (usually ≤ 3) with bounded interaction (edge) length and density of sites. Often the local Hilbert space dimension d_i is taken to be constant over the lattice, but at a minimum it must be bounded. The dynamics of the system are specified by a Hamiltonian consisting of a sum of bounded interactions centered at each site whose strength is decaying suitably quickly with total radius of their support (intuitively, the interactions must be local enough). This condition, combined with the finite valency of the lattice, means that the total norm of all interactions acting on any site of the lattice should be finite.

Quantum many-body spin models are subject to Lieb-Robinson bounds [LR72]. These bounds give a maximum rate for transmission of information or correlations over the lattice (up to exponentially small corrections). The ability to prove such a bound should be understood as the appropriate definition of "decaying quickly" in the previous paragraph. For most purposes, we will deal with either strictly local interactions (those whose interaction strength is precisely zero for interaction ranges beyond some constant value) or exponentially decaying interactions, which both have this property. We will normally use the term local to refer to strictly local interactions, reserving the term 1-local for operations on a single site, and using quasi-local for exponentially decaying terms or other terms decaying fast enough to satisfy a Lieb-Robinson bound.

Often we are most interested in the behaviour of many-body models when the number of sites on the lattice tends to infinity. This can be thought of as taking the thermodynamic limit, where we also increase the total size of the lattice such that the density of sites remains bounded. It is in this limit that notions such as gappedness, phase transition, and so on emerge. These are key features of a condensed matter system that play an important role in characterizing the effective properties of (finite approximations to) such systems in the laboratory. Though the thermodynamic limit may not be well-defined for arbitrary quantum many-body spin models, for most models of interest we will be able to compute these kinds of quantities asymptotically.

Applications of many-body spin models

One major reason to study many-body spin models is that they can represent or approximate natural physical systems such as condensed matter systems, discrete gauge theories, etc. As well as modelling natural systems, many-body spin systems can be specifically engineered in experimental setups as previously mentioned. Apart from straightforwardly describing these physical systems with lattice models, there are several broader reasons to be interested in the study of many-body spin systems.

Toy models are a ubiquitous tool to study interesting phenomena without complicating the analysis with spurious effects. Many-body spin models give a broad framework within which

toy models of varying degrees of realism can be constructed and analysed to give insight into a vast range of physical phenomena. While quantum many-body spin models are mostly inspired by models for condensed matter physics, these kinds of models are also be used to study phenomena in high energy physics and quantum gravity.

Classic examples of toy spin models include the Ising models [Kog79], Bose- and Fermi-Hubbard models [Hub63], and Abelian lattice gauge theories [Kog79]. The kinds of phenomena these models and other spin models can be used to study is almost endless and includes phase transitions, magnetism, superconductivity, condensation, confinement, localization, thermalization, symmetry breaking, and topological order. Many-body spin models also give a general theoretical test-bed for broader physical concepts and theoretical tools such as entanglement (or correlation) measures, variational ansatze, and renormalization group flow.

Of interest in this thesis are the related notions of topological order and topological phases. Compared to their classical counterparts which fall under the Landau symmetry-breaking phase classification, quantum (or topological) phases are not so well understood. Studying explicit spin models as representatives of phases is extremely useful in quantifying the properties of a phase, and how these systems behave as they approach a phase transition. Of course similar analysis has historically played a very important role in understanding classical phases and phase transitions, for instance in the classical Ising models.

Apart from these general considerations, a central motivation of this thesis is in studying the application of many-body spin models to the implementation of topological quantum computation. The systems we consider can generally be thought of as toy models of varying degrees of realism - balancing the possibility of meaningful analysis with the constraint of describing a realizable physical system. Many-body spin models can be used in several different ways to realize quantum computational protocols, several of which we will discuss shortly. Most notably these systems are central to both the topological quantum computation and measurement-based quantum computation paradigms. Interesting examples of common many-body spin models relevant to this thesis include resources for measurement-based quantum computation such as the AKLT state [WAR11, Miy11] and cluster states [RB01, RBB03], and topologically ordered systems and topological codes such as string-net models [LW05], quantum double models [Kit03], and color codes [BMD06]. The cluster states and toric code (the simplest quantum double model) in particular are the prototypical toy models for many phenomena or protocols in measurement-based and topological quantum computation, respectively.

One exciting possible technology for quantum information is a self-correcting quantum memory. In analogy to a classical hard-drive, which can store information robustly over long timescales at finite temperature, it may be possible to construct a quantum many-body model that can store quantum information robustly without the need for active error-correction protocols to be continuously running. This is known to be possible using a local many-body model in 4 spatial dimensions [DKLP02, AHHH10], but remains an open question in 2 or

3 dimensions. Promising partial results have been found in this direction [BH11a, Mic14, PHWL13, BTH+13, BASP14] which have led to significant progress in our understanding of the possible phenomenology of realistic many-body models. Many-body spin models are also important in the study of several other open problems in quantum information theory, notably the quantum probabilistic checkable proofs conjecture [AAV13].

Topological order, topological codes, and topological quantum computation

Topological order in many-body models can be defined in many ways depending on the context and application. Topological order may either be defined for a particular state or space [CGW10], or for a Hamiltonian system [BHM10, BH11b, MZ13] (and typically its associated ground space). We will refer to topologically ordered systems, but this should be understood to either mean topologically ordered states or Hamiltonians as appropriate. Topological phases are a useful related notion. A topological phase is the equivalence class of all systems which have the same topological (i.e. global or long-range) properties. Such a phase can also be defined in several ways depending on context. A common definition that will be useful for this work will be that two gapped, local Hamiltonians are in the same phase if they are connected by a quasi-local adiabatic path (i.e. one that does not close the gap of the Hamiltonian). This definition of a phase also implies a definition of a topologically ordered system: one which is not in the same phase as the trivial system, where the trivial system is a gapped, local Hamiltonian with a product state as its ground state.

Observables of two systems in the same phase can be related by quasi-adiabatic continuation [HW05], and this is the notion that makes concrete the idea that the microscopic details of a particular system do not play a significant role in the topological properties of a system. The topological degrees of freedom, accessible only by global operations, are not adversely affected by this quasi-adiabatic continuation.

Another way to express this robustness to changes in microscopic degrees of freedom is encapsulated in the topological stability theorems [BHM10, BH11b, MZ13]. Loosely speaking, these define topologically ordered systems as those with global degrees of freedom that are inaccessible by local operations. The topological stability theorems prove that for gapped, local, frustration-free Hamiltonians with this kind of topological order, the gap of the system is robust against the addition of sufficiently small quasi-local perturbations. Similarly, the splitting of the ground space of the system is exponentially suppressed in the system size, so that the thermodynamic limits of all such perturbed systems have the same ground space properties. This result proves that all systems that are topologically ordered in the appropriate sense belong to proper phases (as the addition of a perturbation while the gap remains open defines a non-trivial adiabatic path).

Often, we will be interested in topological order specifically in 2D systems. The types of possible topologically ordered systems in 2D are much better understood than the general case, and can be described by models with point-like quasi-particle excitations obeying so-

called anyonic statistics [NSS+08]. These are in contrast to the more familiar bosonic and fermionic statistics that are available to point-like excitations in 3D space. In 3D space the exchange of particles must act as a representation of the permutation group, while in 2D space exchange statistics can act as a representation of the braid group instead. Anyonic statistics may be either Abelian (corresponding to 1D representations of the braid group), in which case some arbitrary phase is accumulated upon exchange of two particles, or non-Abelian (for higher-dimensional representations), where pairs of particles can have multiple possible fusion outcomes and exchanging the particles acts as some unitary on this space of fusion products.

Physically, anyon models are expected to describe the excitations of experimentally relevant natural systems such as fractional quantum hall liquids or engineered systems such as neutral atoms in optical lattices [Wen07, Pac12]. Mathematically, a particular anyon model is described by a ribbon category [Wan10]. This contains the information about the types of particles (or charges), how they may fuse, and how they act under exchange or braiding. Such anyon models can also be studied in the continuum as topological quantum field theories [Wan10]. This connection has allowed the development of new quantum algorithms to compute topological invariants of manifolds efficiently for which no efficient classical algorithm is known [AJL09]. It has also advanced our understanding of the simulability of topological quantum field theories (which are both efficiently simulable by a quantum computer and can efficiently simulate a quantum computer [FKW02]).

The canonical microscopic test-bed for topological order in 2D systems is the toric code [Kit03]. This simple model is amenable to study through the Pauli stabilizer formalism [Got99b] and supports Abelian anyons. The ground space of this system can be studied abstractly as a quantum code and is the prototypical example of a topological code. Topological codes are, loosely speaking, codes corresponding to the ground spaces of topologically ordered systems. This then means that the codespace is inaccessible to local noise operations and so has robustness to common sources of noise (or common errors). Topological codes can also often be used to implement computation via code deformation [BMD09, Bom11], a process by which the code itself is gradually changed in a way that encodes, manipulates, and measures quantum information.

A related notion to topological order is symmetry protected topological order [GW09, CGW11, SPGC11] (SPTO), or simply symmetry protected order. Systems with SPTO share many features with topological ordered systems such as robustness of to certain deformations - though in this case the deformations must respect the relevant symmetry. SPTO systems may also be used to encode classical information, though they do not typically give good quantum codes as do true topologically ordered systems [ZZ14].

Computation by anyon braiding

A pair of non-Abelian anyons may fuse to several possible distinct particle types, in contrast to Abelian anyons whose fusion products are unique. The space of possible fusion outcomes of pairs (or sets) of non-Abelian anyons may be used to encode information in a topologically protected way, as it is inaccessible to local operations if the anyons are kept well separated [Kit03]. Only by bringing a pair of anyons together may their total charge be measured, and so far-separated anyon pairs have fusion spaces robust to local noise sources.

Computation can be performed on this fusion space by braiding pairs of particles [NSS+08]. Non-Abelian anyon braiding statistics give rise to a non-Abelian representation of the braid group that acts on the relevant fusion spaces. If the anyon model is sufficiently complicated, then this braiding may be sufficient to efficiently perform any desired unitary gate on some subspace of the fusion space to arbitrary precision. This anyon model is then said to be universal, in the sense that it may be used to implement universal quantum computation by braiding of these particles. Not all non-Abelian anyon models are universal in this sense (in fact the braiding of some non-Abelian anyons can be efficiently simulated on a classical computer [Bra06]), though there are many known families of universal anyon models, most notably the Fibonacci anyons [NSS+08].

A quantum algorithm generally consists of three main stages: initalization, evolution, and measurement. Given a universal anyon model, the initalization step may be performed by creating suitable particle-antiparticle pairs from the vacuum. This process places the fusion space in a known state, which can then be evolved by braiding the anyons to give any desired gate to a given accuracy. Finally, measurement may be performed on the encoded information by bringing pairs of anyons together and determining the particle type of their fusion product.

It is also possible to supplement the computational power of a non-universal anyon model with non-topological operations that complete a universal gate set. The common topological operations would then inherit the inherent robustness of the topological protocol, and only the non-topological operations would need to be made fault tolerant by hand. This is often envisaged in systems whose anyons may be experimentally accessible but do not have the ability to perform universal computation by braiding, such as the Ising anyons [Bra06].

Computation by code deformation

An alternative method for implementing topological quantum computation is by topological code deformation [BMD09, Bom11]. Instead of using the fusion space of several anyons to encode information, in these kinds of schemes quantum information is encoded in global degrees of freedom corresponding to topological defects. Topological codes and topologically ordered systems allow for several kinds of topological defects to arise, most notably holes [BMD09] and twists [Bom11]. These can be considered to represent defects in the manifold itself on which the topologically ordered system lives.

Holes are punctures in the surface of the manifold, and each hole may contain anyonic (or more generally topological) charge. The charge of a hole can be made inaccessible to local operations by making the size of the hole macroscopic. Only operations that can enclose the entire hole may measure its charge. In this way we can encode topological information in a set of holes and manipulate it by braiding them.

Twists are the endpoints of domain walls in anyon systems [KK12]. A domain wall is a defect line along which the particle type of different anyon species is confused. By travelling around a twist, an anyon may change its charge. Due to charge conservation, this associates a residual charge with the domain wall and its twists that may be measured by annihilating the twists with one another (destroying the domain wall). The charge associated with a pair of well separated twists is again inaccessible to local operations and may be manipulated by braiding twists with either anyons or other twists.

These kinds of topological defects should not be considered excitations of the anyon system, rather deformations of the system itself. Holes and twists are usually imagined to be produced by, for example, adiabatically deforming the Hamiltonian to move from one defect configuration to another [CLB+14]. This process should be done sequentially via local changes to avoid closing the gap along the adiabatic path. If we interpret the system as a topological code, this style of procedure can be classed as code deformations. Code deformations change the definition of the codespace step by step until we arrive at an alternative code encoding the output of the desired computation. Examples of braiding of twists and holes as code deformation can be conveniently expressed in the stabilizer formalism [BMD09, Bom11, Bom10a].

Measurement-based quantum computation

Measurement-based quantum computation [RB01] is a paradigm for quantum information processing that proceeds quite differently to the standard circuit model. The circuit model typically specifies a computation by initialization of data registers in a product state, unitary evolution of the registers, and measurements on each register. In contrast, the measurement-based model assumes that a suitable highly entangled resource state has been prepared prior to computation. It then evolves the state by selectively measuring single particles one at a time and choosing subsequent measurements based on prior outcomes. These measurements can be thought of as consuming the entanglement prepared at the beginning of the protocol, as compared to the circuit model where entanglement can be created or destroyed at will by many-particle unitary gates.

In some experimental implementations, measurements are relatively cheap, and so if a suitable resource can easily be prepared then measurement-based quantum computation may be much simpler than implementing the circuit model or other computational protocols. The complexity of a measurement-based computation scheme thus largely rests on the difficulty of preparing an appropriate resource state. The prototypical resource state is the 2D cluster state [RBB03], which is very amenable to study within the stabilizer formalism. The cluster

state is the ground state of gapped, local, commuting Hamiltonian, and can also be prepared as the output of a constant depth quantum circuit. Other resource states that are ground states of more realistic Hamiltonians have also been proposed, most notably the 2D AKLT states [WAR11, Miy11]. These are the ground states of 2-body Hamiltonians, and so may be possible to prepare more easily in the laboratory, but this realism is traded for some of the simplicity of analysis present in the cluster states.

Elements of the measurement-based quantum computation paradigm may also be blended with those of other paradigms, most notably the topological and adiabatic approaches to quantum computation. Using a 3D cluster state, it is possible to simulate code deformation on a toric code by measurement [RHG07], thus combining some of the robustness of a topological computation scheme with the possible experimental advantages of a measurement-based protocol. The measurements in a cluster state computation can also be simulated by adiabatic fields, allowing a modular approach to adiabatic quantum computing by importing the tools of cluster state computation [BF10, BFC13, AMA14].

Many-body state ansatze

The problem of efficiently describing and manipulating quantum many-body states is an important one. Simply writing down a many-body spin model is of little use if there exist no tools to derive its properties. To this end, several extremely successful ansatze have been proposed to assist in the description and analysis of many-body states. We will discuss two main frameworks for describing many-body systems: stabilizer formalism and tensor network ansatze.

Pauli stabilizer formalism [Got99b] is very simple and can only describe a very restricted class of states of many-spin-$\frac{1}{2}$ systems. Happily, this small class includes important examples of many interesting many-body systems such as the toric code, color code, and cluster states. Pauli stabilizer states can be described as common $+1$ eigenstates of a set of Pauli operators called stabilizers. Using this Heisenberg picture description of the state, we can easily determine expectation values of operators by looking at their commutation relations with the stabilizers, or compute the effect of certain evolutions that take stabilizer states to stabilizer states. These allowed evolutions, called Clifford operations, and stabilizer states in general, are significant to the study of quantum information broadly, but when combined with locality constraints can also be used to describe many-body models of interest.

The Pauli stabilizer formalism has been extended in several ways. The first obvious extension is to higher dimensional Pauli algebras [Got99a], where most of the structure is inherited directly. Further generalizations have been less successful in giving useful tools to analyse evolution or properties of states, but are still useful to describe certain classes of quantum many-body states. Generalized stabilizer formalisms include the XS stabilizer formalism [NBVdN15], the normalizer circuit formalism [VdN13, BVVdN14, BVLVdN14], and the monomial stabilizer formalism [VdN11].

Tensor network ansatze are variational classes of quantum states that allow for efficient representation and manipulation of a desired class of states. Tensor network ansatze have been developed specifically to represent states of quantum many-body spin models, and have allowed for rapid advances in the numerical simulation of such systems. A prototypical such ansatz is that of matrix product states (MPS) [AKLT88, FNW92, PGVWC07]. This is suited to describing states of 1D spin chains, and in fact can provably be used to efficiently approximate the ground space of any gapped 1D system of locally interacting spins [Has07].

One way of understanding MPS is by considering pairs of maximally entangled "virtual" d-dimensional spins arranged on a line. Neighbouring qudits belonging to different maximally entangled pairs are then grouped and projected into some D-dimensional "physical" Hilbert space. The projection map thus defines a particular matrix product state. Expectation values of local observables and correlation functions can be efficiently extracted from such a description of the state, and for a given Hamiltonian the density matrix renormalization group procedure may be used to quickly determine a good MPS description for the ground state of such a system. MPS are equivalent to mean field theory (the variational class of product states) for trivial virtual systems (i.e. $d = 1$).

A natural generalization of MPS to higher dimension is projected entangled pair states [Has06, VWPGC06a] (PEPS). In this ansatz, pairs of virtual spins are placed on each edge of a graph, and then a projection map acts on all of the spins collected at each vertex (an MPS corresponds to a PEPS on a line graph). Though many of the guarantees of efficiency of representation or calculation that MPS provides do not survive to the general case of PEPS, it is nonetheless quite successful in practice at numerically determining the ground states of (usually gapped) quantum many-body spin systems and calculating their expectation values.

Apart from their use as numerical tools, states with MPS and PEPS representations can also be analysed analytically. For example, a PEPS representation by construction constrains the scaling of entanglement entropy in a system. The existence of a PEPS representation with certain properties for a state also guarantees the existence of a local, gapped, frustration-free parent Hamiltonian that has the desired PEPS as its ground state [PGVCW08]. Symmetries of a PEPS representation can be related to the properties of the state itself [SCPG10], and the PEPS representation of the cluster states can even be used to understand measurement-based quantum computation as a teleportation-based computation scheme on the virtual systems [VC04]. Additionally, PEPS have been used to construct interesting examples of states such as resonating valence bond states [SPCPG12], as well as the cluster states [VWPGC06b], quantum double ground states [SCPG10], and string-net states [BAV09, GLSW09].

Finally, we briefly mention a third major tensor network ansatz, though we will not make particular use of it in this thesis. The multiscale entanglement renormalization ansatz [Vid08] (MERA) is a class of tensor network states that are suited to describing critical many-body systems as opposed to MPS and PEPS, which are typically used to describe ground states of gapped systems.

1.1 Thesis overview

In this thesis we will develop several families of quantum many-body spin models that may be of use for topological quantum information processing. In developing these models, there are several competing factors: it is desirable that the models have interesting phenomenology, are analytically tractable, and are experimentally realistic. Of course, it is not always possible to optimize these constraints all at once and so at different stages of this thesis we will focus on either the first or last of these values, while still maintaining a high enough level of tractability that it is possible to demonstrate the relevant features.

In Chapter 2, we consider the topologically ordered quantum double models first described by Kitaev. These models are one of the main theoretical test-beds for concrete proposals of topological quantum computation by either braiding anyons or code deformation, and have the toric code as their simplest member. Although the simplicity of these models lends itself to theoretical study, the Hamiltonians of these systems are not particularly realistic, involving at least 4-body operators. We develop a method to approximate these systems by 2-body interactions using the tools of perturbation theory. The approximation we develop in fact gives the quantum double model in an encoded form as its low energy limit, so that each qudit of the target model is encoded in a fixed number of qudits of our system. The construction is motivated by the PEPS descriptions of the quantum double ground states. The interactions involved in our construction are local, and retain much of the algebraic structure of the original quantum double models, enabling the analysis of these new, more realistic models.

Following this theme, in Chapter 3 we construct 2-body parent Hamiltonians for a broad class of PEPS. Typically parent Hamiltonians of PEPS require many-body interactions, as is the case for the quantum double models. We can again use the structure of the PEPS description and ideas from perturbation gadgets to build a gapped Hamiltonian involving only 2-local interactions that gives the desired PEPS as its ground state under some conditions. These conditions are inspired by several known important natural classes of PEPS with amenable algebraic structure such as injective, G-injective, H-injective, etc. PEPS. Topological order of the states is also important in demonstrating the stability of the result. The additional complexity of the general case means that some of the elegant features of the quantum double construction presented in Chapter 2 do not survive. As in the previous chapter, the main result of Chapter 3 is a 2-local Hamiltonian with the desired ground state, providing an avenue for more experimentally realistic realizations of PEPS.

Chapter 4 departs from this programme of producing more realistic parent Hamiltonians for desirable states. In this chapter, we begin to construct new examples of many-body spin states that may have interesting phenomenology or be amenable to application in quantum information processing protocols. We start by introducing a formalism for generalizing a given qubit CSS state to a family of states labelled by arbitrary finite group. In this picture, the original qubit state corresponds to the group $\mathbb{Z}_2$. We relate the algebraic structure of a

CSS state to the group algebra of $\mathbb{Z}_2$ or the (isomorphic) representation algebra, and show how this may be straightforwardly generalized. This construction is applied to the cluster states to produce a family of generalized cluster states. The relationship between the standard qubit cluster state and the toric code generalizes to a relationship between the generalized cluster states and the relevant quantum double model. We also explore some properties of these states such as their symmetries and PEPS representations, as well as discussing possible applications of these states, including to generalizing the topological cluster state computation scheme (also making use of adiabatic quantum computation techniques).

Chapter 5 follows this programme by proposing a generalization of the topologically ordered color codes to arbitrary finite group. The color codes are of significant interest for topological coding and topologically ordered systems, having many useful properties. However, these systems cannot support non-Abelian anyons, precluding the possibility to implement topological quantum computation by braiding of color code anyons. Roughly following the prescription outlined in Chapter 4 we define a family of generalized color codes that allow for non-Abelian anyons and study their properties. An equivalence between these generalized color codes and the quantum double models is demonstrated and is particularly useful in determining the topological properties of these systems.

Finally, in Chapter 6 we comment on the broader relevance of the models introduced and the tools used in this thesis, before providing concluding remarks.

Each of the main chapters 2-5 can be read as a stand-alone unit, and has a self-contained introduction to the relevant background material. For the reader's convenience, at the conclusion of each of these chapters is a brief summary of the main results and discussion points covered.

2 Toric Codes and Quantum Doubles from Two-Body Hamiltonians

Abstract

We present a procedure to obtain the Hamiltonians of the toric code and Kitaev quantum double models as the low-energy limits of entirely two-body Hamiltonians. Our construction makes use of a new type of perturbation gadget based on error-detecting subsystem codes. The procedure is motivated by a PEPS description of the target models, and reproduces the target models' behavior using only couplings which are natural in terms of the original Hamiltonians. This allows our construction to capture the symmetries of the target models.

2.1 Introduction

There has been a surge of interest recently in spin lattice models because of their strange and wonderful properties. From the perspective of condensed matter physics and quantum many-body theory, they have recently led to major advances in our understanding of the nature of quantum phase transitions and topological order in two-dimentional systems. The topological properties of these models are also of interest in quantum computing and quantum error correction. A system with topological order can possess intrinsic error correction or protection capabilities. These are exploited for quantum data storage [DKLP02, WHP03, DCP10] or quantum information processing [RH07, RHG06, RHG07] with high error thresholds. The encoded logical operations in topological models are associated with non-trivial homology cycles on a lattice of spins. A lattice which has a non-trivial topology (such as a torus or punctured disk) can encode quantum information into its ground states which is robust to small local perturbations of the Hamiltonian.

Many models which are relatively simple (from a theoretical point of view) contain topologically ordered ground states. The toric code and its generalization to the quantum dou-

ble models [Kit03] are a significant class of exactly solvable models containing a range of different topological orders. Quantum double models of non-Abelian groups can support non-Abelian anyons, quasiparticles whose exchange statistics transcend the traditional Bose-Einstein/Fermi-Dirac dichotomy that is ubiquitous in three dimensions. Braiding such quasiparticles can be used for universal quantum computation [Moc03, Moc04, Pre98, WOP99].

However, these models (and other more general topological models [LW05]) consist of many-body interactions that are quite challenging to implement experimentally, as they usually involve interactions between four or more bodies. By contrast, most natural couplings are only 2-body. It is therefore of interest to find systems with only 2-body interactions which can realize topologically ordered phases.

An example of a 2-body system with a topologically-ordered ground state is the Kitaev honeycomb model [Kit06]. This well-studied model is being pursued experimentally in a number of systems, but unfortunately it cannot be used for universal quantum computation.

Aside from explicitly finding 2-body models which reproduce a particular desired type of topological order (certainly challenging), one can use perturbative techniques to reproduce an existing many-body model as the low energy effective behaviour of a 2-body system. The perturbative gadgets approach [KKR06, BDLT08, JF08, OT08] is the standard tool to achieve this, but it has a number of drawbacks. By tailoring the perturbation gadgets to specific classes of models, one might hope the result is a simpler construction circumventing many of these difficulties.

Here we present a new type of perturbation gadget that works by encoding the logical qudits of the target models in quantum error-detecting codes. This allows us to reproduce the properties of topological models as the low-energy effective Hamiltonians of 2-body systems. Here we concentrate specifically on the quantum double models, but we anticipate that a similar mechanism could be tailored to other classes of models (e.g. string net models [LW05]). Our construction is natural, in the sense that all of the interactions of our system are very closely related to the interactions of the target model, and because of this, an extensive number of symmetries of the target model are preserved exactly from the level of the physical lattice.

Unlike Kitaev's honeycomb model, our constructions are not known to be exactly solvable. However, our results are a significant extension of Kitaev's method in that they can yield any type of topological order (i.e. different types of anyons) within the class spanned by the quantum double models, including those which are universal for quantum computation.

2.2 Results and Methods

In this section we give an overview of our results and the methods we use to obtain them. To avoid obscuring the essence of our work with unnecessary technical details, we will use the toric code model as a concrete example in many places. However, we stress that our results

immediately carry over to all of the cyclic ($\mathbb{Z}_d$) quantum double models, and extend to the general non-Abelian quantum double models with just minor adjustments.

2.2.1 The Quantum Double Models

The quantum double models [Kit03] are a class of spin-lattice models which exhibit topological order. They can be used as topological quantum error-correcting codes based on the algebra of the Drinfeld double $\mathcal{D}(G)$ of a group G. The simplest member, corresponding to the group $\mathbb{Z}_2$, is the well-studied toric code model.

For simplicity, we define the quantum double models on a square lattice (although they can be defined on any oriented graph) with qudits (d-level quantum systems) on the edges, as in Figure 2.1. The lattice can be embedded into any 2-dimensional orientable surface, such as a torus. The Hamiltonian for the model takes the form

$$H_{\mathrm{QD}} = -\sum_{v} A(v) - \sum_{p} B(p)\,, \tag{2.1}$$

where v denotes a vertex of the lattice and p denotes a plaquette. In the simple case of the toric code, the vertex and plaquette operators are defined by

$$A(v) \equiv \bigotimes_{e\in+(v)} X_e \qquad \text{and} \qquad B(p) \equiv \bigotimes_{e\in\square(p)} Z_e \quad , \tag{2.2}$$

where the form for the star of a vertex $+(v)$ and the boundary of a plaquette $\square(p)$ can be seen in Figure 2.1, and X_e and Z_e are Pauli matrices acting on the qubit located on the edge e. Since we are working on a square lattice, each of these terms are clearly 4-body. For more complicated quantum double models, the $A(v)$ and $B(p)$ operators take slightly different forms, but will always consist of operators acting on the star of a vertex or the boundary of a plaquette. The exact details of the quantum double construction are given in Sec. 2.4.

When the surface in which the lattice is embedded has genus g, then the ground space of the toric code is 4^g-fold degenerate, and thus can encode $2g$ qubits. This particular encoding has generated so much interest because it is in some ways naturally robust to local errors [Kit03, DKLP02, BHM10, BH11b]. The dimension of the codespace for a non-Abelian quantum double model is more complicated, but on a torus the degeneracy of the ground space is equal to the total number of particle types [NSS$^+$08, Agu11].

2.2.2 Methods

Overview of Our Construction

Our main result is the construction of a wholly 2-body Hamiltonian that reproduces the quantum double Hamiltonian of Eq. (2.1) as its low-energy limit. Our procedure uses only

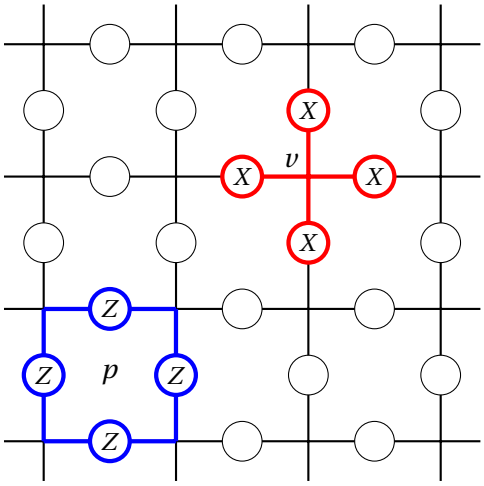

Figure 2.1 – The toric code defined on a square lattice with qubits on the edges. Each colored region represents one of the two types of terms in the Hamiltonian. The star terms (in red) act around a vertex v with a Pauli X on each qubit and the plaquette terms (in blue) act on the qubits around the boundary of p with a Pauli Z operator.

qudits of the same dimension as in the target model. Furthermore, the couplings that we use have the same form as in the original model. As an example, notice how each $A(v)$ and $B(p)$ term from Eq. (2.2) consists of the tensor product of four Pauli X terms or 4 Pauli Z terms, respectively. Our construction for the toric code will involve products of only two Pauli X terms or Z terms.

Each qudit on the edges of the original model is encoded in four physical qudits, shown in Fig. 2.2. The 2-body interactions among these four qudits will give us an effective single-qudit degree of freedom in the low-energy limit. This gives a 4-fold increase in the number of qudits required to construct our model as compared with the target model. We will couple neighbouring encoded qudits perturbatively, and the perturbation expansion will yield the desired Hamiltonian at 4^{th} order. This order is related to the coordination number of the underlying lattice and the number of edges bordering each plaquette, both of which are four for a square lattice. In contrast, on a honeycomb lattice terms will arise at 3^{rd} and 6^{th} order in perturbation theory (though there would still only be a 4-fold increase in the number of physical qudits required).

We achieve these results with a blend of techniques from condensed matter physics and quantum information theory. Before sketching how we use these techniques, we briefly mention each one in turn.

Projected Entangled Pair States.

Our construction is inspired by *projected entangled pair states* (PEPS), a class of quantum states particularly well suited for describing the ground states of interacting quantum many-

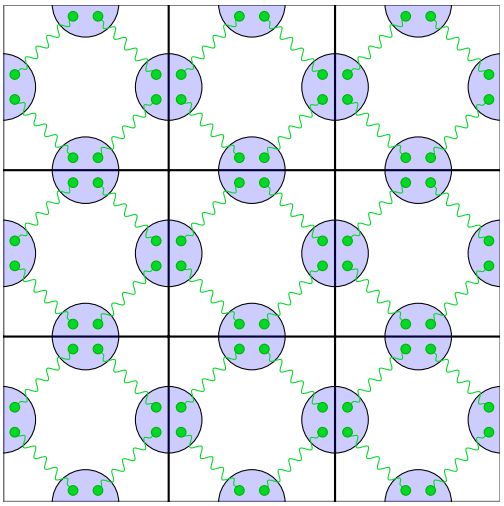

Figure 2.2 – PEPS description on a square lattice. Each qubit (for the toric code, or qudit in general) on an edge in the original model is replaced by four qubits (or qudits in general). Qubits connected by a wavy line are in a maximally entangled state. Each blue circle represents a projection down to a single encoded qubit. The quantum states in the support of these projectors are encoded qubits, entangled with each other. The global state space contains exactly the states in the ground space of the original toric code model. With toroidal boundary conditions, the ground space is four-fold degenerate. Our construction proceeds by simulating these local projections and the entangling interactions with 2-body Hamiltonians.

body systems [AKLT88, FNW92, Has06, PGVWC07, VWPGC06a, Vid03]. Indeed, for the case of 1-dimensional systems this is provably the case [Has07]. The basic idea of these states is to use virtual pairs of entangled systems to simulate correlations. For every coupling between neighboring systems on a lattice, a maximally entangled state (of some chosen dimension) is introduced between the systems. These virtual entangled pairs are then projected down to a "physical" subspace with a dimension equal to the that of the spins in the original model. An illustrative construction is depicted in Figure 2.2 for the special case of a square lattice.

One would expect the kinds of models we are studying to have an efficient PEPS representations of their ground spaces because of the facts that they obey an area law, possess a spectral gap above the ground state, and contain finite correlations. In fact, the PEPS representation of the toric code ground space has been studied by Verstraete *et al.* [VWPGC06b], and a PEPS representation of general quantum double models is also known [SCPG10]. PEPS descriptions have also been developed for all of the string-net ground spaces [GLSW09, BAV09] and the symmetries of these PEPS descriptions have been explored [SCPG10]. The quantum double models on trivalent lattices can be mapped to string net models [BA09], and generalisations of the quantum double models are also being interpreted as extended string net models [BCKA13]. In our construction we have an implicit PEPS representation for the quantum double models which is presumably equivalent to those already known (this is provably the case for our construction of the toric code).

Perturbation Gadgets.

The next technique that we use is that of *perturbation gadgets* [KKR06, OT08, BDLT08, JF08]. Perturbation gadgets are a method for systematically reducing the complexity of a many-body coupling between a large number of quantum systems. The gadgets generally consist of introducing some ancilla qudits which act as *conductors*, in the sense of the conductor of an orchestra. By having a strong coupling to the conductor, n separate primary qudits can synchronize their behavior in a way which mimics an n-body coupling at low energies, but by using couplings having only a fraction of the "body-ness". By recursively applying these general constructions, one can arrive at a strictly 2-body Hamiltonian for an arbitrary n-body coupling. The cost is that this coupling only occurs at a higher order in perturbation theory.

Our construction is a new variant on the perturbation gadgets approach. The concept is very similar, but instead of beginning from the original lattice and adding ancilla qubits to break up many-body interactions, we begin by encoding the qudits of the original lattice into a 4-qudit system. These systems are then coupled via relatively weak 2-body interactions, which enable us to treat the entire model perturbatively and show that it reproduces the target model in the low-energy limit. We will refer to these 4-qudit encoded systems as "code gadgets". Apart from the intrinsic interest of a new approach, we also manage to bypass a number of pitfalls that naive application of the perturbation gadgets can encounter. In particular, the resource cost of perturbative gadget schemes scales poorly with the system complexity, and a naive application of the technique can lead to the energy gap scaling with the system size or the fidelity of the topologically ordered states [VdNLDB08, OT08]. While this can be avoided, it remains a problem with applying the method in general. Additionally, while the couplings can be reduced to only 2-body, the nature of these 2-body couplings is in general vastly different from the couplings of the original model. It is plausible that by taking advantage of structure a much simpler construction could be devised that is specifically tailored to the model, using couplings that exploit this structure. This is the approach taken by Koenig [Koe10], who showed that a simple "clock" gadget could reduce the complexity of the quantum double models to only 3-body terms. Our construction also follows a similar strategy in some sense, but uses perturbative couplings that are direct analogues of the original models' terms on simple surfaces.

The type of gadgets that we use are adapted for use with states that are ground states of local Hamiltonians and have a simple PEPS description [BR06]. The virtual entangled pairs of the PEPS description are promoted into real physical systems with a coupling such that their ground state is a maximally entangled state. Then the PEPS projection can be done by using strong interactions between the systems within a code gadget which energetically favors the subspace defined by the PEPS projection. When this coupling within a site is much stronger than the entangling coupling between sites, the resulting Hamiltonian at low energy approximates the desired many-body Hamiltonian, with the same ground space up to perturbative corrections. This technique was originally used [BR06, GB08] to find 2-body Hamiltonians whose ground state encodes the cluster state [RB01], a state which is universal

for measurement-based quantum computing. Our technique is very similar, in that the target models are reproduced in an encoded manner, i.e. the 4-qudit code gadgets of our construction serve as the logical spins of the target model.

Subsystem Quantum Error Detecting Codes.

Finally, we make use of quantum error-detecting codes [Sho95, Ste96, Got97] to ensure that all of the undesirable terms in the perturbative expansion do not couple to the low-energy sector of our model. Recall that a quantum error-detecting code consists of a subspace of a larger Hilbert space, which is protected from some set of errors on the large Hilbert space. This protected subspace, the codespace, is used to store encoded logical information. The mapping between the codespace and the physical Hilbert space defines the encoded logical operators. Detectable errors move the system out of the codespace, and so can be detected by a suitable measurement.

Specifically, we use a particular type of quantum code known as a subsystem code [KLP05, KLPL06]. Compared to stabilizer codes, subsystem codes are no more powerful in terms of the number of errors they can detect, rather, their power lies in a simplification of the recovery operations required to fix the errors. The physical Hilbert space is partitioned into distinct subsystems: the logical subsystem and a "gauge" subsystem. As in a stabilizer code [Got97], stabilizer operators are defined such that the logical codespace is in the mutual +1 eigenspace of these operators. If an error moves the system out of this +1 eigenspace, it can be detected by measurement of the stabilizer, and must actively be corrected. In contrast, the logical state is taken to be invariant under a transformation on the gauge system, and so any errors that occur on this gauge space are passively avoided.

The code we use on our gadget construction is designed so that any operations contributing to unwanted terms in the perturbative expansion will be detected as errors, and map the ground space to another energy eigenspace with higher energy. In this way, the code ensures that the low energy behavior of our system will remain error free, in the sense that only desirable terms (i.e. those of the target model) will remain. Errors which move the system out of the codespace need not explicitly be corrected because they will be suppressed heavily by an energy penalty for doing so. Note that the "errors" that occur in the gadget code are unrelated to errors appearing in the target model we are trying to replicate. Instead, they mix the protected low-energy sector with higher energy (unprotected) sectors, thus preventing our system from mimicking the target model perfectly.

Our models are similar in many respects to the topological subsystem codes of Bombin [Bom10b]. These models, based on the color codes [BKMD09, KBMD10] and their qudit generalizations [Sar10], yield a subsystem code using local 2-body gauge generators. We note that the construction of [Bom10b] requires a 3-colorable lattice, whereas our method applies to any lattice for which the desired model possesses a PEPS description. Additionally, Bombin's models possess an exactly degenerate ground space while our models' ground spaces are

only approximately degenerate (as in the Kitaev honeycomb model [Kit06]), but where the degeneracy is only broken at very high order (roughly the linear size of the system). One consequence of this exact degeneracy in the Bombin model is that it is straightforward to define quantum error correction in the ground space [SBT11] where perfect recovery operations will yield perfect recovery from correctable errors. By contrast, in our model even perfect recovery operations will yield some small error due to the splitting of the ground space. While the small error in recovery seems unavoidable in our model, it might still be the case that our model yields higher thresholds due to the substantially simpler stabilizer measurements that are required. It is an open problem to define error correction and exactly quantify the errors incurred by the splitting for our model. Aside from both of our constructions being viewed as a generalization of the honeycomb model, we are not aware of any deeper connection between them.

2.2.3 Discussion

Our results allow us to replicate in the low-energy limit the Hamiltonians of certain topological models, but a more ambitious goal is to reproduce the topological order in the ground state wavefunctions of these models, as well as in their low-lying excited states. To demonstrate that our constructions reproduce *all* the topological properties of the original models, we would need to show additional properties. First, we would need to show that these topological orders are stable under the kinds of perturbative corrections that our procedure introduces. There are two separate types of corrections which could threaten the stability of the topological properties of our models. The first are the very high-order corrections where perturbation terms can form non-trivial homology cycles on the surface of the model. These will occur at order $2L$ in perturbation theory (with L the smallest linear dimension of the surface) and split the ground space degeneracy of the encoded model. They can be heavily suppressed by increasing L or by increasing the bare energy gap of the system. The second kinds of corrections to consider are those which leave the protected ground space of our code gadgets. These allow transitions into higher energy subspaces where our encodings fail. These kinds of corrections are suppressed energetically by the energy gap. Thus, we would also need to demonstrate stability of the energy gap in the thermodynamic limit. It would also be quite interesting to compute the topological entanglement entropy in the ground state [HIZ05, KP06, LW06, FHHW09]. Like the toric code model in two dimensions [DKLP02, NO08, CC07], the topological order of Kitaev's non-Abelian quantum double model is not expected to persist at finite temperature. We expect that our models will have similar behaviour to the original quantum double model at finite temperature, and in particular, that they will suffer from the same "thermal fragility" of the topological order.

Even more ambitiously, one might hope to show that our models remain gapped even in the presence of arbitrary local perturbations, with only very small splitting of the ground state degeneracy and the degeneracy of the excited states. For topological models whose Hamiltonians consist of a sum of commuting projectors, just such a result was shown by

Bravyi, Hastings and Michalakis [BHM10, BH11b]. Unfortunately, their techniques cannot be directly applied to our models since our Hamiltonians are not sums of commuting projectors. In fact, our models do not have frustration-free ground states either (meaning the ground states are not minimum-energy eigenstates of each term separately in the Hamiltonian) and hence other results on frustration-free systems also do not apply.

As one might expect from a perturbative construction, our effective Hamiltonian can be thought of as the target Hamiltonian plus perturbative corrections. Generically in this type of construction, the symmetries of the target model will be recovered approximately, up to these corrections. In our model, the encoded string operators of the target models will not commute with the perturbative terms in the Hamiltonian, and the corresponding ground space degeneracy will also be split. This splitting will be exponentially suppressed by the size of the lattice (as noted above), and so these symmetries will be recovered approximately as one might expect. In the quantum double models, there are also an extensive number of vertex and plaquette operators which commute with the Hamiltonian and form a quantum double algebra. It is possible to construct encoded counterparts of these operators on our model which also commute with our full Hamiltonian and form an equivalent algebra. In contrast to a generic perturbative construction, this large symmetry group is reproduced exactly by our model. This symmetry group severely constrains the arbitrarily high order terms arising from the perturbation expansion, and prevents undesirable terms from appearing. In fact, higher order terms in our effective Hamiltonian will act on the logical codespace as products of (commuting) lower order terms until the perturbative order is sufficiently high to form non-trivial loops over the lattice and break the ground space degeneracy.

As well as capturing symmetries of the target models, our construction is also natural in the sense that it is built from miniature quantum double models overlaid on each other. In the case of Abelian quantum double models (including the toric code), there is an exact correspondence between our constructions and quantum double models on simple surfaces. For these models, the ground space of our code gadget is chosen to coincide with a subspace of the quantum double ground space on a 4-qudit torus (see Sec. 2.6.2). That is, our codespace is stabilized by the same operators as the ground space of the quantum double Hamiltonian on this torus. These stabilizers would normally be 4-body, so in order for our codespace to obtain this property from a 2-body Hamiltonian we must sacrifice the degeneracy of one of the two qudits a torus can typically encode. In addition, the perturbative bond terms we introduce can be interpreted as quantum double models on a 2-qudit sphere (see Sec. 2.6.3). All the terms present in our model reflect the construction of the quantum double models on small surfaces. In non-Abelian models, the correspondence in the Hamiltonian is not as precise due to the distinction between left and right regular representations. However it will still be true that the ground spaces of our code gadgets will correspond to a subspace of the quantum double ground space on a 4-qudit torus, and the ground space of the perturbative bond terms will correspond to the ground space of the relevant quantum double model on a 2-qudit sphere.

Our work is inspired by the construction of Bartlett and Rudolph [BR06], who used encoded qubits to reproduce the cluster state as the ground state of a 2-body Hamiltonian. As with the model we present, the encoding is closely related to the PEPS description of the target state. Our work generalises this type of construction by using a subsystem code (as opposed to a subspace code). In order to reproduce the PEPS space as the ground space of a 2-body Hamiltonian, we have had to sacrifice the extra gauge degrees of freedom in our model. This would not have been possible if we had used a subspace code, where these gauge degrees of freedom are not available.

The procedure we present reproduces the quantum double Hamiltonian in the perturbative coupling limit. If we consider the opposite (strong coupling) limit in our model, the system will act as a disconnected set of maximally entangled pairs. In this limit, the lattice can be thought of as a set of disconnected quantum double models on spheres (up to the caveats noted above). There must be some phase transition(s) between these states, and the respective topologies in the two limits are suggestive of the kind of behavior studied by Gils *et al.* [GTK$^+$09]. The phase transition would be between different topologies in the sense that the quantum double model would act on the entire lattice together in one limit, and at some critical coupling strength break down to act on disconnected portions of it.

A robust topologically ordered system would also have anyonic low-energy excitations which, ideally, would be similar to those of the desired quantum double model. One would need to consider the effect of the perturbative corrections in our model on these anyons and any other excitations, as for example in [DSV08, SDV08, VSD08]. The perturbative nature of our construction means that the target model is only realized up to a quasi-local unitary transformation. Attempting to manipulate excitations in the model using local unitary operations would generally cause the quasi-particles to delocalize or create additional undesired excitations [DSV08, VSD08]. One method to avoid these complications is to transport the excitations by local adiabatic deformation of the Hamiltonian [BP08, LP09].

It would also be interesting to explicitly and rigorously show that cooling our Hamiltonians by coupling to a local bath can bring them to the ground space quickly. (Cooling to a particular ground *state* of the degenerate ground space is more difficult, but also quite interesting.) Because of the frustration in the model, it isn't immediately obvious that this can be achieved efficiently, i.e. in an amount of time polynomial in the size of the system. But because the low-energy effective theory is frustration-free, it certainly seems plausible that the cooling can be done efficiently.

It is noteworthy that the codes we utilise in our construction for general quantum double models are examples of extensions of the stabilizer formalism to non-Abelian groups. This has not been closely studied previously, and in that sense the quantum codes we use may be of interest in their own right.

We believe that the kind of approach we employ here to reproduce topological orders may be more generally applicable to other systems with efficient PEPS representations. Some work

towards extending this treatment to the class of string net models [LW05] supports this belief, with some caveats, and will be presented in a future publication.

2.3 Example: The Toric Code

As a simple and illustrative example of our scheme, we now demonstrate how to construct a two-body Hamiltonian for which the low-energy behavior reproduces the standard toric code Hamiltonian on a square lattice. This simple example possesses all of the key features of our general construction for the quantum double models.

2.3.1 PEPS Representation of the Toric Code

We begin our construction by replacing each qubit on the edges of the toric code lattice with four qubits, as in Fig. 2.2 on page 17. We use the term *bond* to refer to the wavy lines in Fig. 2.2 that connect the maximally entangled pairs of physical qubits. By contrast, we use the word *edge* to denote the edges of the original lattice. In the PEPS description, the projection operators acting on each edge will entangle these four qubits into a single qubit. We achieve this projection in the ground space of a Hamiltonian defined on each edge e.

$$H(e) = -\left(\begin{array}{c|c} X & I \\ X & I \end{array}\right)_e - \left(\begin{array}{c|c} I & X \\ I & X \end{array}\right)_e - \left(\begin{array}{c|c} Z & Z \\ I & I \end{array}\right)_e - \left(\begin{array}{c|c} I & I \\ Z & Z \end{array}\right)_e . \tag{2.3}$$

This notation is a convenient visual shorthand for the tensor product of the operators acting on the given physical qubits. For each edge, the collection of 4 qubits forms our "code gadget". The Hamiltonian contains only two-body terms acting within the gadget itself.

Instead of the explicit projection mechanism of the PEPS scheme to reduce the Hilbert space, our model simply suppresses by energy penalty states which lie outside the desired PEPS projection. It can be shown that the projectors to the ground space of our edge Hamiltonian are equivalent to the PEPS projectors given in Ref. [VWPGC06b] for the toric code. These two formulations are not identical – they give different encodings of the "physical" PEPS space in the "virtual" qubits. However, this difference can be regarded as a gauge freedom in the PEPS representation that does not affect the PEPS itself. Explicitly demonstrating this equivalence is tedious (though straightforward) so we omit this.

Next, we introduce entanglement across the bonds by coupling sites on different edges. Thus for each bond b, define the perturbation term

$$V(b) = -\ X \overset{b}{\sim\sim} X \ -\ Z \overset{b}{\sim\sim} Z \ , \tag{2.4}$$

chosen because it possesses a maximally entangled state as its ground state[1]. Our unpertubed Hamiltonian is summed over all edges e:

$$H_0 = \sum_e H(e)\,, \tag{2.5}$$

and our perturbation term is summed over all bonds b:

$$V = \sum_b V(b)\,. \tag{2.6}$$

For those readers familiar with PEPS, it may seem counterintuitive to treat the bond term as small compared to the code gadget Hamiltonian (which is simulating the PEPS projection). We will see that this is in fact the correct approach to recover the target model. We introduce a coupling strength λ which is a small parameter compared to the strength of the main terms in our Hamiltonian (which we have taken to have unit norm). The full Hamiltonian describing our lattice is then given by

$$H = H_0 + \lambda V\,. \tag{2.7}$$

Now we need to compute the perturbative low-energy effective Hamiltonian to leading non-trivial order in λ. We will find the exact ground space of $H(e)$ in the next section, and then show that the perturbations λV will generate operators which reproduce an encoded toric code Hamiltonian (Eq. 2.1-2.2) at fourth order in λ.

2.3.2 Solving the Code Gadget Hamiltonians

We must first demonstrate that $H(e)$ of an edge e has a two-dimensional degenerate ground space. We will show that this ground space is in fact the codespace of a subsystem quantum error-detecting code, which will greatly assist the perturbative analysis in the next section. Our analysis of this Hamiltonian for the toric code construction follows Bacon [Bac01]. Because we are always working on a particular arbitrary edge (within a particular code gadget), we will suppress the label e in this section.

The code gadget Hamiltonian $H(e)$ (Eq. 2.3) posesses a number of constants of motion. That is, we can define operators that commute with each other, and with the Hamiltonian. In fact some of these operators are the *stabilizers* of a quantum code, so we label them S. They form a

[1] An alternative choice would be $V(b) = -$ 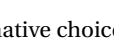 . This choice also approximately realizes the toric code Hamiltonian in the limit of small perturbation strength. The resulting Hamiltonian Eq. (2.7) is precisely equivalent to Kitaev's exactly solvable honeycomb model on a mosaic tiling [YZS07]. We do not consider this possibility further since it is unclear how to generalize it to more complicated quantum double models. It is interesting to note, however, that this alternative choice results in a model with topological order in the limit of large perturbation strength, in contrast to our models which become valence bond solids.

commutative group, and are generated by

$$S_X \equiv \left(\begin{array}{c|c} X & X \\ X & X \end{array}\right) \quad \text{and} \quad S_Z \equiv \left(\begin{array}{c|c} Z & Z \\ Z & Z \end{array}\right). \tag{2.8}$$

We can also define other joint operators to complete the algebra of our code gadget. We will call these operators *gauge* operators and *logical* operators, and denote them with appropriate subscripts.

$$X_{\mathsf{G}} \equiv \left(\begin{array}{c|c} I & X \\ I & X \end{array}\right), \quad Z_{\mathsf{G}} \equiv \left(\begin{array}{c|c} Z & Z \\ I & I \end{array}\right), \quad \text{and} \quad X_{\mathsf{L}} \equiv \left(\begin{array}{c|c} X & X \\ I & I \end{array}\right), \quad Z_{\mathsf{L}} \equiv \left(\begin{array}{c|c} I & Z \\ I & Z \end{array}\right). \tag{2.9}$$

These Pauli algebras define qubit Hilbert spaces that we denote G and L respectively.

We see immediately that these operators encode two orthogonal copies of the Pauli algebra, so they define two encoded qubits. In terms of these new operators, we can rewrite the gadget Hamiltonian

$$H(e) = -X_{\mathsf{G}}(1+S_X) - Z_{\mathsf{G}}(1+S_Z)\,. \tag{2.10}$$

The protected subspace of our code, also corresponding to the ground space of the Hamiltonian, is a subspace of the $+1$ eigenspace of the stabilizers S_X and S_Z. Any single qubit error will anticommute with at least one of these, and so could be detected (though not unambiguously) by measurement of the stabilizers. This means that any single qubit error will neccesarily move the system out of its ground space, and will be suppressed by the energy penalty for doing so.

We can easily check that the logical operators X_{L} and Z_{L} also commute with $H(e)$. However, neither X_{G} nor Z_{G} commutes with H. Given all these facts, H decomposes into a direct sum of four copies of $\mathsf{L}\otimes\mathsf{G}$, each labeled by the pairs of eigenvalues $(\pm1,\pm1)$ of S_X and S_Z, and furthermore the energies in the logical space are degenerate. Thus, we only have to solve the Hamiltonian on the gauge subspace of each stabilizer eigenvalue to find the ground space.

It turns out the ground space is contained in the $(+1,+1)$ block, and it is exactly two-fold degenerate. We provide a proof of this statement and its generalization to all the quantum double models in Sec. 2.10. It can be shown that within this codespace the encoded computational

basis states take the (unnormalised) form:

$$|0_L\rangle = \left(1+\sqrt{2}\right)$$ 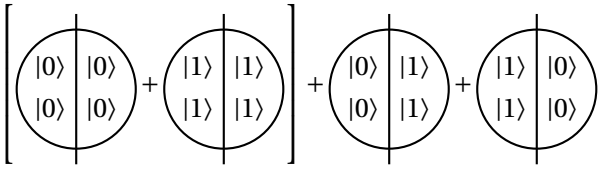 (2.11)

$$|1_L\rangle = \left(1+\sqrt{2}\right)$$ 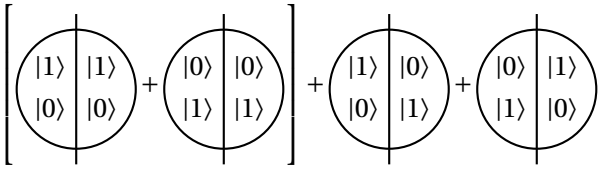 (2.12)

Now that we have determined that the ground space encodes a qubit in an error-detecting code, we can perform the perturbative analysis to compute the low-energy effective Hamiltonian.

2.3.3 Perturbation Analysis

We now introduce the perturbative coupling of Eq. (2.4) between our encoded qubits on the lattice. We use the Green's function perturbation method, following Kitaev [Kit06] (see also [BSFB07]) to calculate the leading non-trivial order in the effective Hamiltonian, defined as $H_{\text{eff}} = E_0 + \Sigma(E_0)$, with the unperturbed ground state energy of the lattice E_0 and Σ the self-energy. In this, we have approximated the self energy as being independent of E, for $E \approx E_0$. More details of our perturbation formalism are in Sec. 2.7.

The key to our analysis is the fact that quantum codes map detectable errors to orthogonal states. In terms of the gadget Hamiltonians $H(e)$, this means that any single-qubit Pauli operator anti-commutes with either (or both) of S_X or S_Z, and hence maps ground states to orthogonal states, since these states must lie in some block of $H(e)$ other than the $(+1,+1)$ block.

The consequence is that the perturbation analysis greatly simplifies. It immediately gives the result that all odd-order perturbation terms will vanish, as they will necessarily leave two code gadgets in excited states. The terms at second order only contribute an energy shift, since those that don't vanish act twice on the same qubits, hence they act proportionally to the identity. The first non-trivial terms appear at fourth order, and we can write the 4th-order effective Hamiltonian as follows:

$$H_{\text{eff}}^{(4)} = \lambda^4 \Upsilon V \big(G_0(E_0) V\big)^3 \Upsilon\,, \tag{2.13}$$

where Υ is the projector to the ground space of the unperturbed system and $G_0(E) = (E - H_0)^{-1}(1-\Upsilon)$ is the Green's function (resolvent) projected to vanish on ground states. The Υ will project the stabilizer and gauge degrees of freedom down to a single state, but will act identically on the logical degree of freedom.

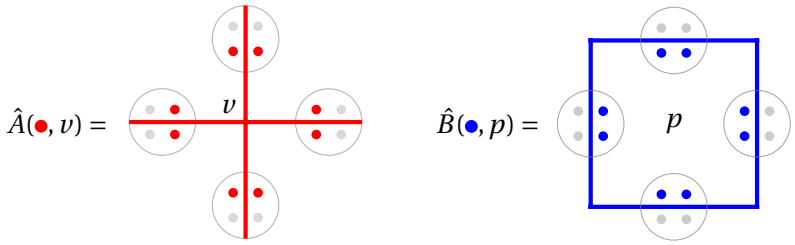

Figure 2.3 – Encoded operators. For each operator, the non-trivial operator acts on the colored qubits. For example, $\hat{A}(X, v)$ is a tensor product of X operators on each of the colored qubits surrounding the vertex v.

The non-trivial fourth order terms arise by constructing joint operators around a plaquette or around a vertex which leave all the code gadgets in the ground space. By expanding Eq. 2.13 and ignoring constant energy shifts, we can express the effective Hamiltonian to 4^{th} order as

$$H_{\text{eff}} \propto -\lambda^4 \sum_v \Upsilon \hat{A}(v) \Upsilon - \lambda^4 \sum_p \Upsilon \hat{B}(p) \Upsilon \,, \tag{2.14}$$

where v and p sum over all vertices and plaquettes, respectively. The operators $\hat{A}(v)$ and $\hat{B}(p)$ are each a sum of two terms,

$$\hat{A}(v) = \hat{A}(X, v) + \hat{A}(Z, v) \quad \text{and} \quad \hat{B}(p) = \hat{B}(X, p) + \hat{B}(Z, p) \,, \tag{2.15}$$

where these terms are quite cumbersome to express algebraically, so we define them pictorially in Fig. 2.3. Basically, these operators act on the pairs of qubits in an edge that are nearest to the center of a given plaquette or vertex.

We can derive from Fig. 2.3 that $\hat{A}(X, v)$ acts like a tensor product of logical X_{L} operators on each of the edges surrounding v. This is not immediately obvious; we must use the fact that in the ground space $X_{\text{L}} = S_X X_{\text{L}}$ to exchange the action of the logical operators between pairs of qubits at a particular edge. Similarly, $\hat{B}(Z, p)$ acts like a tensor product of logical Z_{L} operators around the plaquette p. The other operators $\hat{A}(Z, v)$ and $\hat{B}(X, p)$ act like gauge operators in a similar fashion. When these encoded gauge operators are mapped back to the ground space by Υ, they contribute only a constant energy shift, which we can ignore.

We can think of these $\hat{A}$ and $\hat{B}$ operators as acting equivalently to some logical operators within the ground space. If we define

$$\hat{A}_{\text{L}}(v) \equiv \bigotimes_{e \in +(v)} X_{\text{L}}^e \qquad \text{and} \qquad \hat{B}_{\text{L}}(p) \equiv \bigotimes_{e \in \square(p)} Z_{\text{L}}^e \,, \tag{2.16}$$

then we can see that within the codespace, they are equivalent (up to muliplicative and additive constants) to $\hat{A}$ and $\hat{B}$ respectively. That is,

$$\Upsilon \hat{A}_{\text{L}}(v) \Upsilon \propto \Upsilon \hat{A}(v) \Upsilon - \text{const} \qquad \text{and} \qquad \Upsilon \hat{B}_{\text{L}}(p) \Upsilon \propto \Upsilon \hat{B}(p) \Upsilon - \text{const} \,. \tag{2.17}$$

We can think of the logical Hamiltonian acting within the codespace as being comprised of these operators, such that

$$H_{\mathsf{L}} = -\lambda^4 \sum_{v} \hat{A}_{\mathsf{L}}(v) - \lambda^4 \sum_{p} \hat{B}_{\mathsf{L}}(p)\,. \tag{2.18}$$

When restricted to the codespace, this is exactly the effective Hamiltonian we previously derived (again, up to multiplicative constants and energy shifts), so that

$$H_{\text{eff}} \propto \Upsilon H_{\mathsf{L}} \Upsilon + \text{const} \tag{2.19}$$

Noting that the logical operators $\hat{A}_{\mathsf{L}}$ and $\hat{B}_{\mathsf{L}}$ act on the logical state exactly like the toric code vertex and plaquette terms, we can see that on the logical space, our effective Hamiltonian is the toric code Hamiltonian of Eq. (2.2) up to constants, as claimed.

The higher order terms in the expansion for the self-energy (see Sec. 2.7) will generally act on the logical space like products of the terms appearing in Eq. (2.18). Moreover, for low energies all these terms will be negative, since the perturbation term and the Green's function will both be non-positive and so each term in the expansion will be negative. All these terms in the self-energy expansion will commute, and so the ground space should remain the +1 eigenspace of the terms in Eq. (2.18) as desired. There will be some corrections to the excited spectrum of the effective Hamiltonian due to these higher order corrections and due to the energy dependence of the self-energy as discussed in Sec. 2.7, but as we are mainly interested in the topologically ordered ground space, this does not concern us especially. At very high order it will be possible to construct terms which run all the way around the torus. These errors will corrupt the logical state. If the linear size of the torus is N, these terms will appear at $2N^{\text{th}}$ order, and will be suppressed by a factor of λ^{2N}.

This result allows us to take a system of only two-body couplings, and in the low energy limit reproduce the Hamiltonian of the toric code. This means we might expect to be able to use the topological properties of the toric code to protect quantum information without the requirement for experimentally problematic many-body couplings. A similar result of obtaining the toric code in a limit was observed in Kitaev's honeycomb model [Kit06]. In contrast to our construction, this honeycomb model is exactly solvable. Although we can only solve our model perturbatively, we can generalize it relatively easily to more complicated quantum double models (and lattices other than square), as will be seen in the following sections.

2.4 Review of Quantum Double Models

The quantum double models consist of coupled finite-dimensional quantum systems on the edges of a lattice, and their ground states exhibit topological order [Kit03]. In this section,

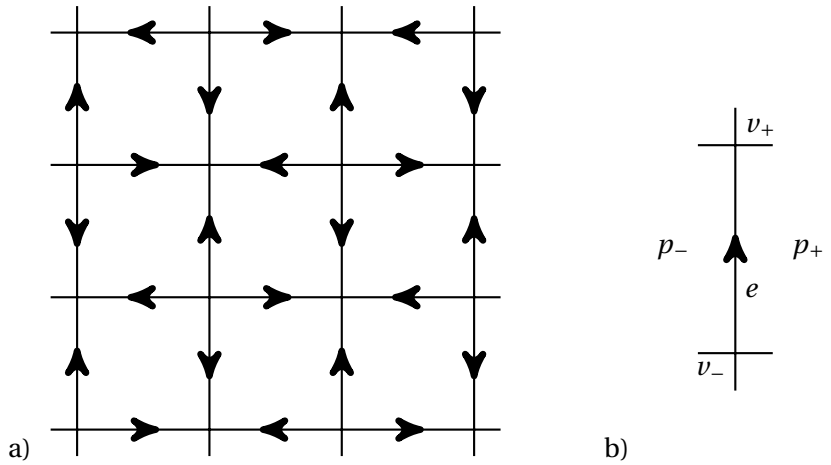

Figure 2.4 – a) A directed square lattice, and the orientation of + and − vertices and plaquettes relative to edge direction. Each vertex consists either of all "inward" edges or all "outward" edges. Plaquettes consist of alternately directed edges as you traverse their boundary. b) If an edge spans the pair of vertices (v_+, v_-), then the edge is oriented toward v_+. The plaquettes are labeled with signs, where p_+ is on the right of the edge, following the given orientation.

we will define the quantum double Hamiltonian that will become the target model of the perturbative two-body systems that we will work with in the subsequent sections.

As with the toric code, we will work with a square lattice for concreteness. The lattice can be embedded into any orientable 2-dimensional surface. To each edge e of the lattice we will associate an orientation, as in Figure 2.4. Although this orientation could be arbitrary, we chose the orientation in Figure 2.4 because it has the convenient feature that each vertex can be labeled with either a "+" or a "−" sign. In fact, any bipartite lattice can be partitioned in such a way.

We associate each quantum double model with a finite group G, and a local Hilbert space for each edge $\mathbb{C}^{|G|}$, with $|G|$ the order of the group. On each edge e of the lattice, there exists a natural orthonormal basis $\{|g\rangle_e, g \in G\}$, for these degrees of freedom. The total Hilbert space is then the tensor product of the local Hilbert spaces over all the edges.

We now define a number of operators that act on these edge degrees of freedom. For each edge e, define operators associated with left (+) and right (−) group multiplication and group projectors as follows:

$$L_+^g(e) \equiv \sum_h |gh\rangle\langle h|_e\,, \qquad L_-^g(e) \equiv \sum_h |hg^{-1}\rangle\langle h|_e\,, \tag{2.20}$$

$$T_+^g(e) \equiv |g\rangle\langle g|_e\,, \qquad T_-^g(e) \equiv |g^{-1}\rangle\langle g^{-1}|_e\,. \tag{2.21}$$

The operators on a single edge form an algebra defined by commutation relations

$$L_{\pm}^{g} T_{\pm}^{h} = T_{\pm}^{gh} L_{\pm}^{g} \quad , \quad L_{\pm}^{g} T_{\mp}^{h} = T_{\mp}^{hg^{-1}} L_{\pm}^{g} . \tag{2.22}$$

Clearly, operators acting on different edges commute.

We also associate a sign $\pm$ to each vertex and plaquette relative to their incident edge. This is illustrated in Figure 2.4. If an edge spans the vertices (v_-, v_+), then the arrow along the edge points away from v_- and toward v_+. Plaquettes to the left of an edge when looking along its direction are labelled p_-, while those to the right are labelled p_+.

It is convenient to associate a particular operator with a (plaquette, edge) pair or a (vertex, edge) pair. That is, depending on the sign of the vertex or plaquette under consideration at the time ($v_\pm$ or $p_\pm$) respective to the edge under consideration, the sign of the group multiplication and projection operators can be inferred. Explicitly, we define

$$L^{g}(e, v_{\pm}) \equiv L_{\pm}^{g}(e) \quad , \quad T^{g}(e, p_{\pm}) \equiv T_{\pm}^{g}(e) . \tag{2.23}$$

The L operators play the role of a generalized Pauli X operator in the group element basis, insofar as they move a particular state $|g\rangle$ through the space of elements. To make the analogy with the toric code more apparent, we can also construct some operators which act as generalized Pauli Z's for an arbitrary group algebra. Let π be a unitary irreducible representation of G. Then we can define a type of Fourier transform by

$$Z_{\pm}^{\pi_{ij}} \equiv \sum_{g} [\pi(g)]_{ij} T_{\pm}^{g} , \tag{2.24}$$

where $[\pi(g)]_{ij}$ is the $(i,j)^{\text{th}}$ element of the representation matrix for group element g in representation π. Equivalently, we can invert this expression to obtain

$$T_{\pm}^{g} = \frac{1}{|G|} \sum_{\pi} d_{\pi} \sum_{ij} [\pi(g)]_{ij} Z_{\pm}^{\pi_{ij}} , \tag{2.25}$$

where the sum is over the complete set of unitarily inequivalent irreps of G and d_π is the dimension of the irrep π. Although the quantum doubles are typically defined in terms of T operators, the algebra of these generalized Z operators gives the most convenient form for a particular calculation later on.

Given these preliminary operators, for each vertex v we can define operators

$$A^{g}(v) \equiv \bigotimes_{e \in +(v)} L^{g}(e, v) , \tag{2.26}$$

where $+(v)$ is the set of edges incident on the vertex v (recall Figure 2.1). We can average these

operators over the group to give the projector

$$A(v) \equiv \frac{1}{|G|} \sum_g A^g(v) . \tag{2.27}$$

Given a plaquette p and a fiducial edge on its boundary that we label e_1, we can define an operator

$$B^g(p) \equiv \sum_{g_k \cdots g_1 = g} \bigotimes_{e_i \in \square(p)} T^{g_i}(e_i, p) , \tag{2.28}$$

where e_i are the boundary edges taken as the plaquette is traversed clockwise starting with e_1, and there are k total edges on the boundary of p. These operators are all orthogonal projectors, but note that this definition depends on the choice of the fiducial edge e_1. However, if we consider the operator

$$B(p) \equiv B^1(p) , \tag{2.29}$$

where 1 is the identity element of the group G, then it is easy to see that B no longer depends on the choice of this fiducial edge.

For all p and all v, the $B(p)$ operators and the $A(v)$ commute pairwise amongst themselves and each other. Finally, the following Hamiltonian defines the quantum double model

$$H = -\sum_v A(v) - \sum_p B(p) , \tag{2.30}$$

in a fashion which directly generalizes the toric code.

2.4.1 Simplifications in the Case of Cyclic Groups

It will be instructive to treat the cyclic groups $\mathbb{Z}_d$ before moving on to the general case. For that reason, we revisit the above discussion specialized to this setting. Because each of the $|G|$ representations of the (Abelian) groups $\mathbb{Z}_d$ are 1-dimensional, we can relate the L and Z operators by a simple discrete Fourier transform for these groups. In cyclic groups (with $d = |G|$), the group multiplication operation is addition (modulo d), and so the left and right multiplication operations are equivalent. Following this, the convention for the identity element in cyclic groups is 0 as opposed to 1 for general groups. With no need for unique left and right multiplication operators, we define the cyclic L operator by

$$L \equiv \sum_{h=0}^{d-1} |h+1\rangle\langle h| . \tag{2.31}$$

The addition within the ket is performed modulo d. Note that the group action of any other element can be achieved in these models by taking powers of this (unitary) operator. We also

define a set of group projection operators

$$T^g \equiv |g\rangle\langle g|\,, \tag{2.32}$$

Following the general case, we also define a generalized Pauli Z operator. As representations of the cyclic groups are 1-dimensional, we can define a primitive Z corresponding to a representation ω

$$Z \equiv \sum_{h=0}^{d-1} \omega^h T^h\,, \tag{2.33}$$

where ω is a primitive d^{th} root. Other representations of the group correspond to powers of ω, so to obtain the operators corresponding to these representations, we need only take powers of this Z operator. Thus we regard the powers of Z as being labelled by representations of $\mathbb{Z}_d$.

If we take a discrete fourier transform on the basis $\big|g\rangle$, we obtain:

$$|\gamma\rangle = \frac{1}{\sqrt{d}} \sum_j \omega^{\gamma j} |j\rangle \tag{2.34}$$

where we label the Fourier basis with Greek letters (corresponding to irreps). This transformation diagonalizes the L operators:

$$L = \sum_\gamma \omega^{-\gamma} |\gamma\rangle\langle\gamma|\,, \tag{2.35}$$

and so we can see that the Z and L operators are simply a basis change away from each other in these cyclic models, as was the case with the Pauli matrices for the toric code. As they are both unitary, we can also say

$$L^\dagger = L^{-1} = L^{d-1}\,, \tag{2.36}$$

$$Z^\dagger = Z^{-1} = Z^{d-1}\,. \tag{2.37}$$

In terms of the definition of the quantum double model for cyclic groups, the only changes we need make to become consistent with this simplified set of operators is to slightly redefine the associations of L and T operators with $\pm$ vertices and plaquettes, i.e.

$$L^g(e, v_\pm) \equiv L^{\pm g}(e) \quad , \quad T^g(e, p_\pm) \equiv T^{\pm g}(e)\,. \tag{2.38}$$

With this in mind, the quantum double Hamiltonian is defined exactly as in the general case.

2.5 Our Construction for the Cyclic Quantum Double Models

In this section we will show how our construction on the toric code generalizes naturally to the quantum doubles of cyclic groups. The toric code model corresponds to the quantum double of the group $\mathbb{Z}_2$; here we extend this treatment to the quantum double of $G = \mathbb{Z}_d$, where $|G| = d$ is the order of the group. This analysis could be extended to general Abelian groups. However, for simplicity, and because the fully general case is considered in the next section, we restrict our attention to cyclic groups in this section.

In order to reproduce the cyclic quantum double models, two features must be added to the simple toric code construction. To begin with, qubits at each site must be replaced by d-dimensional qudits, with appropriate generalized Pauli operators defined on them, as introduced in Sec. 2.4. The group multiplication operator L plays the role of the X operator in the toric code, and the newly generalized Z operator plays the role of the Pauli Z. These operators obey the commutation relation

$$Z^a L^b = \omega^{ab} L^b Z^a \tag{2.39}$$

The other feature we will add to our construction at this juncture is the notion of directed edges, as discussed in Sec. 2.4. As in the toric code ($\mathbb{Z}_2$) case, we will now proceed with our construction explicitly on the square lattice.

2.5.1 Code Gadgets on Lattice Edges

We use a very similar construction to the toric code to encode our qudits for cyclic quantum double models. Each logical qudit is encoded using a subsystem code constructed from 4 physical qudits (Figure 2.2 shows the scheme). The d^4-dimensional space of these edges is partitioned as

$$\mathscr{H}(e) = \bigoplus_S \mathscr{H}_{\mathsf{L}}^S \otimes \mathscr{H}_{\mathsf{G}}^S \tag{2.40}$$

where the direct sum is over eigenvalues of stabilizers S. Our codespace is in the +1 eigenspace of two stabilizer operators S_L and S_Z defined below. The remaining d-dimensional degrees of freedom are encoded as qudits, one of which (the gauge qudit $\mathscr{H}_{\mathsf{G}}$) we fix in a single state in the codespace. The other qudit is used as our logical space $\mathscr{H}_{\mathsf{L}}$. If an error occurs, it will flip a stabilizer operator, move the code gadget out of the codespace, and incur an energy penalty.

Physically, we provide the codespace with these properties as the ground space of a 2-body Hamiltonian. Before we write it, we will first introduce the gauge, logical, and stabilizer joint

operators as we did for the toric code.

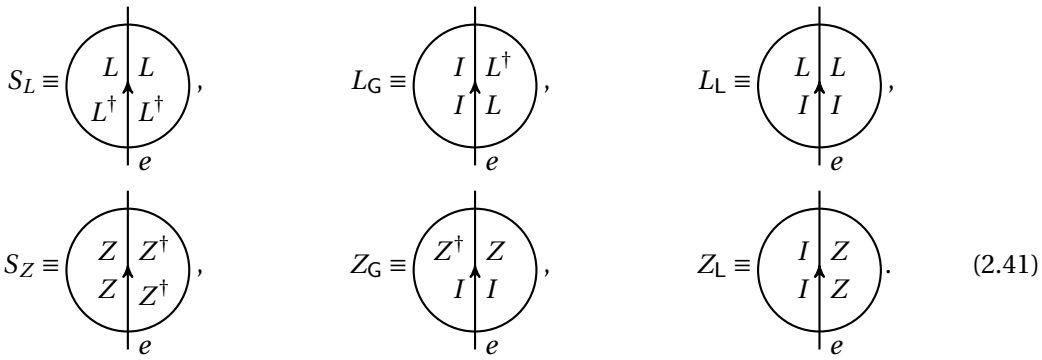

(2.41)

To avoid confusion as much as possible, we will distinguish typographically G for gauge and G for group, similarly L for logical and L for group multiplication. It is simple to verify that the operators defining each seperate degree of freedom commute with each other (i.e., stabilizers commute with gauge and logical operators, and gauge operators commute with logical operators). It can also be seen that the logical operators satisfy the desired algebra of the cyclic quantum double models:

$$Z_\mathsf{L}^a L_\mathsf{L}^b = \omega^{ab} L_\mathsf{L}^b Z_\mathsf{L}^a \tag{2.42}$$

and the gauge operators satisfy an equivalent algebra:

$$Z_\mathsf{G}^a L_\mathsf{G}^{-b} = \omega^{ab} L_\mathsf{G}^{-b} Z_\mathsf{G}^a . \tag{2.43}$$

We define the Hamiltonian on a single code gadget (associated with edge e) as

$$H(e) = -\frac{1}{d}\sum_{k=0}^{d-1}\left[L_\mathsf{G}^k + (L_\mathsf{G}^k S_L^k)^\dagger + Z_\mathsf{G}^k + (Z_\mathsf{G}^k S_Z^k)^\dagger\right]_e . \tag{2.44}$$

This equation can be represented diagrammatically as

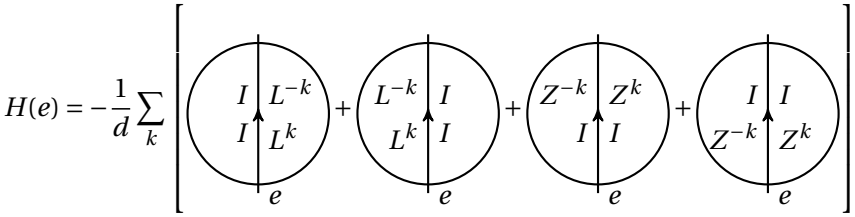

(2.45)

In this form, it is easy to see that each term in the Hamiltonian acts only on two qudits.

Multiplication by the stabilizers (as in $L_\mathsf{G} S_L$) effectively moves a gauge operator from two qudits onto the opposite two. In the $d = 2$ case, this Hamiltonian does not directly reduce to the one quoted for the toric code earlier (Eq. (2.10)) because of the inclusion of the identity

($k = 0$) term. However this term only induces a constant energy shift, and so can be disregarded for our purposes.

We now turn to the properties of the ground space of this Hamiltonian. It is clear that this Hamiltonian commutes with the logical operators, but less obvious that its ground space possesses the other properties we require. In Sec. 2.9, we prove the following theorem:

Theorem 1. *The Hamiltonian Eq. (2.44) has a d-fold degenerate ground space that is in the common $+1$ eigenspace of S_L and S_Z.*

This result, combined with the fact that our logical operators commute with the Hamiltonian, gives us a ground space to use as an encoded logical codespace $\mathscr{H}_{\mathsf{L}}$.

2.5.2 Coupling the Code Gadgets

The lattice is connected exactly as was the case for the toric code (Fig. 2.2), with qudits from neighbouring edges linked via an entangling bond. We have an unperturbed Hamiltonian for each edge qudit given as in the previous section:

$$H_0 = \sum_e H(e) \tag{2.46}$$

where the index e denotes a particular edge qudit. We then introduce the bond term:

$$V = \sum_b V(b) \tag{2.47}$$

$$= -\sum_b \sum_{k=0}^{d-1} \left[L^k \overset{b}{\sim\sim} L^k + Z^k \overset{b}{\sim\sim} Z^{-k} \right] \tag{2.48}$$

coupling the physical qudits connected by bond b. The ground state of this bond term is a maximally entangled state of dimension d between the two qudits.

We are interested in reproducing the quantum double Hamiltonian in an encoded form, so to concisely state our objective, we define the encoded A and B operators

$$\hat{A}(v) \equiv \frac{1}{|G|} \sum_g \bigotimes_{e \in +(v)} L_{\mathsf{L}}^g(e, v) \tag{2.49}$$

$$\hat{B}(p) \equiv \sum_{g_k \ldots g_1 = 0} \bigotimes_{e_i \in \square(p)} T_{\mathsf{L}}^{g_i}(e_i, p) \tag{2.50}$$

with L_{L} defined in Eq. (2.41) and $T_{\mathsf{L}} = \frac{1}{d} \sum_k \omega^k Z_{\mathsf{L}}^k$ is the encoded group projection operator. We can then state main result of this section as Theorem 2.

Theorem 2. *The Hamiltonian $H = H_0 + \lambda V$ with H_0 and V defined as in Eq. (2.46) and Eq. (2.47)*

on a square lattice has a low energy behaviour described by an effective Hamiltonian of the form

$$H_{\text{eff}} = c_I I - \left(c_A \lambda^4\right) \sum_v \hat{A}(v) - \left(c_B \lambda^4\right) \sum_p \hat{B}(p) + \mathcal{O}(\lambda^5) \tag{2.51}$$

for some constants c independent of λ and N, where N is the number of sites on the lattice.

The consequence of this theorem is our system's low energy effective Hamiltonian replicating the low-energy sector of the quantum double model (for cyclic groups at this stage).

Proof of Theorem 2.

We again follow the perturbative analysis described in Sec. 2.7. As such, this will require evaluating terms in the perturbative expansion of the self-energy at order n:

$$\Sigma^{(n)}(E_0) = \lambda^n \Upsilon V (G_0(E_0) V)^{(n-1)} \Upsilon \tag{2.52}$$

with G_0 the Green's function for the system (vanishing on ground states) and Υ is the projector to the mutual ground space of each of the code gadgets.

Before we begin our the proof in earnest, it is useful to comment on the kinds of terms which will be preserved and those that will vanish in the ground space. All the operators defined for cyclic groups have some commutation relation $MN = \alpha NM$ for some complex α. It is then a simple result to show that for our set of stabilizers any operator which does not commute with each stabilizer will neccessarily excite a ground state to an orthogonal state. This means that an operator M with $\alpha \neq 1$ for N any stabilizer will become a detectable error on the gadget's quantum code, and will take the gadget to an orthogonal subspace. This implies that it will vanish in our perturbative treatment, as terms arising in our effective Hamiltonian are restricted to the ground space. In this way we need only consider error-free terms (i.e. terms which commute with all stabilizers) in our effective Hamiltonian.

From this discussion, we immediately see that first order terms will vanish, as they will necessarily leave two code gadgets in excited states. The only non-vanishing second order terms will be proportional to identity. In contrast to the toric code as presented earlier, there will be non-vanishing third order terms due to the inclusion of an identity component in the perturbation term Eq. (2.47). However, these terms will be proportional to the second order terms, and so will be trivial. At 4^{th} order we find non-trivial vertex and plaquette terms which survive. To write each of these terms more explicitly, we must now distinguish between inwards directed vertices (v_+) and outward directed vertices (v_-) as well as the two kinds of plaquettes. We will label the plaquettes left (p_l) and right (p_r) depending on the orientation of the top edge. In this scheme, the effective Hamiltonian will take the form

$$H_{\text{eff}}^{(4)} = \text{const} - \sum_{k=0}^{d-1} \left[\sum_{v_+} H_{v_+}^k + \sum_{v_-} H_{v_-}^k + \sum_{p_l} H_{p_l}^k + \sum_{p_r} H_{p_r}^k \right] \tag{2.53}$$

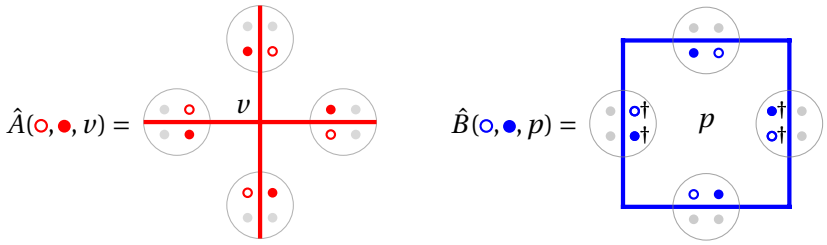

Figure 2.5 – Physical operators for a cyclic quantum double model. Qudits at locations denoted by open circles will be acted upon by the same single-qudit operator (and similarly for those represented by full circles). The adjoint (†) of a given operator is applied to the qudits so labelled. Note the similarity of this diagram with Figure 2.3, however in contrast to the toric code case, the operators acting on adjacent qubits are now different.

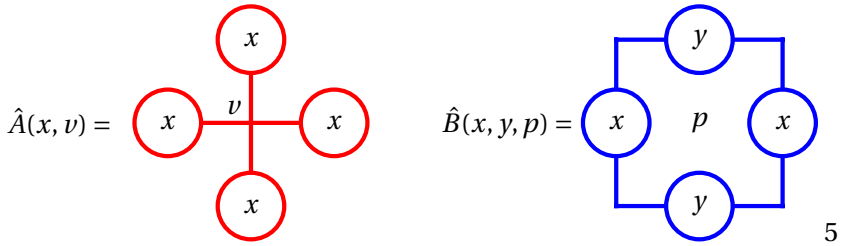

Figure 2.6 – Encoded operators for a cyclic quantum double model. Here each of x or y represents a 4-qudit logical or gauge operator. We use an overloaded notation here for $\hat{A}$ and $\hat{B}$ such that when their arguments are encoded 4-qudit operators they take this form, while if the arguments are single qudit operators, then they take the form of Fig. 2.5.

We can write each of these parts individually using the notation of Figure 2.5.

$$H^k_{v_+} = \kappa^L_v \lambda^4 \Upsilon \hat{A}(L^k, L^k, v)\Upsilon + \kappa^Z_v \lambda^4 \Upsilon \hat{A}(Z^k, Z^{-k}, v)\Upsilon \tag{2.54}$$

$$H^k_{v_-} = \kappa^L_v \lambda^4 \Upsilon \hat{A}(L^k, L^k, v)\Upsilon + \kappa^Z_v \lambda^4 \Upsilon \hat{A}(Z^k, Z^{-k}, v)\Upsilon \tag{2.55}$$

$$H^k_{p_l} = \kappa^L_p \lambda^4 \Upsilon \hat{B}(L^k, L^{-k}, p)\Upsilon + \kappa^Z_p \lambda^4 \Upsilon \hat{B}(Z^k, Z^k, p)\Upsilon \tag{2.56}$$

$$H^k_{p_r} = \kappa^L_p \lambda^4 \Upsilon \hat{B}(L^k, L^{-k}, p)\Upsilon + \kappa^Z_p \lambda^4 \Upsilon \hat{B}(Z^k, Z^k, p)\Upsilon \tag{2.57}$$

The κ are constants which take into account the sum of products of the Green's functions in the perturbation. They can be calculated for given d once the spectrum of H_0 has been found. They must be nonzero for each of these terms because they do not return to the ground state before the end of the perturbation, and so the Green's function will never vanish.

In terms of encoded logical, gauge and stabilizer operators, we can use a similar notation (as

seen in Fig. 2.6) to write these terms.

$$H^k_{v_+} = \kappa^L_v \lambda^4 \Upsilon \hat{A}(L^k_{\mathsf{L}} S^{-k}_L, v)\Upsilon + \kappa^Z_v \lambda^4 \Upsilon \hat{A}(Z^{-k}_{\mathsf{G}} S^{-k}_Z, v)\Upsilon \quad (2.58)$$

$$H^k_{v_-} = \kappa^L_v \lambda^4 \Upsilon \hat{A}(L^k_{\mathsf{L}}, v)\Upsilon + \kappa^Z_v \lambda^4 \Upsilon \hat{A}(Z^{-k}_{\mathsf{G}}, v)\Upsilon \quad (2.59)$$

$$H^k_{p_l} = \kappa^L_p \lambda^4 \Upsilon \hat{B}(L^k_{\mathsf{G}}, L^{-k}_{\mathsf{G}} S^{-k}_L, p)\Upsilon + \kappa^Z_p \lambda^4 \Upsilon \hat{B}(Z^{-k}_{\mathsf{L}} S^{-k}_Z, Z^k_{\mathsf{L}}, p)\Upsilon \quad (2.60)$$

$$H^k_{p_r} = \kappa^L_p \lambda^4 \Upsilon \hat{B}(L^k_{\mathsf{G}} S^k_L, L^{-k}_{\mathsf{G}}, p)\Upsilon + \kappa^Z_p \lambda^4 \Upsilon \hat{B}(Z^{-k}_{\mathsf{L}}, Z^k_{\mathsf{L}} S^k_Z, p)\Upsilon \quad (2.61)$$

We now evaluate the Υ projectors. Stabilizers S_Z and S_L act as identity on the ground space by Theorem 1, and each gauge operator will simply evaluate as a constant (expectation value) in the ground space. We can again disregard these constant terms as irrelevant energy shifts. This leaves us with:

$$H^k_{v_+} = \kappa^L_v \lambda^4 \Upsilon \hat{A}(L^k_{\mathsf{L}}, v)\Upsilon \quad (2.62)$$

$$H^k_{v_-} = \kappa^L_v \lambda^4 \Upsilon \hat{A}(L^k_{\mathsf{L}}, v)\Upsilon \quad (2.63)$$

$$H^k_{p_l} = \kappa^Z_p \lambda^4 \Upsilon \hat{B}(Z^{-k}_{\mathsf{L}}, Z^k_{\mathsf{L}}, p)\Upsilon \quad (2.64)$$

$$H^k_{p_r} = \kappa^Z_p \lambda^4 \Upsilon \hat{B}(Z^{-k}_{\mathsf{L}}, Z^k_{\mathsf{L}}, p)\Upsilon \quad (2.65)$$

By subsitituting the definitions of the Z operators in terms of T projectors, and using the orthogonality of the characters ω, it is simple to verify that these B terms are identical to the B terms of Eq. (2.29). Although the $\pm$ signs associated with the vertices (and edges in general) in these definitions may not immediately seem consistent with the quantum double Hamiltonian presented earlier (2.30) for cyclic groups, we have the freedom to rearrange the sums over k in the Hamiltonian. When we consider that we can take $k \to -k$ whenever we like, it becomes clear that these terms are indeed identical to those appearing in the quantum double Hamiltonian. This gives the result that the effective Hamiltonian will take the form Eq. (2.51). □

At all orders $< 2L$ (L the smallest linear dimension of the surface into which the model is embedded) the terms in the self-energy expansion (see Sec. 2.7) will act on the logical state like products of the 4^{th} order terms. These terms all commute and will not map the ground space of the quantum double model out of the +1 eigenspace of the encoded vertex and plaquette terms (2.62-2.65).

2.6 Our Construction for General Quantum Double Models

General quantum double models can have a much more complicated algebra than the simple cyclic ones studied previously (see Sec. 2.4). However, this class includes non-Abelian models which are able to perform universal quantum computation, and so they are of key interest in

this study.

2.6.1 Code Gadget Operators

As in the previously studied $\mathbb{Z}_d$ quantum double models, we encode each logical qudit in a code gadget consisting of four strongly coupled physical qudits (the scheme is again as in Fig. 2.2). For a given group G, the code gadget on each edge then has a $|G|$-fold degenerate ground space which we use as a logical qudit. The difference in this scheme is that the generalizations of the gauge operators and stabilizers will not commute in general, and so these degrees of freedom are not separable. This is contrary to the normal use of the terms "stabilizer" and "gauge", but we will abuse the terminology and continue to use these terms in analogy to their cyclic counterparts. The operators we define here directly generalise those used in the previous sections. The differences arise from the non-commutativity of the group multiplication operations and the fact that the irreducible representations of these general groups can be multidimensional (as opposed to the cyclic groups, which have 1-dimensional irreps). With this in mind, we can define logical and "gauge" operators on the code gadget as follows:

$$L^g_{\mathsf{L}+} \equiv \left(\begin{array}{c|c} L^g_+ & L^g_+ \\ I & I \end{array}\right), \qquad T^g_{\mathsf{L}+} \equiv \sum_{g_2 g_3 = g} \left(\begin{array}{c|c} I & T^{g_2}_+ \\ I & T^{g_3}_+ \end{array}\right),$$
$$L^g_{\mathsf{G}-} \equiv \left(\begin{array}{c|c} I & L^{\underline{g}} \\ I & L^g_+ \end{array}\right), \qquad T^g_{\mathsf{G}+} \equiv \sum_{g_1 g_2 = g} \left(\begin{array}{c|c} T^{\underline{g}_1} & T^{g_2}_+ \\ I & I \end{array}\right). \tag{2.66}$$

We can also define operators to describe the "stabilizer" degrees of freedom:

$$S^g_L \equiv \left(\begin{array}{c|c} L^{\underline{g}^{-1}} & L^{\underline{g}^{-1}} \\ L^{g^{-1}}_+ & L^{g^{-1}}_+ \end{array}\right), \qquad S_L \equiv \frac{1}{|G|}\sum_g S^g_L, \tag{2.67}$$
$$S^g_T \equiv \sum_{g_1 g_2 g_3 g_4 = g} \left(\begin{array}{c|c} T^{\underline{g}_1} & T^{g_2}_+ \\ T^{\underline{g}_4} & T^{g_3}_+ \end{array}\right), \qquad S_T \equiv S^1_T. \tag{2.68}$$

where here the identity group element is denoted 1. These operators are clearly defined in a very natural way with respect to the quantum double algebra. In these models, the only operators which we strictly require to stabilize (act identically within) the ground space of our edge qudits are the projectors S_L and S_T. Despite this, we will extend our notational abuse and continue to refer to S^g_L and S^g_T as "stabilizer operators".

The operators we have defined now constitute a minimum operator basis for the degrees of

freedom of our encoded qudit. We can also define addititonal operators:

$$L^g_{\mathsf{L}-} \equiv \left(\begin{array}{c|c} I & I \\ L^g_- & L^g_- \end{array}\right), \qquad T^g_{\mathsf{L}-} \equiv \sum_{g_4 g_1 = g} \left(\begin{array}{c|c} T^{g_1}_- & I \\ T^{g_4}_- & I \end{array}\right),$$
$$L^g_{\mathsf{G}+} \equiv \left(\begin{array}{c|c} L^g_- & I \\ L^g_+ & I \end{array}\right), \qquad T^g_{\mathsf{G}-} \equiv \sum_{g_3 g_4 = g} \left(\begin{array}{c|c} I & I \\ T^{g_4}_- & T^{g_3}_+ \end{array}\right). \tag{2.69}$$

The + and − subscripts on the joint operators here refer to whether these operators obey the algebra of left or right multiplication (or projection) operators, i.e.

$$L^g_\pm T^h_\pm = T^{gh}_\pm L^g_\pm \tag{2.70}$$
$$L^g_\pm T^h_\mp = T^{hg^{-1}}_\mp L^g_\pm \tag{2.71}$$

The stabilizer operators themselves satisfy the quantum double algebra

$$S^g_L S^h_T = S^{g^{-1}hg}_T S^g_L \tag{2.72}$$

The logical operators commute with both the gauge and stabilizer operators, but in this scheme the gauge and stabilizer operators do not commute with each other.

We can also derive the Z operators corresponding to our T operators (see Sec. 2.4):

$$Z^{\pi_{ij}}_{\mathsf{L}+} = \sum_m \left(\begin{array}{c|c} I & Z^{\pi_{im}}_+ \\ I & Z^{\pi_{mj}}_+ \end{array}\right), \qquad Z^{\pi_{ij}}_{\mathsf{G}+} = \sum_m \left(\begin{array}{c|c} Z^{\pi_{im}}_- & Z^{\pi_{mj}}_+ \\ I & I \end{array}\right)$$
$$Z^{\pi_{ij}}_{\mathsf{L}-} = \sum_m \left(\begin{array}{c|c} Z^{\pi_{mj}}_- & I \\ Z^{\pi_{im}}_- & I \end{array}\right), \qquad Z^{\pi_{ij}}_{\mathsf{G}-} = \sum_m \left(\begin{array}{c|c} I & I \\ Z^{\pi_{mj}}_- & Z^{\pi_{im}}_+ \end{array}\right). \tag{2.73}$$

By construction, the sets of operators $\{Z^{\pi_{ij}}_{\mathsf{L}\pm}\}$ and $\{Z^{\pi_{ij}}_{\mathsf{G}\pm}\}$ give independent representations of the $Z^{\pi_{mj}}_\pm$.

We have now defined operators on the code gadget corresponding to both the left regular representation and the right regular representation of the group G for the encoded gauge and logical qudits. These definitions are redundant, in that the gauge or logical state can be uniquely defined through the action of only one L operator and only one T operator (or equivalently Z operator). This gives us some freedom in the definition of the logical state. We will choose to define it through the action of $L^g_{\mathsf{L}-}$ and $T^g_{\mathsf{L}+}$. The action of $L^g_{\mathsf{L}+}$ and $T^g_{\mathsf{L}-}$ will then be poorly defined in general with respect to the logical state, but we will choose the codespace such that they act appropriately within it.

In order to understand how these operators act on the logical state, it is useful at this point to explicitly identify the encoding scheme of our code gadget. We can label the state of each physical qudit within a given code gadget as follows:

$$|h_a, h_b, k_\mathsf{G}, k_\mathsf{L}\rangle = \left(\begin{array}{c|c} |h_a\rangle & |k_\mathsf{G} h_a\rangle \\ \left|h_b^{-1} h_a^{-1} k_\mathsf{L}\right\rangle & \left|h_a^{-1} k_\mathsf{G}^{-1} k_\mathsf{L}\right\rangle \end{array} \right) \tag{2.74}$$

Here the logical and gauge states of the system are labelled by k_L and k_G respectively, and will transform under the action of the logical or gauge operators. The remaining labels h define how the stabilizers S_L and S_G act on the system. We can directly see the action of our encoded operators on these states. For example,

$$L^g_{\mathsf{L}-}|h_a, h_b, k_\mathsf{G}, k_\mathsf{L}\rangle = |h_a, h_b, k_\mathsf{G}, k_\mathsf{L} g^{-1}\rangle \tag{2.75}$$

$$T^g_{\mathsf{L}+}|h_a, h_b, k_\mathsf{G}, k_\mathsf{L}\rangle = \delta_{g k_\mathsf{L}}|h_a, h_b, k_\mathsf{G}, k_\mathsf{L}\rangle. \tag{2.76}$$

We chose to define the logical state k_L by the action of these two operators, and as such they act on k_L as might be expected. The stabilizer operators act as

$$S^g_L|h_a, h_b, k_\mathsf{G}, k_\mathsf{L}\rangle = \left|h_a g, g^{-1} h_b g, k_\mathsf{G}, k_\mathsf{L}\right\rangle \tag{2.77}$$

$$S^g_T|h_a, h_b, k_\mathsf{G}, k_\mathsf{L}\rangle = \delta_{g h_b}|h_a, h_b, k_\mathsf{G}, k_\mathsf{L}\rangle\,. \tag{2.78}$$

The action of the remaining encoded operators is not so simple. In general, these will mix the logical or gauge states with the h_a or h_b. However, we will construct the codespace such that within it, logical operators will act only on the logical state, and gauge operators similarly act appropriately.

2.6.2 Code Gadget Hamiltonian

Now that we have defined a set of operators we consider the Hamiltonian of a code gadget. We require that this Hamiltonian consist only of 2-body terms and possess a ground space which can be used as a codespace for our logical qudit. For this to happen, the ground space must be stabilized by S_L and S_T, and be exactly $|G|$-fold degenerate. The significance of these two stabilizers is that they are terms in the quantum double Hamiltonian defined on a small 4-qudit torus (as depicted in Fig. 2.7). In that sense, we are creating a code which is very similar to a miniature quantum double model. Of course, our code gadget will consist of only two-body terms, and to achieve this we must sacrifice the gauge degrees of freedom in our model.

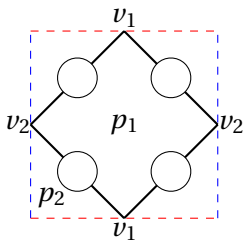

Figure 2.7 – The 4-qudit torus is constructed by identifying the opposite vertices of a square. The dashed horizontal (red) lines are identified, and the dashed vertical (blue) lines are identified. There are two equivalent plaquette stabilizers corresponding to p_1 and p_2 and two (generally inequivalent) vertex stabilizers corresponding to v_1 and v_2 in this quantum double model. Our stabilizers S_L and S_T are obtained by choosing one of each. For Abelian models the two vertex stabilizers are also equivalent, and so S_L and S_T generate the full stabilizer group of the quantum double model on this surface for those groups.

To this end, we generalize the Hamiltonian we used for cyclic groups previously to give

$$H(e) = -\frac{J_L}{|G|}\sum_g \left[L^g_{\mathsf{G}+} + L^g_{\mathsf{G}-}\right] - \frac{J_Z}{|G|}\sum_{\pi,i} d_\pi \left[Z^{\pi_{ii}}_{\mathsf{G}+} + Z^{\pi_{ii}}_{\mathsf{G}-}\right] \tag{2.79}$$

$$= -\frac{J_L}{|G|}\sum_g \left[L^g_{\mathsf{G}+} + L^g_{\mathsf{G}-}\right] - J_Z\left[T^1_{\mathsf{G}+} + T^1_{\mathsf{G}-}\right] \tag{2.80}$$

These two forms can be seen to be equivalent using the definitions of the Z_{G} operators (Eq. (2.73)). In the latter form, it is clear that our unperturbed Hamiltonian is very closely related to the quantum double Hamiltonian (Eq. (2.30)). It is also clear that the logical operators will commute with the Hamiltonian (as each term is a gauge operator), and so we can expect at least the $|G|$-fold degeneracy of our logical qubit. The following theorem encapsulates the remaining requirements of our codespace.

Theorem 3. *The Hamiltonian Eq. (2.79) has a $|G|$-fold degenerate ground space that is in the common $+1$ eigenspace of S_L and S_T.*

We provide a proof of this theorem in Sec. 2.10. This theorem places restrictions on the form of the ground space which ensure that undesirable terms in the effective Hamiltonian will couple to higher energy sectors and vanish. Now we have a suitable codespace for our logical qudit, we proceed to reproducing the target model.

2.6.3 Coupling the Code Gadgets

We place our code gadgets on the edges of the lattice and couple them using the same geometric scheme as the toric code and cyclic group cases (illustrated in Fig. 2.2), where each physical qudit is perturbatively coupled to a physical qudit from a neighbouring code gadget.

Our uncoupled (unperturbed) Hamiltonian for each edge of the lattice is as given in Eq. (2.79).

$$H_0 = \sum_e H(e) \tag{2.81}$$

$$= \sum_e \left[-\frac{J_L}{|G|} \sum_g [L^g_{\mathsf{G}+} + L^g_{\mathsf{G}-}] - \frac{J_Z}{|G|} \sum_{\pi,i} d_\pi \left[Z^{\pi_{ii}}_{\mathsf{G}+} + Z^{\pi_{ii}}_{\mathsf{G}-} \right] \right]_e \tag{2.82}$$

As before, the subscript e refers to a particular edge (a particular code gadget). The perturbation term is generalized straightforwardly from the cyclic case to take the form:

$$V = \sum_b V(b) \tag{2.83}$$

$$= -\sum_b \left[\sum_k L^k \overset{b}{\sim\sim} L^k + \sum_{\pi,k,m} d_\pi \; Z^{\pi_{km}} \overset{b}{\sim\sim} Z^{\pi_{mk}} \right] \tag{2.84}$$

where the L or Z operator associated with a particular qudit has definite $\pm$ subscript depending on its location as follows

L: $\begin{pmatrix} + & + \\ - & - \end{pmatrix}$ $\qquad\qquad$ Z: $\begin{pmatrix} - & + \\ - & + \end{pmatrix}$

e.g. an L operator in the top right hand corner of a code gadget (with the edge taken running up the page) will take the form L_+. This is motivated by the definitions of $v_\pm$ and $p_\pm$ of the quantum double model in Sec. 2.4. As in the $\mathbb{Z}_d$ models, it is clear that the coupling terms are very closely related to the quantum double Hamiltonian. In fact, these bond terms could be considered a quantum double Hamiltonian on a small (2-qudit) sphere, with the corresponding non-degenerate ground state (see Fig. 2.8).

Again we must define the encoded A and B operators we will reproduce in our perturbative expansion (with 1 the identity group element for general groups)

$$\hat{A}(v) \equiv \frac{1}{|G|} \sum_g \bigotimes_{e \in +(v)} L^g_{\mathsf{L}}(e, v) \tag{2.85}$$

$$\hat{B}(p) \equiv \sum_{g_k \ldots g_1 = 1} \bigotimes_{e_i \in \square(p)} T^{g_i}_{\mathsf{L}}(e_i, p) \tag{2.86}$$

The main result of this section is Theorem 4.

Theorem 4. *The Hamiltonian $H = H_0 + \lambda V$ with H_0 and V defined as in Eq. (2.81) and Eq. (2.83) on a square lattice has a low energy behaviour described by an effective Hamiltonian of the form*

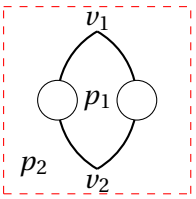

Figure 2.8 – The 2-qudit sphere is constructed by identifying every point on the boundary of a plane. This boundary is represented by dashed red lines. The solid lines correspond to edges on the lattice, with a qudit located on each edge. The loop formed by these edges is homologically equivalent to an equator around the sphere. There exists a plaquette stabilizer for each plaquette p_1 and p_2 and similarly a vertex stabilizer for each vertex v_1 and v_2 in this quantum double model. The terms in our bond Hamiltonian are obtained by choosing one plaquette and one vertex stabilizer from these. For Abelian models the two vertex stabilizers are also equivalent, as are the two plaquette stabilizers, and so the bond Hamiltonian consists of a full generating set of the stabilizer group of the quantum double model on this surface for these groups.

$$H_{\text{eff}} = c_I I - \left(c_A \lambda^4\right) \sum_v \hat{A}(v) - \left(c_B \lambda^4\right) \sum_p \hat{B}(p) + \mathcal{O}(\lambda^5) \tag{2.87}$$

for constants c independent of λ and N, where N is the number of sites on the lattice. The encoded low energy behavior of the system to this order is described by the quantum double Hamiltonian Eq. (2.30) up to additive and multiplicative constants.

This theorem implies that our effective Hamiltonian correctly reproduces the low energy sector of the quantum double Hamiltonian for any group. Before we prove it, we make some comment on the operators that will arise in the perturbative treatment. For cyclic models, we were able to make some general arguments to exclude all unwanted operators from arising in the effective Hamiltonian. Unfortunately, no equivalent general argument has been found for the general quantum double models. For this reason, we have explicitly shown this property for the relevant operators in Sec. 2.11. The results are an intuitive generalization of the cyclic case, in that the only non-vanishing operators will be those contributing encoded operators which act on the gauge or logical subspaces. We use these results now to calculate the non-vanishing terms in the effective Hamiltonian.

Proof of Theorem 4.

We follow the perturbative treatment as used previously (see Sec. 2.7). The results of Sec. 2.11 effectively show that no 2^{nd} order terms are able to survive except those proportional to identity (exactly as in the cyclic case). Similarly, all first order terms, and all non-trivial third order terms will vanish. It is clear then, that no non-trivial operators will appear below 4th order. The effective Hamiltonian at order 4 is given in Eq. (2.13).

At this order we will find non-trivial terms around plaquettes and vertices consisting of products of Z or L operators. As in the $\mathbb{Z}_d$ case, it is useful to distinguish the two different kinds of vertices and the two different kinds of plaquettes here (see Fig. 2.4). We have defined the lattice such that vertices can either consist of all inwardly directed edges (v_+) or all outwardly directed edges (v_-). Plaquettes can either have their top edge directed left (p_l) or right (p_r).

Disregarding constant energy shifts, we can then separate terms in the Hamiltonian by vertex or plaquette type:

$$H_{\text{eff}}^{(4)} = -\Upsilon\left[\sum_{v_+} H_{v_+} + \sum_{v_-} H_{v_-} + \sum_{p_l} H_{p_l} + \sum_{p_r} H_{p_r}\right]\Upsilon \tag{2.88}$$

As we did for the cyclic groups, we will write these operators pictorially to make the physical location of a particular operator obvious. For simplicity, we have neglected to draw those qudits on the outer edge of the vertex/plaquette under consideration, where these terms will act trivially. With this in mind, the individual terms in the effective Hamiltonian can be written as:

$$H_{v_+} = \kappa_v^L \lambda^4 \sum_g$$

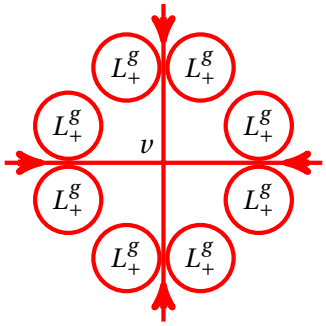

$$+\kappa_v^Z \lambda^4 \sum_{\pi,i,r,m,n} d_\pi^4 \sum_j$$

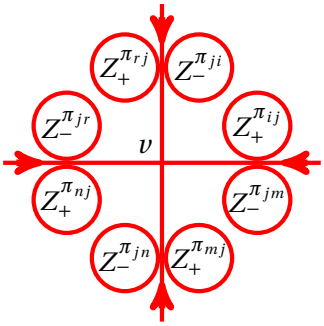

(2.89)

$$H_{v_-} = \kappa_v^L \lambda^4 \sum_g$$

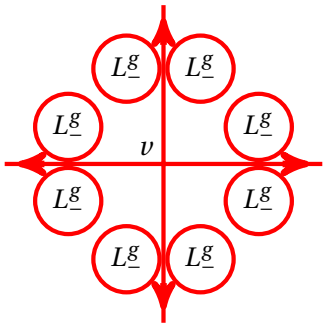

$$+\kappa_v^Z \lambda^4 \sum_{\pi,i,r,m,n} d_\pi^4 \sum_j$$

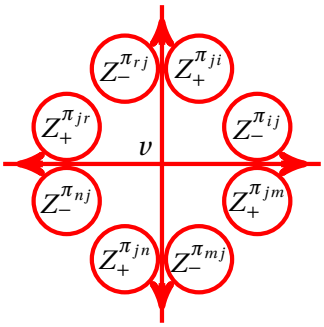

(2.90)

$$H_{p_l} = \kappa_p^L \lambda^4 \sum_g$$

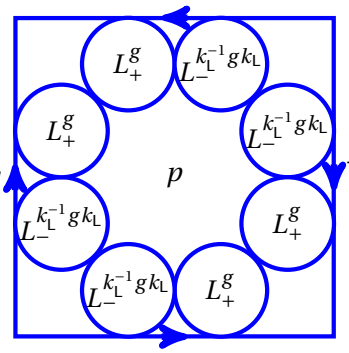

$$+\kappa_p^Z \lambda^4 \sum_{\pi,i,r,m,n} d_\pi^4 \sum_j$$

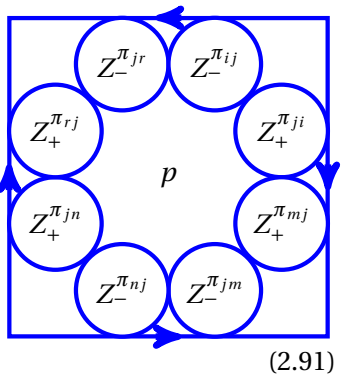

(2.91)

$$H_{p_r} = \kappa_p^L \lambda^4 \sum_g$$

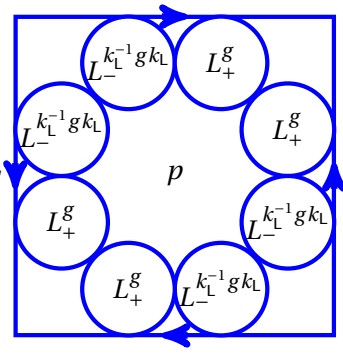

$$+\kappa_p^Z \lambda^4 \sum_{\pi,i,r,m,n} d_\pi^4 \sum_j$$

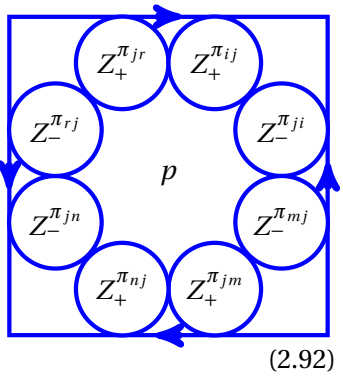

(2.92)

Here the κ's are proportionality constants arising from the pertubation treatment. For a specific model, they can readily be calculated. It should be reasonably clear that no other non-trivial 4^{th} order terms (or lower) than those shown above will survive (see Sec. 2.11). The higher order terms will act in the logical space as products of the 4^{th} order terms, until the order is sufficiently high to form non-contractible loops over the lattice.

The most illustrative of the 4^{th} order terms are the plaquette Z terms. As such, we will present a brief demonstration of how these operators arise. On our plaquette, at 4th order the most general Z operator to be constructed has the form:

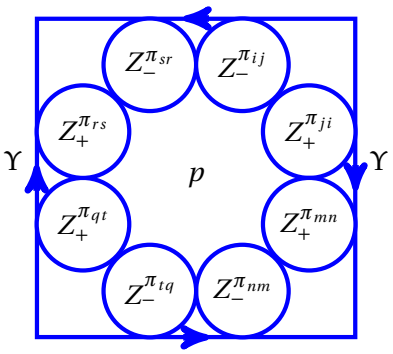

Here we have already used the fact that Z operators with different representations will move out of the ground space, and so we have only used one representation π. It will be shown in Sec. 2.11, Eq. (2.184, 2.186) that we find the condition $j = s = n = q$ for non-vanishing terms. From this, we immediately obtain the term appearing above in the effective Hamiltonian for this plaquette. Similar considerations give the other plaquette and vertex terms.

Given the operators (2.89-2.92) in their current form, it is difficult to immediately see how many of them act on the logical state. In order to study this, we must revisit the encoding scheme defined in Eq. (2.74) and the ground space studied in Sec. 2.10. We will study the action of each operator on the basis

$$|\sigma_{mn}, h, k_{\mathsf{G}}, k_{\mathsf{L}}\rangle \equiv \frac{\sqrt{d_\sigma}}{\sqrt{|G|}} \sum_{g_\sigma \in G} [\sigma(g_\sigma)]_{mn} |g_\sigma, g_\sigma^{-1} h g_\sigma, k_{\mathsf{G}}, k_{\mathsf{L}}\rangle \tag{2.93}$$

particularly in the ground space where $\sigma_{mn} = I_{11}$ and $h = 1$. This basis is introduced in Sec. 2.10.1 as the "gauge element basis". From this we can examine the effect on the logical state k_{L} in the codespace. The operators in question act on these states as follows

$$\left(\begin{array}{c|c} L^g_+ & I \\ L^{k_{\mathsf{L}}^{-1} g k_{\mathsf{L}}}_- & I \end{array}\right) |I_{11}, 1, k_{\mathsf{G}}, k_{\mathsf{L}}\rangle = \frac{1}{\sqrt{|G|}} \sum_{g_\sigma} |g g_\sigma, 1, k_{\mathsf{G}} g^{-1}, k_{\mathsf{L}}\rangle \tag{2.94}$$

$$= \frac{1}{\sqrt{|G|}} \sum_{\tilde{g}_\sigma} |\tilde{g}_\sigma, 1, k_{\mathsf{G}} g^{-1}, k_{\mathsf{L}}\rangle \tag{2.95}$$

$$= |I_{11}, 1, k_{\mathsf{G}} g^{-1}, k_{\mathsf{L}}\rangle \tag{2.96}$$

and

$$\left(\begin{array}{c|c} I & L^g_+ \\ I & L^{k_{\mathsf{L}}^{-1} g k_{\mathsf{L}}}_- \end{array}\right) |I_{11}, 1, k_{\mathsf{G}}, k_{\mathsf{L}}\rangle = \frac{1}{\sqrt{|G|}} \sum_{g_\sigma} |g_\sigma, 1, g k_{\mathsf{G}}, k_{\mathsf{L}}\rangle \tag{2.97}$$

$$= |I_{11}, 1, g k_{\mathsf{G}}, k_{\mathsf{L}}\rangle \tag{2.98}$$

In the codespace, these operators have the effective action equivalent to $L^g_{\mathsf{G}-}$ or $L^g_{\mathsf{G}+}$ respectively. They differ from the previously defined versions, but the key is that they act only on the gauge state in this subspace. We will denote these operators $L^g_{\mathsf{G}'-}$ and $L^g_{\mathsf{G}'+}$. In a similar way, we can look at the action of the Z-like operators:

$$\sum_m \left(\begin{array}{c|c} Z^{\pi_{mj}}_- & Z^{\pi_{im}}_+ \\ I & I \end{array}\right) |I_{11}, 1, k_{\mathsf{G}}, k_{\mathsf{L}}\rangle = [\pi(k_{\mathsf{G}})]_{ij} |I_{11}, 1, k_{\mathsf{G}}, k_{\mathsf{L}}\rangle \tag{2.99}$$

This operator acts quite similarly (identical up to conjugacy) to $Z_{\mathsf{G}+}^{\pi_{ij}}$. In the ground space, we will be able to ignore it as a constant expectation value (as the gauge state will be fixed). As such, we will denote this operator $Z_{\mathsf{G}'+}^{\pi_{ij}}$. The second of the Z operators is a little more complicated. To this end, we must consider the exact form of the ground states:

$$|\psi_0\rangle = |I_{11}, 1, 1, k_{\mathsf{L}}\rangle + |I_{11}, 1, I_{11}, k_{\mathsf{L}}\rangle \tag{2.100}$$

This allows us to see the action of these operators.

$$\sum_m \left(\begin{array}{c|c} I & I \\ Z_-^{\pi_{im}} & Z_+^{\pi_{mj}} \end{array} \right) |I_{11}, 1, 1, k_{\mathsf{L}}\rangle = [\pi(k_{\mathsf{L}}^{-1} k_{\mathsf{L}})]_{ij} |I_{11}, 1, 1, k_{\mathsf{L}}\rangle \tag{2.101}$$

$$= \delta_{ij} |I_{11}, 1, 1, k_{\mathsf{L}}\rangle \tag{2.102}$$

$$\sum_m \left(\begin{array}{c|c} I & I \\ Z_-^{\pi_{im}} & Z_+^{\pi_{mj}} \end{array} \right) |I_{11}, 1, I_{11}, k_{\mathsf{L}}\rangle = \frac{1}{\sqrt{|G|}} \sum_{g_\pi} [\pi(k_{\mathsf{L}}^{-1} g_\pi^{-1} k_{\mathsf{L}})]_{ij} |I_{11}, 1, g_\pi, k_{\mathsf{L}}\rangle \tag{2.103}$$

On the ground space, this acts not dissimilarly to $Z_{\mathsf{G}-}^{\pi_{ij}}$. The gauge state becomes mixed up somewhat, but because of the particular definite gauge state we have in the code space, an operator of this form can be evaluated as a constant. This is a result of the fact that the overlap of this state (Eq. (2.103)) with the ground space is independent of k_{L} (as can be easily verified). With this in mind, we will write this operator as $Z_{\mathsf{G}'-}^{\pi_{ij}}$ from now on.

Given these definitions, we can now write the terms in the effective Hamiltonian in a more succinct format:

$$H_{v_+} = \kappa_v^L \lambda^4 \sum_g \; L_{\mathsf{L}+}^g \; L_{\mathsf{L}+}^g \; L_{\mathsf{L}+}^g \; L_{\mathsf{L}+}^g \; v + \kappa_v^Z \lambda^4 \sum_{\pi,i,r,m,n} d_\pi \; Z_{\mathsf{G}'+}^{\pi_{ri}} \; Z_{\mathsf{G}'+}^{\pi_{nr}} \; Z_{\mathsf{G}'+}^{\pi_{im}} \; Z_{\mathsf{G}'+}^{\pi_{mn}} \; v \tag{2.104}$$

$$H_{v_-} = \kappa_v^L \lambda^4 \sum_g \; L_{\mathsf{L}-}^g \; L_{\mathsf{L}-}^g \; L_{\mathsf{L}-}^g \; L_{\mathsf{L}-}^g \; v + \kappa_v^Z \lambda^4 \sum_{\pi,i,r,m,n} d_\pi \; Z_{\mathsf{G}'-}^{\pi_{ri}} \; Z_{\mathsf{G}'-}^{\pi_{nr}} \; Z_{\mathsf{G}'-}^{\pi_{im}} \; Z_{\mathsf{G}'-}^{\pi_{mn}} \; v \tag{2.105}$$

$$H_{p_l} = \kappa_p^L \lambda^4 \sum_g$$ 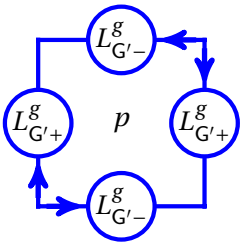 $$+ \kappa_p^Z \lambda^4 \sum_{\pi,i,r,m,n} d_\pi$$ 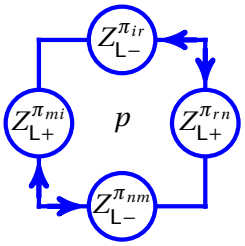 (2.106)

$$H_{p_r} = \kappa_p^L \lambda^4 \sum_g$$ 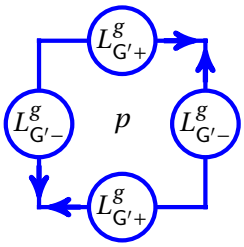 $$+ \kappa_p^Z \lambda^4 \sum_{\pi,i,r,m,n} d_\pi$$ 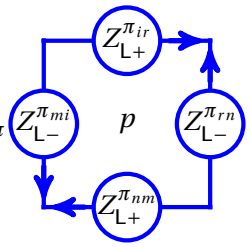 (2.107)

We have been able to treat each code gadget in the Z terms separately, even though in the previous definitions they shared a common index (j). The reason that we are able to separate them in this way is because in the ground space for any given j we can use Eq. (2.184 - 2.190) to rewrite each term as an average over all values of j. This allows us to rewrite each term as a summation over different indices, which gives us their quoted form. The factor of d_π appearing in the terms (2.104-2.107) then comes from the remaining sum over j. As a simplified explicit example, consider:

$$\Upsilon \sum_j \left(\begin{array}{c|c} Z_-^{\pi_{jm}} & Z_+^{\pi_{ij}} \\ I & I \end{array} \right) \otimes \left(\begin{array}{c|c} Z_-^{\pi_{jp}} & Z_+^{\pi_{mj}} \\ I & I \end{array} \right) \Upsilon = \Upsilon \sum_j \sum_{j'} \frac{1}{d_\pi} \left(\begin{array}{c|c} Z_-^{\pi_{j'm}} & Z_+^{\pi_{ij'}} \\ I & I \end{array} \right) \otimes \left(\begin{array}{c|c} Z_-^{\pi_{jp}} & Z_+^{\pi_{mj}} \\ I & I \end{array} \right) \Upsilon \tag{2.108}$$

We can disregard all the terms in the Hamiltonian which do not act on the logical subspace (as they will only introduce some constant energy shift for our purposes). We now also drop the $\pm$ subscript on logical operators, with the observation that they are consistent with the edge orientation conventions introduced in Sec. 2.4. With this in mind, our effective Hamiltonian reduces to:

$$H_{\text{eff}} = -\lambda^4 \Upsilon \Bigg[\sum_v \kappa_v^L \sum_g$$ 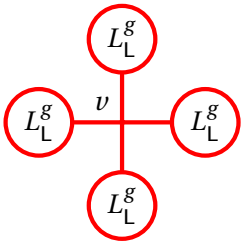 $$+ \sum_p \kappa_p^Z \sum_{\pi,i,r,m,n} d_\pi$$ 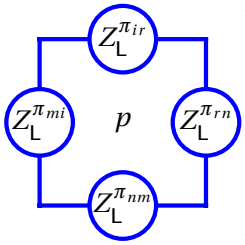 $$\Bigg] \Upsilon$$ (2.109)

with each operator defined as in Eq. (2.104 - 2.107), and the ± of the logical operators defined by the edge orientation. Using the definitions of the Z operators in terms of T operators, and the orthogonality of group characters, it is not difficult to show that these operators are indeed equivalent to those of the target quantum double Hamiltonian. This gives our Hamiltonian the form Eq. (2.87) as claimed. □

Additionally, the low energy effective Hamiltonian is gapped to arbitrary order of perturbation theory, and the degeneracy of the ground space is lifted only at the order of the linear lattice size.

As in the Abelian case, to all orders $< 2L$ (L the smallest linear dimension of the surface into which the model is embedded), the terms in the self-energy expansion (see Sec. 2.7) will act on the logical space like products of the 4^{th} order terms. These terms all commute and will not map the ground space of the quantum double model out of the +1 eigenspace of the encoded vertex and plaquette terms (2.62-2.65). As such, they will preserve the gap of the effective Hamiltonian. Beyond this order perturbative corrections to the self-energy will be able to form homologically non-trivial loops on the surface. These will act to lift the degeneracy of the ground space, though this splitting will be exponentially suppressed in L.

2.7 Perturbation Theory

We will now give a brief introduction to the formalism we will use to perform perturbation calculations, such as to introduce lattice couplings between edge qudits. We follow the resolvent or Green's function approach in [Kit06] and in general we are only interested in the leading non-constant order in the effective Hamiltonian. Consider the Hamiltonian

$$H = H_0 + \lambda V \tag{2.110}$$

where H_0 has a subspace of degenerate eigenvectors with energy E_0. Let Υ be the projector onto the eigenspace of the eigenvalue E_0 of H_0. In our case we are interested in the situation where E_0 is the ground state energy of H_0. In degenerate perturbation theory one generally aims to find an effective Hamiltonian H_{eff} that acts on the subspace given by Υ and that has the same eigenvalues as H, in other words, an effective Hamiltonian that describes how the perturbation term V acts within the ground space of the unperturbed Hamiltonian. We use the Green's function formalism of [Kit06] for this calculation and find the self-energy $\Sigma(E)$ which is given by the perturbation expansion:

$$\Sigma(E_0) = \sum_n \Sigma^{(n)}(E_0) \tag{2.111}$$

$$\Sigma^{(n)}(E_0) = \lambda^n \Upsilon V (G_0(E_0)V)^{(n-1)} \Upsilon \tag{2.112}$$

To the lowest non-trivial order of perturbation theory we have

$$H_{\text{eff}} \simeq E_0 + \Sigma(E_0) \tag{2.113}$$

The unperturbed Green's function for excited states of H_0 is denoted by $G_0(E) = (E - H_0)^{-1}(1 - \Upsilon)$, such that this function vanishes in the ground space. At higher orders in perturbation theory, one would need to take into account the E dependence of the self-energy around $E \approx E_0$ in order to find the effective Hamiltonian; however, as we are interested only in the lowest non-trivial order in perturbation theory throughout this paper, we do not. As such, the Green's function G_0 will always be evaluated at the unperturbed ground state energy E_0, and will be non-positive.

The product of operators obtained between between Υ's will vanish unless it remains within (or at least overlaps in some nontrivial way) the ground space of every code gadget on the lattice. It will be simple to eliminate many operators which will vanish or act trivially on the ground space. At n^{th} order, the self-energy will consist of a sum of terms

$$\Sigma^{(n)}(E_0) = \sum_j \lambda^n \Upsilon \kappa_j A_j \Upsilon \tag{2.114}$$

with κ_j constants. They take into account the Green's function terms appearing in the perturbative analysis. Summed over each possible ordering of the V terms which will give the same A_j, κ_j is the product of the $(n-1)$ Green's functions appearing in the n^{th} order terms. In our case, this sum will run over the $n!$ ways of ordering the perturbations which multiply together to give the operator A_j.

2.8 Extension to Arbitrary Graph

It is not difficult to extend our treatment from the explicit square lattice to an arbitrary directed graph. As each edge is associated with two plaquettes on any nonintersecting 2D graph (neglecting boundaries), each edge qudit is associated with exactly 4 nearest neighbours regardless of the form of the lattice. This allows us to retain our previous definitions for edge qubit gauge and logical operators as in Sec. 2.6.1.

If we apply a perturbation to the uncoupled edge qudits exactly as before, we will again see plaquette and vertex terms arising in the effective Hamiltonian. Of course, they may not arise at the same order in this treatment (e.g. for a hexagonal lattice plaquettes arise at 6^{th} and vertices arise at 3^{rd} order, and on a general graph plaquette boundaries and vertex stars will not be uniform in size). It is possible that this may have some undesirable effect on excited states of the effective Hamiltonian, but the higher order terms that will be able to survive the perturbation will act in the logical space as products of existing (commuting) terms until the perturbative order is high enough to form non-trivial homology cycles over the lattice. Below this order, the ground space of the effective Hamiltonian will remain within the ground space

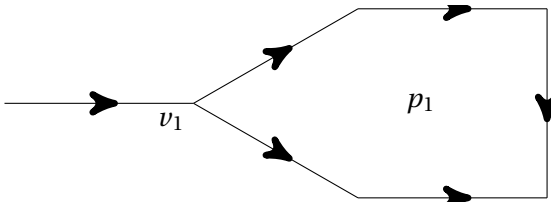

Figure 2.9 – A section of a simple directed graph

of the encoded quantum double Hamiltonian.

We can see in Fig. 2.9 part of a simple directed graph. If we consider the perturbation term exactly as in the general group square lattice treatment (Eq. (2.83)), the vertex term will take the form (up to additive and multiplicative constants)

$$H(v) \sim \Upsilon \sum_g \prod_{e\to v} L^g_{\mathsf{L}+} \prod_{e\leftarrow v} L^g_{\mathsf{L}-} \Upsilon + \Upsilon \sum \prod_{e\to v} Z_{\mathsf{G}'+} \prod_{e\leftarrow v} Z_{\mathsf{G}'-} \Upsilon \tag{2.115}$$

where $e \leftarrow v$ denotes those edges which run out of the vertex v, and $e \rightarrow v$ denotes those that run towards the vertex. The exact form of the Z term is not difficult to calculate but is only sketched in this notation for clarity. In any case, the vertex Z term will evaluate as a constant in the ground space and so can be disregarded for our purposes. This leaves the products of terms for inwards directed edges and outwards directed edges. If we look back to the definitions of the quantum double model in Sec. 2.4, we can see that this will give a vertex term consistent with the target Hamiltonian.

Similarly, as we traverse a plaquette, two kinds of terms will arise,

$$H(v) \sim \Upsilon \sum_g \prod_{e\to p} L^g_{\mathsf{G}-} \prod_{e\leftarrow p} L^g_{\mathsf{G}+} \Upsilon + \Upsilon \sum \prod_{e\to v} Z_{\mathsf{L}+} \prod_{e\leftarrow v} Z_{\mathsf{L}-} \Upsilon \tag{2.116}$$

Here the notation $e \rightarrow p$ is taken to mean the edge is on the left of the plaquette, when looking along e, and similarly $e \leftarrow p$ has the edge on the right of p. The indices of the Z terms are here suppressed for clarity, but they can easily be restored by comparing with Eq. (2.109), and can be verified to be consistent with the quantum double Hamiltonian. Of course, the gauge L term will be evaluated as a constant and disregarded. This will leave us only with the desired logical operators on both plaquettes and vertices, and we will have successfully reproduced the quantum double Hamiltonian (with the caveat that the terms may arise at different order, and with different coefficients).

2.9 Proof of Theorem 1

Proof. We will label eigenstates of Z by group elements $|h\rangle$, and the corresponding eigenstates of L by (unitary, irreducible) representations $|\sigma\rangle = \frac{1}{\sqrt{d}} \sum_h \omega^{\sigma h} |h\rangle$. Note that for these cyclic

groups, the representations are all one dimensional. We begin by defining projectors

$$P_i^k = \frac{1}{d}\sum_l \omega^{kl} S_i^l, \tag{2.117}$$

with inverses

$$S_i^k = \sum_l \omega^{-kl} P_i^l. \tag{2.118}$$

where $i \in \{L, Z\}$. We can then write our Hamiltonian as

$$H(e) = -\frac{1}{d}\sum_k \left[L_{\mathsf{G}}^k \left(1 + \sum_h \omega^{-kh} P_L^h\right) + Z_{\mathsf{G}}^k \left(1 + \sum_\sigma \omega^{-k\sigma} P_Z^\sigma\right)\right]. \tag{2.119}$$

If we block diagonalize with respect to both h and σ, our proof will amount to showing that the unique ground state is in the $h = 0$ and $\sigma = 0$ block. In group theoretic terms, this corresponds to h the identity group element and σ the trivial representation (which we will denote now as $\sigma = I$). Our Hamiltonian within the (h, σ) block takes the form (suppressing the (e) argument)

$$H^{h,\sigma} = -\frac{1}{d}\sum_k \left[L_{\mathsf{G}}^k (1 + \omega^{-kh}) + Z_{\mathsf{G}}^k (1 + \omega^{-k\sigma})\right]. \tag{2.120}$$

We can rewrite the $\sum_k L_{\mathsf{G}}^k$ and $\sum_k Z_{\mathsf{G}}^k$ operators as projectors on the gauge subspace onto group elements or representations:

$$\sum_k \omega^{-kh} L_{\mathsf{G}}^k = d|h\rangle\langle h| \quad \text{and} \quad \sum_k \omega^{-k\sigma} Z_{\mathsf{G}}^k = d|\sigma\rangle\langle\sigma|, \tag{2.121}$$

with $|\sigma\rangle$ a representation state and $|h\rangle$ a group element state. The representation states are discrete Fourier transforms of the element states. Then we have

$$H^{h,\sigma} = -\left[|0\rangle\langle 0| + |h\rangle\langle h| + |I\rangle\langle I| + |\sigma\rangle\langle\sigma|\right]. \tag{2.122}$$

Here $|0\rangle$ is the group identity element and $|I\rangle$ corresponds to the trivial representation of the group. Since $H^{h,\sigma}$ is a negative sum of projectors, all its eigenvalues are non-positive. We can then write a triangle inequality for the magnitude of least eigenvalue by taking the operator norm,

$$\left\| H^{h,\sigma} \right\| \leq \left\| |0\rangle\langle 0| + |I\rangle\langle I| \right\| + \left\| |h\rangle\langle h| + |\sigma\rangle\langle\sigma| \right\|. \tag{2.123}$$

We know that this inequality is saturated only if $(|0\rangle\langle 0| + |I\rangle\langle I|)$ is parallel to $(|h\rangle\langle h| + |\sigma\rangle\langle\sigma|)$ in their largest eigenspace. But unless $(h, \sigma) = (0, I)$, these vectors are never parallel. Then we

have

$$\left\| H^{0,I} \right\| = 2\left\| |0\rangle\langle 0| + |I\rangle\langle I| \right\| > \left\| H^{h,\sigma} \right\| \quad \text{when } (h,\sigma) \neq (0,I)\,. \tag{2.124}$$

We can now say that the ground space must have $h = 0$ and $\sigma = I$. Furthermore, when this is the case, we see from Eq. (2.122) that the only non-vanishing eigenvectors of this block are linear combinations of $|0\rangle$ and $|I\rangle$. We find by inspection that the two independent eigenvectors are

$$|\psi_\pm\rangle = |0\rangle \pm |I\rangle\,, \tag{2.125}$$

with eigenvalues

$$\lambda_\pm = -2\left[1 \pm \frac{1}{\sqrt{d}}\right]. \tag{2.126}$$

This gives for the unique ground state of the gauge qudit

$$|\psi_0^{\mathsf{G}}\rangle = |0\rangle + |I\rangle\,. \tag{2.127}$$

Given that the stabilizer and gauge degrees of freedom have a unique ground state, and the fact that the Hamiltonian commutes with the logical operators, we can also say that the Hamiltonian Eq. (2.44) has a d-fold degenerate ground space encoding the logical state. □

2.10 Proof of Theorem 3

Proof. We wish to prove that the ground space of our Hamiltonian Eq. (2.79) is stabilized as claimed. The key to proving this theorem is choosing a suitable basis. We have previously defined the states as in the physical basis of Eq. (2.74). Here we will need to look at some more sophisticated bases that make the actions of our encoded operators even more transparent.

2.10.1 Alternative Bases

Consider first the gauge representation basis:

$$|\sigma_{mn}, h, \pi_{ij}, k_{\mathsf{L}}\rangle \equiv \frac{\sqrt{d_\pi d_\sigma}}{|G|} \sum_{g_\pi, g_\sigma \in G} [\pi(g_\pi g_\sigma)]_{ij} [\sigma(g_\sigma)]_{mn} |g_\sigma, g_\sigma^{-1} h g_\sigma, g_\pi, k_{\mathsf{L}}\rangle \tag{2.128}$$

Here π and σ are (unitary irreducible) representations of dimension d_π and d_σ respectively. The π_{ij} variable defines the gauge state, which is why we call this the gauge representation basis. It is clear that there are a total of $|G|^4$ basis states, as needed, and orthonormality can be easily verified. We would like to know how the $\sum_g L^g_{\mathsf{G}_\pm}$ projectors in the Hamiltonian Eq. (2.79)

will act on this basis.

It can be easily verified that these operators act in the following way on the physical basis

$$L^{\tilde{g}}_{\mathsf{G}+}|h_a,h_b,k_{\mathsf{G}},k_{\mathsf{L}}\rangle = \left|h_a\tilde{g}^{-1},\tilde{g}h_b\tilde{g}^{-1},k_{\mathsf{G}}h_a\tilde{g}h_a^{-1},k_{\mathsf{L}}\right\rangle \tag{2.129}$$

$$L^{\tilde{g}}_{\mathsf{G}-}|h_a,h_b,k_{\mathsf{G}},k_{\mathsf{L}}\rangle = \left|h_a,h_b,k_{\mathsf{G}}h_a\tilde{g}^{-1}h_a^{-1},k_{\mathsf{L}}\right\rangle . \tag{2.130}$$

This gives for the action of the L projectors in our new basis:

$$\frac{1}{|G|}\sum_{\tilde{g}} L^{\tilde{g}}_{\mathsf{G}+}|\sigma_{mn},h,\pi_{ij},k_{\mathsf{L}}\rangle = \frac{\sqrt{d_\pi d_\sigma}}{|G|^2}\sum_{g_\pi,g_\sigma,\tilde{g}}[\pi(g_\pi g_\sigma)]_{ij}[\sigma(g_\sigma)]_{mn} \cdot|g_\sigma\tilde{g}^{-1},\tilde{g}g_\sigma^{-1}hg_\sigma\tilde{g}^{-1},g_\pi g_\sigma\tilde{g}g_\sigma^{-1},k_{\mathsf{L}}\rangle \tag{2.131}$$

introducing substitutions

$$g'_\sigma = g_\sigma\tilde{g}^{-1} \tag{2.132}$$

$$g'_\pi = g_\pi g_\sigma\tilde{g}g_\sigma^{-1} \tag{2.133}$$

we find

$$\frac{1}{|G|}\sum_{\tilde{g}} L^{\tilde{g}}_{\mathsf{G}+}|\sigma_{mn},h,\pi_{ij},k_{\mathsf{L}}\rangle = \frac{\sqrt{d_\pi d_\sigma}}{|G|^2}\sum_{g'_\pi,g'_\sigma,\tilde{g}}\sum_s[\pi(g'_\pi g'_\sigma)]_{ij}[\sigma(g'_\sigma)]_{ms}[\sigma(\tilde{g})]_{sn} \cdot|g'_\sigma,g_\sigma'^{-1}hg'_\sigma,g'_\pi,k_{\mathsf{L}}\rangle \tag{2.134}$$

The grand orthogonality theorem (Eq. (2.182)) can then be used over $\tilde{g}$ to give

$$\frac{1}{|G|}\sum_{\tilde{g}} L^{\tilde{g}}_{\mathsf{G}+}|\sigma_{mn},h,\pi_{ij},k_{\mathsf{L}}\rangle = \delta_{\sigma I}\frac{\sqrt{d_\pi d_\sigma}}{|G|}\sum_{g'_\pi,g'_\sigma}[\pi(g'_\pi g'_\sigma)]_{ij}[\sigma(g'_\sigma)]_{11} \cdot|g'_\sigma,g_\sigma'^{-1}hg'_\sigma,g'_\pi,k_{\mathsf{L}}\rangle \tag{2.135}$$

$$= \delta_{\sigma I}|\sigma_{mn},h,\pi_{ij},k_{\mathsf{L}}\rangle \tag{2.136}$$

where I is the trivial irrep of the group G. We can perform a similar treatment for the other L projector, giving

$$\frac{1}{|G|}\sum_{\tilde{g}} L^{\tilde{g}}_{\mathsf{G}-}|\sigma_{mn},h,\pi_{ij},k_{\mathsf{L}}\rangle = \frac{\sqrt{d_\pi d_\sigma}}{|G|^2}\sum_{g'_\pi,g_\sigma,\tilde{g}}\sum_s[\pi(g'_\pi g_\sigma)]_{is}[\pi(\tilde{g}^{-1})]_{sj}[\sigma(g_\sigma)]_{mn} \cdot|g_\sigma,g_\sigma^{-1}hg_\sigma,g'_\pi,k_{\mathsf{L}}\rangle \tag{2.137}$$

with substitutions

$$g'_\pi = g_\pi g_\sigma \tilde{g} g_\sigma^{-1} \tag{2.138}$$

Again, this can be simplified through orthogonality to give

$$\begin{aligned}\frac{1}{|G|}\sum_{\tilde{g}} L_{\mathsf{G}-}^{\tilde{g}}|\sigma_{mn},h,\pi_{ij},k_{\mathsf{L}}\rangle &= \delta_{\pi I}\frac{\sqrt{d_\pi d_\sigma}}{|G|}\sum_{g'_\pi,g_\sigma}[\pi(g'_\pi g_\sigma)]_{11}[\sigma(g_\sigma)]_{mn} \\ &\quad \cdot|g_\sigma, g_\sigma^{-1}hg_\sigma, g'_\pi, k_{\mathsf{L}}\rangle \qquad (2.139)\\ &= \delta_{\pi I}|\sigma_{mn},h,\pi_{ij},k_{\mathsf{L}}\rangle \qquad (2.140)\end{aligned}$$

To treat the $T_{G\pm}$ operators analogously, we need to look at another basis in which the gauge state takes a particular goup element as opposed to an element of a representation. We define this gauge element basis as

$$|\sigma_{mn},h,k_{\mathsf{G}},k_{\mathsf{L}}\rangle \equiv \frac{\sqrt{d_\sigma}}{\sqrt{|G|}}\sum_{g_\sigma\in G}[\sigma(g_\sigma)]_{mn}|g_\sigma, g_\sigma^{-1}hg_\sigma, k_{\mathsf{G}},k_{\mathsf{L}}\rangle \tag{2.141}$$

i.e. instead of using a representation for the gauge degree of freedom, here a single group element is used. In terms of the physical basis, the $T^1_{G\pm}$ projectors act in the following way:

$$\begin{aligned}T^1_{\mathsf{G}+}|h_a,h_b,k_{\mathsf{G}},k_{\mathsf{L}}\rangle &= \delta_{1k_{\mathsf{G}}}|h_a,h_b,k_{\mathsf{G}},k_{\mathsf{L}}\rangle \qquad (2.142)\\ T^1_{\mathsf{G}-}|h_a,h_b,k_{\mathsf{G}},k_{\mathsf{L}}\rangle &= \delta_{(h_ah_bh_a^{-1})k_{\mathsf{G}}}|h_a,h_b,k_{\mathsf{G}},k_{\mathsf{L}}\rangle \qquad (2.143)\end{aligned}$$

where 1 is the identity group element. We are now in a position to demonstrate that the T operators explicitly project to single states in the gauge element basis:

$$\begin{aligned}T^1_{\mathsf{G}+}|\sigma_{mn},h,k_{\mathsf{G}},k_{\mathsf{L}}\rangle &= \delta_{1k_{\mathsf{G}}}\frac{\sqrt{d_\sigma}}{\sqrt{|G|}}\sum_{g_\sigma}[\sigma(g_\sigma)]_{mn}|k_{\mathsf{G}},\sigma_{mn},h,k_{\mathsf{L}}\rangle \qquad (2.144)\\ &= \delta_{ek_{\mathsf{G}}}|R_{mn},h,k_{\mathsf{G}},k_{\mathsf{L}}\rangle \qquad (2.145)\\ T^1_{\mathsf{G}-}|\sigma_{mn},h,k_{\mathsf{G}},k_{\mathsf{L}}\rangle &= \delta_{(g_\sigma g_\sigma^{-1}hg_\sigma g_\sigma^{-1})k_{\mathsf{G}}}\frac{\sqrt{d_\sigma}}{\sqrt{|G|}}\sum_{g_\sigma}[\sigma(g_\sigma)]_{mn}|g_\sigma,g_\sigma^{-1}hg_\sigma,k_{\mathsf{G}},k_{\mathsf{L}}\rangle \qquad (2.146)\\ &= \delta_{hk_{\mathsf{G}}}|\sigma_{mn},h,k_{\mathsf{G}},k_{\mathsf{L}}\rangle \qquad (2.147)\end{aligned}$$

2.10.2 Computing the code gadget ground space

The Hamiltonian of interest is given by

$$H(e) = -\sum_g L^g_{\mathsf{G}+} - \sum_g L^g_{\mathsf{G}-} - T^1_{\mathsf{G}+} - T^1_{\mathsf{G}-} \tag{2.148}$$

Given that we now know explicitly what states each of these terms project to, we can write instead

$$\begin{aligned} H(e) = &- \sum_{\pi_{ij},h,k_{\mathsf{L}}} |I_{11},h,\pi_{ij},k_{\mathsf{L}}\rangle\langle I_{11},h,\pi_{ij},k_{\mathsf{L}}| - \sum_{\sigma_{mn},h,k_{\mathsf{L}}} |\sigma_{mn},h,I_{11},k_{\mathsf{L}}\rangle\langle\sigma_{mn},h,I_{11},k_{\mathsf{L}}| \\ &- \sum_{\sigma_{mn},h,k_{\mathsf{L}}} |\sigma_{mn},h,1,k_{\mathsf{L}}\rangle\langle\sigma_{mn},h,1,k_{\mathsf{L}}| - \sum_{\sigma_{mn},h,k_{\mathsf{L}}} |\sigma_{mn},h,h,k_{\mathsf{L}}\rangle\langle\sigma_{mn},h,h,k_{\mathsf{L}}| \end{aligned} \tag{2.149}$$

Each of these terms are pairwise orthogonal for different values of h or k_{L}. We can then immediately block diagonalize the Hamiltonian by these two variables. As these labels will not participate overly in the calculation, we will suppress them henceforth for clarity. We can also block diagonalize by a representation and one of its indices as follows (suppressing (e) labels)

$$H^{h,k_{\mathsf{L}}}_{\sigma,n} = -\sum_m \Big[|I_{11},\sigma_{mn}\rangle\langle I_{11},\sigma_{mn}| + |\sigma_{mn},I_{11}\rangle\langle\sigma_{mn},I_{11}| + |\sigma_{mn},1\rangle\langle\sigma_{mn},1| + |\sigma_{mn},h\rangle\langle\sigma_{mn},h| \Big] \tag{2.150}$$

That projectors in each block are orthogonal to those in different blocks can be verified by examining the inner products presented in Sec. 2.10.3.

Looking only in one block of the Hamiltonian, we can split the terms into two operators:

$$\begin{aligned} -H^{h,k_{\mathsf{L}}}_{\sigma,n} = &\Big[\sum_m |I_{11},\sigma_{mn}\rangle\langle I_{11},\sigma_{mn}| + \sum_m |\sigma_{mn},1\rangle\langle\sigma_{mn},1| \Big] \\ &+ \Big[\sum_m |\sigma_{mn},I_{11}\rangle\langle\sigma_{mn},I_{11}| + \sum_m |\sigma_{mn},h\rangle\langle\sigma_{mn},h| \Big] \end{aligned} \tag{2.151}$$

We can bound the length of each of these operators individually by considering them as subhamiltonians

$$-H_A = \sum_m |I_{11},\sigma_{mn}\rangle\langle I_{11},\sigma_{mn}| + \sum_m |\sigma_{mn},1\rangle\langle\sigma_{mn},1| \tag{2.152}$$

$$-H_B = \sum_m |\sigma_{mn},I_{11}\rangle\langle\sigma_{mn},I_{11}| + \sum_m |\sigma_{mn},h\rangle\langle\sigma_{mn},h| \tag{2.153}$$

each of these subhamiltonians can be further block diagonalized by m:

$$-H_A^m = |I_{11}, \sigma_{mn}\rangle\langle I_{11}, \sigma_{mn}| + |\sigma_{mn}, 1\rangle\langle\sigma_{mn}, 1| \tag{2.154}$$
$$-H_B^m = |\sigma_{mn}, I_{11}\rangle\langle\sigma_{mn}, I_{11}| + |\sigma_{mn}, h\rangle\langle\sigma_{mn}, h| \tag{2.155}$$

We can solve these subhamiltonians in each block by calculating the overlap of the two projectors (these calculations are shown in Sec. 2.10.3):

$$\langle I_{11}, \sigma_{mn}|\sigma_{mn}, 1\rangle = \frac{1}{\sqrt{|G|}} \tag{2.156}$$
$$\langle\sigma_{mn}, I_{11}|\sigma_{mn}, h\rangle = \frac{1}{\sqrt{|G|}} \tag{2.157}$$

It can be shown that the eigenvalues of these subhamiltonians will then be

$$\lambda_m = -1 \pm |C| \tag{2.158}$$

where C is the inner product calculated above. As such, we can say that the norm of the subhamiltonians are equal, independent of m block and have value $1 + \frac{1}{\sqrt{|G|}}$. Importantly, their length is independent of the choice of σ_{mn}, π_{ij}, h and k_L.

In terms of the full Hamiltonian and block structure, we have two operators whose norms are constant for a given group. We can then bound the eigenvalues of the full Hamiltonian as follows. We can use a triangle inequality argument to give

$$\left\| H_{\sigma,n}^{h,k_\mathrm{L}} \right\| \leq \left\| \sum_m |I_{11}, \sigma_{mn}\rangle\langle I_{11}, \sigma_{mn}| + \sum_m |\sigma_{mn}, 1\rangle\langle\sigma_{mn}, 1| \right\| + \left\| \sum_m |\sigma_{mn}, I_{11}\rangle\langle\sigma_{mn}, I_{11}| + \sum_m |\sigma_{mn}, h\rangle\langle\sigma_{mn}, h| \right\| \tag{2.159}$$

We know that each individual operator has a constant norm. We also know that this inequality will only be saturated when the two operators are equal. This is also when $\sigma = I$, $n = 1$, and $h = e$. As desired, there is no dependence on k_L.

Since the eigenvectors of H are non-positive, the largest magnitude eigenvalue will correspond to the ground space. The triangle inequality argument amounts to showing that the ground state must rest in the block defined by $H_{I,1}^{1,k_\mathrm{L}}$. By inspection, there will be 2 independent eigenvectors in this block for each value of k_L (we return the h index, but the k_L index remains suppressed here)

$$|\psi_\pm\rangle = |I_{11}, 1, 1\rangle \pm |I_{11}, 1, I_{11}\rangle \tag{2.160}$$

with eigenvalues

$$\lambda_{\pm} = -2\left(1 \pm \frac{1}{\sqrt{|G|}}\right)$$

Clearly $|\psi_+\rangle$ defines a $|G|$-fold degenerate ground space of our system. It is simple to verify that the stabilizers have the desired relations with this state

$$\sum_g S_L^g |\psi_+\rangle = |\psi_+\rangle \tag{2.161}$$

$$S_T^1 |\psi_+\rangle = |\psi_+\rangle \tag{2.162}$$

and thus the Hamiltonian Eq. (2.79) behaves as claimed. □

2.10.3 Useful Inner Products

Here we wish to calculate inner products between states in the gauge representation basis and the gauge element basis. In general, we have

$$\begin{aligned}
\langle \sigma_{mn}, h, \pi_{ij}, k_{\mathsf{L}} | \sigma'_{m'n'}, h', k_{\mathsf{G}}, k'_{\mathsf{L}} \rangle &= \frac{\sqrt{d_\pi d_{\sigma'} d_\sigma}}{|G|^{3/2}} \sum_{g_\pi, g_\sigma, g_{\sigma'}} [\pi(g_\pi g_\sigma)]^*_{ij} [\sigma(g_\sigma)]^*_{mn} [\sigma'(g_{\sigma'})]_{m'n'} \\
&\quad \times \langle g_\sigma, g_\sigma^{-1} h g_\sigma, g_\pi, k_{\mathsf{L}} | g_{\sigma'}, g_{\sigma'}^{-1} h' g_{\sigma'}, k_{\mathsf{G}}, k'_{\mathsf{L}} \rangle \qquad (2.163) \\
&= \frac{\sqrt{d_\pi d_{\sigma'} d_\sigma}}{|G|^{3/2}} \sum_{g_\pi, g_\sigma, g_{\sigma'}} [\pi(g_\pi g_\sigma)]^*_{ij} [\sigma(g_\sigma)]^*_{mn} \sigma'(g_{\sigma'})]_{m'n'} \\
&\quad \times \delta_{g_\sigma g_{\sigma'}} \delta_{hh'} \delta_{g_\pi k_{\mathsf{G}}} \delta_{k_{\mathsf{L}} k'_{\mathsf{L}}} \qquad (2.164) \\
&= \frac{\sqrt{d_\pi d_{\sigma'} d_\sigma}}{|G|^{3/2}} \sum_{g_\sigma} [\pi(k_{\mathsf{G}} g_\sigma)]^*_{ij} [\sigma(g_\sigma)]^*_{mn} [\sigma'(g_\sigma)]_{m'n'} \\
&\quad \times \delta_{hh'} \delta_{k_{\mathsf{L}} k'_{\mathsf{L}}} \qquad (2.165)
\end{aligned}$$

In particular, the special cases we are interested can be simplified. With I the trivial representation, we have

$$\begin{aligned}
\langle \sigma_{mn}, h, I_{11}, k_{\mathsf{L}} | \sigma'_{m'n'}, h', k_{\mathsf{G}}, k'_{\mathsf{L}} \rangle &= \frac{\sqrt{d_{\sigma'} d_\sigma}}{|G|^{3/2}} \delta_{hh'} \delta_{k_{\mathsf{L}} k'_{\mathsf{L}}} \sum_{g_\sigma} [\sigma(g_\sigma)]^*_{mn} [\sigma'(g_\sigma)]_{m'n'} \qquad (2.166) \\
&= \frac{1}{|G|^{1/2}} \delta_{hh'} \delta_{k_{\mathsf{L}} k'_{\mathsf{L}}} \delta_{\sigma\sigma'} \delta_{mm'} \delta_{nn'} \qquad \forall\, k_{\mathsf{G}} \qquad (2.167)
\end{aligned}$$

and

$$\langle I_{11}, h, \pi_{ij}, k_{\mathsf{L}} | \sigma'_{m'n'}, h', k_{\mathsf{G}}, k'_{\mathsf{L}} \rangle = \frac{\sqrt{d_\pi d_{\sigma'}}}{|G|^{3/2}} \delta_{hh'} \delta_{k_{\mathsf{L}} k'_{\mathsf{L}}} \sum_{g_\sigma} [\pi(k_{\mathsf{G}} g_\sigma)]^*_{ij} [\sigma'(n_R)]_{m'n'} \tag{2.168}$$

$$= \frac{\sqrt{d_\pi d_{\sigma'}}}{|G|^{3/2}} \delta_{hh'} \delta_{k_{\mathsf{L}} k'_{\mathsf{L}}} \sum_{g_\sigma} \sum_{s} [\pi(k_{\mathsf{G}})]^*_{is} [\pi(g_\sigma)]^*_{sj} [\sigma'(n_R)]_{m'n'} \tag{2.169}$$

$$= \frac{1}{|G|^{1/2}} \delta_{hh'} \delta_{k_{\mathsf{L}} k'_{\mathsf{L}}} \delta_{\pi\sigma'} \delta_{jn'} [\pi(k_{\mathsf{G}})]^*_{im'} \tag{2.170}$$

particularly,

$$\langle I_{11}, h, \pi_{ij}, k_{\mathsf{L}} | \sigma'_{m'n'}, h', 1, k'_{\mathsf{L}} \rangle = \frac{1}{|G|^{1/2}} \delta_{hh'} \delta_{k_{\mathsf{L}} k'_{\mathsf{L}}} \delta_{\pi\sigma'} \delta_{im'} \delta_{jn'} \tag{2.171}$$

The orthonormality of the gauge representation basis is also useful when written in the form

$$\langle I_{11}, h, \pi_{ij}, k_{\mathsf{L}} | \sigma_{mn}, h', I_{11}, k'_{\mathsf{L}} \rangle = \delta_{\pi\sigma} \delta_{\sigma I} \delta_{i1} \delta_{nj} \delta_{m1} \delta_{n1} \delta_{hh'} \delta_{k_{\mathsf{L}} k'_{\mathsf{L}}} \tag{2.172}$$

2.11 Error Operations in General Quantum Double Models

In the case of cyclic quantum double models, we were able to provide a simple general argument as to why many of the terms in the effective Hamiltonian vanished. In the more general case, this kind of simple argument is no longer applicable, and so we are forced to take an exhaustive survey of the terms that may arise in the effective Hamiltonian. We aim to show that any undesired terms will vanish in the ground space.

In order to undertake this study, it is useful to note the following relations:

$$Z_\pm^{\pi_{ij}} L_\pm^g = \sum_k [\pi(g)]_{ik} L_\pm^g Z_\pm^{\pi_{kj}} \tag{2.173}$$

$$Z_\pm^{\pi_{ij}} L_\mp^g = \sum_k L_\mp^g Z_\pm^{\pi_{ik}} [\pi(g^{-1})]_{kj} \tag{2.174}$$

The kinds of operators we consider will take the form:

$$z_a = \left(\begin{array}{c|c} Z_-^{\pi_{ij}} & Z_+^{\sigma_{kl}} \\ I & I \end{array} \right), \quad z_b = \left(\begin{array}{c|c} I & I \\ Z_-^{\pi_{ij}} & Z_+^{\sigma_{kl}} \end{array} \right), \quad z_c = \left(\begin{array}{c|c} I & Z_+^{\pi_{ij}} \\ I & Z_+^{\sigma_{kl}} \end{array} \right), \quad z_d = \left(\begin{array}{c|c} Z_-^{\pi_{ij}} & I \\ Z_-^{\sigma_{kl}} & I \end{array} \right)$$

$$l_a = \left(\begin{array}{c|c} L_+^g & L_+^{g'} \\ I & I \end{array} \right), \qquad l_b = \left(\begin{array}{c|c} I & I \\ L_-^g & L_-^{g'} \end{array} \right), \qquad l_c = \left(\begin{array}{c|c} I & L_+^g \\ I & L_-^{g'} \end{array} \right), \qquad l_d = \left(\begin{array}{c|c} L_+^g & I \\ L_-^{g'} & I \end{array} \right) \tag{2.175}$$

We will refer to these as "error terms" or "error operators". For each error term $\hat{E}$ we will calculate $\Upsilon\hat{E}\Upsilon$ where Υ is the projector on to the ground state. Note that $\Upsilon = S\Upsilon$ for either of the stabilizers S_T or S_L. First consider the error term z_c:

$$\begin{aligned}
\Upsilon z_c \Upsilon &= \Upsilon z_c S_L \Upsilon && (2.176)\\
&= \frac{1}{|G|}\sum_g \Upsilon z_c S_L^g \Upsilon && (2.177)\\
&= \frac{1}{|G|}\sum_g \Upsilon \left(\begin{array}{c|c} L_-^{g^{-1}} & Z_+^{\pi_{ij}} L_-^{g^{-1}} \\ L_+^{g^{-1}} & Z_+^{\sigma_{kl}} L_+^{g^{-1}} \end{array}\right) \Upsilon && (2.178)\\
&= \frac{1}{|G|}\sum_g \Upsilon (S_L^{g^{-1}})^\dagger \sum_{m,n} [\pi(g)]_{mj}[\sigma(g^{-1})]_{kn} \left(\begin{array}{c|c} I & Z_+^{\pi_{im}} \\ I & Z_+^{\sigma_{nl}} \end{array}\right) \Upsilon && (2.179)
\end{aligned}$$

Now, because the ground state is stabilized by the projector S_L, it is easy to check that it must also be stabilized by each of S_L^g individually. This allows us to write:

$$\begin{aligned}
\Upsilon z_c \Upsilon &= \frac{1}{|G|}\Upsilon \sum_{m,n,g} [\pi(g)]_{mj}[\sigma(g^{-1})]_{kn} \left(\begin{array}{c|c} I & Z_+^{\pi_{im}} \\ I & Z_+^{\sigma_{nl}} \end{array}\right) \Upsilon && (2.180)\\
&= \frac{1}{|G|}\Upsilon \sum_{m,n,g} [\pi(g)]_{mj}[\sigma(g)]^*_{nk} \left(\begin{array}{c|c} I & Z_+^{\pi_{im}} \\ I & Z_+^{\sigma_{nl}} \end{array}\right) \Upsilon && (2.181)
\end{aligned}$$

where we have used the unitarity of the representation σ in the last line. Now we make use of the Grand Orthogonality Theorem for unitary representations:

$$\sum_g [\pi(g)]^*_{ij}[\sigma(g)]_{kl} = \frac{|G|}{d_\pi}\delta_{\pi\sigma}\delta_{ik}\delta_{jl} \qquad (2.182)$$

and we can write

$$\begin{aligned}
\Upsilon z_c \Upsilon &= \Upsilon \sum_{m,n} \frac{1}{d_\pi}\delta_{\pi\sigma}\delta_{mn}\delta_{jk} \left(\begin{array}{c|c} I & Z_+^{\pi_{im}} \\ I & Z_+^{\sigma_{nl}} \end{array}\right) \Upsilon && (2.183)\\
&= \Upsilon \sum_{m} \frac{1}{d_\pi}\delta_{\pi\sigma}\delta_{jk} \left(\begin{array}{c|c} I & Z_+^{\pi_{im}} \\ I & Z_+^{\sigma_{ml}} \end{array}\right) \Upsilon && (2.184)
\end{aligned}$$

This gives us the result that all errors of this type will vanish from the effective Hamiltonian unless they satisfy the conditions $\pi = \sigma$ and $j = k$. It also allows us to rewrite an operator of the form z_c satisfying these conditions as an average over the shared index in the ground state.

This will become important when we undertake the perturbation calculations.

We can find analogous results for the other z error terms,

$$\Upsilon z_d \Upsilon = \Upsilon \sum_{m,n,g} [\pi(g^{-1})]_{im} [\sigma(g)]_{nl} \left(\begin{array}{c|c} Z_-^{\pi_{mj}} & I \\ Z_-^{\sigma_{kn}} \uparrow & I \end{array} \right) \Upsilon \tag{2.185}$$

$$= \Upsilon \sum_m \frac{1}{d_\pi} \delta_{\pi\sigma} \delta_{il} \left(\begin{array}{c|c} Z_-^{\pi_{mj}} & I \\ Z_-^{\sigma_{km}} \uparrow & I \end{array} \right) \Upsilon \tag{2.186}$$

$$\Upsilon z_a \Upsilon = \Upsilon \sum_{m,n,g} [\pi(g^{-1})]_{im} [\sigma(g)]_{nl} \left(\begin{array}{c|c} Z_-^{\pi_{mj}} & Z_+^{\sigma_{kn}} \\ I \uparrow & I \end{array} \right) \Upsilon \tag{2.187}$$

$$= \Upsilon \sum_m \frac{1}{d_\pi} \delta_{\pi\sigma} \delta_{il} \left(\begin{array}{c|c} Z_-^{\pi_{mj}} & Z_+^{\sigma_{km}} \\ I \uparrow & I \end{array} \right) \Upsilon \tag{2.188}$$

$$\Upsilon z_b \Upsilon = \Upsilon \sum_{m,n,g} [\pi(g)]_{mj} [\sigma(g^{-1})]_{kn} \left(\begin{array}{c|c} I & I \\ Z_-^{\pi_{im}} \uparrow & Z_+^{\sigma_{nl}} \end{array} \right) \Upsilon \tag{2.189}$$

$$= \Upsilon \sum_m \frac{1}{d_\pi} \delta_{\pi\sigma} \delta_{jk} \left(\begin{array}{c|c} I & I \\ Z_-^{\pi_{im}} \uparrow & Z_+^{\sigma_{ml}} \end{array} \right) \Upsilon \tag{2.190}$$

The l error terms require slightly different treatment. Consider first l_a:

$$\Upsilon l_a \Upsilon = \Upsilon l_a S_T^1 \Upsilon \tag{2.191}$$

$$= \Upsilon \sum_{g_1 g_2 g_3 g_4 = 1} \left(\begin{array}{c|c} L_+^g T_-^{g_1} & L_+^{g'} T_+^{g_2} \\ T_-^{g_4} \uparrow & T_+^{g_3} \end{array} \right) \Upsilon \tag{2.192}$$

$$= \Upsilon \sum_{g_1 g_2 g_3 g_4 = 1} \left(\begin{array}{c|c} T_-^{g_1 g^{-1}} & T_+^{g' g_2} \\ T_-^{g_4} \uparrow & T_+^{g_3} \end{array} \right) l_a \Upsilon \tag{2.193}$$

$$= \Upsilon \sum_{g_1 g g'^{-1} g_2 g_3 g_4 = 1} \left(\begin{array}{c|c} T_-^{g_1} & T_+^{g_2} \\ T_-^{g_4} \uparrow & T_+^{g_3} \end{array} \right) l_a \Upsilon \tag{2.194}$$

The first operator is now orthogonal to the projector S_T^1 unless $g' g^{-1} = 1$. Because the ground

space is stabilized by S^1_T, we can say that this vanishes unless $g = g'$. This gives:

$$\Upsilon l_a \Upsilon = \Upsilon \delta_{gg'} \left(\begin{array}{c|c} L^g_+ & L^{g'}_+ \\ I & I \end{array} \right) \Upsilon \tag{2.195}$$

i.e. error terms of the form l_a will vanish unless they obey $g = g'$. The procedure for l_b proceeds similarly to yield:

$$\Upsilon l_b \Upsilon = \Upsilon \sum_{g_1 g_2 g_3 g' g^{-1} g_4 = 1} \left(\begin{array}{c|c} T^{g_1}_- & T^{g_2}_+ \\ T^{g_4}_- & T^{g_3}_+ \end{array} \right) l_b \Upsilon \tag{2.196}$$

$$= \Upsilon \delta_{gg'} \left(\begin{array}{c|c} I & I \\ L^g_- & L^{g'}_- \end{array} \right) \Upsilon \tag{2.197}$$

The error operators l_c and l_d are more complicated.

$$\Upsilon l_c \Upsilon = \Upsilon l_c \sum_{g_1 g_2 g_3 g_4 = 1} \left(\begin{array}{c|c} T^{g_1}_- & T^{g g_2}_+ \\ T^{g_4}_- & T^{g_3 g'^{-1}}_+ \end{array} \right) \Upsilon \tag{2.198}$$

We can imagine the second operator acting on state $|h_a, h_b, k_\mathsf{G}, k_\mathsf{L}\rangle$. This leads to this operator vanishing unless

$$h_a^{-1} g^{-1} k_\mathsf{L} g' k_\mathsf{L}^{-1} h_a h_b = 1$$

In the ground subspace, we know $h_b = 1$, this implies

$$g = k_\mathsf{L} g' k_\mathsf{L}^{-1} \tag{2.199}$$

i.e. the nonvanishing operators of the form l_c depend explicitly on the logical state. A similar result is obtained for the error term l_d:

$$\Upsilon l_d \Upsilon = \Upsilon l_d \sum_{g_1 g_2 g_3 g_4 = 1} \left(\begin{array}{c|c} T^{g_1 g^{-1}}_- & T^{g_2}_+ \\ T^{g' g_4}_- & T^{g_3}_+ \end{array} \right) \Upsilon \tag{2.200}$$

The second operator vanishes unless

$$h_a^{-1} g k_\mathsf{L} g'^{-1} k_\mathsf{L}^{-1} h_a h_b = 1$$

In the codespace this is equivalent to:

$$g = k_{\mathrm{L}} g' k_{\mathrm{L}}^{-1} \tag{2.201}$$

There are two remaining kinds of terms which will arise in our perturbation treatment. They may take a diagonal form, e.g.

$$\hat{E} \sim \left(\begin{array}{c|c} \hat{A} & I \\ I & \hat{B} \end{array} \right)$$

in which case they will not contribute to low order terms (and will have little impact on the form of higher order terms). A similar treatment to Sec. 2.11 and Eq.(2.94-2.103) reveals that these operators act as both gauge and logical operators, just as in the cyclic case.

Alternatively, error operators may consist of mixed L and Z operators, e.g.

$$\hat{E} \sim \left(\begin{array}{c|c} Z_{-}^{\pi_{ij}} & L_{+}^{g} \\ I & I \end{array} \right)$$

It is a simple calculation to show that these kinds of operators will vanish when conjugated by Υ, except when $\pi = I$ (the trivial representation) and $g = 1$. That is, the only non-vanishing operator of this form is the identity operator. These results show that the encoding we use will indeed prevent undesirable excitations from being permitted, leaving only the terms from the target Hamiltonian to arise in our perturbative treatment.

Chapter Review

We construct perturbative 2-local Hamiltonians that reproduce the Kitaev quantum double models as their low-energy limits.

- The main conceptual tool introduced is a form of perturbation gadget based on error-detecting subsystem codes that we call a "code gadget". These are related to similar tools used to produce the cluster state Hamiltonian in earlier work.
- In contrast to previous perturbation gadget approaches, our construction produces an encoded form of the target model. That is, each qudit of the target model is encoded in the set of qudits forming a code gadget.
- The structure of the Hamiltonian and code gadgets are closely related to the PEPS descriptions of the quantum double ground states.
- The low-energy effective Hamiltonian is shown to be gapped and has the target quantum double ground state to arbitrary order in perturbation theory.
- The local symmetries of the target quantum double model are exactly reproduced in our construction.
- We give a simplified analysis for the quantum doubles of cyclic groups, as well as using the toric code as a pedagogical example.

3 Perturbative Two-body Parent Hamiltonians for Projected Entangled Pair States

Abstract

We construct parent Hamiltonians involving only local 2-body interactions for a broad class of Projected Entangled Pair States (PEPS). Making use of perturbation gadget techniques, we define a perturbative Hamiltonian acting on the virtual PEPS space with a finite order low energy effective Hamiltonian that is a gapped, frustration-free parent Hamiltonian for an encoded version of a desired PEPS. For topologically ordered PEPS, the ground space of the low energy effective Hamiltonian is shown to be in the same phase as the desired state to all orders of perturbation theory. An encoded parent Hamiltonian for the double semion string net ground state is explicitly constructed as a concrete example.

3.1 Introduction

Projected Entangled Pair States (PEPS) are a class of quantum states particularly well suited for describing the ground states of interacting quantum many-body systems [AKLT88, FNW92, Has06, PGVWC07, VWPGC06a, Vid03]. They are a form of tensor network ansatz amenable to both numerical and analytical study, and encompass many interesting classes of states. In particular, they offer exact analytical descriptions of such states as the topologically ordered ground states of quantum double models [Kit03] and string-net models [LW05], as well as resources for measurement-based quantum computation such as the cluster states [RB01] and Affleck-Kennedy-Lieb-Tasaki (AKLT) states [AKLT88, WAR11, DBB12], among others.

For a given PEPS (representing the state of a quantum many-body system defined on a graph), there is an associated parent Hamiltonian for which it is a ground state [PGVCW08]. For certain classes of PEPS, these Hamiltonians can be defined using only local interactions (i.e., interactions whose support lies only on qudits within some bounded size region) such that

their ground states are unique. Though these interactions act only within a finite sized region, there will still generally be a large number of qudits within this region. For this reason these interactions may be challenging to implement experimentally, and it may be preferable to find an alternative parent Hamiltonian with interactions involving at most two neighbouring quantum systems (2-local[1] interactions), whose ground state is a desired PEPS.

In this chapter, we construct such a parent Hamiltonian involving only 2-local interactions for PEPS with certain properties. The strategy we use to show this is based on the perturbation gadget [KKR06, OT08, BDLT08, JF08] approach. Perturbation gadgets allow k-body interactions (those involving k systems) to be approximated by 2-body interactions through the introduction of ancilla qudits coupled perturbatively. Applied to infinite systems, a naive perturbation gadgets approach can encounter a number of pitfalls. In particular, the resource cost of a general perturbation gadget scheme scales poorly with the system complexity, and application of the technique can lead to the energy gap scaling with the system size or the fidelity of target states [VdNLDB08, OT08]. Additionally, while interactions can be reduced to only 2-body, the nature of these interactions is in general complicated and unnatural when viewed in terms of the target model. By taking advantage of structure and tailoring the gadgets to a particular class of models, we can circumvent these difficulties. Our construction involves interactions that are natural from the point of view of the PEPS ansatz, and captures the structure of the standard PEPS parent Hamiltonian.

We present a perturbation gadget scheme that works by encoding the qudits of the model in question in a quantum code, and weakly coupling neighbouring encoded qudits. The encodings and couplings are directly inspired by the PEPS descriptions of the target ground states. As such, our scheme is specifically suited to constructing 2-local Hamiltonians whose ground space is (an encoded form of) a desired PEPS. This generalizes the ideas of Refs. [BR06] and [BFBD11], where similar techniques were used to reproduce encoded forms of the cluster state and the quantum double ground states, respectively, as the ground states of entirely 2-local Hamiltonians, based on their PEPS descriptions. The model studied in this chapter is not precisely equivalent to those developed previously, which take advantage of structure that is not generally available for all the PEPS we discuss here. As well as the quantum double and cluster states, we expect our construction to apply to broad classes of topologically ordered states with similar structure, such as the string net ground states, isometric H-injective PEPS [BMCA13], and (G,ω)-isometric PEPS [Bue14]. In this direction, we argue that isometric MPO-injective PEPS [SWB$^+$14] with trivial so-called generalized inverse satisfy the requirements of our construction; this class is known to include string-net ground states and (G,ω)-isometric PEPS. In fact, we conjecture that our results extend to any PEPS that satisfy certain topological order conditions.

Our analysis proceeds in two parts. In the first part, we show that for a given PEPS satisfying

[1] The term k-local is used sometimes in the literature to refer to any interaction whose support is restricted to at most k sites, regardless of their geometric arrangement. We will use the term k-body to refer to these types of interactions, and reserve the term k-local for interactions whose support is localized geometrically.

certain criteria there exists a finite-order low energy effective Hamiltonian for our system which is a valid (gapped) parent Hamiltonian for the desired PEPS satisfying these conditions. Our perturbation analysis is based on the Schrieffer-Wolff transformation [SW66, BDL11]. In the second part of our analysis, we study the robustness of this effective Hamiltonian to contributions from higher order terms in the perturbation expansion. In doing so, we prove that the effective Hamiltonian is in the same phase as the desired parent Hamiltonian to arbitrary order.

We make use of stability results for topologically ordered states [BHM10, BH11b, MZ13, CMPGS13] to prove that the ground space of our effective Hamiltonian remains in the same phase to arbitrarily high order of perturbation theory. For this reason, our results apply only to states with parent Hamiltonians satisfying the local topological quantum order conditions [MZ13]. Note that these states need not be topologically ordered in the more colloquial sense, and may have non-degenerate ground spaces, for example.

As an explicit new example of our construction, we demonstrate our procedure for the double semion string-net model [LW05], which has an exact PEPS description [GLW08, GLSW09, BAV09].

In Sec. 3.2 we will introduce the PEPS formalism and define the class of PEPS to which our construction applies. In Sec. 3.3 we briefly outline our model and main results. Following this, Sections 3.4 and 3.5 are devoted to the proofs of our results. Sec. 3.6 contains a discussion of our results and concluding remarks, followed by an explicit example of our construction in Sec. 3.7.

3.2 Projected Entangled Pair States

PEPS is an ansatz for describing states of many-body quantum systems. For a given PEPS satisfying certain criteria, we will exploit the structure of this ansatz in order to construct a 2-local Hamiltonian whose ground state is in the same phase as the desired PEPS.

A PEPS is typically associated with a graph or lattice Λ, and can be defined constructively by beginning with maximally entangled pairs of qudits of dimension D on each edge $e = (i, j)$ of the graph, such that one qudit from each pair is associated with each of the sites i and j. These qudits are conventionally called virtual qudits. A linear map $\mathscr{P}_s : \left(\mathbb{C}^D\right)^{\otimes \deg(s)} \to \mathbb{C}^d$ is then applied to the $\deg(s)$ virtual qudits at each site s of the graph (with $\deg(s)$ the degree of s), mapping the combined Hilbert spaces of all the virtual qudits at s to an encoded space of dimension d. The space $\mathbb{C}^d$ is often called the physical space, but we will refer to it as the code space, associated with an encoding of a d-dimensional qudit in the $\deg(s)$ D-dimensional virtual qudits. The map $\mathscr{P}_s$ is often referred to as the projection map, though it need not be a projector in the strict sense.

This structure of a PEPS is illustrated in Fig. 3.1. In general, the projection map and the

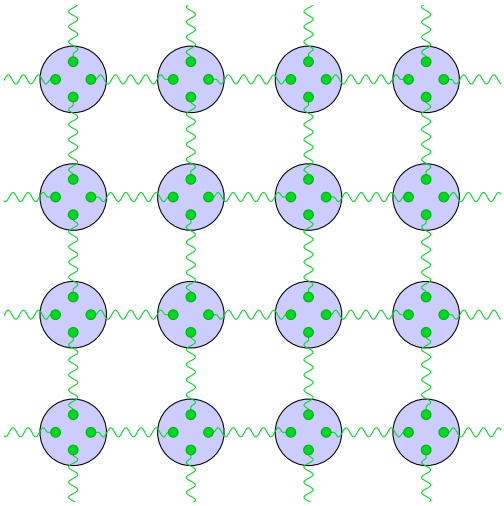

Figure 3.1 – PEPS construction on a square lattice. Virtual systems are shown in green, while code qudits are shown in blue, encoded in the enclosed virtual qudits. Wavy lines run along edges of the PEPS graph, and connect virtual qudits in maximally entangled states.

dimensions d and D can vary with location, but for notational simplicity we will restrict our attention to the translation-invariant case (extension to the general case is straightforward). We also take the graph Λ to have a bounded coordination number, i.e. $\deg(s)$ is finite. Because each edge $e = (i, j)$ of the PEPS graph has an associated pair of virtual qudits, we define $|\Phi_D(e)\rangle \equiv \sum_{k=0}^{D-1} |k\rangle_{e,i} |k\rangle_{e,j}$ as the maximally entangled state on edge e, where $|\cdot\rangle_{e,i}$ refers to the state of the virtual qudit at site i corresponding to edge e. With this in mind, we can write the PEPS state (up to normalization) as

$$|\psi_{\mathrm{PEPS}}\rangle_c = \prod_s \mathscr{P}_s \prod_e |\Phi_D(e)\rangle_v \tag{3.1}$$

where e runs over edges of Λ, and s runs over sites of Λ. Note that $|\psi_{\mathrm{PEPS}}\rangle_c$ is defined on the code space, as opposed to the virtual qudits. We denote states and operators on the code qudits and virtual qudits by subscript c and v, respectively.

A parent Hamiltonian of a PEPS (or more generally any state or space) is a local Hamiltonian that has the desired state as its ground state. We will exclusively consider gapped parent Hamiltonians. It is often conventional to also require that a parent Hamiltonian is frustration-free, but we will still refer to a frustrated Hamiltonian as a parent Hamiltonian so long as it is local and gapped. For any given PEPS, there is a special class of parent Hamiltonians, *canonical* parent Hamiltonians [PGVCW08], defined as follows.

A canonical parent Hamiltonian is specified by a set of regions $\{R\}$ on the PEPS lattice, where $\{R\}$ must contain a region of a large enough size around each site of the lattice. We call the largest required region size r_*. This size r_* generally depends on the details of the PEPS under consideration, but in the cases we consider it can always be taken to be finite (see [PGVCW08] for details). For each R, we define the projector ϖ_R onto the support of

$\rho_R = \mathrm{Tr}_{\setminus R} |\psi_{\mathrm{PEPS}}\rangle\langle\psi_{\mathrm{PEPS}}|$, the reduced state in region R. The associated canonical parent Hamiltonian is then

$$H_{\mathrm{can},c} = -\sum_R \omega_R \tag{3.2}$$

This Hamiltonian will have the desired PEPS as a frustration-free ground state. The Hamiltonian (3.2) acts on the code qudits of the model (as denoted by the subscript c), and the virtual qudits are seen only as a mathematical tool used in the definition of the PEPS.

Virtual qudits and code qudits

A PEPS is a state defined on the code qudits as in Eq. (3.1). However, we will consider the virtual qudits to be those that are manipulated in the laboratory and we regard the code qudits to simply be encoded within a subspace of these virtual systems. This is the sense in which we will recover an encoded form of the PEPS.

Generically in perturbation gadget approaches, ancilla qudits are required to mediate effective many-body correlations. In standard approaches, these ancillae are introduced beside the original qudits of the model being considered and simply mediate the interactions between the model qudits. However, in our construction each qudit of the desired model is encoded into several ancilla qudits, and so the additional qudits are integrated into the structure of the model itself. In this way we have aligned the structure of our perturbation gadgets with that of PEPS to reproduce these states more naturally.

For clarity, for the bulk of our analysis the interactions we use will not generally be 2-local on these virtual systems, but instead be 2-local on the collection of virtual qudits that encodes each code qudit. We call this collection a *code gadget*. We stress this distinction between 2-locality of an interaction with respect to the code gadgets as opposed to the virtual qudits as it is a departure from previous similar work [BR06, BFBD11]. We discuss in Sec. 3.6.1 how to subsequently construct Hamiltonians whose interactions involve at most 2 virtual qudits.

3.2.1 Types of PEPS

Because we take a perturbative approach in this work, we will construct a parent Hamiltonian for a state within the same phase as a given PEPS, such that the ground state of our model can be made arbitrarily close to the PEPS by taking the perturbation parameter to be small enough. For this to be a sensible approach, we require parent Hamiltonians for the PEPS under consideration to be gapped and stable (in an appropriate sense) with respect to small perturbations. This criterion is formalized as *topological order*, and will be defined later in this section. As well as the topological order condition, our procedure will require the PEPS we treat to possess additional structure as compared to the most general definition of PEPS. We are interested in the broadest such structure that will allow us to demonstrate our result.

Apart from topologically ordered PEPS, there are two main subclasses of PEPS that we will need to consider: *isometric* PEPS and *quasi-injective* PEPS. Isometric PEPS are a natural and important subclass of PEPS, and are renormalization fixed points [SPGC11]. Quasi-injectivity is the least natural of the classes we consider and is mainly a technical tool required in our analysis. We argue that it is a generalization of several known classes of PEPS such as injective PEPS [PGVCW08] and G-injective PEPS [SCPG10], which have properties that make them amenable to our construction.

Isometric PEPS

Definition 5 (Isometric PEPS [SPGC11, SCPG10])**.** *A PEPS is isometric if the projection maps $\mathscr{P}_s$ are isometries.*

Notably, for isometric PEPS $P_s \equiv \mathscr{P}_s^\dagger \mathscr{P}_s$ is a (Hermitian, idempotent) projector acting on the virtual qudit space.

Apart from being renormalization fixed-points, isometric PEPS also give a simpler form for the parent Hamiltonian than the general case [SCPG10]. In this work, we will require all PEPS we treat to be isometric, as we will make use of the additional structure of their parent Hamiltonians in our analysis. For isometric PEPS, we can write a canonical parent Hamiltonian on the virtual space as

$$H_{\mathrm{can},v} = \mathscr{P}_\Lambda^\dagger H_{\mathrm{can},c} \mathscr{P}_\Lambda \tag{3.3}$$
$$= -\sum_R \mathscr{P}_\Lambda^\dagger \omega_R \mathscr{P}_\Lambda \tag{3.4}$$

where $\mathscr{P}_\Lambda = \prod_{s\in\Lambda} \mathscr{P}_s$. Explicitly, this Hamiltonian will be be a parent Hamiltonian for the encoded PEPS state

$$|\psi_{\mathrm{PEPS}}\rangle_v = \prod_s P_s \prod_e |\Phi_D(e)\rangle_v \tag{3.5}$$

defined on the virtual space.

Quasi-injective PEPS

We will define a class of PEPS that we call *quasi-injective* PEPS, inspired by several known classes of PEPS. The most fundamental of these known classes is injective PEPS [PGVCW08], which are technically defined as those PEPS whose projection maps have left inverses. Injectivity has important consequences for properties of the parent Hamiltonian, and in particular injective PEPS can be shown to be unique ground states of their canonical parent Hamiltonians, which can be defined to be 2-local [PGVCW08]. Broader classes of PEPS with similar structure have been proposed, such as G-injective PEPS [SCPG10] for finite groups G, (G,ω)-injective PEPS [Bue14] for a finite group G and 3-cocycle ω, and H-injective PEPS [BMCA13]

for finite-dimensional C^* Hopf algebras H. Recently, a notion of injectivity based on the use of a projection matrix product operator (MPO) that includes many (perhaps all) of these previous classes has been developed [SWB+14], known as MPO-injectivity. MPO-injective PEPS can describe a large class of topologically ordered states including the ground states of string-net models [LW05]. In contrast to injective PEPS, which represent unique ground states of local Hamiltonians, these other classes typically represent the ground states of topologically ordered systems that would generally have degenerate ground spaces.

For all of these classes of PEPS (injective, G-injective, etc.), the canonical parent Hamiltonians can be shown to have additional structure that is not present in the general case. In particular, isometric PEPS that are also injective or G-injective have canonical parent Hamiltonians (3.2) whose terms take a particularly simple form:

$$\omega_R = \mathscr{P}_R \cdot \left(\prod_{e \in R} |\Phi_D(e)\rangle\langle\Phi_D(e)|_v \right) \cdot \mathscr{P}_R^\dagger \tag{3.6}$$

Importantly, the Hamiltonian (3.2) can be chosen to be both local and gapped for these PEPS [PGVCW08, SPGC11, SCPG10].

Our construction will, among other things, require the PEPS under consideration to have canonical parent Hamiltonians that are local, gapped, and whose terms take the form of Eq. (3.6). Injective or G-injective isometric PEPS have these properties, but we wish to be as general as possible. We will therefore define the class of quasi-injective PEPS to be those that satisfy the loosest such conditions that are sufficient to prove our main results. We believe that, for isometric PEPS, our definition of quasi-injectivity generalizes the known classes of PEPS mentioned earlier (injective, G-injective, (G,ω)-injective, H-injective, and MPO-injective). Loosely speaking, the conditions we impose require that the PEPS is stabilized by a set of operators $\Upsilon_{\{R_{P_i}, R_{E_i}\}}$ defined below, in the sense that the PEPS is an eigenstate of each $\Upsilon_{\{R_{P_i}, R_{E_i}\}}$ corresponding to its highest eigenvalue. Explicitly, these (Hermitian) operators acting on the virtual space take the form

$$\Upsilon_{\{R_{P_i}, R_{E_i}\}} = \frac{1}{2} P_{\bigcup_j \{R_{P_j}, R_{E_j}\}} \left(\prod_i P_{R_{P_i}} \left(\prod_{e \in R_{E_i}} |\Phi_D(e)\rangle\langle\Phi_D(e)|_v \right) \right) P_{\bigcup_j \{R_{P_j}, R_{E_j}\}} + \text{h.c.} \tag{3.7}$$

where the R are connected regions of the graph and $P_R = \prod_{s \in R} \mathscr{P}_s^\dagger \mathscr{P}_s$. The set $\{R_{P_i}, R_{E_i}\} = \{R_{P_1}, R_{P_2}, \ldots, R_{E_1}, R_{E_2}, \ldots\}$ is a set of regions, with $\bigcup_j \{R_{P_j}, R_{E_j}\}$ their union.

PEPS is a tensor network ansatz in the sense that the projection map can be defined by a tensor with indices corresponding to each virtual and code qudit. In this picture, the operators $\Upsilon_{\{R_{P_i}, R_{E_i}\}}$ can be thought of as contractions of the tensors defining the PEPS projector in various ways. This is because each P_s can be thought of as a tensor with input and output indices for each virtual qudit, and $|\Phi_D(e)\rangle\langle\Phi_D(e)|_v$ acts to contract the relevant indices of these tensors on the sites e connects. In particular, $\Upsilon_{\{\emptyset, R\}} = P_R \left(\prod_{e \in R} |\Phi_D(e)\rangle\langle\Phi_D(e)|_v \right) P_R = \mathscr{P}_R^\dagger \omega_R \mathscr{P}_R$ corresponds to the contraction of all of the pairs of indices of P_R corresponding to

edges in R.

Given these $\Upsilon_{\{R_{P_i},R_{E_i}\}}$ operators, we can explicitly define the quasi-injectivity condition as follows:

Definition 6 (Quasi-injective PEPS)**.** *An isometric PEPS is quasi-injective if*

$$\Upsilon_{\{R_{P_i},R_{E_i}\}}|\psi_{\mathrm{PEPS}}\rangle_v = \eta_{\{R_{P_i},R_{E_i}\}}|\psi_{\mathrm{PEPS}}\rangle_v\,, \tag{3.8}$$

for $\eta_{\{R_{P_i},R_{E_i}\}}$ the largest eigenvalue of $\Upsilon_{\{R_{P_i},R_{E_i}\}}$.

Most significantly, isometric quasi-injective PEPS have the property that

$$H_{\mathrm{par},v} = -\sum_{\{R_{P_i},R_{E_i}\}} c_{\{R_{P_i},R_{E_i}\}}\Upsilon_{\{R_{P_i},R_{E_i}\}}\,, \tag{3.9}$$

is a valid frustration-free parent Hamiltonian for any choice of $c_{\{R_{P_i},R_{E_i}\}} > 0$. This is a direct consequence of the condition (3.8). It is also clear from the fact that $H_{\mathrm{par},v}$ contains all terms in the canonical parent Hamiltonian that if (3.2) is gapped, the Hamiltonian (3.9) is also gapped. This follows from the fact that every term is minimized in the ground space, and so additional terms can only increase the size of the gap.

We emphasise that the notion of quasi-injectivity is designed to be the loosest notion required for our results to hold, and it is expected (in the isometric case) to encompass the broad class of PEPS listed above, including injective, G-injective, (G,ω)-injective, H-injective, and MPO-injective PEPS. To illustrate this, we provide a proof sketch that all MPO-injective PEPS for which the 'generalized inverse' (defined in Ref. [SWB$^+$14]) is the identity map are quasi-injective, noting that this class includes injective, G-injective, (G,ω)-injective and string-net PEPS. For isometric PEPS, as we consider in this chapter, it is believed that all MPO-injective PEPS have a generalized inverse equal to the identity. We also believe that quasi-injectivity captures the relevant features of higher dimensional analogues of these classes, such as projected entangled pair operator (PEPO)-injective PEPS that are the natural extension of MPO-injective PEPS. We leave the development of a formal proof of the relationship between quasi-injectivity and other forms of injectivity to future work. The close relationship between MPO-injective PEPS and topologically ordered PEPS in 2 dimensions may also suggest a close relationship between quasi-injective PEPS and topologically ordered PEPS in general.

Proof sketch: Consider the operator $\Upsilon_{\{R_{P_i},R_{E_i}\}}$ acting on an MPO-injective PEPS. Consider each projection factor of $\Upsilon_{\{R_{P_i},R_{E_i}\}}$ as defined in Eq. (3.7) to be applied sequentially. As we apply projectors on maximally-entangled states associated with some set of bonds on the lattice, this acts to block sites. This is because for MPO-injective PEPS, the generalised inverse tensor can be considered to be a blocking operation. For those MPO-injective PEPS with trivial generalized inverse, this simply corresponds to a contraction of the relevant bond, which in our context is implemented by the projection onto the maximally entangled state. Applying PEPS projectors on some set of sites then removes these sites from any blocks. The

pull-through condition of MPO-injective PEPS ensures that blocks with such sites removed indeed remain blocks. Note that $\Upsilon_{\{R_{P_i},R_{E_i}\}}$ is composed of a sequence of such bond projections that block sites followed by PEPS projectors that remove sites from blocks. At the conclusion of this sequence, the state is described by blocks of sites (not necessarily geometrically local); however, applying the PEPS projector at all sites restores the original PEPS state, thereby guaranteeing that the PEPS is stabilized by all $\Upsilon_{\{R_{P_i},R_{E_i}\}}$ as required by quasi-injectivity.

Topological Order

The quasi-injective and isometric conditions discussed above are specific to the PEPS framework. In contrast, the topological order condition applies more generally to frustration-free, gapped, local Hamiltonian systems. Systems with topological order have inherent stability to quasi-local perturbations (defined below). Since we will be using a perturbative approach, we must consider the effect of high order corrections in the perturbation expansion, and topological stability results will be crucial to establishing the robustness of our results to these corrections. In our context, the topological order condition will be applied to the family of canonical parent Hamiltonians (3.2) for a given PEPS.

The following results have been developed in a sequence of works [BHM10, BH11b, MZ13] on the definition and stability of topologically ordered systems (see also related work on stability of tensor network states [SW15, CMPGS13]). It is not our intention to provide a complete discussion of topological order, and we will we will simply paraphrase the relevant definitions and results here. We neglect several details (in particular, we restrict our discussion to infinite length scales); interested readers should consult Ref. [MZ13] for a more thorough treatment and for technical details of these conditions.

Definition 7 (Local-TQO)**.** *Consider a gapped Hamiltonian $H_0 = \sum_{u\in\Lambda} L_u$ for some L_u supported in local regions around site u of a graph Λ. Let $P_0(R)$ be the projector to the ground space of the restricted Hamiltonian $H_R = \sum_{u\in R} L_u$ for a region $R \subseteq \Lambda$. The system is said to obey* Local-TQO *iff for all operators X_R acting on a finite region R, there exists a superpolynomially decaying function $f(r)$ such that*

$$\left\| P_0(R_r) X_R P_0(R_r) - \frac{\operatorname{Tr} P_0(R_r) X_R}{\operatorname{Tr} P_0(R_r)} P_0(R_r) \right\| \leq \|X_R\| f(r) \tag{3.10}$$

for all finite r, where R_r is a region enclosing all points within distance r from R (including R itself).

Definition 8 (Local-Gap)**.** *Given a gapped, local Hamiltonian H_0, we say that it obeys the* Local-Gap *condition iff for each $R \subseteq \Lambda$ and $r \geq 0$, we have that H_{R_r} has gap at least $g(r)$ for g a function decaying at most polynomially in r.*

The Local-TQO condition formalises the colloquial definition of a topologically ordered system as one whose ground states cannot be distinguished by local operations. The Local-Gap condition is required to prove the topological stability results below.

If at least one canonical parent Hamiltonian for the PEPS satisfies Local-TQO and Local-Gap, we say that the PEPS is topologically ordered. One might be concerned that in general some special choices of canonical parent Hamiltonian will satisfy these conditions while the rest will not. It can easily be seen that if one canonical parent Hamiltonian defined by a set of regions $\{R\}$ satisfies the topological order conditions, then the family of canonical parent Hamiltonians defined by region sets $\{R'\} \supseteq \{R\}$ are also topologically ordered. Thus for large enough sets of regions the Local-TQO and Local-Gap conditions are universal properties of a PEPS, rather than properties of a specific canonical parent Hamiltonian.

We will also require a notion of quasi-locality for operators. An operator X will be called (J,μ)-quasi-local iff it has a local decomposition $X = \sum_{s\in\Lambda}\sum_r X_{s,r}$ for $X_{s,r}$ with support only within radius r of site s, and $\|X_{s,r}\| \leq J\mu^r$ for some $\mu < 1$.

Given a PEPS that is topologically ordered, we can make use of the topological stability theorem:

Theorem 9 (Topological Stability [MZ13])**.** *Given a frustration-free Hamiltonian H_0 with $O(1)$ gap, satisfying the Local-TQO and Local-Gap conditions, there exists $\varepsilon > 0$ such that $H = H_0 + \varepsilon V$ has spectral gap $O(1)$ for quasi-local V.*

Note that systems satisfying both Local-TQO and Local-Gap conditions need not have degenerate ground spaces as one might expect for a conventional notion of a topologically ordered system. In particular, canonical parent Hamiltonians of injective PEPS as well as G-injective PEPS, etc. are topologically ordered by this definition. It seems natural to conjecture that the appropriate definition of quasi-injectivity is really equivalent to (or at least implied by) the topological order conditions. Unfortunately it is unclear to us how to prove this conjecture.

3.3 Overview of results

In this section we give an outline of our method and results. Given a suitable PEPS, our goal is to construct a quantum spin model with 2-body interactions that is a parent Hamiltonian for a state within the same phase as this PEPS. We will first describe the form of the Hamiltonian by which we achieve this, before stating our main theorems. Sections 3.4 and 3.5 will be devoted to proving these theorems.

3.3.1 Construction

Our strategy will be to use a perturbative Hamiltonian to simulate the different elements of the PEPS construction. In contrast to a conventional PEPS parent Hamiltonian, our model acts on the virtual qudit space, as opposed to the code qudit space. The unperturbed dynamics of our model will be such that the ground space of our system is an encoded form of the relevant PEPS code space.

Our main tool is the code gadget [BFBD11], which can be understood as the collection of virtual qudits at each site of the PEPS lattice, together with a Hamiltonian whose ground space is the desired code space (i.e. an encoding of a physical qudit in the PEPS language). From this point on all operators act on the virtual qudits unless otherwise stated, and so we will suppress v subscripts on operators and states. The encoding of the d-dimensional code qudit in the virtual space is given (up to 1-local unitaries) by the projection map $\mathscr{P}_s$. The simplest way to achieve this encoding in the ground space of a code gadget is by using the Hamiltonian

$$Q_s = 1 - P_s \tag{3.11}$$

with $P_s \equiv \mathscr{P}_s^\dagger \mathscr{P}_s$ the projector to the PEPS code space (for an isometric PEPS). Each of these code gadgets therefore corresponds to a single code qudit.

Note that the Q_s act on a single code gadget, but this corresponds to $\deg(s)$ virtual qudits. Thus, in terms of the virtual qudits of the model, this is a $\deg(s)$-body interaction. We will generally analyse this model as written, and in Sec. 3.6.1 discuss how to reduce the interactions from $\deg(s)$-body to 2-body on the virtual qudits if required.

We couple the code gadgets perturbatively according to the structure of the PEPS lattice Λ, and this coupling will mediate the correlations present in the PEPS. For each edge e of the PEPS lattice, we define a coupling term

$$M_e = |\Phi_D(e)\rangle\langle\Phi_D(e)| \tag{3.12}$$

with M the projector to the maximally entangled state of the relevant virtual space dimension D.

The Hamiltonian of our system is then given by

$$H = \sum_{s\in\Lambda} Q_s - \varepsilon \sum_e M_e \tag{3.13}$$

where $\varepsilon \ll 1$. This is a 2-body Hamiltonian (considering each code gadget to be a single particle), and we will show that it is a valid parent Hamiltonian for a state in the same phase as the desired isometric, quasi-injective, topologically ordered PEPS.

A simple example of this construction is analysed in Sec. 3.7. The analysis uses a simplified formalism and is much more accessible than the main technical sections; some readers may wish to read it before tackling the technical issues that are required to treat the general case.

3.3.2 Results

Our analysis of the model described above proceeds in several stages. The main idea is to compute a perturbation expansion in ε for a low-energy effective Hamiltonian of the system and analyse its properties. To achieve this, we use the global Schrieffer-Wolff perturbation

method [SW66, BDL11] as described in Sec. 3.4. We find the following result:

Theorem 10. *Given an isometric, quasi-injective PEPS with gapped canonical parent Hamiltonian, there exists finite n_* such that the global Schrieffer-Wolff effective Hamiltonian for our model to order n_* in the perturbation parameter ε is a frustration-free parent Hamiltonian for the PEPS and has gap $O(\varepsilon^{n_*})$ for sufficiently small $\varepsilon > 0$.*

This theorem is proved in Sec. 3.4 and is the most crucial part of our analysis.

Beyond this result, we would like to demonstrate that the full Hamiltonian (3.13) is gapped and has ground state in the same phase as the desired PEPS. In this direction, we analyse the stability of the gap of the n_*^{th} order effective Hamiltonian to the addition of higher order terms in the perturbation expansion. Such stability would guarantee that the n_*^{th} order effective Hamiltonian is adiabatically connected to the full effective Hamiltonian at arbitrary order in perturbation theory, and so their ground states are in the same phase.

In order to guarantee any kind of stability against the additional contribution from higher order terms in the perturbation expansion, we appeal to known results for topologically ordered systems [MZ13, BHM10, CMPGS13]. If a given PEPS is topologically ordered as well as isometric and quasi-injective, then we can use Theorem (10) together with the local Schrieffer-Wolff perturbation method [DFRBF96, BDL11] to demonstrate the following theorem:

Theorem 11. *Given an isometric, quasi-injective, topologically ordered PEPS, there exists perturbation strength $\varepsilon > 0$ such that the effective Hamiltonian for our model to any order $k > n_*$ is in the same phase as the n_*^{th} order effective Hamiltonian.*

Here we define two ground states of gapped quasi-local Hamiltonians H_1 and H_2 to be in the same phase iff H_1 can be connected to H_2 by a quasi-local adiabatic evolution that does not close the spectral gap. Theorems 10 and 11 straightforwardly imply the following theorem, which is the main result of this chapter.

Theorem 12. *There exists perturbation strength $\varepsilon > 0$ such that the low-energy effective Hamiltonian corresponding to the system (3.13) is a gapped parent Hamiltonian for a state in the same phase as the quasi-injective, isometric, topologically ordered PEPS under consideration to any order $k > n_*$ of perturbation theory.*

Our proof of Theorem 11 is given in Sec. 3.5 and involves two stages. We first transform the effective Hamiltonian derived from the global Schrieffer-Wolff method to one defined by the related local Schreiffer-Wolff method [DFRBF96, BDL11]. Although the global SW expansion has structure which allows for the proof of Theorem 10, the higher-order terms in its expansion cannot easily be bounded. Conversely, the local SW expansion has explicit locality properties that allow us to analyse higher-order terms, but does not allow for a direct proof of Theorem 10. By transforming between these two effective Hamiltonian expansions, we are able to make use of the convenient features of both. This transformation between the global and local

Schrieffer-Wolff effective Hamiltonians can be treated as a quasi-local perturbation, and is thus guaranteed to preserve the gap by the topological stability theorem.

Once we have demonstrated that the local SW effective Hamiltonian is in the same phase as the global SW effective Hamiltonian, we show that the higher order contributions to the local SW effective Hamiltonian can also be treated as quasi-local perturbations on the n_*^{th} order Hamiltonian and so will not induce a phase transition. A caveat to this statement that will be made clear in the analysis is that we use a slightly modified effective Hamiltonian as compared to the standard definition of the local SW expansion. The composition of each of these results defines an adiabatic path from the n_*^{th} order global SW effective Hamiltonian to our effective Hamiltonian at arbitrary finite order, proving Theorem 11.

In addition, one would ideally like to show stability against contributions from the excited space of the unperturbed Hamiltonian, which are neglected in the effective Hamiltonian. While we expect that it may be possible to prove this kind of rigorous result using similar tools to those used here, the bounds from Ref. [BDL11] on the size of these additional high-energy terms are insufficient for this purpose, and so a complete proof of stability against such terms is beyond the scope of this work. Our analysis demonstrates that the low energy effective Hamiltonian of our model is a parent Hamiltonian for the desired state, but it does not prove that this effective Hamiltonian is a good description of the low energy physics of our system (i.e., that perturbation theory is accurate in this regime). While in principle, states from the excited space of the unperturbed Hamiltonian could contribute to the low energy physics of our model, we do not know of any examples for which such unusual behaviour occurs. We leave the investigation of such breakdowns of perturbation theory to future work.

3.4 Perturbation Analysis

3.4.1 Preliminaries

As in Sec. 3.3.1, we define our system by a Hamiltonian of the form $H = H_0 + \varepsilon V$ with

$$H_0 = \sum_{s\in\Lambda} Q_s\,, \qquad V = -\sum_e M_e \tag{3.14}$$

where $\varepsilon \ll 1$. The projector to the ground space of the unperturbed Hamiltonian H_0 is defined as $P_0 = P_\Lambda = \prod_s P_s$, and $P_0 H_0 = H_0 P_0 = 0$. It will also be convenient to define the projector to the unperturbed excited space $Q_0 \equiv 1 - P_0$. Let Δ_0 be the gap of H_0 and note that $\Delta_0 = 1$. We define $N \equiv |\Lambda|$ to be the total number of sites of the PEPS graph.

We can motivate this choice of perturbative Hamiltonian by noticing that the low-energy behaviour of the Hamiltonian (3.13) will involve projectors to maximally entangled states of virtual qudits acting within the code space (or the unperturbed ground space), much as in the terms of the canonical parent Hamiltonian (3.6). This will allow us to argue that the low-energy effective Hamiltonian of our model is a valid parent Hamiltonian for a given PEPS, albeit in an

encoded form. We will revisit this intuitive picture before proceeding to the general analysis, but first let us define our perturbation formalism.

3.4.2 Global Schrieffer-Wolff perturbation expansion

We are interested in the low energy effective Hamiltonian of our system. To derive this effective Hamiltonian, we will make use of the global Schrieffer-Wolff (SW) perturbation expansion [SW66, BDL11]. We give a brief review of some relevant properties of the global SW method here, following Ref. [BDL11]. We will focus on the relevant case where the unperturbed Hamiltonian is 1-local and the perturbation is 2-local on the lattice Λ, which has bounded degree.

The effective Hamiltonian derived from the global SW method is based on a transformation $e^S H e^{-S}$ that block diagonalizes H with respect to the ground and excited spaces of the unperturbed Hamiltonian H_0. We define an anti-Hermitian operator S such that

$$P_0 e^S H e^{-S} Q_0 = Q_0 e^S H e^{-S} P_0 = 0 \tag{3.15}$$

That is, the transformed Hamiltonian $e^S H e^{-S}$ has vanishing block-off-diagonal components.

Together with (3.15), the conditions $P_0 S P_0 = Q_0 S Q_0 = 0$ and $\|S\| < \frac{\pi}{2}$ uniquely define S. We will expand S in a Taylor series in ε and use this to compute an effective Hamiltonian expansion, but before we proceed we will introduce some notations. Define

$$\mathscr{L}(X) = \frac{Q_0}{H_0} X P_0 - P_0 X \frac{Q_0}{H_0} \tag{3.16}$$

$$X_{\mathrm{d}} = P_0 X P_0 + Q_0 X Q_0 \tag{3.17}$$

$$X_{\mathrm{od}} = P_0 X Q_0 + Q_0 X P_0 \tag{3.18}$$

for any operator X, where we define $\frac{Q_0}{H_0}$ in the obvious way to vanish on the image of P_0.

Without loss of generality, we set $H_0 P_0 = P_0 H_0 = 0$, i.e., the unperturbed ground state energy is set to zero. Because of this zero eigenvalue, we note that we can express $\frac{Q_0}{H_0}$ as $Q_0 \tilde{g}$ with

$$\tilde{g} = \tilde{\Delta} P_0 + \frac{Q_0}{H_0} \tag{3.19}$$

for an *arbitrary* constant $\tilde{\Delta}$. We will make extensive use of this identity, and the freedom to set $\tilde{\Delta}$, to prove our result.

Equipped with these notations, and following Ref. [BDL11], we expand $S = \sum_{j=1}^{\infty} \varepsilon^j S_j$ as a

series of anti-Hermitian operators $S_j = -S_j^\dagger$, finding

$$S_1 = \mathscr{L}(V) \tag{3.20}$$

$$S_j = \mathscr{L}\left([S_{j-1}, V_{\mathrm{d}}]\right) + \sum_{i=1}^{\left\lfloor \frac{j-1}{2} \right\rfloor} a_{2i} \mathscr{L}\left(W_{2i}^{(j-1)}\right) \qquad \text{for } j > 1 \tag{3.21}$$

for $a_i = \frac{2^i B_i}{i!}$ with B_i the Bernoulli numbers, and

$$W_m^{(k)} = \sum_{\substack{j_1,\ldots,j_m \geq 1 \\ j_1+\ldots+j_m=k}} [S_{j_1}, [S_{j_2}, [\cdots, [S_{j_m}, V_{\mathrm{od}}] \cdots]]] \tag{3.22}$$

This yields an effective Hamiltonian to order n of the form

$$H_{\mathrm{eff}}^{\langle n \rangle} = P_0 H_0 P_0 + \sum_{j=1}^{n} \varepsilon^j P_0 V^{(j-1)} P_0 \tag{3.23}$$

where

$$V^{(0)} = V \tag{3.24}$$

$$V^{(j-1)} = \sum_{i=1}^{\left\lfloor \frac{j}{2} \right\rfloor} b_{2i-1} W_{2i-1}^{(j-1)}, \qquad j > 1 \tag{3.25}$$

with $b_{2i-1} = \frac{2(2^{2i}-1)B_{2i}}{(2i)!}$.

The terms in Eq. (3.23) can be systematically calculated through a diagrammatic technique [BDL11], but for our purposes, we will not need to calculate the exact expansion of the effective Hamiltonian for a general PEPS to arbitrary order. It will suffice for us to note that each term $P_0 V^{(j)} P_0$ in (3.23) can be written as a linear combination of operators of the form

$$\Gamma(q_1, \ldots, q_j) = P_0 \left(\prod_{i=1}^{j} V g_{q_i} \right) V P_0 \tag{3.26}$$

for integers q_i with $\sum_i |q_i| = j$, and where g_q is defined by

$$g_0 = P_0 \tag{3.27}$$

$$g_q = \tilde{g}^q = \tilde{\Delta}^q P_0 + \frac{Q_0}{H_0^q} \qquad \text{for } q \geq 1 \tag{3.28}$$

$$g_q = P_0 \tilde{g}^{|q|} = \tilde{\Delta}^{|q|} P_0 \qquad \text{for } q \leq -1\,. \tag{3.29}$$

This can be seen by the application of Eqs. (3.20-3.25) and making use of the identities $\frac{Q_0}{H_0} = Q_0 \tilde{g}$, $Q_0 = 1 - P_0$, and $H_0 P_0 = P_0 H_0 = 0$.

We will also make use of the fact that the effective Hamiltonian Eq. (3.23) obeys the linked cluster theorem [Kle74], which loosely states that all terms in the perturbative expansion at order n are $O(n)$-local. More precisely, recall that the perturbation V is a sum of 2-local terms. Then the effective Hamiltonian at order n can be decomposed into a sum of terms, each of which correspond to the product of n such 2-local perturbations. The linked cluster theorem states that the effective Hamiltonian terms corresponding to any product of perturbations which are "unlinked" (there exists a bipartition of the perturbations such that the supports of these sets are disjoint), must vanish. This implies that at order n, the terms in the effective Hamiltonian can act on at most $(n+1)$ sites, which must all be within a local region of size $(n+1)$.

3.4.3 Ground space of the effective Hamiltonian

In this section, we prove Theorem 10. That is, we will show that to some finite order n_*, the effective Hamiltonian expansion of Eq. (3.13) is a gapped parent Hamiltonian for the desired quasi-injective, isometric PEPS with a gapped canonical parent Hamiltonian. Before we begin the proof in earnest, let us briefly attempt to give some intuition for our construction.

The effective Hamiltonian (3.23) can be written as a linear combination of $\Gamma(q_1,\ldots,q_j)$ operators as defined in Eq. (3.26). Imagine for the moment that we were able to neglect the g_q terms in these operators (i.e. neglect the dependence on the spectrum of H_0). These operators would then reduce to $P_0 V^{j+1} P_0$, and for isometric, quasi-injective PEPS the effective Hamiltonian would take the form

$$H_{\text{eff}}^{\langle n\rangle} \sim -\sum_{j=0}^{n} \varepsilon^n P_0 \left(\sum_e M_e\right)^j P_0 \qquad \text{(neglecting constants and } g_q \text{ factors)} \tag{3.30}$$

$$\sim -\sum_R \mathscr{P}_\Lambda^\dagger \bar{\omega}_R \mathscr{P}_\Lambda \tag{3.31}$$

where R runs over all regions containing at most n edges.

Equation (3.31) is precisely the encoded parent Hamiltonian (3.4), and so for $n \sim O(r_*)$ will have the desired PEPS as its ground state. (Recall from Sec. 3.2 that r_* is the maximum required region size to guarantee the canonical parent Hamiltonian has the correct ground space.) The following sections will be devoted to giving this simple intuition a level of rigor.

Analysis

In order to analyse the ground space of the effective Hamiltonian (3.23), it will be useful to split it into two parts: $H_{\text{eff}}^{\langle n\rangle} = \tilde{H}_{\text{eff}}^{\langle n\rangle} + \tilde{H}_{\text{else}}$, where $\tilde{H}_{\text{eff}}^{\langle n\rangle}$ contains all $\Gamma(q_1,\ldots,q_j)$ terms with all q_i positive, and $\tilde{H}_{\text{else}}$ contains the terms with at least one $q_i \leq 0$. The motivation for this split is that g_q for $q \leq 0$ are proportional to P_0, while those with $q > 0$ are not. This distinction will prove crucial in the analysis.

The constraint $\sum_i |q_i| = j$ implies that the only Γ terms with all positive q_i have all $q_i = 1$. It is straightforward to demonstrate that $\tilde{H}_{\text{eff}}^{\langle n \rangle}$ can be written as

$$\tilde{H}_{\text{eff}}^{\langle n \rangle} = P_0 H_0 P_0 + \sum_{j=1}^{n} (-1)^j \varepsilon^j P_0 \Gamma(\underbrace{1,1,\ldots 1,1}_{j}) P_0 \,, \tag{3.32}$$

where we have made use of the fact that $b_1 = \frac{1}{2}$. The behavior of Eq. (3.32) actually depends on the value of $\tilde{\Delta}$, in contrast to the complete effective Hamiltonian (3.23) which is independent of $\tilde{\Delta}$. This is because we have neglected some terms which would otherwise cancel out the effect of $\tilde{\Delta}$ in the Hamiltonian.

Our proof of Theorem 10 will proceed in two parts. In the first, we will expand the restricted Hamiltonian $\tilde{H}_{\text{eff}}^{\langle n \rangle}$ of Eq. (3.32) to some finite order $n_* \sim r_*$ (recall the definition of r_* in Sec. 3.2), and show that this is a valid parent Hamiltonian for a given (quasi-injective, isometric) PEPS for sufficiently large $\tilde{\Delta}$. This may seem suspicious at first glance, as our proof only holds for sufficiently large values of an unphysical parameter. However, since r_* is finite for the PEPS we consider, $\tilde{\Delta}$ should be understood as a placeholder for some $O(1)$ (i.e. intensive) constant that will be important in the subsequent analysis. Although the value of $\tilde{\Delta}$ chosen does not affect the behavior of the effective Hamiltonian (3.23), the value of $\tilde{\Delta}$ required to demonstrate this result captures the magnitude of a relevant energy scale in the problem.

In the second part of the proof, we will restore the neglected terms $\tilde{H}_{\text{else}}$ to analyse the complete effective Hamiltonian (3.23) at order n_*. We will show that there exists sufficiently small ε that the physics of (3.23) is dominated by $\tilde{H}_{\text{eff}}^{\langle n \rangle}$. That is, the additional contributions from $\tilde{H}_{\text{else}}$ do not affect the ground space nor gappedness of the Hamiltonian. The required value of ε will be set in part by the value of $\tilde{\Delta}$. The neglected terms that we restore in this part of the analysis have some properties that will be quite useful. Recall that every neglected term has at least one $q_i < 1$, and $g_q \propto P_0$ for all $q < 1$. This allows us to decompose any such term into a product of $\Gamma(1,1,\ldots,1,1)$ terms. Putting our Hamiltonian into this form (i.e. a sum of products of $\Gamma(1,1,\ldots,1,1)$ terms) will allow us to analyse it effectively.

We now prove Theorem 10, beginning with the following lemma.

Lemma 13. *There exists $O(1)$ (i.e. intensive) constants $\tilde{\Delta}$ and $n = n_*$ such that $\tilde{H}_{\text{eff}}^{\langle n \rangle}$ is a valid parent Hamiltonian for a given quasi-injective, isometric PEPS with ground state energy < 0.*

Proof. Consider one of the terms in the restricted effective Hamiltonian of Eq. (3.32):

$$(-1)^j \Gamma(1,1,\ldots 1,1) = (-1)^j P_0 \left(\prod_{i=1}^{j-1} V \tilde{g} \right) V P_0 \tag{3.33}$$

$$= -P_0 \left(\prod_{i=1}^{j-1} \left(\sum_e M_e \right) \tilde{g} \right) \left(\sum_e M_e \right) P_0 \tag{3.34}$$

Similarly to Eq. (3.31), if we could ignore the $\tilde{g}$ terms, this would become a sum of $\mathscr{P}_\Lambda^\dagger \omega_R \mathscr{P}_\Lambda$

operators. Thus we begin our analysis by expanding the operator $\tilde{g}$ as follows:

$$\tilde{g} = \tilde{\Delta} P_0 + \frac{Q_0}{H_0} = \tilde{\Delta} P_0(\Lambda) + \frac{1}{\Delta_0} P_1(\Lambda) + \frac{1}{2\Delta_0} P_2(\Lambda) + \ldots + \frac{1}{N\Delta_0} P_N(\Lambda) \tag{3.35}$$

for $P_i(\Lambda)$ the projector to the i^{th} excited space of H_0. This follows from the equally spaced spectrum of the unperturbed Hamiltonian H_0. In fact, we will be interested only in the effect of $\tilde{g}$ on local regions R, and so we will generally need only consider excited states up to energy $|R|\Delta_0$. Define the restricted operator

$$\tilde{g}(R) = \tilde{\Delta} P_0(R) + \frac{1}{\Delta_0} P_1(R) + \frac{1}{2\Delta_0} P_2(R) + \ldots + \frac{1}{|R|\Delta_0} P_{|R|}(R) \tag{3.36}$$

where the $P_i(R)$ involve only states with excitations localized within R.

Since H_0 is a sum of commuting projectors Q_s, we can easily enumerate all possible states with i excitations localized within a region R. The corresponding projectors $P_i(R)$ can each be expanded as

$$P_i(R) = P_{\Lambda\setminus R} \sum_{R'\subseteq R:|R'|=i} \left(\prod_{s'\in R'} Q_{s'} \right) \left(\prod_{s\in R\setminus R'} P_s \right) \tag{3.37}$$

$$= P_{\Lambda\setminus R} \sum_{k=0}^{i} \left(\sum_{R''\subseteq R:|R''|=(i-k)} (-1)^k \binom{|R|-(i-k)}{k} \left(\prod_{s\in R\setminus R''} P_s \right) \right) \tag{3.38}$$

where $R_1 \setminus R_2$ contains the sites of R_1 that are not in R_2, and we have expanded the $Q_s = 1 - P_s$ on the second line. Noting that $\sum_{R''\subseteq R:|R''|=j} \prod_{s\in R\setminus R''} P_s = \sum_{R'\subseteq R:|R'|=|R|-j} P_{R'}$, we find

$$\begin{aligned} \tilde{g}(R) = &\left(\tilde{\Delta} + \sum_{i=1}^{|R|} (-1)^i \frac{1}{i\Delta_0} \binom{|R|}{i} \right) \cdot P_0 \\ &+ \sum_{j=1}^{|R|} \left(\sum_{k=0}^{|R|-j} (-1)^k \frac{1}{(j+k)\Delta_0} \binom{|R|-j}{k} \right) \cdot \sum_{R'\subseteq R:|R'|=|R|-j} P_{R'} P_{\Lambda\setminus R} \end{aligned} \tag{3.39}$$

The sums over k can be evaluated explicitly, and yields the result

$$\tilde{g}(R) = \left(\tilde{\Delta} - \frac{1}{\Delta_0} h_{|R|} \right) P_0 + \sum_{j=1}^{|R|} \left(j \binom{|R|}{j} \right)^{-1} \cdot \left(\sum_{R'\subseteq R:|R'|=|R|-j} P_{R'} P_{\Lambda\setminus R} \right) \tag{3.40}$$

for $h_{|R|} = \sum_{j=1}^{|R|} \frac{1}{j}$. We can guarantee that the first term in this expression is positive by choosing $\tilde{\Delta} > \frac{1}{\Delta_0} h_{|R|}$, while it is clear that $\left(j \binom{|R|}{j} \right)^{-1}$ is positive for all $j > 0$. It is clear that as long as $|R|$ is finite, we can also choose $\tilde{\Delta}$ finite.

Now returning to $\Gamma(1,1,\ldots 1,1)$, we notice that

$$(-1)^j \Gamma(1,1,\ldots 1,1) = -P_0 \left(\prod_{i=1}^{j-1} \left(\sum_e M_e \right) \tilde{g} \right) \left(\sum_e M_e \right) P_0 \tag{3.41}$$

$$= - \sum_{\substack{\{R_{E_i}\} \\ \sum_i |R_{E_i}|=j}} \sum_{\{R_{P_i}\}} c_{\{R_{E_i},R_{P_i}\}} P_0 \Upsilon_{\{R_{E_i},R_{P_i}\}} P_0 \tag{3.42}$$

for some constants c, recalling the definitions of $\Upsilon_{\{R_{E_i},R_{P_i}\}}$ presented in (3.7) as part of our definition of quasi-injectivity, and using $\tilde{g}(R)$ for $\tilde{g}$ as appropriate. We have also used the fact that the global SW effective Hamiltonian obeys the linked cluster theorem so that all terms in $\tilde{H}_{\text{eff}}^{\langle n \rangle}$ act within regions of size $O(n)$. Further, we can see by comparison with Eq. (3.40) that for sufficiently large $\tilde{\Delta}$, the constants c will all be positive.

Thus, the restricted effective Hamiltonian at nth order can be expressed as

$$\tilde{H}_{\text{eff}}^{\langle n \rangle} = - \sum_{j=0}^{n} \varepsilon^j \sum_{\substack{\{R_{E_i}\} \\ \sum_i |R_{E_i}|=j}} \sum_{\{R_{P_i}\}} c_{\{R_{E_i},R_{P_i}\}} P_0 \Upsilon_{\{R_{E_i},R_{P_i}\}} P_0 \tag{3.43}$$

This Hamiltonian takes the form of Eq. (3.9), and so as demonstrated in Sec. 3.2.1 it will be a valid parent Hamiltonian for a quasi-injective isometric PEPS for sufficiently large n. We can always find some finite order $n_* \sim O(r_*)$ that will contain all regions in the canonical parent Hamiltonian (3.2).

Additionally, because all the terms in (3.43) are negative semi-definite, the ground space energy of $\tilde{H}_{\text{eff}}^{\langle n \rangle}$ cannot be higher than that of $\tilde{H}_{\text{eff}}^{\langle n-1 \rangle}$, and so cannot be higher than 0. □

The proof of Lemma 13 is the main part of our analysis that depends explicitly on the spectrum of H_0. If one were interested in analysing a modified construction with an alternative unperturbed Hamiltonian (3.14) that is 2-body on the virtual qudits as well as the code qudits (as discussed in Sec. 3.6.1), then the analogue of Lemma 13 may need alternative proof techniques.

We have thus far considered the restricted Hamiltonian (3.32). Now we will restore terms from $\tilde{H}_{\text{else}}$ to analyse the complete effective Hamiltonian (3.23). We will demonstrate that there exists sufficiently small but non-zero ε such that the ground spaces of these two Hamiltonians coincide.

The terms neglected in $\tilde{H}_{\text{eff}}^{\langle n \rangle}$ are linear combinations of the terms $\Gamma(q_1,\ldots,q_j)$ where there exists some i such that $q_i < 1$. Since $g_q \propto \left(g_q\right)^2$ for $q < 1$, these $\Gamma(q_1,\ldots,q_j)$ can be rewritten as $\Gamma(q_1,\ldots,q_{i-1})\Gamma(q_{i+1},\ldots,q_j)$ up to constant factors. By making use of the decomposition (3.40) we can expand any $\Gamma(q_1,\ldots,q_j)$ into linear combinations of Υ terms. Decomposing each Γ in this way, we can rearrange the effective Hamiltonian into sums of terms acting on each region of the lattice. The linked-cluster theorem shows that all non-local terms vanish.

Together with the guarantee that the degree of Λ is bounded, this guarantees that for finite n only a finite number of terms act on each region. Thus there exist finite constants $c_i > 0$ and $\tilde{c}_i \in \mathbb{R}$ such that

$$H_{\text{eff}}^{\langle n\rangle} = -\sum_{j=0}^{n}\sum_{k=0}^{n-j}\sum_{\substack{\{R_{E_i}\}\\ \sum_i |R_{E_i}|=j}}\sum_{\{R_{P_i}\}}\sum_{\substack{\{R_{E'_i}\}\\ \sum_i |R_{E'_i}|=k}}\sum_{\{R_{P'_i}\}}\Big(\varepsilon^j c_{\{R_{E_i},R_{P_i}\}} P_0 \Upsilon_{\{R_{E_i},R_{P_i}\}} P_0 + \varepsilon^k c_{\{R_{E'_i},R_{P'_i}\}} P_0 \Upsilon_{\{R_{E'_i},R_{P'_i}\}} P_0 + \varepsilon^{j+k} \tilde{c}_{\{R_{E_i},R_{P_i}\},\{R_{E'_i},R_{P'_i}\}} P_0 \Upsilon_{\{R_{E_i},R_{P_i}\}} \Upsilon_{\{R_{E'_i},R_{P'_i}\}} P_0\Big) \tag{3.44}$$

where $\tilde{c}_{\{R_{E_i},R_{P_i}\},\{R_{E'_i},R_{P'_i}\}} = 0$ if $|R_{E_i}| = 0$ or $|R_{E'_i}| = 0$. If we could also guarantee that all $\tilde{c}_i > 0$, then the proof that $H_{\text{eff}}^{\langle n\rangle}$ is a parent Hamiltonian would be immediate. Unfortunately this will not be the case in general, but noting that $\varepsilon^j, \varepsilon^k \geq \frac{1}{\varepsilon}\varepsilon^{j+k}$ for terms with non-vanishing $\tilde{c}$, we use following simple lemma (given without proof) to show that the ground spaces of $H_{\text{eff}}^{\langle n\rangle}$ and $\tilde{H}_{\text{eff}}^{\langle n\rangle}$ coincide for sufficiently small ε.

Lemma 14. *Consider Hermitian operators A, B with eigenvalues $\eta_1(A) \geq \eta_2(A) \geq \ldots \geq \eta_n(A)$ and $\eta_1(B) \geq \eta_2(B) \geq \ldots \geq \eta_n(B)$. If A and B share a common eigenspace $\mathcal{H}$ with eigenvalues $\eta_1(A)$ and $\eta_1(B)$ respectively, then $\mathcal{H}$ is also an eigenspace of*

$$C = A - \lambda B \tag{3.45}$$

corresponding to the largest eigenvalue of C, for $\lambda < \lambda_c = \frac{\Delta_A}{2||B||}$, with $\Delta_A = \eta_1(A) - \eta_2(A)$. Furthermore, C has a finite gap $\Delta_C > 2||B||(\lambda_c - \lambda)$ between largest and second largest eigenvectors.

Since $\varepsilon^j, \varepsilon^k \geq \frac{1}{\varepsilon}\varepsilon^{j+k}$, we can immediately apply Lemma 14 to conclude that there exists $\varepsilon > 0$ such that each bracketed term has the same ground space as if all $\tilde{c}$ were zero (since we are guaranteed that an isometric, quasi-injective PEPS state corresponds to the highest eigenvalue of any Υ operator). Immediately we can conclude that $H_{\text{eff}}^{\langle n\rangle}$ has the same ground space as $\tilde{H}_{\text{eff}}^{\langle n\rangle}$. If we consider each bracketed term as a (local) operator, this Hamiltonian is also frustration-free. Since the c and $\tilde{c}$ were implicitly functions of $\tilde{\Delta}$, the critical value of ε will similarly be set in part by the value of $\tilde{\Delta}$.

Finally, to complete the proof of Theorem 10, we note that because all of the $c, \tilde{c}$ coefficients in Eq. (3.44) are $O(1)$, the gap of the effective Hamiltonian for our system must be at least $O(\varepsilon^n)$. Additionally, we can similarly see that ε can be chosen small enough that $H_{\text{eff}}^{\langle n\rangle}$ has ground space energy no greater than $H_{\text{eff}}^{\langle 0\rangle}$. Because the energy of any state in the image of Q_0 is 0, and the ground state energy of $H_{\text{eff}}^{\langle 0\rangle}$ is 0, at least one ground state of $H_{\text{eff}}^{\langle n\rangle}$ must be in the support of P_0. This means that it is sensible to discuss the restriction of Eq. (3.44) to P_0. In particular, this is useful because (3.44) in its general form is not a sum of local terms (note that P_0 is a highly non-local operator, having support on the entire lattice), while it does have this feature after being restricted to P_0.

3.5 Stability of Effective Hamiltonian

Having proved Theorem 10, we will now show that the ground space of $H_{\text{eff}}^{\langle n \rangle}$ does not change dramatically (i.e., will remain in the same phase) as we include additional contributions from higher order terms in the perturbation expansion, as detailed in Theorem 11. In this context, we will say that $H_{\text{eff}}^{\langle n \rangle}$ is *stable* to these additional terms. To prove Theorem 11, we will require that the canonical parent Hamiltonian of the PEPS under consideration obeys the Local-TQO and Local-Gap conditions, and so the PEPS is topologically ordered. This will allow us to use the results on stability of topologically ordered systems under quasi-local perturbations [MZ13, BHM10].

Let us outline the proof strategy, which proceeds in two stages. In order to analyse the stability of the effective Hamiltonian, it will be convenient to make use of the *local* Schreiffer-Wolff perturbation method in contrast to the global SW method used in Sec. 3.4. The local SW method produces an effective Hamiltonian expansion with locality properties that we will exploit to prove our stability results. With this in mind, the first stage of our proof will be to transform the global SW effective Hamiltonian derived in the previous section into the corresponding local SW effective Hamiltonian and showing that the properties of the ground space are preserved under this transformation. This is captured by the following lemma.

Lemma 15. *For a quasi-injective, isometric, topologically ordered PEPS, the global SW effective Hamiltonian of our model at order n_* is in the same phase as the local SW effective Hamiltonian at order n_* for sufficiently small $\varepsilon > 0$.*

In order to prove this lemma, we will show that the transformation between the global and local effective Hamiltonians can be achieved by the addition of a sufficiently small quasi-local operator. This allows us to use the topological stability theorem to argue that the two Hamiltonians are in the same phase. We then also give a lemma showing that if the global SW effective Hamiltonian is topologically stable, then so is the local SW effective Hamiltonian.

At this point in the analysis we will simply have demonstrated that the ground space of one finite order effective Hamiltonian is in the same phase as the ground space of another finite order effective Hamiltonian. For the second stage of our proof, we will use the structure of the local SW perturbation expansion to argue that the higher-order contributions to the local SW Hamiltonian are both small and quasi-local. This will allow us to again apply the topological stability theorem and prove the following:

Lemma 16. *For a quasi-injective, isometric, topologically ordered PEPS, the local SW Hamiltonian of our model at order n_* is in the same phase as our effective Hamiltonian at any order $k \geq n_*$, for sufficiently small $\varepsilon > 0$.*

The two lemmas 15-16 constitute a proof of Theorem 11.

Throughout the following analysis, we will make use of the fact that both n_* and the maximum

coordination number of Λ are $O(1)$ constants in N and ε. We will also often use locality properties of operators in this section. Although the majority of the Hamiltonians and operators we consider in this section are highly non-local (e.g., the unperturbed ground space projector P_0), we will often use the fact that these operators are local when restricted to the image of P_0. We will often loosely refer to an operator as local or quasi-local, when in fact it is clear from context that this is only true after the restriction to the unperturbed ground space.

3.5.1 Transformation to local Schrieffer-Wolff effective Hamiltonian

To analyse the stability properties of the effective Hamiltonian (3.23), we will consider a related effective Hamiltonian derived from the local Schrieffer-Wolff method [DFRBF96, BDL11]. (The previous method has been referred to as the global SW method to avoid confusion.) As with the global SW method, the local SW method is based on a transformation that block diagonalizes the Hamiltonian with respect to the ground space and excited space of the unperturbed Hamiltonian. In contrast to the global SW transformation, the local SW transformation does not achieve this block diagonalization exactly, but only up to corrections of order $O(\varepsilon^{n+1})$ for a given order n. However, it is constructed in a manifestly local way, which allows us to analyse some properties of this expansion much more directly.

Local Schrieffer-Wolff transformation

Before proceeding, we will briefly define and review some relevant properties of the local SW method, following Ref. [BDL11]. At a given order n we construct a sequence of anti-Hermitian operators

$$T^{\langle n\rangle} = \sum_{q=1}^{n} \varepsilon^q T_q \tag{3.46}$$

such that all T_q are $(q+1)$-local and

$$\left\| P_0 \mathrm{e}^{T^{\langle n\rangle}} H \mathrm{e}^{-T^{\langle n\rangle}} Q_0 + Q_0 \mathrm{e}^{T^{\langle n\rangle}} H \mathrm{e}^{-T^{\langle n\rangle}} P_0 \right\| \leq O(N\varepsilon^{n+1}) \tag{3.47}$$

for sufficiently small ε. We can decompose the transformed Hamiltonian into a block-diagonalized part and a "garbage" part as

$$\mathrm{e}^{T^{\langle n\rangle}} H \mathrm{e}^{-T^{\langle n\rangle}} = H_{\mathrm{loc}}^{\langle n\rangle} + H_{\mathrm{garbage}} \tag{3.48}$$

where $Q_0 H_{\mathrm{loc}}^{\langle n\rangle} P_0 = P_0 H_{\mathrm{loc}}^{\langle n\rangle} Q_0 = 0$. We use the subscript 'loc' to denote operators derived from the local SW method where there may be confusion with similar operators from the global SW method. Because $H_{\mathrm{loc}}^{\langle n\rangle}$ is block-diagonal, Eq. (3.47) implies that $\|H_{\mathrm{garbage}}\|$ is $O(N\varepsilon^{n+1})$.

The effective Hamiltonian at order n is defined as the restriction of $H_{\mathrm{loc}}^{\langle n\rangle}$ to the ground space

of the unperturbed Hamiltonian H_0:

$$H_{\text{eff,loc}}^{\langle n\rangle} = P_0 H_{\text{loc}}^{\langle n\rangle} P_0 \tag{3.49}$$

In order to explicitly compute $H_{\text{loc}}^{\langle n\rangle}$, we first define a series of Hermitian operators

$$\begin{aligned} V_{\text{loc}}^{(j)} = &\sum_{q=2}^{j+1} \frac{1}{q!} \sum_{\substack{1\le j_1,\ldots,j_q\le n \\ j_1+\ldots+j_q=j+1}} [T_{j_1},[T_{j_2},[\cdots,[T_{j_q},H_0]\cdots]]] \\ &+ \sum_{q=1}^{j} \frac{1}{q!} \sum_{\substack{1\le j_1,\ldots,j_q\le n \\ j_1+\ldots+j_q=j}} [T_{j_1},[T_{j_2},[\cdots,[T_{j_q},V]\cdots]]] \end{aligned} \tag{3.50}$$

where $V_{\text{loc}}^{(0)} = V$. We represent each of these operators as a sum of local terms

$$V_{\text{loc}}^{(j)} = \sum_{R\subseteq\Lambda} V_{R,\text{loc}}^{(j)} \tag{3.51}$$

where each $V_{R,\text{loc}}^{(j)}$ is Hermitian and acts non-trivially only on spins within region R. This decomposition is chosen as the expansion of $V_{\text{loc}}^{(j)}$ in some orthogonal operator basis. Is can be shown [BDL11] that $V_{\text{loc}}^{(j)}$ is $(j+2)$-local, so we can guarantee that this local decomposition need only consider $(j+2)$-local regions R. Each of the T_j operators take the form

$$T_j = \sum_{R\subseteq\Lambda} \left(\frac{Q_R}{H_R} V_{R,\text{loc}}^{(j-1)} P_R - P_R V_{R,\text{loc}}^{(j-1)} \frac{Q_R}{H_R} \right) \tag{3.52}$$

where $P_R \equiv \prod_{s\in R} P_s$, $Q_R \equiv 1 - P_R$, and $H_R \equiv \sum_{s\in R} Q_s$. Equations (3.50) and (3.52) can be solved recursively. Given this solution, we find

$$H_{\text{loc}}^{\langle n\rangle} = H_0 + \sum_{j=1}^{n} \varepsilon^j \sum_{R\subseteq\Lambda} \left(P_R V_{R,\text{loc}}^{(j-1)} P_R + Q_R V_{R,\text{loc}}^{(j-1)} Q_R \right) \tag{3.53}$$

Properties of the local Schrieffer-Wolff transformation

Here we will state a number of known properties of the local Schrieffer-Wolff transformation that will be useful in our analysis [BDL11].

Although Eqns. (3.50) and (3.52) define $V_{\text{loc}}^{(j)}$ for arbitrary (positive, integral) j, only those $V_{\text{loc}}^{(j)}$ with $j < n$ appear in $H_{\text{loc}}^{\langle n\rangle}$. The remaining terms can be used to write H_{garbage} as

$$H_{\text{garbage}} = \sum_{j=n+1}^{\infty} \varepsilon^j V_{\text{loc}}^{(j-1)} \tag{3.54}$$

As would be expected, $V_{\text{loc}}^{(j)}$ is independent of n for $j < n$, while it is implicitly dependent on

n for $j \geq n+1$. For sufficiently small ε, the norm of H_{garbage} can be bounded as $\|H_{\text{garbage}}\| \leq c\Delta_0 N\varepsilon^{n+1}$ for a constant c that depends on n.

The local SW method obeys the linked-cluster theorem, and so we can guarantee that $H^{\langle n\rangle}_{\text{eff,loc}}$ is $O(n)$-local. It is also the case that at a fixed order n, the effective Hamiltonians found by the global and local SW methods can be related by a transformation $K^{\langle n\rangle}$ up to an error

$$H^{\langle n\rangle}_{\text{eff,glob}} - \mathrm{e}^{K^{\langle n\rangle}} H^{\langle n\rangle}_{\text{eff,loc}} \mathrm{e}^{-K^{\langle n\rangle}} \equiv \hat{\delta} \tag{3.55}$$

with $\|\hat{\delta}\| \leq O(N|\varepsilon|^{n+1})$ for a system with N sites and $|\varepsilon| < 1$, and where $K^{\langle n\rangle}$ is $O(n)$-local. This is shown in Ref. [BDL11, Lemma 4.4]. We denote the global SW effective Hamiltonian by $H^{\langle n\rangle}_{\text{eff,glob}}$ and the local SW effective Hamiltonian by $H^{\langle n\rangle}_{\text{eff,loc}}$ to avoid confusion. In the following analysis, we will prove that $\hat{\delta}$ is quasi-local with favourable decay parameters. In doing so, we will prove Lemma 15.

Because $H^{\langle n\rangle}_{\text{eff,glob}}$, $H^{\langle n\rangle}_{\text{eff,loc}}$ and $K^{\langle n\rangle}$ are all $O(n)$-local, we can decompose them into operators acting non-trivially only on connected regions of Λ with bounded size. Denote such a decomposition of an operator X as $X = \sum_R X_R$. We now define a bound on the strength of an operator as

$$\|X\|_{\max} = \max_{s\in\Lambda} \left\| \sum_{R \ni s} X_R \right\| \tag{3.56}$$

It can be shown that $\|K^{\langle n\rangle}\|_{\max} = O(|\varepsilon|)$ [BDL11]. In fact, we can expand $K^{\langle n\rangle}$ as a Taylor series in ε as

$$K^{\langle n\rangle} = \sum_{j=1}^{n} \varepsilon^j K_j \tag{3.57}$$

for some $O(j)$-local, block-diagonal K_j with $\|K_j\|_{\max} \sim O(1)$.

Transforming from global to local Schrieffer-Wolff effective Hamiltonians

Given the properties of the local Schrieffer-Wolff transformation noted above, we now demonstrate that $\hat{\delta}$ of Eq. (3.55), the operator that relates the local and global SW effective Hamiltonians, is quasi-local. This quasi-locality will allow us to argue that $H^{\langle n\rangle}_{\text{eff,glob}}$ is stable under addition of $\hat{\delta}$, and thus the gap does not close along a path from $H^{\langle n\rangle}_{\text{eff,glob}}$ to $H^{\langle n\rangle}_{\text{eff,loc}}$.

Lemma 17. *$\hat{\delta}$ is $\left(O(1), O(\varepsilon^{O(1)})\right)$-quasi-local when restricted to the space P_0.*

Proof. Recall from our definition of quasi-locality in Sec. 3.2, a (J,μ)-quasi-local operator has interaction strength that decays with radius r as $J\mu^r$. In order to show that $\hat{\delta}$ is quasi-local, we will explicitly construct a local decomposition for it. For this purpose it will be convenient to

introduce operators

$$\Theta_R(k) = \sum_{j=0}^{k} \frac{1}{j!} [K^{\langle n \rangle}, \cdot]^j H^{\langle n \rangle}_{\text{eff,loc},R} \tag{3.58}$$

for $H^{\langle n \rangle}_{\text{eff,loc}} = \sum_R H^{\langle n \rangle}_{\text{eff,loc},R}$ an $O(n)$-local decomposition of $H^{\langle n \rangle}_{\text{eff,loc}}$ with $\| H^{\langle n \rangle}_{\text{eff,loc},R} \| = O(1)$, and where $[A, \cdot]^j B$ is the j-fold nested commutator of A and B, e.g. $[A, \cdot]^0 B = B$, $[A, \cdot]^1 B = [A, B]$, $[A, \cdot]^2 B = [A, [A, B]]$, etc.

Note that $\Theta_R(\infty) = \mathrm{e}^{K^{\langle n \rangle}} H^{\langle n \rangle}_{\text{eff,loc},R} \mathrm{e}^{-K^{\langle n \rangle}}$. Because $K^{\langle n \rangle}$ and $H^{\langle n \rangle}_{\text{eff,loc},R}$ are both $O(n)$-local (when restricted to the image of P_0), this leads us to consider $\Theta_R(k)$ to be a $O(kn)$-local truncation of $\mathrm{e}^{K^{\langle n \rangle}} H^{\langle n \rangle}_{\text{eff,loc},R} \mathrm{e}^{-K^{\langle n \rangle}}$. To relate this new operator to $\hat{\delta}$, it is convenient to rewrite the global SW effective Hamiltonian as [BDL11]

$$H^{\langle n \rangle}_{\text{eff,glob}} = \sum_{j=0}^{n} \sum_{\substack{1 \le q_0, q_1, \ldots, q_j \le n \\ q_0 + \ldots + q_j \le n}} \frac{1}{j!} \varepsilon^{q_0 + \ldots + q_j} [K_{q_1}, [K_{q_2}, \ldots [K_{q_j}, H^{\langle q_0 \rangle}_{\text{eff,loc}} - H^{\langle q_0 - 1 \rangle}_{\text{eff,loc}}] \ldots]] \tag{3.59}$$

Because we are interested in the local decomposition of $\hat{\delta}$, we also define

$$H^{\langle n \rangle}_{\text{eff,glob},R} = \sum_{j=0}^{n} \sum_{\substack{1 \le q_0, q_1, \ldots, q_j \le n \\ q_0 + \ldots + q_j \le n}} \frac{1}{j!} \varepsilon^{q_0 + \ldots + q_j} [K_{q_1}, [K_{q_2}, \ldots [K_{q_j}, H^{\langle q_0 \rangle}_{\text{eff,loc},R} - H^{\langle q_0 - 1 \rangle}_{\text{eff,loc},R}] \ldots]] \tag{3.60}$$

where we note that $H^{\langle n \rangle}_{\text{eff,glob},R}$ need not act only within R, even when restricted to the P_0 subspace (though it is local). It is then straightforward to see that the difference between $H^{\langle n \rangle}_{\text{eff,glob},R}$ and $\Theta_R(n)$ consists only of those terms in the sum with $\sum_i q_i > n$, i.e.

$$\begin{aligned} H^{\langle n \rangle}_{\text{eff,glob},R} - \Theta_R(n) = - \sum_{j=0}^{n} \frac{1}{j!} \sum_{\substack{1 \le q_0, q_1, \ldots, q_j \le n \\ q_0 + \ldots + q_j > n}} & \varepsilon^{q_0 + \ldots + q_j} \\ & \cdot [K_{q_1}, [K_{q_2}, \ldots [K_{q_j}, H^{\langle q_0 \rangle}_{\text{eff,loc},R} - H^{\langle q_0 - 1 \rangle}_{\text{eff,loc},R}] \ldots]] \end{aligned} \tag{3.61}$$

The norm of this difference is

$$\| H^{\langle n \rangle}_{\text{eff,glob},R} - \Theta_R(n) \| \sim O(\varepsilon^{n+1}) \tag{3.62}$$

for sufficiently small ε, since each $H^{\langle q_0 \rangle}_{\text{eff,loc},R}$ fails to commute with at most a constant number of local terms in each K_q.

We now define a local decomposition of $\hat{\delta}$ making use of these $\Theta_R(n)$ operators. This decomposition is not unique, and we may choose it as convenient so long as it has the property that $\hat{\delta} = \sum_{s,r} \hat{\delta}_{s,r}$ for $\hat{\delta}_{s,r}$ acting only within a region of radius r around site s. For our purposes,

we are interested mainly in decay of $\hat{\delta}$ on long length scales, and so we simply collect all the terms with radius smaller than some critical length scale κ. Specifically, we choose $\kappa \sim n^2$ as the maximum radius of operators $H^{\langle n\rangle}_{\text{eff,glob},R} - \Theta_R(n)$ over all R. With this in mind, for all s we define

$$\hat{\delta}_{s,r} = 0 \qquad \text{for } r < \kappa \tag{3.63}$$

$$\hat{\delta}_{s,\kappa} = H^{\langle n\rangle}_{\text{eff,glob},R_s} - \Theta_{R_s}(n) \tag{3.64}$$

where the regions R_s here have been put into one-to-one correspondence with the sites s in some canonical way.

In a similar spirit, we need not define $\hat{\delta}_{s,r}$ for all r. Instead, we will only define it for some set of radii r_k for each $k > n$, as follows

$$\hat{\delta}_{s,r_k} = \Theta_{R_s}(k) - \Theta_{R_s}(k+1) \qquad \text{for } k > n \tag{3.65}$$

such that $\hat{\delta}_{s,r_k}$ acts within radius r_k of site s as required. Since $\Theta_R(k)$ is $O(kn)$-local, this implies that $r_k \sim O(kn)$. It can clearly be seen that $\sum_{s,r} \hat{\delta}_{s,r} = \hat{\delta}$. Given the facts that $\|\hat{\delta}_{s,\kappa}\| \sim O(\varepsilon^{n+1})$ and (since $\|K^{\langle n\rangle}\| \sim O(\varepsilon)$ and n, $\|H^{\langle n\rangle}_{\text{eff,loc},R}\| = O(1)$)

$$\|\hat{\delta}_{s,r_k}\| \leq \|[K^{\langle n\rangle}, \cdot]^{k+1} H^{\langle n\rangle}_{\text{eff,loc},R_s}\| \leq O(\varepsilon^{k+1}) \tag{3.66}$$

we conclude that $\hat{\delta}$ is $\left(O(1), O(\varepsilon^{O(1)})\right)$-quasi-local (when acting on the space P_0) as claimed. □

Now we can make use of the fact that $\|\hat{\delta}_{s,r}\| \leq O(\varepsilon^{n+1})$ for all s, r to provide some alternative quasi-local parameters for $\hat{\delta}$. Consider the following Lemma (presented without proof).

Lemma 18. *Consider a function $f(r)$ where $f(r) \leq ab^r$ and $f(r) \leq c$ for $0 < b < 1$ and $a, c > 0$. Then $f(r) \leq c^{1-\lambda} a^{\lambda} b^{r\lambda}$ for all $0 < \lambda < 1$.*

This implies that $\hat{\delta}$ is $\left(O(\varepsilon^{(n+1)(1-\lambda)}), O(\varepsilon^{\lambda O(1)})\right)$-quasi-local for any choice of $0 < \lambda < 1$. Particularly, let us choose $\lambda < \frac{1}{n+1}$. Importantly, this means that by choosing ε sufficiently small, we can make the first parameter of the quasi-local decay arbitrarily small compared to the $O(\varepsilon^n)$ gap of $H^{\langle n\rangle}_{\text{eff,glob}}$, and the second parameter can be made arbitrarily small simultaneously by decreasing ε.

Because $H^{\langle n_*\rangle}_{\text{eff,glob}}$ is frustration free, satisfies Local-TQO and Local-Gap by assumption, and has a gap of $O(\varepsilon^{n_*})$, we can apply the topological stability theorem of Ref. [MZ13] for sufficiently small ε to show that the gap of $H^{\langle n_*\rangle}_{\text{eff,glob}}$ remains $O(\varepsilon^{n_*})$ along a path to $\mathrm{e}^{K^{\langle n_*\rangle}} H^{\langle n_*\rangle}_{\text{eff,loc}} \mathrm{e}^{-K^{\langle n_*\rangle}}$. In particular, this shows that $\mathrm{e}^{K^{\langle n_*\rangle}} H^{\langle n_*\rangle}_{\text{eff,loc}} \mathrm{e}^{-K^{\langle n_*\rangle}}$ is in the same phase as $H^{\langle n_*\rangle}_{\text{eff,glob}}$.

Since the Hamiltonians we consider are only local when restricted to the space P_0, one might be concerned that the topological stability theorems do not apply. However, we could instead consider Hamiltonians which are manifestly local on the entire Hilbert space by replacing each operator H_R acting on a region R with $P_R H_R P_R$, and considering $\sum P_R H_R P_R$ instead of

$\sum P_0 H_R P_0$. Though we do not present it in this way for clarity, the analysis would proceed in the same way and the same conclusions would be reached.

To complete the proof of Lemma 15, we appeal to the following lemma, as proven in Ref. [CGW10]

Lemma 19 ([CGW10])**.** *Given a gapped quasi-local Hamiltonian H and local Hamiltonian X, the ground states of $e^{iX} H e^{-iX}$ are in the same phase as those of H.*

Because $iK^{\langle n\rangle}$ can be regarded as a local Hamiltonian, the proof of Lemma 15 is an immediate corollary to Lemma 19. That is, the local SW effective Hamiltonian at order n_* has the desired quasi-injective, isometric, topologically ordered PEPS as its ground state. This is the main result of this section.

Before we proceed, it will be useful to demonstrate an additional property of the effective Hamiltonian $H^{\langle n_*\rangle}_{\text{eff,loc}}$. In the following sections, we would like to apply the topological stability theorem (Theorem 9) to demonstrate that the ground space of $H^{\langle n_*\rangle}_{\text{eff,loc}}$ is stable against some additional terms. Since the Local-TQO property itself is stable against perturbations which do not close the (local) gap [CMPGS13], we can also argue that $H^{\langle n_*\rangle}_{\text{eff,loc}}$ satisfies Local-TQO and Local-Gap. Unfortunately we have not shown that $H^{\langle n\rangle}_{\text{eff,loc}}$ is frustration-free, and so we cannot directly apply Theorem 9. However, the following Lemma will allow us to leverage the topological stability of $H^{\langle n_*\rangle}_{\text{eff,glob}}$ to prove topological stability of $H^{\langle n_*\rangle}_{\text{eff,loc}}$.

Lemma 20. *Consider a Hamiltonian H_{TO} satisfying the assumptions of Theorem 9. That is, for any quasi-local perturbation V there exists some $\varepsilon_0 > 0$ such that $H_{TO} + \varepsilon V$ is in the same phase as H_{TO} for all $0 \le \varepsilon < \varepsilon_0$. Then for each Hamiltonian H' in the same phase as H_{TO}, there exists some $\varepsilon'_0 > 0$ such that $H' + \varepsilon' V$ is in the same phase as H' for all $0 \le \varepsilon' < \varepsilon'_0$.*

Proof. Define a smooth, invertible, linear quasi-local transformation $\mathcal{T}$ that relates H_{TO} and H', i.e. $\mathcal{T}(H_{TO}) = H'$. We are guaranteed that such a transformation exists from the fact that H' and H_{TO} are in the same phase. This implies that $\mathcal{T}^{-1}(V) \equiv V'$ is quasi-local and $\mathcal{T}^{-1}(H' + \varepsilon' V) = H_{TO} + \varepsilon' V'$. Because there exist non-zero ε such that $H_{TO} + \varepsilon V'$ is in the same phase as H_{TO} by the quasi-locality of V', this also implies that there exist non-zero ε' such that $H' + \varepsilon' V$ is in the same phase as H'. □

3.5.2 Stability to higher order contributions

Now that we have shown that $H^{\langle n_*\rangle}_{\text{eff,loc}}$ is in the same phase as $H^{\langle n_*\rangle}_{\text{eff,glob}}$, we can make use of the explicit locality structure of the local SW transformation to bound the effect of higher order contributions to the effective Hamiltonian. The main technical result we will derive here is the fact that H_{garbage} is quasi-local, and so the ground state and gap of $H^{\langle n_*\rangle}_{\text{eff,loc}}$ are stable under addition of this garbage term. Following this, we can define a sequence of effective Hamiltonians to arbitrary order (very similar to the local SW effective Hamiltonians) that are in the same phase as $H^{\langle n_*\rangle}_{\text{eff,loc}}$ to arbitrary finite order, completing the proof of Lemma 16.

Our analysis is based on the fact that $H_{\text{loc}}^{\langle n\rangle}$ obeys the linked cluster theorem. This follows directly from the fact that $V_{\text{loc}}^{(j-1)}$ is $(j+1)$-local. Any non-local term arising in the expansion of $V_{\text{loc}}^{(j)}$ must vanish. Defining $V_{s,\text{loc}}^{(j)} = \sum_{R\ni s} V_{R,\text{loc}}^{(j)}$, we can also bound the strength of $V_{\text{loc}}^{(j)}$ as

$$\|V_{\text{loc}}^{(j)}\|_{\max} = \max_{s\in\Lambda} \|V_{s,\text{loc}}^{(j)}\| \leq \alpha \left(\frac{n^2}{\Delta_0\beta}\right)^j \tag{3.67}$$

for some constants $\alpha, \beta > 0$ [BDL11].

Now, because $V_{R,\text{loc}}^{(j)}$ are components of $V_{\text{loc}}^{(j)}$ in an orthogonal operator basis, removing some set of them from $V_{s,\text{loc}}^{(j)}$ cannot increase $\|V_{s,\text{loc}}^{(j)}\|$. That is, $\left\|\sum_{R'\subseteq\{R:R\ni s\}} V_{R',\text{loc}}^{(j)}\right\| \leq \|V_{s,\text{loc}}^{(j)}\|$.

This allows us to define a decomposition of H_{garbage} (recall Eq. (3.54)) into terms acting within a region of radius r around each site s. These will be operators of the form $\varepsilon^{r-1}\sum_{R'\subseteq\{R:R\ni s\}} V_{R',\text{loc}}^{(r-2)}$. For a fixed n, we then have that for $\varepsilon < \frac{\Delta_0\beta}{n^2}$ we can bound the norms of these operators by the exponential decay

$$\left\|\varepsilon^{r-1}\sum_{R'\subseteq\{R:R\ni s\}} V_{R',\text{loc}}^{(r-2)}\right\| \leq \left(\frac{\alpha\Delta_0^2\beta^2}{\varepsilon n^4}\right)\left(\frac{\varepsilon n^2}{\Delta_0\beta}\right)^r. \tag{3.68}$$

Therefore, H_{garbage} is $\left(O(\varepsilon^{-1}), O(\varepsilon)\right)$-quasi-local.

Because we also know that $\|H_{\text{garbage}}\|$ does not include terms $V^{(r-2)}$ for $r \leq n+1$, we can give an alternative bound on the decay parameters of H_{garbage}. Making use of Lemma 18, we find that H_{garbage} is also $\left(O(\varepsilon^{n+1-\lambda(n+2)}), O(\varepsilon^{\lambda})\right)$-quasi-local. Importantly, for $\lambda < \frac{1}{n+2}$, the first of these parameters is $O(\varepsilon^{n+\delta})$ for $\delta > 0$, and both parameters can be made arbitrarily small by decreasing ε. This is convenient as it allows us to use the topological stability theorem to analyse the stability of $H_{\text{eff,loc}}^{\langle n\rangle}$ to contributions from H_{garbage}.

As the gap of $H_{\text{eff,loc}}^{\langle n_*\rangle}$ is $O(\varepsilon^{n_*})$, by making ε small enough, we can make the strength of H_{garbage} arbitrarily small compared to the gap for $\lambda < \frac{1}{n_*+2}$. By the topological stability theorem, we can find $\varepsilon > 0$ such that $H_{\text{eff,loc}}^{\langle n_*\rangle} + H_{\text{garbage}}$ is in the same phase as $H_{\text{eff,loc}}^{\langle n_*\rangle}$ and has a gap of $O(\varepsilon^{n_*})$.

Given this result, we can write a sequence of effective Hamiltonians of the form

$$H_{\text{eff,loc+}}^{\langle k\rangle} \equiv P_0 e^{T^{\langle k\rangle}} H e^{-T^{\langle k\rangle}} P_0 \tag{3.69}$$

$$= H_{\text{eff,loc}}^{\langle k\rangle} + P_0 H_{\text{garbage}}^{\langle k\rangle} P_0 \tag{3.70}$$

where we note that H_{garbage} has previously been implicitly dependent on the order of perturbation theory, and so we restore this explicit dependence here. Given the fact that $H_{\text{eff,loc}}^{\langle n_*\rangle}$ +

$H_{\text{garbage}}^{\langle n_*\rangle}$ is in the same phase as $H_{\text{eff,loc}}^{\langle n_*\rangle}$, we can now write for any $k \geq n_*$

$$H_{\text{eff,loc+}}^{\langle k\rangle} = P_0 e^{T^{\langle k\rangle}} e^{-T^{\langle n_*\rangle}} \left(H_{\text{loc}}^{\langle n_*\rangle} + H_{\text{garbage}}^{\langle n_*\rangle}\right) e^{T^{\langle n_*\rangle}} e^{-T^{\langle k\rangle}} P_0 \tag{3.71}$$

$$= P_0 e^{T^{\langle k\rangle}} e^{-T^{\langle n_*\rangle}} \left(H_{\text{eff,loc}}^{\langle n_*\rangle} + H_{\text{garbage}}^{\langle n_*\rangle}\right) e^{T^{\langle n_*\rangle}} e^{-T^{\langle k\rangle}} P_0 \tag{3.72}$$

Because $iT^{\langle k\rangle}$ are local Hamiltonians for any finite k, we can appeal to Lemma 19 to show that $H_{\text{eff,loc+}}^{\langle k\rangle}$ and $H_{\text{eff,loc}}^{\langle n_*\rangle}$ are indeed in the same phase when restricted to P_0, and because both Hamiltonians act trivially outside of P_0, this concludes the proof of both Lemma 16 and Theorem 11.

3.6 Discussion

Our construction yields a 2-body Hamiltonian described by Eq. (3.13) that is a gapped parent Hamiltonian for a state in the same phase as a desired PEPS to all orders of perturbation theory. We have made use of the fact that two ground states of gapped local Hamiltonians are in the same phase if one Hamiltonian can be smoothly deformed into the other without closing the gap. This also implies that expectation values of local observables deform smoothly along the same path. Because in the limit $\varepsilon \to 0$ both the global and local Schrieffer-Wolff transformations tend to the identity, our construction gives a parent Hamiltonian for a state which tends towards the desired PEPS state as $\varepsilon \to 0$. Expectation values of local observables can therefore be made arbitrarily close to those of the PEPS under consideration by choosing ε arbitrarily small.

3.6.1 Locality on virtual qudits

Our model as defined in Sec. 3.3.1 gives a 2-local Hamiltonian where the code gadgets of our construction are considered as indivisible quantum systems. Instead of treating a code gadget as a single quantum system, we could also be interested in implementing the virtual qudits as distinct physical systems. The code gadget Hamiltonian as defined at a site s would then involve $\deg(s)$-body interactions in general. There are two strategies that can be applied to also reduce these interactions to 2-body terms on the virtual qudits. The first approach is more elegant but less general, while the second is universally applicable.

The most important feature of a code gadget that we must preserve in a procedure like this is its ground space. With this in mind, the first strategy involves simply finding an explicit 2-body Hamiltonian whose ground space is identical to the code gadget Hamiltonian in Eq. (3.14). This is the approach taken in Refs. [BR06] and [BFBD11]. When making use of this strategy, the modification of the spectral structure of the code-gadget Hamiltonian means that our technical proofs in Sec. 3.4 are not immediately applicable (particularly Lemma 13). However, it seems reasonable to conjecture that the construction is insensitive to these details and similar results could be found for any sensible choice of code gadget Hamiltonian.

The second strategy is to simply apply more conventional perturbation gadget techniques to the code gadget Hamiltonian directly, reducing it to 2-body interactions using further perturbative ancillae (for example following Ref. [JF08]). Because these perturbation gadgets could be applied within each code gadget separately, they would be approximating systems involving only a fixed finite number of qudits. For this reason, many of the difficulties with applying general perturbation gadgets to infinite systems could be avoided. Additionally, because the effective Hamiltonian of this system will be identical to Eq. (3.14), we expect that the proofs in Sec. 3.4 could be adapted to this situation (given an appropriately chosen perturbative hierarchy). Although it could be applied to an arbitrary system, this is clearly the less elegant option.

3.6.2 Symmetries of the model

In previously studied examples of these techniques [BR06, BFBD11], the local symmetries of the states were exactly captured by this construction. That is, for each local symmetry of these models, a corresponding encoded symmetry can be found which commutes with the full Hamiltonian of the system, including the perturbative couplings. In generic perturbative approaches one would expect only to recover these symmetries approximately.

Exactly capturing the local symmetries of the target states is not a feature of our construction in general. There exist cases where some or all of the local symmetries are exactly captured, but this does not seem to be generic. An example of this is shown in Sec. 3.7, where a subset of the full symmetries of the model are preserved exactly, and the rest only preserved approximately.

3.6.3 Application to RVB states

Constructing and analysing parent Hamiltonians for resonating valence bond (RVB) states is of interest for modelling spin liquids and other exotic quantum phases. Methods to construct such parent Hamiltonians for the Kagome lattice require at least 12-body interactions [Sei09]. Recently, an alternative construction for parent Hamiltonians of these states has been proposed, based on a PEPS representation of the RVB states on this lattice [SPCPG12]. Canonical parent Hamiltonians for this PEPS require at least 19-body interactions.

Because the RVB PEPS is $\mathbb{Z}_2$-injective [SPCPG12], we anticipate that our analysis could be applied to this case and as such a 2-body parent Hamiltonian of the form (3.13) may be obtained for a state in the same phase as the RVB state (and in the limit that the perturbation parameter vanishes, should reproduce the RVB state precisely). In this context, we remind the reader that our construction yields an encoded version of the desired state. The dimension of the Hilbert spaces associated with each site will be larger, and there will also be ancilla systems required to mediate coupling between the sites (corresponding to tensors with no physical indices in the description of Ref. [SPCPG12]).

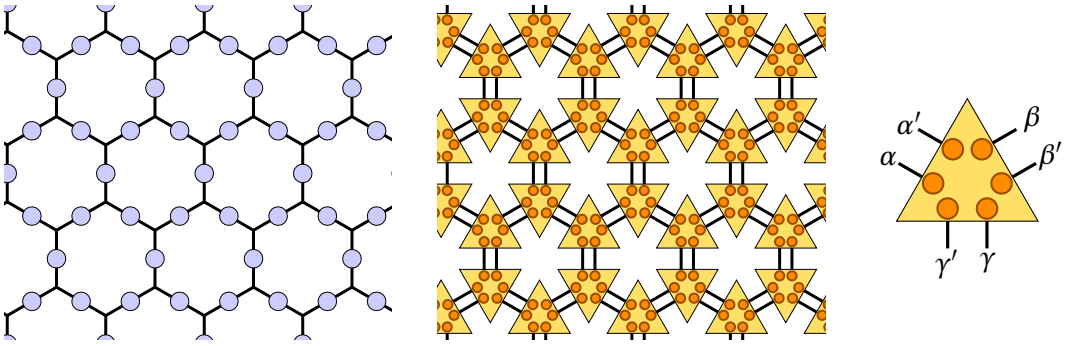

(a) (b) (c)

Figure 3.2 – (a) The double semion model is typically presented on a honeycomb lattice with qubits (blue) on links. (b) The PEPS representation of the same region of the lattice. At vertices of the honeycomb lattice, we place 6 virtual (orange) qubits, which will be projected into a 4-dimensional (yellow) code qudit. Solid lines here denote edges of the PEPS graph, and so connect virtual qubits in maximally entangled states. (c) Virtual qubit labels. For triangles oriented in the opposite direction, rotate these definitions by π. States are labelled as $|\alpha\alpha';\beta\beta';\gamma\gamma'\rangle$.

3.7 Example: The Double Semion Model

We now present an illustrative example of our construction. The double semion model is a simple example of a string-net model [LW05], whose ground states are known to have exact PEPS descriptions [GLSW09, BAV09]. In fact, the double semion model has a particularly simple PEPS description [GLW08, GLSW09] that we can exploit to construct a 2-body system whose low energy effective Hamiltonian is an encoded parent Hamiltonian for the double semion ground space. These states are examples of both (G,ω)-injective PEPS and MPO-injective PEPS.

We will use the double semion model to demonstrate some of the features of our construction. The analysis in this section should be understood as illustrative of the features of the Hamiltonian (3.13) rather than as an example of the theorems proven in Sections 3.4 and 3.5. As such, we make use of a simplified formalism that sacrifices some rigor for clarity. The general analysis as shown in Sections 3.4 and 3.5 can be applied to this example to demonstrate the relevant features more rigorously.

The double semion state is typically defined on a honeycomb lattice with qubits on the edges, as in Fig. 3.2a. It is conventionally defined as the ground state of the Hamiltonian [LW05]

$$H_{\text{ds}} = -\sum_{v}\prod_{j\sim v}\sigma_j^z + \sum_{p}\left(\prod_{k\in p}\sigma_k^x\right)\left(\prod_{m\sim p} i^{\frac{1-\sigma_m^z}{2}}\right) \tag{3.73}$$

where v (p) are vertices (plaquettes) of the honeycomb lattice, σ are the Pauli matrices, $j\sim v$ runs over qubits incident to vertex v, $k\in p$ runs over edges bounding plaquette p, and $m\sim p$

runs over edges incident to p (i.e. edges sharing one vertex with p).

We can represent the ground state of this Hamiltonian as a PEPS by placing 2 pairs of maximally entangled pairs of qubits between each vertex of the honeycomb lattice, as shown in Fig. 3.2b, and applying a projection map $\mathscr{P}_s$ at each vertex s to map from the 2^6-dimensional virtual space to a 4-dimensional code space. (Note this is a slightly different PEPS representation for the double semion ground state as compared to those presented in Refs. [GLW08, GLSW09, BAV09].) The correspondence between these code qudits and the qubits of the double semion model is not obvious at this stage, but will become clear as we proceed. At this point we should emphasise the distinction between the honeycomb lattice, on which the double semion model is typically defined (Fig. 3.2a), and the PEPS lattice, whose edges correspond to maximally entangled virtual pairs (Fig. 3.2b). In particular, we stress that the sites of the PEPS lattice (where $\mathscr{P}_s$ is applied) correspond to vertices of the honeycomb lattice, and not edges.

For the most part of this analysis, we will neglect normalization for the sake of clarity. With this in mind, and the labelling conventions of Fig. 3.2c, we can write the projection map $\mathscr{P}_s$ as:

$$\mathscr{P}_s = \sum_{\alpha,\beta,\gamma,i,j,k\in\mathbb{Z}_2} T_{\alpha\beta\gamma}\cdot\delta_{i=\alpha+\beta}\delta_{j=\beta+\gamma}\delta_{k=\gamma+\alpha}|ijk\rangle_c\langle\alpha\beta;\beta\gamma;\gamma\alpha|_s \tag{3.74}$$

where the c subscript on the ket indicates that it is a code space state, addition is modulo 2, and we have defined

$$T_{\alpha\beta\gamma} = \begin{cases} 1 & \alpha+\beta+\gamma = 0,3 \\ i & \alpha+\beta+\gamma = 1 \\ -i & \alpha+\beta+\gamma = 2 \end{cases} \tag{3.75}$$

It should be clear that although there are in principle 8 states that could be labelled by i, j, and k, these variables are not independent. In fact, there are only 4 non-vanishing states of this form, given explicitly by

$$\mathscr{P}^\dagger|000\rangle_c = |00;00;00\rangle + |11;11;11\rangle \tag{3.76}$$
$$\mathscr{P}^\dagger|110\rangle_c = i|10;01;11\rangle - i|01;10;00\rangle \tag{3.77}$$
$$\mathscr{P}^\dagger|101\rangle_c = i|01;11;10\rangle - i|10;00;01\rangle \tag{3.78}$$
$$\mathscr{P}^\dagger|011\rangle_c = i|11;10;01\rangle - i|00;01;10\rangle \tag{3.79}$$

We call these values of $\{ijk\}$ the *allowed* values. The site projector is then

$$P_s = \sum_{\{ijk\}} \mathscr{P}_s^\dagger|ijk\rangle\langle ijk|_{c,s}\mathscr{P}_s \tag{3.80}$$

where the sum only runs over allowed values of $\{ijk\}$, and the c,s subscript denotes code space states associated with site s.

The reason we use this redundant description of these states is that it allows us to identify the states i, j, and k as the states of the qubits of the double semion model. That is, each variable is associated with an edge of the honeycomb model. That some states (e.g. $|100\rangle_c$) are not in the image of $\mathscr{P}_s$ is a consequence of the fact that these states do not belong to the double semion ground state, which is what this PEPS describes. One might also worry that we have two variables labelling the state of each edge (one for each vertex on which the edge ends). However, we will see that this is resolved in our analysis.

Our construction proceeds by simulating the projection maps with code gadgets, using a Hamiltonian of the form of Eq. (3.13). Recall that the Hamiltonian for a code gadget is simply $Q_s = 1 - P_s$. Because our virtual systems are qubits, each edge of the PEPS lattice has an associated operator

$$M_e = |00\rangle\langle 00|_e + |11\rangle\langle 11|_e + |00\rangle\langle 11|_e + |11\rangle\langle 00|_e \tag{3.81}$$

The full Hamiltonian of our system is then given by

$$H = \sum_s Q_s - \varepsilon \sum_e M_e \tag{3.82}$$

where s (e) runs over the sites (edges) of the PEPS lattice.

3.7.1 Effective Hamiltonian

In this example, we will not use the more rigorous global Schrieffer-Wolff perturbation method as in Sections 3.4.2 and 3.4.3. We instead use the simpler self-energy expansion as used in Refs. [Kit06, BFBD11]. This amounts to neglecting the $\Gamma(q_1, \ldots, q_j)$ terms in the global SW expansion with any $|q_i| \neq 1$.

Given the Hamiltonian

$$H = H_0 + \varepsilon V \tag{3.83}$$

the self-energy low energy effective Hamiltonian is given by

$$H_{\text{eff,SE}} = E_0 + \sum_n \varepsilon^n P_0 V \left(\frac{Q_0}{H_0} V\right)^{(n-1)} P_0 \tag{3.84}$$

where P_0 is the projector to the ground space of H_0 with energy 0, and $\frac{Q_0}{H_0}$ is defined to vanish on ground states of H_0. In writing the effective Hamiltonian in this way, we have neglected the dependence of the ground state energy on the perturbation. For our purposes, $O(1)$ constants are unimportant, so we will commonly neglect them in our analysis.

If we now explicitly evaluate the expansion (3.84) for the double semion model, we will see that the terms arising will provide a parent Hamiltonian for the desired state. We have for the

low energy effective Hamiltonian

$$H_{\text{eff,ds}} = -\sum_n \varepsilon^n P_0 \left(\sum_e M_e\right)\left(\frac{Q_0}{H_0}\left(\sum_e M_e\right)\right)^{(n-1)} P_0 \tag{3.85}$$

We now evaluate this sum order by order. At 0^{th} order, the effective Hamiltonian can simply be taken to be

$$H^{\langle 0\rangle}_{\text{eff,ds}} = -P_0 \tag{3.86}$$

This term may seem trivial, but in fact it is not so if we consider it in terms of the qubits in the double semion model. This term enforces the constraint that only allowed values of $|ijk\rangle_p$ at each vertex are in the ground space. Thinking about these variables i, j, and k as labels for the states of the three qubits on the edges incident to any given vertex, this constraint plays the same role as the term $-\prod_{j\sim v}\sigma_j^z$ in Eq. (3.73).

At 1^{st} order, we find that the only terms to appear are also proportional to P_0, and so we can absorb them into constants of the 0^{th} order Hamiltonian. At 2^{nd} order, non-trivial terms can appear corresponding to each edge of the honeycomb lattice. Neglecting $O(1)$ constants, the effective Hamiltonian will take the form

$$H^{\langle 2\rangle}_{\text{eff,ds}} \sim -P_0 - \varepsilon^2 \sum_{\substack{s\\ s'\sim s}} P_0 C_{s,s'} P_0 \tag{3.87}$$

$$C_{s,s'} \equiv \sum_{\substack{i,j,k\\ i',j',k'}} \mathscr{P}^\dagger_{s,s'} \delta^{ijk}_{i'j'k'}(s,s') |ijk\rangle\langle ijk|_{c,s} \cdot |i'j'k'\rangle\langle i'j'k'|_{c,s'} \mathscr{P}_{s,s'} \tag{3.88}$$

where $s'\sim s$ runs over all s' neighbouring s (with s and s' sites of the PEPS lattice). The function $\delta^{ijk}_{i'j'k'}(s,s')$ takes the form of a Kronecker delta $\delta_{ii'}$, $\delta_{jj'}$, or $\delta_{kk'}$ for s and s' connected by an edge running northeast, northwest, or vertically respectively. These second order terms arise from the product of M_e on the two PEPS edges connecting s and s'. Recalling that each site has its own label for the state of the double semion qubit on incident edges of the honeycomb lattice, the $C_{s,s'}$ terms can be interpreted as requiring that the two labels for the state (one each from s and s') are consistent. This resolves the apparent overcounting of degrees of freedom present in the model.

If we continue expanding the effective Hamiltonian order by order, we will find that no new terms (that are not products of 2^{nd} order terms) arise until 6^{th} order. At this order, a new term will arise from the product of M_e terms around the inside of a hexagonal plaquette. We can write the effective Hamiltonian (neglecting products of 2^{nd} order terms and constant factors) as

$$H^{\langle 6\rangle}_{\text{eff,ds}} \sim -P_0 - \varepsilon^2 \sum_{\substack{s\\ s'\sim s}} P_0 C_{s,s'} P_0 - \varepsilon^6 \sum_p P_0 B_p P_0 \tag{3.89}$$

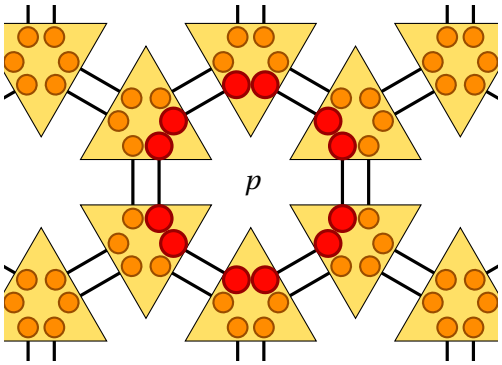

Figure 3.3 – The B_p operator acts on the edges of the PEPS lattice closest to the centre of the plaquette p. The affected qubits are shown here in red.

where the action of B_p can be described as

$$B_p \sim \prod_{e=(s,s')\in p} \left(|00\rangle\langle 11|_{s,s'} + |11\rangle\langle 00|_{s,s'}\right) \tag{3.90}$$

with $e = (s, s')$ the edges of the PEPS lattice comprising the interior of the plaquette p (see Fig. 3.3).

We can more clearly examine the effect of B_p by restricting to the image of all $P_0 C_{s,s'} P_0$. Call the projector to this subspace P_C, and note that it is the ground space of $H^{\langle 2\rangle}_{\text{eff,ds}}$. Within this subspace, we can unambiguously assign code space state labels to the edges of the honeycomb lattice as in the standard definition of the double semion model. If we then evaluate $P_C B_p P_C$, we find that phases accumulate depending on the state of the edges leading out of the plaquette under consideration (the legs of the plaquette). This is due to the asymmetry between the phase factors defining the $|ijk\rangle_c$ states of Eqs. (3.76)-(3.79).

On the double semion model states (i.e. those associated with the honeycomb lattice), we can describe this by

$$P_C B_p P_C \sim \left(\prod_{k\in p} \sigma^x_k\right)\left(\prod_{m\sim p} i^{\frac{1-\sigma^z_m}{2}}\right) \tag{3.91}$$

where k runs over honeycomb lattice edges comprising p and m runs over edges incident to p, precisely as in Eq. (3.73).

Given also that the $P_0 B_p P_0$ commute with the $P_0 C_{s,s'} P_0$, this completes the specification of the ground space of this model. The effect of each type of term arising in the effective Hamiltonian on the low energy space can be summarized as follows.

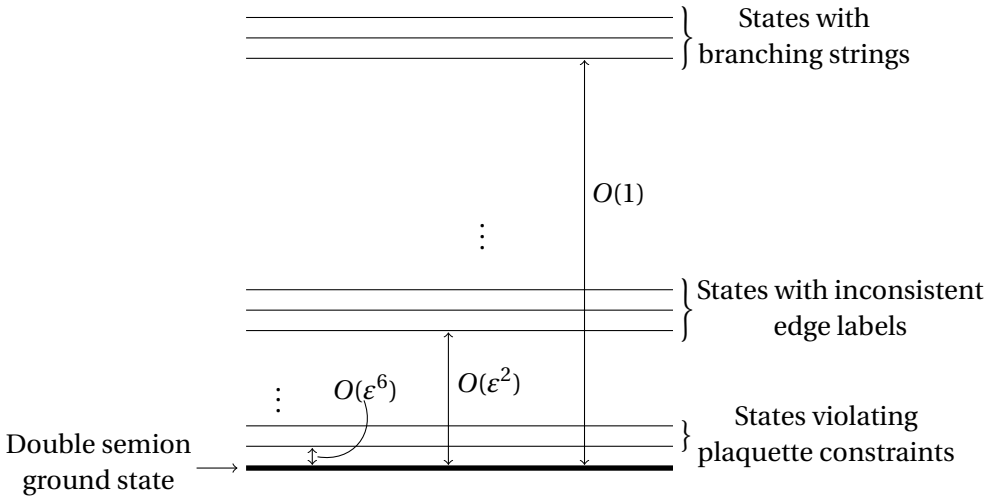

Figure 3.4 – A schematic of the energy level structure of our effective Hamiltonian for the double semion model defined by Eq. (3.89), showing the lowest excited states for each characteristic energy scale (each order of perturbation theory).

0^{th} order:	Forbids disallowed vertex configurations (branching strings)
2^{nd} order:	Enforces consistency between the two descriptions of the state on each edge of the honeycomb lattice (only one qubit per edge)
6^{th} order:	Gives rise to plaquette energetics of the double semion model

Each of these types of term acts on a different characteristic energy scale, based on the order of perturbation theory at which they arise. This gives the spectrum of our system as in Fig. 3.4. The ground state can easily be identified as (an encoded form of) the double semion ground state.

In previous examples of this kind of construction [BR06, BFBD11], the local symmetries of the target model were exact (i.e. not approximate) symmetries of the full Hamiltonian (including perturbation). However, as discussed in Sec. 3.6.2, this is not a general feature of our construction. In this double semion example, note that the 2^{nd} order terms correspond to exact symmetries of the model, while the 6^{th} order terms do not.

The Hamiltonian we presented is 2-local if a code gadget is considered as one system. However, if we consider the virtual qubits to be distinct particles, we would need to use further perturbation gadgets techniques as outlined in Sec. 3.6.1 to reduce the Hamiltonian interactions to 2-local. Examples of our construction that would naturally allow for a 2-local Hamiltonian even on the virtual qudits include those reproducing the quantum double ground states [BFBD11].

Chapter Review

We construct perturbative 2-local parent Hamiltonians for a broad class of PEPS.

- Similarly to Chapter 2, we make use of a perturbation gadgets approach based on code gadgets. As such, the target models are again reproduced in an encoded form.
- Our construction applies to isometric, topologically ordered PEPS satisfying a condition we call "quasi-injectivity", which we believe to be a generalization of known classes such as injective, G-injective, (G,ω)-injective, and H-injective PEPS.
- The structure of our Hamiltonian and code gadgets again is directly inspired by the PEPS construction.
- In contrast to the construction of Chapter 2 for the toric code and quantum double models, we make use of the more rigorous Schrieffer-Wolff perturbation expansion. This avoids approximating the self-energy as independent of energy, and allows for explicit error bounds on several important quantities.
- We show that there exists a finite order of perturbation theory such that the low-energy effective Hamiltonian of our model has the target isometric, quasi-injective PEPS as its ground state and is gapped.
- We also show that for topologically ordered, isometric, quasi-injective PEPS, the low-energy effective Hamiltonian of our model remains gapped and has a ground state in the same phase as the desired PEPS to arbitrary order of perturbation theory.
- In contrast to the construction of Chapter 2, we treat each code gadget as an indivisible particle, as opposed to being composed of several component particles, for the purposes of defining 2-locality. We discuss how this issue may be reconciled by the use of specially tailored encodings or further perturbation gadgets.
- We find that the local symmetries of the PEPS are not generally reproduced exactly in our construction, as compared to the special case of the quantum double models treated in Chapter 2.
- We include a concrete demonstration of the double semion string-net state arising as the ground state of our model.

4 Generalized Cluster States Based on Finite Groups

Abstract

We define generalized cluster states based on finite group algebras in analogy to the generalization of the toric code to the Kitaev quantum double models. We do this by showing a general correspondence between systems with CSS structure and finite group algebras, and applying this to the cluster states to derive their generalization. We then investigate properties of these states including their PEPS representations, global symmetries, and relationship to the Kitaev quantum double models. We also comment on possible applications of these states including a protocol for universal adiabatic topological cluster state quantum computation.

4.1 Introduction

Cluster states (or graph states) [RB01, RBB03] are the prototypical resource for measurement-based quantum computation (MBQC) [BBD$^+$09]. This is broad category of strategies for implementing fault-tolerant quantum information processing equivalent but in contrast to the quantum circuit model, adiabatic quantum computation, and topological quantum computation. MBQC proceeds by taking a suitable entangled many-particle resource state and performing computation by sequential single-particle measurements that may be chosen adaptively based on previous measurement results.

The cluster states have a particularly simple structure that allows for straightforward analysis of their properties. They also have many desirable features for a resource state: for example, they are the output of a finite-depth quantum circuit, and also the frustration-free ground states of a (gapped) commuting local Hamiltonian.

Apart from their usefulness for standard MBQC, the cluster states are also related to topologically ordered systems such as the toric code [Kit03, DKLP02, RBH05, HRD07, BSK$^+$11] and

the color codes [BMD06, BMD08b]. In fact, this relationship can be leveraged to define a protocol for MBQC that exploits the natural fault-tolerance properties of topological quantum computation schemes [RHG07]. The cluster states can also be used to study general stabilizer states, as all stabilizer states are equivalent to cluster states under local Clifford operations [VdNDDM04]. Additionally, the cluster states have been used in studies of such diverse topics as the origin of quantum computational power [AB09] and contextuality [Rau13].

Since the cluster states are such an important theoretical tool for studying these topics, it is of interest to ask if their properties can be generalized in any interesting ways. In this chapter we take steps towards answering this question, in particular motivated by the relation between cluster states and topologically ordered systems. In so doing, we provide a general framework for similar generalization programmes.

The toric code is the simplest member of the family of topologically ordered Kitaev quantum double models [Kit03]. These models are defined by a finite group G (of which the toric code corresponds to $\mathbb{Z}_2$). These models are of significant interest for condensed matter physics, where they are an important testbed for the phenomenology of topological order, as well as quantum information, where they can be used to implement topological quantum computation, for example through braiding of quasiparticles [NSS+08] or code deformation [BMD09], or can be used as quantum memories [DKLP02]. Though extensions of the Kitaev quantum double models have also been proposed based on a Hopf algebra H [BMCA13], or twisted quantum doubles labelled by a finite group G and a 3-cocycle ω [HWW13], we will restrict our consideration to the finite group case here. Most of the important phenomenology of these generalizations can be captured by finite groups, and in particular the qualitative distinction between Abelian and non-Abelian topological phases is manifested in Kitaev quantum double models for Abelian and non-Abelian groups respectively. Abelian phases such as the toric code cannot be used for quantum computation by braiding of quasi-particles, and are not known to be able to implement universal topological quantum computation via code-deformation. It is known that code-deformation in topological stabilizer codes such as the toric code cannot produce a universal gate set [BK13], though universal quantum computation can still be achieved by using non-topological operations such as magic state distillation [BK05, CLB+14].

For these reasons, we define a family of generalized cluster states based on arbitrary finite groups G, where the standard qubit cluster state corresponds to the simplest group $\mathbb{Z}_2$. The previously known higher-qudit cluster states [ZZXS03, Hal07] correspond to the cyclic groups $\mathbb{Z}_d$. In order to make this generalization process as clear as possible, we first make a general connection between general qubit CSS states and the group $\mathbb{Z}_2$. This allows an intuitive generalization of any such system, which may be more generally applicable.

We explore the properties of the generalized cluster states defined in this way, such as their global symmetries and PEPS representations, in analogy to the qubit case [SAF+11, VC04]. We also show how the generalized cluster states retain a relation to the corresponding quantum double models, and discuss possible applications of the generalized cluster states making use

of this relation.

This chapter is organized as follows. In Sec. 4.2 we outline the group structure of CSS states and the general method of generalization we will follow. This is then used in Sec. 4.3 to define the generalized cluster states for arbitrary finite groups G. Sec. 4.4 is devoted to exploring some properties of these states. Finally, in Sec. 4.5 we briefly consider applications for generalized cluster states including preparation of the Kitaev quantum double states and a generalization of the topological cluster state computation scheme, before discussing possible extensions of the kind of generalization scheme proposed here and providing some concluding remarks.

4.2 From CSS structure to finite groups

In this chapter, we will generalize the familiar qubit cluster state to states based on finite group algebras. In order to do this, we will make use of a general prescription to translate from a system with CSS structure [CS96, Ste96] to one based on the group $\mathbb{Z}_2$.

Many interesting models defined on spin-$^1/_2$ systems have a CSS structure. While the term CSS has a specific technical meaning as a class of stabilizer codes, we will use it in its more colloquial sense to mean any system involving interactions that consist either of products of Pauli X operators or products of Pauli Z operators.

Systems with a CSS structure have a natural interpretation in terms of the group algebra of $\mathbb{Z}_2$. Recall that $\mathbb{Z}_2$ has two elements (labelled 1 and the identity 0), group multiplication is addition modulo 2 ($\oplus$), and there are two irreducible representations. The trivial and alternating irreps we label + and − respectively, with $\Gamma_+(0) = \Gamma_+(1) = \Gamma_-(0) = 1$ and $\Gamma_-(1) = -1$.

We can associate qubit states and operators with objects related to the group $\mathbb{Z}_2$ by considering the computational basis states of our qubit to be labelled by group elements. That is, we take $|0\rangle$ and $|1\rangle$ to be associated with the respective group elements 0 and 1. Following this, the Pauli X operator can be seen to act as group multiplication by the 1 element. For this reason we denote it by $X_1 \equiv X$. We can also see that $X_0 \equiv X^0 = I$ acts as group multiplication by the 0 element. Thus we consider X_g to act as group multiplication by an element $g \in \mathbb{Z}_2$. We can also interpret the CNOT gate in this context as a controlled group multiplication operation. This can easily be seen by $\mathrm{CNOT}|g\rangle|h\rangle = |g\rangle|g \oplus h\rangle$.

The conjugate basis states $|+\rangle$ and $|-\rangle$ can be associated with the irreducible representations of $\mathbb{Z}_2$ by noticing that $|\pm\rangle \propto \Gamma_\pm(0)|0\rangle + \Gamma_\pm(1)|1\rangle$ (throughout this chapter we will consider only unitary irreducible representations over $\mathbb{C}$ unless otherwise specified). We can similarly consider the powers of the Pauli Z operator to be associated with the representations of $\mathbb{Z}_2$ as $Z_+ \equiv Z^1$ and $Z_- \equiv Z^0$. Notice then that $Z_\pm|g\rangle = \Gamma_\pm(g)|g\rangle$.

The group $\mathbb{Z}_2$ has much structure that is absent for general groups. In particular, since it is Abelian there is a natural isomorphism between the group and its dual. The elements of the dual group corresponding to irreps of $\mathbb{Z}_2$, this gives a natural map between group elements

and irreps that takes 0 to + and 1 to −. In this way we can interpret the Hadamard gate as implementing this bijection. Although the CPHASE gate has no fundamental interpretation in terms of objects from the group, it can be brought into this framework by noticing that CPHASE can be constructed from a circuit of Hadamard and CNOT gates.

This entire structure is summarized in the first two columns of Table 4.1. It also gives us an avenue to generalize many of these concepts to arbitrary groups. In interpreting the structure of the qubit in terms of $\mathbb{Z}_2$, the most significant property of this group that does not still hold in the general case is the existence of a natural isomorphism from group elements to irreps. The fact that this is not available for a general group G is the reason that the CSS structure is important when generalizing to arbitrary finite groups, as we will show.

Now that the properties of the qubit have been related to properties of $\mathbb{Z}_2$, the generalization to an arbitrary finite group G is relatively straightforward. 2-dimensional qubits are replaced by $|G|$-dimensional qudits. The analogue of computational basis states for these qudits are labelled by group elements $g \in G$ (we call this the group element basis). It is worthwhile noting that there is a preferred state corresponding to the identity group element e. Thus the $|0\rangle$ state of the qubit corresponds in general to the $|e\rangle$ state of the group element basis.

The Pauli X operator of the qubit generalizes to left and right group multiplication operators $X_g^{\leftarrow}$ and $X_g^{\rightarrow}$ acting as

$$X_g^{\leftarrow}|h\rangle = |gh\rangle \text{ and} \tag{4.1}$$

$$X_g^{\rightarrow}|h\rangle = |hg^{-1}\rangle. \tag{4.2}$$

Similarly, the CNOT gate generalizes straightforwardly to a controlled left or right group multiplication gate.

The conjugate basis of the qubit was interpreted as representation states, and in the general case we label these states by matrix elements of an unitary irreducible representation (or irrep) of G, and define

$$|\Gamma^{ij}\rangle = \sqrt{\frac{d_\Gamma}{|G|}} \sum_{g\in G} [\Gamma(g)]_{ij}|g\rangle, \tag{4.3}$$

where $[\Gamma(g)]_{ij}$ is given by the matrix element (i, j) associated with the action of a group element g in representation Γ, and d_Γ is the dimension of Γ. We call this basis the representation basis as compared to the group element basis. Noting that $\sum_\Gamma d_\Gamma^2 = |G|$, orthonormality of the representation basis follows directly from the grand orthogonality theorem of group representations:

$$\sum_{g\in G} [\Gamma_\lambda(g)]^*_{ij}[\Gamma_\sigma(g)]_{i'j'} = \delta_{\lambda\sigma}\delta_{ii'}\delta_{jj'}\frac{|G|}{d_\lambda}. \tag{4.4}$$

$\mathbb{Z}_2$	Qubit	Qudit	G
Elements $\{0,1\}$	$\|0\rangle, \|1\rangle$	$\|g\rangle$ $(d = \|G\|)$	Elements $g \in G$
Multiplication $\oplus g$	$X_g\|h\rangle = \|g \oplus h\rangle$	$X_g^{\leftarrow}\|h\rangle = \|gh\rangle$ $X_g^{\rightarrow}\|h\rangle = \|hg^{-1}\rangle$	Multiplication
Irreps $\{\Gamma_+, \Gamma_-\}$	$\|\pm\rangle = \frac{1}{\sqrt{2}}(\Gamma_\pm(0)\|0\rangle + \Gamma_\pm(1)\|1\rangle)$	$\|\Gamma^{ij}\rangle = \sqrt{\frac{d_\Gamma}{\|G\|}} \sum_g [\Gamma(g)]_{ij} \|g\rangle$	Irreps $\Gamma \in \mathrm{Rep}(G)$
Irrep Action $\Gamma(g)$	$Z_\Gamma\|h\rangle = \Gamma(h)\|h\rangle$	$Z_{\Gamma^{ij}}\|h\rangle = [\Gamma(h)]_{ij}\|h\rangle$	Irrep Action $[\Gamma(g)]_{ij}$
$\mathbb{Z}_2 \cong \mathrm{Rep}(\mathbb{Z}_2)$	Hadamard gate	-	-
Controlled Not	$\mathrm{CNOT}\|g\rangle\|h\rangle = \|g\rangle\|g \oplus h\rangle$	$\mathrm{CMULT}^{\leftarrow}\|g\rangle\|h\rangle = \|g\rangle\|gh\rangle$ $\mathrm{CMULT}^{\rightarrow}\|g\rangle\|h\rangle = \|g\rangle\|hg^{-1}\rangle$	Controlled Multiplication

Table 4.1 – Summary of the correspondence between group algebras and states or operators on quantum systems.

The transformation from the representation basis to the group element basis can also be found as

$$|g\rangle = \sum_{\Gamma^{ij}} \sqrt{\frac{d_\Gamma}{|G|}} [\Gamma(g)]_{ij} |\Gamma^{ij}\rangle. \tag{4.5}$$

As in the group element basis, there is a preferred state in the representation basis. This corresponds to the trivial irrep I. The trivial irrep state is given by an equal superposition over all group element states, and reduces to the $|+\rangle$ state in the case that $G = \mathbb{Z}_2$.

The generalizations of the Pauli Z operators are labelled by matrix elements of irreps of G. As in the $\mathbb{Z}_2$ case, they act on group element basis states by accumulating amplitudes corresponding to the relevant matrix element of the group element in the given representation. That is,

$$Z_{\Gamma^{ij}} |h\rangle = [\Gamma(h)]_{ij} |h\rangle. \tag{4.6}$$

These generalizations are summarized in Table 4.1.

The Hadamard gate and CPHASE gate of the qubit have no natural generalization to an arbitrary group in this way. Similarly, interactions that do not have CSS structure cannot be generalized for the following reason. If we consider an operator constructed from mixed X and Z operators on a set of qubits, to generalize this operator to the group G we must associate a group element to the X operator and a representation to the Z operator. There is no natural way to choose a representation corresponding to each group element, and so we cannot consistently generalize a mixed operator of this type. This is a direct consequence of the fact that the Hadamard operator has no analogue for arbitrary groups. Given that we can only consider systems with CSS structure in this framework, it is clear that the Hadamard and CPHASE gates cannot be generalized, as they take CSS systems to non-CSS systems.

One way to interpret Table 4.1 is as a prescription to design quantum systems with algebraic properties inherited from an arbitrary finite group. In general, the structure of these algebraic properties will be closely related to the quantum double of the group under consideration, as is the case for example in the Kitaev quantum double models, which can be interpreted in this framework. One could also consider generalizing this correspondence from groups to more general objects such as Hopf algebras (as has been done for the Kitaev quantum double models). This will briefly be discussed in Section 4.5.2, as well as speculation on further possible generalizations.

Of course, the machinery introduced here simplifies significantly if G is chosen to be a cyclic group $\mathbb{Z}_d$. In this case, the representations are all 1-dimensional d^{th} roots of unity. The basis change between the group element and representation bases for these groups is simply the discrete Fourier transform. Significantly, there also exists a natural isomorphism from the space of irreps of $\mathbb{Z}_d$ to the space of elements. This allows us to generalize the Hadamard gate and removes the necessity of considering only systems with CSS structure. The cluster states

corresponding to the cyclic groups have been previously defined and studied [ZZXS03, Hal07].

4.3 Generalized cluster states

We can use the general machinery established in the previous section to generalize the cluster state. This will give a family of states labelled by decorated graphs and a group G. As a prelude to the introduction of these general states, let us first review the definition of the qubit cluster state. Since the standard definition does not have CSS structure, we will need to consider a slightly modified definition of the cluster state that is more amenable to generalization.

4.3.1 Qubit cluster states

A qubit cluster state [RB01, RBB03] is uniquely specified by an underlying graph Λ. One convenient way to define these states is as the output of a certain constant depth quantum circuit. Equivalently, they can be described as the common +1 eigenstate of a set of commuting stabilizer operators. We will describe the qubit cluster state in both of these languages, as these two descriptions showcase different desirable features of the cluster state. In the first case, the cluster state can be prepared in constant time by an appropriate parallel quantum circuit, while in the latter case the cluster state can be seen as the unique gapped ground state of a local Hamiltonian, namely that formed by the (negative) sum of the relevant stabilizer operators.

The cluster state is given by

$$|\mathscr{C}_\Lambda\rangle = \prod_{<m,n>} \mathrm{CPHASE}(m,n) \bigotimes_{v\in\Lambda} |+\rangle_v \tag{4.7}$$

with $< m, n >$ running over all edges and v running over all vertices of Λ. The CPHASE gate is given by $\mathrm{CPHASE}(m,n)|a\rangle_m|b\rangle_n = (-1)^{ab}|a\rangle_m|b\rangle_n$ for $a, b \in \mathbb{Z}_2$. As a circuit, we place qubits in the $|+\rangle$ state at each site of Λ and then perform CPHASE gates between the qubits connected by an edge. Since the CPHASE gates commute, this is always a constant-depth circuit (assuming bounded degree of Λ).

It is straightforward to derive the stabilizers of this state by considering the circuit of Eq. (4.7) in the Heisenberg representation. The qubit cluster state is thus the common +1 eigenstate of the stabilizer operators

$$S(v) = X(v) \prod_{w\sim v} Z(w) \tag{4.8}$$

for every site v, where $w \sim v$ runs over neighbours of v. Clearly, this state does not have the CSS structure discussed in Sec. 4.2. This can be seen in two ways: firstly the stabilizers (4.8) involve both X and Z operators in the same stabilizer, and secondly the circuit (4.7) involved CPHASE operators. The toolkit introduced in Sec. 4.2 cannot be used to generalize states of

this form.

We can, however modify the definition of the cluster state to endow it with CSS structure. In order to do this, we must restrict to bipartite graphs Λ. On these graphs, we can partition the sites of Λ into an odd set Λ_o and an even set Λ_e such that all edges of Λ involve one vertex from Λ_o and one vertex from Λ_e. Given this structure, we can define the CSS cluster state as

$$|\mathscr{C}_\Lambda^{CSS}\rangle \equiv \prod_{v\in\Lambda_e} H(v)|\mathscr{C}_\Lambda\rangle, \tag{4.9}$$

where H is the Hadamard operator. This allows us to rewrite the circuit constructing the CSS cluster state as

$$|\mathscr{C}_\Lambda^{CSS}\rangle = \prod_{\substack{<m,n> \\ m\in\Lambda_o, n\in\Lambda_e}} \mathrm{CNOT}(m,n) \bigotimes_{w\in\Lambda_o} |+\rangle_w \bigotimes_{v\in\Lambda_e} |0\rangle_v \tag{4.10}$$

where here the CNOT gates act with the odd qubit m as control and even qubit n as target. We will generally use the notation that a controlled gate takes two site labels as arguments and acts on the first as the control. The bipartite property of Λ guarantees that each CNOT gate acts on one odd and one even qubit. Even though CNOT gates do not commute in general, two CNOT gates with common targets or common controls will commute. This gives us the fact that the circuit specified by (4.10) is again always constant-depth as expected.

The stabilizers of the CSS cluster state are given by

$$S^e(v) = Z(v) \prod_{w\sim v} Z(w), \text{ and} \tag{4.11}$$

$$S^o(w) = X(w) \prod_{v\sim w} X(v) \tag{4.12}$$

for v and w even and odd sites respectively. This demonstrates the claimed CSS structure of these states. This can also be seen by noting that the circuit (4.10) consists only of operators that preserve CSS structure (i.e. CNOT gates). Although it can only be defined on bipartite graphs, when it exists the CSS cluster state is locally equivalent to the corresponding standard cluster state and so has all the same fundamental properties, notably including the ability to perform universal measurement-based quantum computation.

4.3.2 Finite group cluster states

Given the toolkit of Sec. 4.2 and the definition of the CSS cluster state given above, we will now describe the generalization of the cluster state to arbitrary finite groups G. These cluster states will inherit many of the algebraic properties of the group that defines them.

As compared to the qubit cluster states where an undirected graph completely specifies the state, for an arbitrary group G this is insufficient to uniquely determine a generalized cluster state. This is similar to the generalization of the toric code to the quantum double models,

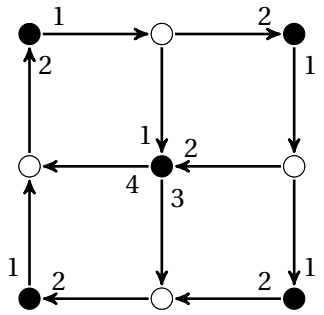

Figure 4.1 – A directed bipartite graph augmented with an ordering of edges incident to each even vertex. Even vertices are shown as solid circles, while odd vertices are represented by open circles. This data is sufficient to specify a generalized cluster state.

where the former is completely specified by an undirected graph, while the latter requires directed edges to specify the model. In particular, to describe a generalized cluster state we require a directed bipartite graph Λ, together with an ordering $\#_v(w)$ of the neighbours w of each even vertex v. An example of such a structure is shown in Fig. 4.1. The roles that are played by the additional direction and ordering parameters will become clear during the construction of the generalized cluster states.

Given such a graph Λ and ordering $\#$, together with a finite group G, the generalized cluster state is a state on a system of $|G|$-dimensional qudits at each site of Λ. It is most convenient to generalize the qubit cluster state by considering the circuit that defines it according to Eq. (4.10). The elements in this circuit are CNOT gates, $|+\rangle$ states and $|0\rangle$ states, each of which has a natural analogue in Table 4.1.

Circuit representation

The qubit $|+\rangle$ state is interpreted as a special case of the trivial irrep state $|I\rangle = \frac{1}{\sqrt{|G|}}\sum_g |g\rangle$. Similarly the $|0\rangle$ state corresponds to the identity group element state $|e\rangle$ in general. Finally, the last ingredient in the CSS cluster state preparation circuit is the CNOT gate, which generalizes to either the left or right controlled multiplication gates $\text{CMULT}^{\leftrightarrows}$.

Loosely speaking then, we define the generalized cluster state as

$$|\mathscr{C}^{CSS}_{\Lambda,\#,G}\rangle \sim \prod_{\substack{<m,n> \\ m\in\Lambda_o, n\in\Lambda_e}} \text{CMULT}(m,n) \bigotimes_{w\in\Lambda_o} |I\rangle_w \bigotimes_{v\in\Lambda_e} |e\rangle_v. \tag{4.13}$$

There are two ways in which (4.13) does not yet constitute a full specification of the state $|\mathscr{C}^{CSS}_{\Lambda,\#,G}\rangle$. The first is that there is an ambiguity regarding whether CMULT gates should act as left or right multiplication. The second is that we have not specified an order in which to apply the CMULT gates, which in general do not commute on their targets. Resolving these ambiguities requires the additional structure we have specified in the $\#$ orderings and in the

directions of the edges of Λ. Note that since the CMULT gates commute on their controls, we need not be concerned about the relative order of gate application on odd qudits, and so need not specify a global order of CMULT application. It suffices to specify the ordering separately at each even vertex.

We can complete the specification of Eq. (4.13) by firstly choosing the ordering of the CMULT gates at a given even site v according to $\#_v$. Secondly, we choose the CMULT(m,n) gate to act as left multiplication if the edge (m,n) runs from n to m, and as right multiplication otherwise. This convention can be remembered by placing the control (odd) qudit on the left of the target (even) qudit. The multiplication sense is then given directly by the direction of the edge connecting the qudits. We denote these conventions in the following way:

$$|\mathscr{C}^{CSS}_{\Lambda,\#,G}\rangle \equiv \prod_{\substack{<m,n> \\ m\in\Lambda_e, n\in\Lambda_o}}^{\#} \text{CMULT}^{\leftrightarrows}(m,n) \bigotimes_{w\in\Lambda_o} |I\rangle_w \bigotimes_{v\in\Lambda_e} |e\rangle_v \tag{4.14}$$

where CMULT$^{\leftrightarrows}(m,n)$ acts as CMULT$^{\rightarrow}$ (CMULT$^{\leftarrow}$) for an edge directed from m to n (n to m). This is now a complete specification of the generalized cluster state $|\mathscr{C}^{CSS}_{\Lambda,\#,G}\rangle$. Note that since the CMULT operators commute on their controls, the circuit (4.14) is always constant-depth as in the qubit case (again assuming Λ has bounded degree).

Strictly speaking, the orderings # contain more information than is necessary to specify the state $|\mathscr{C}^{CSS}_{\Lambda,\#,G}\rangle$. Since left multiplication commutes with right multiplication, we could rearrange the order of CMULT application without affecting the state $|\mathscr{C}^{CSS}_{\Lambda,\#,G}\rangle$ as long as we do not change the relative order of CMULT gates acting on edges directed outwards and the relative order of gates acting on edges direct outwards from a given even vertex. For notational simplicity we will continue to use the redundant description # of the ordering at each even vertex.

The circuit (4.14) is a perfectly adequate definition of the generalized cluster states. However, the stabilizer formalism has proved to be an extremely powerful tool in the analysis of cluster states and similar qubit systems. For this reason we will compute the stabilizer representation of the generalized cluster states.

Stabilizer representation

The term "stabilizer" has slightly different meanings in different contexts. Often it is used to mean a subgroup of the n-qubit Pauli group that does not contain -1. The relevant stabilizer states are then the common $+1$ eigenstates of the stabilizer group. This is the sense in which the qubit cluster state and the CSS cluster state we discussed in Sec. 4.3.1 are stabilizer states of their relative stabilizer groups.

More generally, stabilizer states can be thought of as the $+1$ eigenstates of an arbitrary set of operators. Varying degrees of structure can be introduced to make the set more amenable to study, for example requiring that the stabilizer operators are monomial matrices as in the monomial stabilizer formalism [VdN11]. As with the stabilizers of the Kitaev quantum double

models, the generalized cluster states can be cast in the monomial stabilizer formalism. We may abuse the language slightly by referring to a set of stabilizers in the generalized sense as a group, even if we do not present them in a form that has the algebraic structure of a group.

One of the most attractive features of the Pauli stabilizer formalism is the ability to efficiently simulate operations that map stabilizer states to stabilizer states (through the Gottesman-Knill theorem). This ability carries directly over to stabilizer formalisms based on Abelian group algebras [VdN13, BVVdN14, BVLVdN14]. Such strong simulability properties seem to require more structure than is available for general stabilizer states. However, some notions of classical simulability remain in certain cases. For example, for sufficiently structured states such as the Kitaev quantum double models, the monomial stabilizer formalism allows the efficient evaluation of expectation values for local observables [VdN11]. We expect analogous simulability results to apply to our models as they are based on the same algebraic structure.

Apart from the motivation of classical simulation, the existence of a local stabilizer description guarantees the existence of a local, commuting, gapped parent Hamiltonian for these states. It can also be a useful way of illustrating phenomena that would be more difficult to describe in the Schrodinger representation, for example as is the case in the Kitaev quantum double models where stabilizer operators correspond directly to quantities of interest such as charges or Wilson loops.

In order to explicitly determine a set of stabilizer operators for the generalized cluster states, we examine the action of the circuit implied by Eq. (4.14) in the Heisenberg representation. This circuit begins with a product state of $|I\rangle$ on odd vertices and $|e\rangle$ on even vertices.

Now, notice that the state $|I\rangle = \frac{1}{\sqrt{|G|}} \sum_g |g\rangle$ is stabilized by all group multiplication operators. That is,

$$X_g^{\leftrightarrows} |I\rangle = |I\rangle \tag{4.15}$$

for all g, and either multiplication sense $\leftrightarrows$. Similarly, we can define a set of stabilizers for $|e\rangle$, noting that

$$Z_{\Gamma^{ii}} |e\rangle = |e\rangle \tag{4.16}$$

for all Γ, i.

Although this is a perfectly legitimate stabilizer description of the state $|e\rangle$, for the purposes of calculating the stabilizers of the state $|\mathscr{C}^{CSS}_{\Lambda,\#,G}\rangle$ it will be more convenient to use an alternative representation. Defining the projectors to group element basis states $T_g \equiv |g\rangle\langle g|$, it is clear that $|e\rangle$ is stabilized by T_e. A more roundabout way to see this is to write the T_g operators in terms of the $Z_{\Gamma^{ij}}$ operators as

$$T_g = \frac{1}{|G|} \sum_\Gamma d_\Gamma \sum_{i,j} [\Gamma(g)]^*_{ij} Z_{\Gamma^{ij}} \tag{4.17}$$

and find

$$T_e|e\rangle = \frac{1}{|G|}\sum_{\Gamma} d_\Gamma \sum_{i,j} [\Gamma(e)]^*_{ij} Z_{\Gamma^{ij}}|e\rangle \tag{4.18}$$

$$= \frac{1}{|G|}\sum_{\Gamma} d_\Gamma^2 |e\rangle \tag{4.19}$$

$$= |e\rangle \tag{4.20}$$

as expected.

We thus have that prior to the application of any CMULT gates in Eq. (4.14) there are stabilizers for the system given by

$$\tilde{S}^e(v) = T_e(v), \text{ and} \tag{4.21}$$

$$\tilde{S}^o_g(w) = X^{\overleftrightarrow{}}_g(w) \tag{4.22}$$

for every even site v and odd site w, and all $g \in G$. These stabilizers trivially commute since they each act on distinct sites. In order to determine the stabilizers of the generalized cluster state then, we simply need to study the evolution of these operators under the action of controlled multiplication gates. This can be computed straightforwardly, and found to give

CMULT$^{\leftarrow}$	CMULT$^{\rightarrow}$
$X^{\leftarrow}_g \otimes I \to X^{\leftarrow}_g \otimes X^{\leftarrow}_g$	$X^{\leftarrow}_g \otimes I \to X^{\leftarrow}_g \otimes X^{\rightarrow}_g$
$X^{\rightarrow}_g \otimes I \to \sum_h X^{\rightarrow}_g T_h \otimes X^{\leftarrow}_{hg^{-1}h^{-1}}$	$X^{\rightarrow}_g \otimes I \to \sum_h X^{\rightarrow}_g T_h \otimes X^{\rightarrow}_{hg^{-1}h^{-1}}$
$I \otimes X^{\leftarrow}_g \to \sum_h T_h \otimes X^{\leftarrow}_{hgh^{-1}}$	$I \otimes X^{\leftarrow}_g \to I \otimes X^{\leftarrow}_g$
$I \otimes X^{\rightarrow}_g \to I \otimes X^{\rightarrow}_g$	$I \otimes X^{\rightarrow}_g \to \sum_h T_h \otimes X^{\leftarrow}_{hgh^{-1}}$
$T_g \otimes I \to T_g \otimes I$	$T_g \otimes I \to T_g \otimes I$
$I \otimes T_g \to \sum_h T_h \otimes T_{hg}$	$I \otimes T_g \to \sum_h T_h \otimes T_{gh^{-1}}$

where the first tensor factor is the control qudit and the second the target.

To construct the stabilizers of the generalized cluster states, we now build the state one CMULT gate at a time according to Eq. (4.14). We will first develop the stabilizers for the even sites of the lattice, and then return and compute the stabilizers corresponding to odd sites.

At each even site v of the lattice, prior to the application of any CMULT gates the state is stabilized by $\tilde{S}^e(v) = T_e(i)$. This site will be the target of any CMULT gates applied to it. For each edge directed outwards from v, a CMULT$^{\leftarrow}$ gate will be applied, and similarly a CMULT$^{\rightarrow}$ gate will be applied for each inwards directed edge. In order to describe the evolution of $\tilde{S}^e(v)$, it will be convenient to define $n^{\leftarrow v}_w$ and $n^{\rightarrow v}_u$ as the neighbours of v corresponding to the w^{th} outward directed edge or u^{th} inward directed edge respectively (where the ordering is given by

$\#_v$).

Recalling that CMULT$^{\leftarrow}$ gates commute on common targets with CMULT$^{\rightarrow}$ gates, we will consider first performing the CMULT$^{\leftarrow}$ gates on site v. As we apply the CMULT gates on outward directed edges sequentially in the order specified by $\#_v$, the stabilizer for this site becomes

$$\tilde{S}^e(v) \to \sum_{g_1} T_{g_1}(v) T_{g_1}(n_1^{\leftarrow v}) \tag{4.23}$$

$$\to \sum_{g_1,g_2} T_{g_2 g_1}(v) T_{g_1}(n_1^{\leftarrow v}) T_{g_2}(n_2^{\leftarrow v}) \tag{4.24}$$

$$\vdots$$

$$\to \sum_{\substack{g_w \\ \forall\, w \leftarrow v}} T_{\prod_{w'} g_{w'}}(v) \prod_{w''} T_{g_{w''}}(n_{w''}^{\leftarrow v}) \tag{4.25}$$

where in the final expression w runs over all outward directed neighbours of v and $\prod_w g_w = \cdots g_3 g_2 g_1$ (we also suppress the range of product and summation indices when they are clear from context). We can then similarly apply the gates on the inward directed edges of v (again in the appropriate order) and obtain

$$\tilde{S}^e(v) \to \sum_{\substack{h_u \\ \forall\, u \to v}} \sum_{\substack{g_w \\ \forall\, w \leftarrow v}} T_{(\prod_{w'} g_{w'})(\prod_{u'} h_{u'})^{-1}}(v) \prod_{u''} T_{h_{u''}}(n_{u''}^{\rightarrow v}) \prod_{w''} T_{g_{w''}}(n_{w''}^{\leftarrow v}) \equiv S^e(v). \tag{4.26}$$

Since it now has support on sites other than v, one might now worry that we will also need to calculate how $\tilde{S}^e(v)$ transforms under the other CMULT gates acting on the neighbours of v. However, since these CMULT operations all commute with each other (they share a common control, not target), this is not a concern. Thus (4.26) is the stabilizer corresponding to each even site of our cluster state, acting only on the given site and its nearest neighbours.

We can also derive the stabilizers corresponding to odd sites of Λ in a similar fashion. In this case, the stabilizers of an odd site w prior to the application of any CMULT gates are given by

$$\tilde{S}_g^o(w) = X_g^{\leftrightarrows}(w) \tag{4.27}$$

for all g. Although both the left and right multiplication operators form valid stabilizers for an odd site, only one set is needed to specify the state completely. For simplicity we will choose to study the left multiplication stabilizers though the analysis for the right multiplication operators would proceed in an analogous way. With this in mind, we restrict to the case

$$\tilde{S}_g^o(w) = X_g^{\leftarrow}(w). \tag{4.28}$$

The site w will act as the control for the CMULT gates applied to it. As such, it does not matter in which order the CMULT gates are applied at site w. However, in contrast to the

even sites, the odd site stabilizers will be affected by the order of CMULT gates applied to the neighbouring (even) vertices.

The CMULT gate corresponding to an outward directed edge from w will act as CMULT$^{\rightarrow}$ and inward directed edges correspond to CMULT$^{\leftarrow}$. Applying a CMULT gate on an inward directed edge to neighbour v, we find $\tilde{S}^o_g(w)$ becomes

$$\tilde{S}^o_g(w) \to X^{\leftarrow}_g(w) X^{\leftarrow}_g(v). \tag{4.29}$$

Now this operator has support on v as well as w. This means that we must consider the effects of the CMULT gates acting not only between w and its neighbours, but also between v and its neighbours. In doing so, we will only need to consider the effects of those gates applied to w after that corresponding to the edge $(w \leftarrow v)$. In addition, we need only consider edges with the same direction from v (i.e. outwards from v in this case).

We can make this effect explicit by finding the effect of these CMULT gates on an $X^{\leftarrow}_g$ operator acting on site v. As each successive CMULT$^{\leftarrow}$ is applied to edges connecting v to sites $\tilde{w}_1, \tilde{w}_2, \ldots$ that follow w in the $\#_v$ order, this operator transforms as

$$X^{\leftarrow}_g(v) \to \sum_{h_1} X^{\leftarrow}_{h_1 g h_1^{-1}}(v) T_{h_1}(\tilde{w}_1) \tag{4.30}$$

$$\to \sum_{h_1,h_2} X^{\leftarrow}_{(h_2 h_1) g (h_2 h_1)^{-1}}(v) T_{h_1}(\tilde{w}_1) T_{h_2}(\tilde{w}_2) \tag{4.31}$$

$$\vdots$$

$$\to \sum_{\substack{h_{\tilde{w}} \\ \forall\, \tilde{w} \leftarrow v, \tilde{w} > w}} X^{\leftarrow}_{(\prod_{\tilde{w}'} h_{\tilde{w}'}) g (\prod_{\tilde{w}''} h_{\tilde{w}''})^{-1}}(v) \prod_{\tilde{w}'''} T_{h_{\tilde{w}'''}}(\tilde{w}''') \tag{4.32}$$

where $\tilde{w} > w$ restricts to those $\tilde{w}$ that come after w in $\#_i$.

This operator still acts as multiplication on site v, but by a group element conjugated by terms taking into account states of the neighbours of v. It will be convenient to define this operator for any site v neighbouring w:

$$\tilde{X}^{\leftarrow}_g(v|_w) \equiv \sum_{\substack{h_{\tilde{w}} \\ \forall\, \tilde{w} \leftarrow v, \tilde{w} > w}} X^{\leftarrow}_{(\prod_{\tilde{w}'} h_{\tilde{w}'}) g (\prod_{\tilde{w}''} h_{\tilde{w}''})^{-1}}(v) \prod_{\tilde{w}'''} T_{h_{\tilde{w}'''}}(\tilde{w}'''). \tag{4.33}$$

Now having considered all the effects of site v and its neighbours on the stabilizer for site w, we have the stabilizer

$$\tilde{S}^o_g(w) \to X^{\leftarrow}_g(w) \tilde{X}^{\leftarrow}_g(v|_w). \tag{4.34}$$

As we apply this procedure to each of the edges directed inwards to w, the stabilizer transforms

to

$$\tilde{S}_g^o(w) \to X_g^{\leftarrow}(w) \prod_{v\to w} \tilde{X}_g^{\leftarrow}(v|_w). \tag{4.35}$$

In a similar way, we can also consider the effects of CMULT gates on outwards directed edges from w. If we apply a CMULT gate corresponding to an outward directed edge connecting site w and u, the $X^{\leftarrow}(w)$ operator will be transformed by each gate as

$$X^{\leftarrow}(w) \to X^{\leftarrow}(w)X^{\rightarrow}(u). \tag{4.36}$$

Following an analogous prescription to that used for the analysis of the inward directed edges, we are led to define the operator

$$\tilde{X}_g^{\rightarrow}(u|_w) \equiv \sum_{\substack{h_{\tilde{w}} \\ \forall\, \tilde{w}\to u, \tilde{w}>w}} X^{\rightarrow}_{(\prod_{\tilde{w}'} h_{\tilde{w}'})g(\prod_{\tilde{w}''} h_{\tilde{w}''})^{-1}}(u) \prod_{\tilde{w}'''} T_{h_{w'''}}(\tilde{w}'''). \tag{4.37}$$

This allows us to compute the stabilizers corresponding to each odd site w of a generalized cluster state as

$$\tilde{S}_g^o(w) \to X_g^{\leftarrow}(w) \prod_{v\to w} \tilde{X}_g^{\leftarrow}(v|_w) \prod_{u\leftarrow w} \tilde{X}_g^{\rightarrow}(u|_w) \equiv S_g^o(w). \tag{4.38}$$

In contrast to the qubit cluster state, whose stabilizers only act on a site and its nearest neighbours, in general the operators (4.38) act on a site, its nearest neighbours, and also its next-nearest neighbours.

Together, the even site stabilizers S^e (4.26) and the odd site stabilizers S^o (4.38) completely specify a generalized cluster state. The odd site stabilizers are monomial matrices in their current form, while the even site stabilizers are projectors and so can be made monomials by considering the alternative operators $2S^e - 1$. This means that the generalized cluster states can be studied in the framework of monomial stabilizer groups [VdN11] as claimed.

4.4 Properties of generalized cluster states

We will now explore some salient features of the generalized cluster states defined in the previous section. It is not our intention to provide a comprehensive specification of the properties of the states, but merely to comment on some features of the qubit cluster states and how they are survived in the general case.

One of the most important features of the qubit cluster state is that (on a suitable graph) it is a resource for universal measurement-based quantum computation [RBB03]. Since the qubit cluster state already has this universality property, considering generalized cluster states as re-

Figure 4.2 – Two different 3 qudit cluster states. Solid (open) circles represent even (odd) vertices. The simple structure of these graphs means that a vertex ordering is not required to specify the relevant cluster state. a) An even-odd-even 3 qudit cluster state. b) An odd-even-odd 3 qudit cluster state.

sources for standard measurement-based quantum computation will not give any qualitative advantage in this sense. However, it is possible that generalized cluster states may yield advantages in terms of practical application, for example by finding more efficient implementations of non-Clifford gates or by having desirable spectral properties (when considered as ground states of Hamiltonians). We will not directly address these issues of practical advantage here, though some of the general properties we discuss may be relevant to any such study.

4.4.1 Measurements

The results of measurements in the standard qubit cluster states can easily be determined using the stabilizer formalism. The properties of the resulting states are largely insensitive to the measurement outcomes obtained. By comparison, measurements on generalized cluster states give rise to some qualitatively new phenomena that do not appear in the qubit cluster state, such as significant dependence of the output state on measurement outcomes.

Ideally, we would like to understand the effect of measurements in the group element basis and the representation basis (the analogues of Z and X Pauli measurements) on an arbitrary generalized cluster state. However, since we can no longer use the simple Pauli stabilizer formalism to compute these effects, this general specification is outside the scope of this work. For this reason we will not exhaustively describe the results of measurement procedures on general cluster states. Instead, we will illustrate the kinds of new phenomena that can appear in a simple example. For this purpose, it is sufficient to consider 3 qudits on a line as in Fig. 4.2a or 4.2b.

For a group G, these states are stabilized by the operators

$$S(eoe,1) = \sum_{g\in G} T_g \otimes T_g \otimes I, \qquad S_g(oeo,1) = X_g^{\leftarrow} \otimes X_g^{\leftarrow} \otimes I, \tag{4.39}$$

$$S_g(eoe,2) = X_g^{\leftarrow} \otimes X_g^{\leftarrow} \otimes X_g^{\leftarrow}, \qquad S(oeo,2) = \sum_{g,h\in G} T_g \otimes T_{gh^{-1}} \otimes T_h, \tag{4.40}$$

$$S(eoe,3) = \sum_{g\in G} I \otimes T_g \otimes T_g, \text{ and} \qquad S_g(oeo,3) = I \otimes X_g^{\rightarrow} \otimes X_g^{\rightarrow}, \tag{4.41}$$

where *eoe* or *oeo* represent the even-odd-even and odd-even-odd cluster states of Figs. 4.2a and 4.2b respectively.

Explicitly then, these states can be written as analogues of the GHZ state in different bases:

$$|\mathscr{C}_{\mathrm{eoe}}\rangle = \frac{1}{\sqrt{|G|}} \sum_{g\in G} |g\rangle \otimes |g\rangle \otimes |g\rangle \tag{4.42}$$

$$|\mathscr{C}_{\mathrm{oeo}}\rangle = \frac{1}{|G|} \sum_{g,h\in G} |g\rangle \otimes |gh^{-1}\rangle \otimes |h\rangle. \tag{4.43}$$

The states $|\mathscr{C}_{\mathrm{eoe}}\rangle$ are clearly identical for any different choices of group G with the same order. For a general graph of course this is not true (as with $|\mathscr{C}_{\mathrm{oeo}}\rangle$), but nonetheless we will see group structure arise in the analysis of measurement outcomes on $|\mathscr{C}_{\mathrm{eoe}}\rangle$. This is because the natural measurements to consider are analogues of Pauli X and Z operators in the qubit case, and these operators also inherit structure of the group G.

The two measurements we consider here are those in the group element basis $\{|g\rangle\}$ (corresponding to Pauli Z) and in the representation basis $\{|\Gamma^{ij}\rangle\}$ (corresponding to Pauli X). If we measure the central qubit of our cluster in these bases, we will find that some phenomena arise which have no counterpart in the qubit cluster state.

Let us first recall what happens in the CSS qubit case (i.e. $G = \mathbb{Z}_2$). Since the *eoe* and *oeo* qubit cluster states can be transformed into one another by Hadamard gates on each qubit, we need only consider one of these states (the behavior of the other can be determined by exchanging X and Z). If we measure the central qubit of the *eoe* cluster in the Z basis and find outcome $m_z \in \mathbb{Z}_2$, the state on the remaining qubits becomes a product state $|m_z\rangle \otimes |m_z\rangle$. Alternatively, if we measure in the X basis with measurement outcome $m_X \in \{\pm\}$, we find a maximally entangled state $|0\rangle \otimes |0\rangle + m_x|1\rangle \otimes |1\rangle$.

For a general group G, the group element basis measurement proceeds in much the same fashion. For a outcome $m_g \in G$ of this measurement on an *eoe* cluster state, the resulting state is given by the product state $|m_g\rangle \otimes |m_g\rangle$. Similarly, the *oeo* cluster state is transformed to the maximally entangled state $\sum_{h\in G} |h\rangle \otimes |h^{-1}m_g\rangle$. In contrast, when performing a measurement in the representation basis, we find a qualitative departure from the qubit case. Such a measurement yields a triple of measurement outcomes (m_Γ, m_i, m_j) representing a matrix element of an irrep of G. Beginning with the *eoe* cluster state, we note that it can be rewritten as

$$|\mathscr{C}_{\mathrm{eoe}}\rangle = \sum_g \sum_{\Gamma^{ij}} \frac{\sqrt{d_\Gamma}}{|G|} [\Gamma(g)]^*_{ij} |g\rangle |\Gamma^{ij}\rangle |g\rangle. \tag{4.44}$$

Thus if we measure the central qudit in the representation basis, the resulting state is given as

$$\sum_g \sqrt{\frac{d_{m_\Gamma}}{|G|}} [m_\Gamma(g)]^*_{m_i m_j} |g\rangle |g\rangle. \tag{4.45}$$

For any Abelian group, this will give a maximally entangled state as in the qubit case. However

for a general group, the state (4.45) will be some less-than-maximally entangled state for any representation m_Γ with dimension greater than 1. We can see this by calculating the reduced density matrix of the first qudit as $\rho^{(1)}_{\mathscr{C}_{\text{eoe}}} = \sum_g \frac{d_{m_\Gamma}}{|G|} |[m_\Gamma(g)]_{m_i m_j}|^2 |g\rangle\langle g|$ which is not, in general, equal to $\sum_g \frac{1}{|G|}|g\rangle\langle g|$. Of course, for any Abelian group all $d_{m_\Gamma} = 1 = |[m_\Gamma(g)]_{m_i m_j}|^2$, and we recover the maximally entangled state as claimed.

The analogous measurement on an *oeo* cluster state produces a similar phenomenon. The resulting state after measurement is given by

$$|\mathscr{C}_{\text{oeo}}\rangle \to \sum_{g,h} \frac{\sqrt{d_{m_\Gamma}}}{|G|} [m_\Gamma(gh^{-1})]^*_{m_i m_j} |g\rangle|h\rangle \tag{4.46}$$

$$= \sum_{g,h\in G} \sum_{k=1}^{d_{m_\Gamma}} \frac{\sqrt{d_{m_\Gamma}}}{|G|} [m_\Gamma(g)]^*_{m_i k} [m_\Gamma(h^{-1})]^*_{k m_j} |g\rangle|h\rangle \tag{4.47}$$

$$= \sum_{g,h\in G} \sum_{k=1}^{d_{m_\Gamma}} \frac{\sqrt{d_{m_\Gamma}}}{|G|} [\overline{m_\Gamma}(g)]_{k m_i} [m_\Gamma(h)]_{m_j k} |g\rangle|h\rangle \tag{4.48}$$

$$= \sum_{k=1}^{d_{m_\Gamma}} \frac{1}{\sqrt{d_{m_\Gamma}}} |\overline{m_\Gamma}^{k m_i}\rangle |m_\Gamma^{m_j k}\rangle \tag{4.49}$$

for $\overline{m_\Gamma}$ the conjugate representation to m_Γ (recall that we consider only unitary irreducible representations over $\mathbb{C}$). This leaves us with a maximally entangled state of dimension d_{m_Γ}. For Abelian groups with only 1-dimensional irreps, this gives the product state as in the qubit case. However, for general groups the behavior is non-trivial.

In particular, these phenomena mean that the property of maximal localizable entanglement [PVMDC05] (i.e. any two qudits in the state can be brought into a maximally entangled state with certainty by measurement) is not always present for a generalized cluster state as it is for the qubit cluster state.

In order to develop a standard measurement-based quantum computation protocol making use of the generalized cluster states, compensating for the subtle interplay between measurement outcomes and remaining entanglement would require tools outside the scope of standard cluster state computation methods. It may be possible to develop such a scheme explicitly by making use of techniques in Ref. [GESPG07], combined with the PEPS representation of the generalized cluster states as found in Sec. 4.4.3. However, we will not consider this question further in this work, instead focussing on the relationship between the generalized cluster states and the Kitaev quantum double models as discussed in Sections 4.4.4 and 4.5.1. For this relationship, that the remaining entanglement in the state depends on prior measurement outcomes is crucial in reproducing the phenomenology of non-Abelian topological orders.

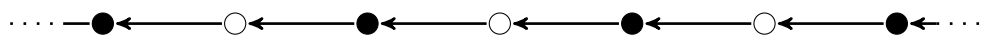

Figure 4.3 – An infinite 1D generalized cluster state graph.

4.4.2 Global symmetries

The 1D cluster state is well known to have a global $\mathbb{Z}_2 \times \mathbb{Z}_2$ symmetry that has a significant effect on its properties [SAF+11, SAV12]. This allows it to be placed in the framework of symmetry-protected topological order (SPTO) [GW09, CGW11, SPGC11]. The symmetry group can also be shown to be related to the power and robustness of the cluster state as a measurement-based resource in both 1 and higher dimensions [ESBD12, EBD12].

The relevant global symmetry group of the infinite 1D CSS cluster state is represented by the operators

$$U^o = \prod_{s\,\text{odd}} X(s), \text{ and} \tag{4.50}$$

$$U^e = \prod_{s\,\text{even}} Z(s). \tag{4.51}$$

Since U^o and U^e clearly commute and are self-inverse, these operators generate a representation of $\mathbb{Z}_2 \times \mathbb{Z}_2$.

Considering the analogous property of a generalized cluster state for arbitrary finite groups G, for simplicity we will restrict to the specific infinite 1D graph as shown in Fig. 4.3.

Explicitly, the cluster state corresponding to this graph can be written as

$$|\mathscr{C}_{\text{line}}\rangle = \sum_{g_i} \cdots |g_i g_{i+1}^{-1}\rangle |g_{i+1}\rangle |g_{i+1} g_{i+2}^{-1}\rangle |g_{i+2}\rangle |g_{i+2} g_{i+3}^{-1}\rangle |g_{i+3}\rangle |g_{i+3} g_{i+4}^{-1}\rangle \cdots . \tag{4.52}$$

It is clear by inspection that the global symmetries of this state can be written as

$$U_g^o = \prod_{s\,\text{odd}} X_g^{\rightarrow}(s) \tag{4.53}$$

$$U_\Gamma^e = \frac{1}{d_\Gamma} \prod_{s\,\text{even}} \sum_{i_s} Z_{\Gamma^{i_{s-2} i_s}}(s) \tag{4.54}$$

as can be directly verified. As in the qubit case the U_g^o and U_Γ^e commute trivially. The U_g^o multiply as elements of G, and the U_Γ^e transform as representations of G (i.e. $U_{\Gamma_1}^e U_{\Gamma_2}^e = U_{\Gamma_1 \otimes \Gamma_2}^e$ and $U_{\Gamma_1}^e + U_{\Gamma_2}^e = U_{\Gamma_1 \oplus \Gamma_2}^e$, with $Z_{\Gamma^{ij}}$ defined in the obvious way for a reducible representation Γ). Thus we deduce that the symmetry algebra of the generalized cluster state is given by the product of the group algebra and the dual (representation) algebra. For Abelian groups such as $\mathbb{Z}_2$, the representation algebra is isomorphic to that of the group itself, which recovers the familiar result for the qubit cluster state.

Although the framework of symmetry protected topological order typically deals with states

that have a group symmetry, we anticipate that many of the tools and results of SPTO may be extended to this more general setting.

4.4.3 PEPS representations

The qubit cluster state has an exact tensor network representation as a projected entangled pair state (PEPS) [VC04]. The PEPS ansatz [AKLT88, FNW92, Has06, PGVWC07, VWPGC06a, Vid03] is extremely useful for both analytical and numerical analysis of states. In particular, the description of the cluster state as a PEPS allows a reinterpretation of measurement-based quantum computation as a teleportation-based computation scheme [VC04] or in the correlation space picture [GESPG07]. Furthermore, it has also enabled an approximate 2-body parent Hamiltonian to be derived for an arbitrary cluster state [BR06, GB08, BBD14a]. Here we show how the PEPS representation of a cluster state generalizes for an arbitrary finite group G.

A PEPS is defined by an interaction graph Λ and a set of "projection" maps $\mathscr{P}_s$ associated with each site of Λ. The state represented by the PEPS can be constructed by beginning with a set of D-dimensional maximally entangled "virtual" pairs $\sum_{i=1}^{D} |i\rangle_{mn}|i\rangle_{nm} \equiv |\Phi_D\rangle_{(m,n)}$ along each edge (m,n) of Λ, with one qudit of each of these pairs associated with each of the vertices forming the edge (i.e. the qudit labelled mn is associated with vertex m and vice versa). At each site $s \in \Lambda$, the projection map $\mathscr{P}_s$ is then applied to the qudits at each site, taking the combined D^k-dimensional virtual Hilbert space (for a site of valency k) to a d-dimensional "physical" Hilbert space. These physical qudits at each site of Λ then typically correspond to the individual qudits of the state being represented. That is, the PEPS state is given by

$$|\psi_{\text{PEPS}}\rangle \equiv \bigotimes_{v\in\Lambda} \mathscr{P}(v) \bigotimes_{(m,n)\in\Lambda} |\Phi_D\rangle_{(m,n)}. \tag{4.55}$$

For the CSS qubit cluster state, the interaction graph Λ is simply the (bipartite) graph specifying the cluster state. $D = d = 2$ and the projection maps $\mathscr{P}$ are defined on odd and even sites of Λ as [VC04]

$$\mathscr{P}^o = |0\rangle\langle 0,\ldots,0| + |1\rangle\langle 1,\ldots,1| \tag{4.56}$$

$$\mathscr{P}^e = |+\rangle\langle +,\ldots,+| + |-\rangle\langle -,\ldots,-|. \tag{4.57}$$

For generalized cluster states, the PEPS interaction graph is again given by the cluster state graph. $D = d = |G|$ as might be expected, and the projection maps are given (up to normalization) by

$$\mathscr{P}^o = \sum_g |g\rangle\langle g,\ldots,g| \tag{4.58}$$

$$\mathscr{P}^e = \sum_{g_1,\ldots,g_k,h_{k+1},\ldots,h_l} \left|\left(\prod_i g_i\right)\left(\prod_j h_j\right)^{-1}\right\rangle\langle g_1,\ldots,g_k,h_{k+1},\ldots,h_l|, \tag{4.59}$$

where the g_i represent the states of qudits corresponding to edges leaving the relevant even vertex, and the h_j correspond to the edges entering the vertex. The products $\prod_i g_i$ and $\prod_j h_j$ are taken in the appropriate order specified by #.

In order to demonstrate that Eqns. (4.58-4.59) define a PEPS for the generalized cluster states as claimed, it is useful to note that the effect of applying controlled multiplication gates on the physical level with target $|e\rangle$ can be reproduced by application of corresponding gates on the virtual level. We will distinguish typographically between CMULT gate acting on a physical target qudit and cmult gates acting on the virtual qudits.

Consider CMULT gates acting on virtual control qudits and a common physical target qudit:

$$\prod_{i=1}^{l\,\#} \mathrm{CMULT}^{\leftrightarrows}(i,s)|g_1,\ldots,g_k,h_{k+1},\ldots,h_l\rangle|e\rangle_s = |g_1,\ldots,g_k,h_{k+1},\ldots,h_l\rangle \left|\left(\prod_i g_i\right)\left(\prod_j h_j\right)^{-1}\right\rangle_s \tag{4.60}$$

where the i index runs over the qudits grouped in the first ket. Compare this to cmult gates acting on virtual control and target qudits, before projecting the target qudits into a single physical qudit space:

$$\begin{aligned} I\otimes\mathscr{P}_s^e \prod \mathrm{cmult}^{\leftarrow}|g_1,\ldots,g_k,h_{k+1},\ldots,h_l\rangle\otimes|e,e,\ldots,e\rangle_s & \\ = I\otimes\mathscr{P}_s^e|g_1,\ldots,g_k,h_{k+1},\ldots,h_l\rangle\otimes|g_1,\ldots,g_k,h_{k+1},\ldots,h_l\rangle_s & \quad (4.61)\\ = |g_1,\ldots,g_k,h_{k+1},\ldots,h_l\rangle\otimes\left|\left(\prod_i g_i\right)\left(\prod_j h_j\right)^{-1}\right\rangle_s & \quad (4.62)\\ = \prod_{i=1}^{l\,\#} \mathrm{CMULT}^{\leftrightarrows}(i,s)|g_1,\ldots,g_k,h_{k+1},\ldots,h_l\rangle|e\rangle_s & \quad (4.63)\end{aligned}$$

where here only one cmult gate acts on each (virtual) control and each (virtual) target qudit. We can use this equivalence to give us the result that

$$\begin{aligned} |\psi_{\mathrm{PEPS}}\rangle &= \left(\bigotimes_{w'\in\Lambda_o}\mathscr{P}^o(w')\bigotimes_{v'\in\Lambda_e}\mathscr{P}^e(v')\right)\bigotimes_{(w,v)\in\Lambda}|\Phi_{|G|}\rangle_{wv} & (4.64)\\ &= \left(\bigotimes_{w'\in\Lambda_o}\mathscr{P}^o(w')\bigotimes_{v'\in\Lambda_e}\mathscr{P}^e(v')\right) \\ &\qquad\cdot\prod_{\substack{<m,n>\\ m\in\Lambda_o,n\in\Lambda_e}}\mathrm{cmult}^{\leftarrow}(m,n)\left(\bigotimes_{w\in\Lambda_o}|I,\ldots,I\rangle_w\bigotimes_{v\in\Lambda_e}|e,\ldots,e\rangle_v\right) & (4.65)\\ &\propto \prod_{\substack{<m,n>\\ m\in\Lambda_o,n\in\Lambda_e}}^{\#}\mathrm{CMULT}^{\leftrightarrows}(m,n)\left(\bigotimes_{w\in\Lambda_o}|I\rangle_w\bigotimes_{v\in\Lambda_e}|e\rangle_v\right) & (4.66)\\ &= |\mathscr{C}_{\Lambda,\#,G}\rangle & (4.67)\end{aligned}$$

as claimed, where on the penultimate line we used the facts that $\mathscr{P}_s^o$ commutes with CMULT on the control qudit, and $|I\rangle_s \propto \mathscr{P}_s^o |I,\ldots,I\rangle_s$.

4.4.4 Generalized cluster states and Kitaev quantum double states

The qubit cluster state is related to the topologically ordered toric code in several ways. One important way is that the toric code can be defined by preparing a suitable cluster state and projecting (or measuring) a subset of the qubits into suitable states [RBH05]. Here we show that this relationship also extends between the generalized cluster states and the Kitaev quantum double models based on the same group. This relationship may also have practical application, for example in preparing certain quantum double states or in generalizing the topological cluster state computation protocol, as we will discuss in Sec. 4.5.1.

Recall that a Kitaev quantum double model is defined on a directed lattice. For simplicity, we make a convenient canonical choice of edge direction (such that the edges around each plaquette either run clockwise or anticlockwise, as shown in Fig. 4.4a) and note that all alternative choices may be reached by local basis change. Quantum double states on these lattices have stabilizers [Kit03]

$$A(s) = \sum_{g\in G} A_g(s) \text{ and} \tag{4.68}$$

$$B(p) = B_e(p) \tag{4.69}$$

for

$$A_g^h(s) = X_g^{\rightarrow}(s_U) X_g^{\leftarrow}(s_L) X_g^{\rightarrow}(s_D) X_g^{\leftarrow}(s_R) \tag{4.70}$$

$$A_g^v(s) = X_g^{\leftarrow}(s_U) X_g^{\rightarrow}(s_L) X_g^{\leftarrow}(s_D) X_g^{\rightarrow}(s_R) \tag{4.71}$$

$$B_g^{CW}(p) = \sum_{g_1 g_2 g_3 g_4 = g} T_{g_1}(p_U) T_{g_2}(p_L) T_{g_3}(p_D) T_{g_4}(p_R) \tag{4.72}$$

$$B_g^{ACW}(p) = \sum_{g_1^{-1} g_2^{-1} g_3^{-1} g_4^{-1} = g} T_{g_1}(p_U) T_{g_2}(p_L) T_{g_3}(p_D) T_{g_4}(p_R). \tag{4.73}$$

with s_U, s_L, s_D, s_R and p_U, p_L, p_D, p_R the neighbouring links located up, left, right, and down from the star s or plaquette p under consideration, where CW or ACW denotes whether the edges around the plaquette p run clockwise or anticlockwise, and where h or v denote whether the horizontal or vertical edges point into the star s. The $A(s)$ and $B(p)$ are projectors, commute pairwise, and the Kitaev quantum double ground state is defined as the common $+1$ eigenspace of all $A(s)$ and $B(p)$ operators.

In order to produce such a quantum double ground state, we begin with a generalized cluster state on a square lattice with half the lattice spacing of the quantum double lattice, as shown in Fig. 4.4b. The even qudits of the generalized cluster state (shown as colored circles) will be projected into suitable states, while the odd sublattice qudits will form the space on which

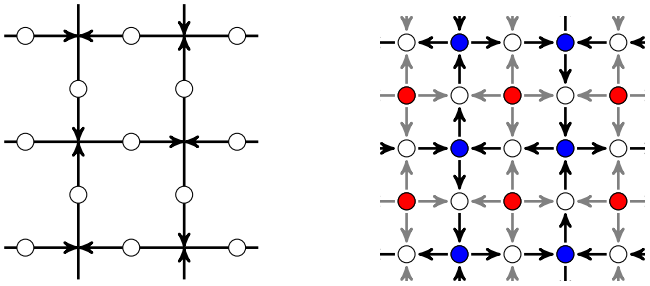

Figure 4.4 – A choice of link directions for a) a quantum double model and b) a set of corresponding cluster state link directions. The qudits in the odd sublattice are shown as open circles, while the even sublattice is shown as colored circles. Qudits on quantum double lattice reside on links. Red qudits in the cluster state are associated with plaquettes of the quantum double, while blue qudits are associated with stars.

the quantum double state is defined. The red odd qudits correspond to plaquettes of the quantum double state, and as such can be labelled as either clockwise or anti-clockwise, depending on the direction of the links around the plaquette. Blue (odd) cluster state qudits correspond to vertices of the quantum double model, and can be labelled as horizontal or vertical depending on whether the horizontal or vertical incident links run into the vertex. An equivalent procedure can be found to project the odd qudits and retain the even qudits, but for simplicity we will treat only one case.

The edge directions and vertex orderings of the cluster state lattice will have a significant effect on the final state. In particular, if we wish to recover a quantum double state on the lattice with edge directions as in Fig. 4.4a, one suitable choice of edge directions is shown in Fig. 4.4b. Explicitly, the edges of the cluster state drawn in black in Fig. 4.4b (i.e. those that will form the quantum double lattice) should run in the opposite direction to the corresponding quantum double links. All grey edges run away from (odd) red sites. For each red site corresponding to an anticlockwise quantum double plaquette, the vertex ordering should be taken anticlockwise beginning from the topmost edge, while for each red site corresponding to a clockwise quantum double plaquette, the vertex ordering should be taken clockwise beginning from the topmost edge. The ordering of the edges around the blue sites is not particularly important, for simplicity we choose them anticlockwise beginning from the topmost edge. The origin of these convention choices may not appear particularly clear at this stage, but it will become apparent how they figure as we proceed in the analysis.

The stabilizers for this generalized cluster state are given for red, blue, and odd sites respec-

tively as

$$S^{r,CW}(p) = \sum_h T_h(p) \sum_{g_1 g_2 g_3 g_4 = h} T_{g_4}(p_U) T_{g_1}(p_L) T_{g_2}(p_D) T_{g_3}(p_R) \tag{4.74}$$

$$S^{r,ACW}(p) = \sum_h T_h(p) \sum_{g_3 g_2 g_1 g_4 = h} T_{g_4}(p_U) T_{g_1}(p_L) T_{g_2}(p_D) T_{g_3}(p_R) \tag{4.75}$$

$$S^{b,v}(s) = \sum_h T_h(s) \sum_{g_3 g_1 g_4^{-1} g_2^{-1} = h} T_{g_4}(s_U) T_{g_1}(s_L) T_{g_2}(s_D) T_{g_3}(s_R) \tag{4.76}$$

$$S^{b,h}(s) = \sum_h T_h(s) \sum_{g_2 g_4 g_1^{-1} g_3^{-1} = h} T_{g_4}(s_U) T_{g_1}(s_L) T_{g_2}(s_D) T_{g_3}(s_R) \tag{4.77}$$

$$S^{o,u}(l) = X_g^{\leftarrow}(l) \tilde{X}_g^{\leftarrow}(l_D|_l) \tilde{X}_g^{\leftarrow}(l_L|_l) \tilde{X}_g^{\rightarrow}(l_U|_l) \tilde{X}_g^{\rightarrow}(l_R|_l) \tag{4.78}$$

$$S^{o,d}(l) = X_g^{\leftarrow}(l) \tilde{X}_g^{\rightarrow}(l_D|_l) \tilde{X}_g^{\rightarrow}(l_L|_l) \tilde{X}_g^{\leftarrow}(l_U|_l) \tilde{X}_g^{\leftarrow}(l_R|_l) \tag{4.79}$$

$$S^{o,l}(l) = X_g^{\leftarrow}(l) \tilde{X}_g^{\leftarrow}(l_D|_l) \tilde{X}_g^{\leftarrow}(l_L|_l) \tilde{X}_g^{\rightarrow}(l_U|_l) \tilde{X}_g^{\rightarrow}(l_R|_l) \tag{4.80}$$

$$S^{o,r}(l) = X_g^{\leftarrow}(l) \tilde{X}_g^{\rightarrow}(l_D|_l) \tilde{X}_g^{\rightarrow}(l_L|_l) \tilde{X}_g^{\leftarrow}(l_U|_l) \tilde{X}_g^{\leftarrow}(l_R|_l) \tag{4.81}$$

where, as in the definition of the quantum double models, CW and ACW refer to the type of plaquette corresponding to the red site, v and h denote the type of star corresponding to the blue site, stabilizers associated to even sites have a u, d, l, r designation according to the direction of the corresponding quantum double link, and vertices of the cluster state have neighbours denoted by U, D, L, and R subscripts.

To produce the Kitaev quantum double ground state from the generalized cluster state we have just described, we project the red even qudits (corresponding to plaquettes of the quantum double model) onto the $|e\rangle$ state, and the blue even qudits (corresponding to vertices) into the $|I\rangle$ state. In the case of the qubit cluster state, this corresponds to projections to the $|0\rangle$ or $|+\rangle$ states, respectively.

Projecting even sites into $|I\rangle$ effectively removes them from the cluster state (indeed, we could alternatively have begun with a cluster state on a lattice lacking the blue sites). After performing just these blue site projections, the red site stabilizers are unchanged, the blue site stabilizers vanish and the odd site stabilizers are transformed to

$$S_g^{o,u}(l) \to X_g^{\leftarrow}(l) \tilde{X}_g^{\leftarrow}(l_D|_l) \tilde{X}_g^{\rightarrow}(l_U|_l) \tag{4.82}$$

$$S_g^{o,d}(l) \to X_g^{\leftarrow}(l) \tilde{X}_g^{\rightarrow}(l_D|_l) \tilde{X}_g^{\leftarrow}(l_U|_l) \tag{4.83}$$

$$S_g^{o,l}(l) \to X_g^{\leftarrow}(l) \tilde{X}_g^{\leftarrow}(l_L|_l) \tilde{X}_g^{\rightarrow}(l_R|_l) \tag{4.84}$$

$$S_g^{o,r}(l) \to X_g^{\leftarrow}(l) \tilde{X}_g^{\rightarrow}(l_L|_l) \tilde{X}_g^{\leftarrow}(l_R|_l) \tag{4.85}$$

where the $\tilde{X}$ operators are now defined with respect to the lattice where the blue sites have been removed.

If we then proceed with the projection of the red sites, the red plaquette stabilizers can easily

be seen to evolve to

$$S^{CW}(p) \to \sum_{g_1 g_2 g_3 g_4 = e} T_{g_4}(p_U) T_{g_1}(p_L) T_{g_2}(p_D) T_{g_3}(p_R) \tag{4.86}$$

$$S^{ACW}(p) \to \sum_{g_1^{-1} g_2^{-1} g_3^{-1} g_4^{-1} = e} T_{g_4}(p_U) T_{g_1}(p_L) T_{g_2}(p_D) T_{g_3}(p_R). \tag{4.87}$$

It is less obvious, but products of the odd site stabilizers around each former blue site s can be rearranged to form the following stabilizers after red site projection:

$$S_g^h(s) = X_g^{\rightarrow}(s_U) X_g^{\leftarrow}(s_L) X_g^{\rightarrow}(s_D) X_g^{\leftarrow}(s_R) \tag{4.88}$$

$$S_g^v(s) = X_g^{\leftarrow}(s_U) X_g^{\rightarrow}(s_L) X_g^{\leftarrow}(s_D) X_g^{\rightarrow}(s_R). \tag{4.89}$$

This can most easily be seen by considering an explicit example of a cluster state in the neighbourhood of a single (removed) h-type blue site:

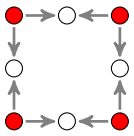

$$\sim \sum_{g_1, g_2, g_3, g_4} \begin{array}{ccc} |g_4 g_1\rangle & |g_4\rangle & |g_3 g_4\rangle \\ |g_1\rangle & & |g_3\rangle \\ |g_2 g_1\rangle & |g_2\rangle & |g_3 g_2\rangle \end{array} . \tag{4.90}$$

This state is not stabilized by the appropriate operator (4.88). However, if we then project the red sites into $|e\rangle$, we find:

$$\sum_{g_1, g_2, g_3, g_4} \delta_{g_2 g_1 = e} \delta_{g_3 g_2 = e} \delta_{g_3 g_4 = e} \delta_{g_4 g_1 = e} \quad \begin{array}{ccc} & |g_4\rangle & \\ |g_1\rangle & & |g_3\rangle \\ & |g_2\rangle & \end{array} \tag{4.91}$$

which is indeed stabilized by S_g^h as claimed. Note that if we had chosen a projection such that, for example, $g_3 g_2 = h$ for some $h \neq e$, then this would no longer be true. If instead, we projected into $\sum_{h \in C} |h\rangle$ for some conjugacy class C, S_g^h would again stabilize the state. In the language of the quantum double anyons, this is due to the fact that only uniform superpositions over conjugacy classes correspond to pure magnetic type excitations.

The stabilizers we just derived (4.86-4.89) are precisely the A_s and B_p stabilizers of the quantum double (4.68-4.69). Thus we have a procedure to define the topologically ordered Kitaev quantum double states by a sequence of projections on the generalized cluster states.

One might hope that for any scheme which builds some interesting state by measurement of Z and X on a (bipartite) qubit cluster state, we could define a generalized model for a finite group G built by performing suitable projections on the generalized cluster state as we have done here. These models may or may not be able to be actually constructed from a cluster state in general by measurement (their interesting properties may or may not survive

the complications of non-ideal measurement outcomes, as will be mentioned in Sec. 4.5.1), but simply being able to define such models may be of independent interest. An example of a model that can be defined in such a way is a non-Abelian generalization of the color codes, presented in Ref. [Bre15b]. One should also note the generality (and hence complexity) of using the projection procedure in this way. We are able to define many generalizations within this same framework by choosing different even and odd sublattices, different link directions, and different link orderings at vertices. Furthermore, alternative projections can be chosen to generalize the measurement of the Z or X operators, as is done in Ref. [Bre15b]. In general, the properties of the resulting state will be significantly affected by the choices of these parameters.

4.5 Discussion

4.5.1 Applications

Producing the quantum double states

In practice, one may be interested in using the relationship between the generalized cluster states and quantum double models discussed in Sec. 4.4.4 as a resource to prepare quantum double states in the laboratory, by replacing the projections by suitable measurements. In the case of the toric code, replacing $|0\rangle$ and $|+\rangle$ projections with measurements in the Z and X bases respectively does not significantly affect the properties of the resulting state. However, in general the effects outlined in Sec. 4.4.1 mean that the situation is not so simple.

To illustrate some of the resulting phenomena, consider replacing the $|e\rangle$ projections at each red site in Fig. 4.4b by measurements in the group element basis. After projection of the blue sites of the cluster state shown in Fig. 4.4b into the $|I\rangle$ state (equivalently, removal of the blue sites), the stabilizers of the state corresponding to the red sites are given as in equations (4.74-4.75), while the remaining odd site stabilizers are as in (4.82-4.85). The effect on the red site stabilizers of measuring these sites in the group element basis is clear: with measurement outcomes $\{m_p\}$, the stabilizers transform to

$$S^{CW}(p) = \sum_{g_1 g_2 g_3 g_4 = m_p} T_{g_4}(p_U) T_{g_1}(p_L) T_{g_2}(p_D) T_{g_3}(p_R) \tag{4.92}$$

$$S^{ACW}(p) = \sum_{g_3 g_2 g_1 g_4 = m_p} T_{g_4}(p_U) T_{g_1}(p_L) T_{g_2}(p_D) T_{g_3}(p_R). \tag{4.93}$$

The effect on the odd site stabilizers is less obvious. As in the previous section where red sites were projected into $|e\rangle$, there will be a stabilizer corresponding to each star of the lattice. These can also be straightforwardly calculated by considering a single isolated vertex and its four neighbouring plaquettes.

We can interpret the state after measurement of the blue sites as a superposition of excited

states of quantum double anyons. Explicitly, anyons in the quantum double models can be created and transported by so-called ribbon operators $F_\rho^{(h,g)}$ corresponding to pairs of group elements (h,g) and fattened paths (ribbons) ρ on the lattice [Kit03, BMD08a]. The ends of ribbons, "sites", are composed of a neighbouring vertex-star pair. Ribbon operators create anyonic charges at each end of the ribbon ρ. In particular, the operator $F_\rho^{(m_p,e)}$ ending on an appropriate site will transform a stabilizer of the form (4.86) or (4.87) into (4.92) or (4.93) respectively. Similarly, the star-type stabilizers can be obtained by transforming the naive stabilizers (4.88) and (4.89) under $F_\rho^{(m_p,e)}$ on suitable ribbons. Further, if we replaced all blue site projections with measurements in the representation basis, we could interpret the remaining state in a similar way.

In some senses, this is a trivial statement, as all states on the lattice (up to boundary conditions) are superpositions of some excited states of the quantum double model. However, using this interpretation may be fruitful for example in a detailed analysis of the adiabatic topological cluster state computation protocol sketched in the following section.

Producing quantum double ground states using generalized cluster states, either by measurement or by adiabatically simulating the projections given in Sec. 4.4.4 [BF10, BFC13, AMA14], faces a fundamental lower bound on the preparation time that scales as the linear size of the system [BHV06, HL08, KP14]. In a measurement-based preparation, this is a limit on how quickly a circuit that transforms the measurement output state into the desired state can be computed.

Adiabatic topological cluster state quantum computation

Apart from standard measurement-based quantum computation, the qubit cluster state can also be used to implement topological cluster state quantum computation [RHG07] (TCSQC). This is a computation scheme that combines practical advantages of measurement-based quantum computation with some natural robustness to noise from topological computation schemes. It is based on the relationship between the cluster states and the toric code discussed and generalized in Sec. 4.4.4.

In the TCSQC protocol, measurements are performed on a cubic lattice cluster state. By interpreting one direction of the lattice as a "simulated time" direction, the resulting procedure can be interpreted as the evolution of punctures in the surface of the toric code in simulated time. The world-lines of the punctures are determined by the chosen measurement settings, while the measurement outcomes may be interpreted as specifying world-lines of toric code anyons, which can then be compensated for by classical post-processing. Though this scheme enjoys the native robustness that accompanies topological computation, the gates that can be performed in this way are insufficient for universal quantum computation, and so must be supplemented with non-topological operations whose fault-tolerance is guaranteed separately.

It is an interesting question as to whether a similar measurement-based computation scheme exists that enjoys universal topological quantum computation. An obvious candidate strategy is to attempt to replace the simulated toric code punctures with simulated defects in another more complicated topological model, such as the quantum doubles. If we were to construct an analogous procedure using the generalized cluster states for a non-Abelian group G, appropriately generalizing the qubit TCSQC protocol would not generally succeed for the reason that the effect of random measurement outcomes could not be efficiently classically processed. Random measurement outcomes would be interpreted as (possibly superpositions of) anyons, and their dynamics - and hence effect on the logical state - is unlikely to be efficiently classically calculable in general (particularly if the anyon dynamics is BQP complete).

One possible way to salvage such a generalized topological cluster state computation scheme is by removing the measurements from the protocol altogether. Adiabatic cluster state computation [BF10, BFC13, AMA14] makes use of the cluster state as a modular prototype for computation by adiabatic deformation of a Hamiltonian. A standard measurement-based cluster state computation may be translated to the adiabatic setting by simulating the measurement with the adiabatic application of a strong field in the direction of the desired measurement result. Thus in this scheme, the analogue of measurement results are not random, and so need not be compensated for by classical post-processing.

Though the adiabatic cluster state computation approach is typically applied to a standard cluster state computation, we could equally well apply it to the topological cluster state scheme. In this setting, the choice of fields would effectively set the world-lines of punctures and anyons in simulated time, without randomness. Making use of these techniques, it should be possible to perform universal topological cluster state computation with the generalized cluster states by simulating the evolution of punctures (as with the standard TCSQC scheme) in a sufficiently complicated Kitaev quantum double model[1]. Alternatively, since the world-lines of anyons may now be controlled directly by choosing the adiabatic fields appropriately, and since braiding of suitable anyons is sufficient to implement universal quantum computation [Kit03, Moc03, Moc04], it should also be possible to compute in a generalized topological cluster state computation scheme by adiabatically simulating the evolution of a suitable class of anyons. These methods for adiabatic topological cluster state computation may be contrasted with the direct approach of adiabatic topological quantum computation [CLB$^+$14].

Universal topological measurement-based quantum computation

In the scheme laid out in Sec. 4.5.1 for adiabatic topological quantum computation with these generalized cluster states, it was in part because of the infeasibility of classical processing that standard measurement-based computing techniques could not be used. The universality of

[1] Though computation by braiding punctures in non-Abelian anyon systems has not been extensively studied, the fact that punctures contain anyonic charges and the braiding of anyonic charges can be sufficient for universal quantum computing [Kit03, Moc03, Moc04] suggests that the braiding of punctures should also be sufficient for universal quantum computation in general.

quasiparticle braiding in the relevant anyon model meant that it was infeasible to calculate the effect of any stray braids caused by undesirable measurement outcomes (the most naive implementation of the scheme would in fact produce superpositions of anyon states which would generally be non-simulable in any case, but we believe that it may be possible to circumvent this with a more sophisticated protocol in some cases).

However, recall that in the qubit topological cluster state computation scheme the computation proceeds not by simulating anyon braiding, but by simulating the braiding of punctures in the surface of the system. It is not clear that the computational power of such puncture braiding and the computational power of anyon braiding in such a model must always coincide. In fact, for another type of topological defect known as a twist, braiding of these objects can be universal for quantum computation while the braiding of the relevant anyons remains classically simulatable [BJQ13c]. Thus it may be possible to find some anyon model where braiding of punctures is universal, while braiding of anyons is classically simulatable. Although the interaction between topological defects and anyons can be quite complex, this could conceivably lead to a universal topological measurement-based quantum computation scheme based on an appropriate generalized cluster state (whether as described in this chapter or from the possible extensions noted below).

4.5.2 Extensions

Although as presented here, the generalized cluster states are based on finite group algebras, there is little in the construction that is particularly restricted to finite groups. Several related or further generalizations of this construction suggest themselves.

The clearest example is the extension from finite groups to Lie groups. In particular, by considering the group of real numbers under addition, our construction reproduces the continuous-variable cluster states [ZB06, MvLG$^+$06]. This gives a unified framework for all previously known variants of the cluster state. This will be presented elsewhere [BM].

As this construction was inspired by the generalization of the toric code to the quantum double models based on finite groups, it is natural to ask if the later generalizations of the toric code to arbitrary finite-dimensional Hopf C^* algebras [BMCA13] and the conjectured generalization to weak Hopf algebras [BMCA13, BCKA13] could also be applied to generalized cluster states. There is an obstacle in directly extending the construction to Hopf algebras, as the natural generalization of the controlled multiplication operation would be according to the coproduct Δ of the Hopf algebra. This is the operation that maps from one system to a tensor product of two systems.

The coproduct of a group algebra is simply $\Delta(g) = g \otimes g$ for $g \in G$. In a general Hopf algebra, the coproduct of an element is given by $\Delta(a) = \sum_i a^{(i)}_{(1)} \otimes a^{(i)}_{(2)}$. The natural generalization of the controlled multiplication gate is defined using this structure, e.g. $\mathrm{CMULT}|a\rangle|b\rangle = \sum_i |a^{(i)}_{(1)}\rangle|a^{(i)}_{(2)} b\rangle$. However, this gate no longer need commute on control qudits. For this reason, if we were to

use this CMULT gate to construct a cluster state, the circuit would no longer be finite-depth and the stabilizer operators derived in analogy to those in Sec. 4.3 would no longer be finite weight in general.

One way to define cluster states based on Hopf algebras that can be constructed by constant depth circuits and have local stabilizers would be to restrict the graphs on which these states are defined. In particular, consider a graph Λ that is bipartite and every site v in the even sublattice Λ_e is 2-valent. Then one edge incident to v could act as controlled left multiplication and the other edge acts as controlled right multiplication. Since these two operations always commute on common targets, this construction would yield a state with the desired properties. Of course choosing graphs of this kind is a very restrictive constraint, and so it would be interesting to see if an alternative mechanism to retain locality is possible.

Apart from Lie groups and Hopf algebras as motivated by the Kitaev quantum double models, it would also be interesting to study generalizations of the cluster states motivated by the Levin-Wen string net models [LW05]. Instead of a group, these models are specified by a fusion category. The simplest choice gives the toric code as in the quantum double models. As in Table 4.1, we could build qudits and associated operator algebras inheriting features of a given fusion category. It would be interesting to develop cluster states for a given fusion category in this way.

Finally, we note that in some of these extensions it may be possible to construct some cluster states that are related to the standard definition (4.7) instead of the CSS definition (4.10). This should be possible when considering algebraic objects which are self-dual in the relevant sense (as with Abelian groups).

4.5.3 Broader implications

As noted in Sec. 4.4.2, the generalized cluster states on an infinite chain extend the standard notion of symmetry protected states with a symmetry group to states that simply have a symmetry algebra. The consequences of this are not clear, and it may be of interest to consider the notion of symmetry protected phases that are labelled by more general objects than groups.

The Pauli stabilizer formalism has proved spectacularly successful at describing a wide variety of states, and making them amenable to both analytical and numerical study. Several similar constructions have been proposed, including the monomial stabilizer formalism [VdN11] mentioned earlier, among others [Got99a, NBVdN15]. It is known that all Pauli stabilizer states are equivalent (under local Clifford circuits) to a qubit cluster state [VdNDDM04]. It may be of interest to determine whether a similar family of states can be defined by local equivalence to a generalized cluster state for any given group G. Although these all fall under the umbrella of monomial stabilizer states, it may be advantageous to define smaller classes that have more structure than the general case.

Chapter Review

We define a family of generalized cluster states based on an arbitrary finite group and explore their properties.

- We offer a general discussion of the algebraic structure of CSS qubit systems, their relationship to the group algebra of $\mathbb{Z}_2$, and how they may be similarly generalized to an arbitrary finite group.
- The relationship between the generalized cluster states and the standard qubit cluster state is analogous to the relationship between the quantum double models and the toric code.
- The generalized cluster states are the ground states of local commuting Hamiltonians and also the outputs of constant depth circuits, as is the case for the standard cluster states.
- We discuss the properties of the generalized cluster states under measurement, as well as giving their PEPS descriptions and discussing their global symmetries.
- The relationship between the qubit cluster state and the toric code is extended to a relationship between the generalized cluster states and the quantum double models.
- Possible applications of the generalized cluster states are discussed, including an adiabatic topological cluster state computation scheme based on the qubit topological cluster state computation scheme.

5 Generalized Color Codes Supporting Non-Abelian Anyons

Abstract

We propose a generalization of the color codes based on finite groups G. For non-Abelian groups, the resulting model supports non-Abelian anyonic quasiparticles and topological order. We examine the properties of these models such as their relationship to Kitaev quantum double models, quasiparticle spectrum, and boundary structure.

5.1 Introduction

Topological codes are a promising avenue to achieve robust quantum memories [DKLP02] or implement fault-tolerant quantum computation [Kit03]. These codes have locality properties that are both advantageous from the perspective of implementation, and give robustness against realistic noise models. Topologically ordered systems can be used for information processing in a number of ways, notably by code deformation [BMD09, Bom11] or by the braiding of quasiparticle excitations [NSS+08]. The latter approach is available only for particular types of topologically ordered systems with non-Abelian anyonic excitations.

The color codes [BMD06, BMD07b] are a family of topological codes with Abelian anyonic excitations. They may be used to perform computation by code deformation, but are particularly notable for having a large class of transversal gates [BMD06], giving rise to high fault-tolerance thresholds [LAR11]. They are also related to many other interesting families of codes such as the toric codes [Kit03], topological subsystem codes [BKMD09, Bom10b], higher-dimensional color codes [BMD07a], and gauge color codes [Bom13]. Small examples of color codes have also been demonstrated and manipulated in the laboratory [NMM+14].

While the color codes have interesting properties and are related to many other interesting models, the ability to support non-Abelian excitations is one feature they lack. Here, we present a generalization of the color code to an arbitrary finite group G (such that the standard

color code corresponds to the group $\mathbb{Z}_2$). This is motivated in analogy to the generalization of the toric code to the quantum double models [Kit03]. These generalized color codes support non-Abelian anyons for non-Abelian groups G and so may in general be used for topological quantum computation by braiding these quasiparticles.

We also study some notable properties of these generalized color codes. Particularly, we demonstrate an equivalence between the generalized color codes and the quantum double models that allows us to easily determine the quasiparticle content of these color codes. We further discuss the structure of the boundaries of these models among other properties.

The layout of the paper is as follows: in Sec. 5.2, we will review the qubit color code model and introduce the generalized color code. We will prove the relation between these models and the quantum double models in Sec. 5.3. Following this, in section 5.4 we will explore the properties of the generalized color codes, before concluding remarks in Sec. 5.5.

5.2 Qubit Color Codes and G-Color Codes

The qubit color code [BMD06] is defined on a trivalent lattice whose plaquettes are 3-colorable (see for example Fig. 5.1). Such lattices are called 2-colexes [BMD07a]. Qubits are placed on vertices of the 2-colex, and each plaquette has two associated projectors, defined as

$$S_p^X = \frac{1}{2}\left(1 + \prod_{i \in p} X(i)\right) \tag{5.1}$$

$$S_p^Z = \frac{1}{2}\left(1 + \prod_{i \in p} Z(i)\right) \tag{5.2}$$

such that $i \in p$ runs over vertices bounding the plaquette p, and where $X(i)$ and $Z(i)$ are the Pauli matrices acting on vertex i. 2-colexes are always bipartite, which means that all cycles of the lattice are even in length, and so S_p^X and S_p^Z commute with each other for the same p. It can also be seen that $[S_p^X, S_{p'}^Z] = 0 \; \forall \, p, p'$. The model is then defined by the Hamiltonian

$$H = -\sum_p \left[S_p^X + S_p^Z\right] \tag{5.3}$$

such that the ground space of the code is the common +1 eigenspace of each of the S_p operators. We will therefore refer to the S^X and S^Z as X- and Z-type stabilizers.

Plaquettes of the 2-colex are colored red, green, and blue, and similarly each link has an associated color, such that it connects two plaquettes of its own color. The elementary excitations of this model can be thought of as (Abelian) anyonic quasiparticles, corresponding to stabilizer operators that are frustrated. Anyon species can be labelled by the color of the plaquette on which they live and the type of stabilizer they frustrate (i.e. X or Z), or can be a composite of these generating anyons.

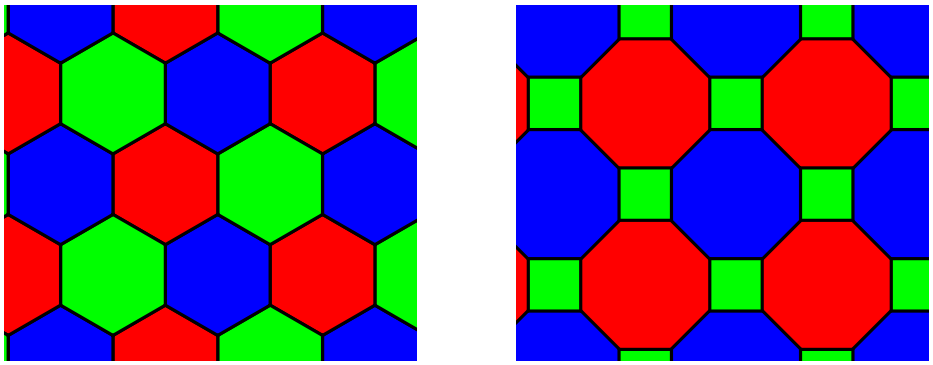

(a) (b)

Figure 5.1 – Two examples of 2-colexes. (a) The 6.6.6 (honeycomb) lattice. (b) The 4.8.8 lattice.

On a torus the qubit color codes are 2^4-fold degenerate, and alternative boundary conditions for these codes are discussed further in Sec. 5.4.3. Logical operators in these codes consist of homologically non-trivial strings of X or Z operators running along edges of a particular color, and can branch if strings along edges of all three colors meet. A X string running along red links will anticommute with a Z string running along blue links, for example, and these string operators will form a Pauli algebra acting on the degenerate codespace.

We can think of the qubit color code as being based on the group $\mathbb{Z}_2$. The qubits on each link have a natural basis labelled by elements of $\mathbb{Z}_2 = \{0, 1\}$ (with 0 the identity element) and we can consider the X operator to act on these states as group multiplication by the 1 element, i.e.

$$X|g\rangle = |g \oplus 1\rangle \tag{5.4}$$

where of course addition modulo 2 is the relevant group multiplication operation for this group. The X operator can also be labelled with a group element superscript such that

$$X^h|g\rangle = |g \oplus h\rangle \tag{5.5}$$

and see that $X^1 = X$, $X^0 = I$.

Let us also introduce operators $T^g = |g\rangle\langle g|$ for each $g \in \mathbb{Z}_2$. This allows us to write

$$Z = T^0 - T^1 \tag{5.6}$$

In particular, this allows us to rewrite

$$S_p^X = \frac{1}{2} \sum_{g \in \mathbb{Z}_2} \prod_{i \in p} X(i)^g \tag{5.7}$$

$$S_p^Z = \sum_{\bigoplus g_i = 0} \prod_{i \in p} T(i)^{g_i} \tag{5.8}$$

where we use notation such that $\bigoplus g_i = 0$ runs over all sets of $g_1, g_2, \ldots, g_n$ such that $g_1 \oplus g_2 \oplus \cdots \oplus g_n = 0$.

When written in this form, these operators bear a close resemblance to the A_v and B_p projectors used to define the quantum double models [Kit03] (in this case for the group $\mathbb{Z}_2$).

5.2.1 G-color codes

Given our interpretation of the qubit color code in terms of the group structure of $\mathbb{Z}_2$, we now define a generalized color code. The desirable characteristics of this code are that its Hamiltonian can be expressed as a (negative) sum of commuting local projectors, and that its excitation spectra includes non-Abelian anyons for a sufficiently complicated group G. The models we present will satisfy both of these conditions. It is worth noting that our models defined for the (Abelian) cyclic groups $\mathbb{Z}_d$ will correspond precisely to the known generalizations of color codes to higher-dimensional spins [Sar10].

A G-color code is defined uniquely by the following set of data:

- A finite group G
- A 2-colex L
- A parity function $s_i = \pm 1$ at each site i of L
- A choice of privileged color (conventionally red), and a choice of "clockwise" and "anti-clockwise" for the remaining colors (conventionally green and blue respectively)

Here we will begin by defining the model for the special case $s_i = +1 \ \forall i$, and subsequently describe how to relate models with different parity functions s_i. To each vertex of the 2-colex L, we associate a qudit with dimension $|G|$ and an orthonormal basis labelled by elements $g \in G$. Define operators corresponding to group multiplication and projection that act at a site as follows

$$X_+^h|g\rangle = |hg\rangle \tag{5.9}$$
$$X_-^h|g\rangle = |gh^{-1}\rangle \tag{5.10}$$
$$T^h|g\rangle = \delta_{h=g}|g\rangle \tag{5.11}$$

As compared to the qubit case, a general group requires a distinction between left and right multiplication, hence we have introduced both X_+ and X_- to distinguish these two operations. Note that $[X_+^g, X_-^h] = 0$, though $[X_+^g, X_+^h] \neq 0 \neq [X_-^g, X_-^h]$ in general.

A further group theoretic concept that will be useful is the commutator subgroup $[G,G] = \langle [g,h] : g,h \in G \rangle$ where $[g,h] = g^{-1}h^{-1}gh$. This subgroup is normal, and the quotient group

$G/[G,G]$ is the Abelianization of G. A particularly useful property of $[G,G]$ is that it can alternatively be defined as the set of elements in G which can be written as some product $g_1 g_2 g_3 \cdots g_n$ that may be reordered such that it evaluates to identity.

In analogy to the qubit color code, the G-color codes are specified by a number of stabilizer operators. As in the qubit case, each plaquette will have an associated X- and Z-type stabilizer. However, in general, the form of these stabilizers will depend on the color of the plaquette under consideration. With this in mind, we can define X-type stabilizers for a plaquette as follows

$$S_p^X = \frac{1}{|G|} \sum_{g \in G} A_p^g \tag{5.12}$$

$$A_p^g = \prod_{i \in p} X^g(i) \tag{5.13}$$

where in Eq. (5.13) the X^g operator acts either as left (X_+^g) or right (X_-^g) multiplication depending on the relative orientation of the three colors at a given site. Explicitly, when considering the X-type stabilizer corresponding to a blue or green plaquette, if the colors of plaquettes around a vertex are ordered $\{r,g,b\}$ when traversed clockwise, then the operator appearing at that vertex will be of the form X_+. Similarly, if the plaquette colors around the vertex are ordered $\{r,b,g\}$ when traversed clockwise, then the operator appearing at that vertex will take the form X_-. When considering red plaquettes, these conventions are reversed, so that $\{r,g,b\}$ clockwise ordering corresponds to X_- and $\{r,b,g\}$ corresponds to X_+. Concrete examples of these conventions are illustrated in Fig. 5.2.

These conventions are chosen so that the S^X operators corresponding to plaquettes of the privileged color (red) commute with the S^X for both blue and green plaquettes. Making all three colored X-type stabilizers commute pairwise is impossible, and so the blue and green S^X will not generally commute with each other for neighbouring plaquettes. Although this may seem at first glance to be a severe problem, it so happens that there exists a common $+1$ eigenspace of all S^X regardless.

The Z-type stabilizers for each of the three plaquette color are then defined as

$$S_{p,\text{red}}^Z = \sum_{\prod g_i \in [G,G]} \prod_{i \in p} T^{g_i}(i) \tag{5.14}$$

$$S_{p,\text{blue}}^Z = \sum_{\prod_{\text{ACW}} g_i = e} \prod_{i \in p} T^{g_i}(i) \tag{5.15}$$

$$S_{p,\text{green}}^Z = \sum_{\prod_{\text{CW}} g_i = e} \prod_{i \in p} T^{g_i}(i) \tag{5.16}$$

where the ACW or CW denotes the product being taken anti-clockwise or clockwise around the plaquette, respectively. The origin of the product can easily be seen not to affect these operators. Additionally, the order of multiplication in S_{red}^Z does not affect the outcome. Since $[G,G]$ can be defined as the set of elements that can be decomposed into a product $h_1 h_2 h_3 \cdots h_n$

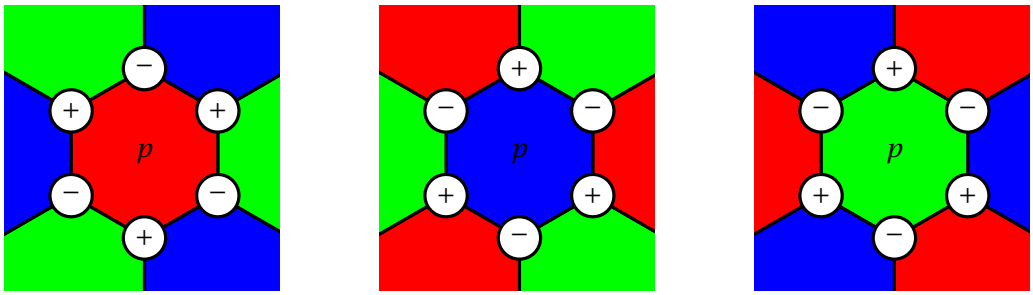

Figure 5.2 – Sign conventions for X-type stabilizers for example red, green, and blue plaquettes. These stabilizers are constructed from products of X operators at each site around the plaquette. Those vertices with a + denote left multiplication (X_+), while those with a − denote right multiplication (X_-). These signs are determined by the order of plaquette colors around a site.

such that it can be rearranged to evaluate to identity, whether or not some product of elements $\prod g_i$ is in $[G,G]$ will be independent of the order of multiplication.

When considering these Z-type stabilizers, it is clear the sense in which the red plaquettes are privileged. Their structure is not related to the full group G. Rather, we can consider $[G,G]$ as the preimage of the identity element of $G/[G,G]$ under the quotient map. Thus the structure of the red Z-type stabilizer is derived from that of the Abelianization of G, as opposed to G itself. For this reason, we will sometimes refer to red plaquettes as "Abelianized". It should also be clear why we identified blue and green plaquettes as "anticlockwise" and "clockwise" respectively.

The reason that we have defined the orderings of products in S^Z operators as above is that this allows these operators to commute with all the S^X, as can easily be verified. That we are unable to preserve this commutativity without Abelianizing the red plaquettes can be seen as a consequence of the fact that the blue and green S^X fail to commute. It is impossible to preserve the full group structure of the red plaquette and have its S^Z commute with both the blue and green S^X. In order to avoid this non-commutativity, we have reverted to the simpler structure of the Abelianization of G, where no such problems exist, for the red plaquettes.

In Abelianizing the red plaquette Z-stabilizers, we have introduced an additional extensive degeneracy to the system. This degeneracy is local in the sense that it can be lifted through the addition of an extra class of local stabilizer operator that has no counterpart in the qubit case (or in fact for any Abelian G-color code), where $[G,G] = \{e\}$. We call these C-type stabilizers, and they are defined for each red link as

$$S^C_{l,\mathrm{red}} = \frac{1}{|[G,G]|} \sum_{n\in[G,G]} C_{l,\mathrm{red}}(n) \tag{5.17}$$

$$C_{l,\mathrm{red}}(n) = X^n_+(l,\uparrow) \otimes X^n_-(l,\downarrow) \tag{5.18}$$

where $X^n_{\pm}(l,\uparrow\downarrow)$ acts on the upper ($\uparrow$) or lower ($\downarrow$) qudit of the red link l after it has been oriented such that the blue plaquette (ACW) is on the left of the link and the green plaquette (CW) on the right. It can be seen that the S^C will commute with all S^Z and S^X. By requiring the ground space to be in the +1 eigenspace of the S^C as well as the S^Z and S^X, the local degeneracies caused by Abelianization of the red plaquettes are lifted.

As noted, the S^X, S^Z, and S^C stabilizers as written do not commute (as the S^X do not in general commute). They nonetheless can be cast in the monomial stabilizer framework [VdN11], and have an associated frustration free ground space. However, commutativity can be restored by restricting the S^X stabilizers for green and blue plaquettes to the +1 eigenspace of the S^C. These modified stabilizers take the form

$$\tilde{S}^X_{p,\text{green}} = S^X_p \prod_{l\in p\cap\text{red}} S^C_l \tag{5.19}$$

$$\tilde{S}^X_{p,\text{blue}} = S^X_p \prod_{l\in p\cap\text{red}} S^C_l \tag{5.20}$$

where $p\cap$ red denotes all red links bounding the plaquette p. This will then give a set of commutative stabilizer operators generated by the S^Z, $\tilde{S}^X$ and S^C operators, allowing us to write the Hamiltonian of a G-color code as

$$H = -\sum_p \left(\tilde{S}^X_p + S^Z_p\right) - \sum_{\text{red } l} S^C_l \tag{5.21}$$

The ground space will be the common +1 eigenspace of all the stabilizer operators, and will be protected from excited states by a constant gap (noting that each of the stabilizers is a projector).

This completes the definition of the G-color code for the special case that the parity function is set to $s_i = 1$ at every site i of the lattice. The parity at a given site may be reversed by making the unitary transformation $|g\rangle \to |g^{-1}\rangle$ at that site. This completely exhausts the freedom we have in choosing the S^X, S^Z and S^C consistently. When viewed in this way, we can see the parity function as being analogous to the edge direction in the quantum double models, where reversing an edge is equivalent to applying the unitary taking $g \to g^{-1}$ on that edge. We will henceforth restrict to the $s_i = 1$ parity case, with the understanding that all results will hold for any possible alternative parity choice.

5.3 Equivalence to copies of the quantum double models

A property of the qubit color code that will be particularly useful to us in understanding the G-color code is that it is locally equivalent to 2 copies of the toric code [Bom14, BDCP12, Haa13]. We will now sketch an alternative proof of this fact (for a particular 2-colex)[1] and demonstrate

[1] The alternative mapping we describe is implicitly defined in [BFBD11].

how it generalizes to a general G-color code.

5.3.1 Qubit color code ↔ toric code equivalence

Before we present the mapping between the color code and the toric code, we first briefly review the toric code [Kit03]. For our purposes, it is sufficient to define the toric code on a square lattice, with qubits on edges. As in the color code, this model is defined by a number of stabilizer operators. Explicitly, for each vertex v and plaquette p of the lattice, we have

$$K_v^X = \frac{1}{2}\left(1 + \prod_{i\sim v} X_v\right) \tag{5.22}$$

$$K_p^Z = \frac{1}{2}\left(1 + \prod_{i\sim p} Z_p\right) \tag{5.23}$$

where we use notation such that $i \sim v$ runs over all qubits incident to v, and $i \sim p$ runs over all qubits bordering p. The toric code Hamiltonian is then given by

$$H_{\text{toric}} = -\sum_v K_v^X - \sum_p K_p^Z \tag{5.24}$$

in a very similar fashion to the color code.

For simplicity, we present a mapping between the color code and two copies of the toric code on a particular 2-colex. Specifically, we consider the 4.8.8 lattice, where the square plaquettes are colored green and the octagonal plaquettes blue and red in such a way as to satisfy 3-colorability (Fig. 5.1b). We will show how to interpret a qubit color code on this 2-colex as 2 copies of the toric code. That is, we will find a local unitary map that transforms color code stabilizers to toric code stabilizers or actions on uncoupled ancilla systems. Intuitively, the mapping we present treats each green plaquette as 2 encoded qubits, one belonging to each copy of the toric code. The blue plaquettes will correspond to vertices (plaquettes) of the first (second) copy of the toric code, while the red plaquettes will correspond to plaquettes (vertices) of the first (second) copy of the toric code (see Fig. 5.3).

Consider the 4 qubits belonging to each green plaquettes as a stabilizer code with a 4-fold degenerate codespace. The stabilizers of this code are simply the green face stabilizers of the color code, i.e.

$$S_{\text{green}}^X = \frac{1}{2}\left(1 + \begin{array}{cc} X & X \\ X & X \end{array}\right) \tag{5.25}$$

$$S_{\text{green}}^Z = \frac{1}{2}\left(1 + \begin{array}{cc} Z & Z \\ Z & Z \end{array}\right) \tag{5.26}$$

where we use a graphical notation for the 4 operators acting on the vertices of the green

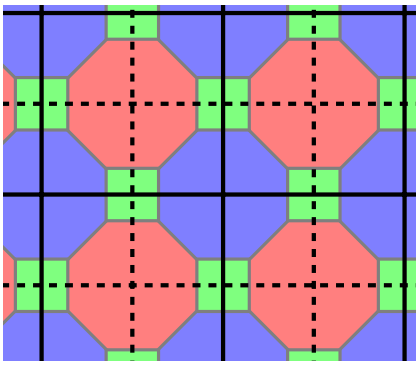

Figure 5.3 – Overlaid on the 4.8.8 color code lattice, the solid lines correspond to the edges of the first toric code lattice, while the dashed lines constitute the second toric code lattice.

plaquette, so that $\begin{matrix} A & B \\ D & C \end{matrix} \equiv A \otimes B \otimes C \otimes D$ on the 4 relevant qubits.

This 4-dimensional codespace corresponding to each green plaquette can be considered as 2 encoded qubits, one for each copy of the toric code. In this way, the qubits of the new toric code lattices have a direct correspondence to the green plaquettes of the color code lattice. It will now be convenient to bipartition these green plaquettes into those with red plaquettes on their right and left (h-type) and those with red plaquettes above and below them (v-type).

On h-type green plaquettes, encoded Pauli algebras can be defined for each of the 2 encoded qubits as

$$X^h_{\text{enc}}(1) = \begin{matrix} X & X \\ I & I \end{matrix} \tag{5.27}$$

$$X^h_{\text{enc}}(2) = \begin{matrix} X & I \\ X & I \end{matrix} \tag{5.28}$$

$$Z^h_{\text{enc}}(1) = \begin{matrix} Z & I \\ Z & I \end{matrix} \tag{5.29}$$

$$Z^h_{\text{enc}}(2) = \begin{matrix} Z & Z \\ I & I \end{matrix} \tag{5.30}$$

where $X^h_{\text{enc}}(2)$ acts as Pauli X on the 2^{nd} encoded qubit for the h-type green plaquette under consideration.

For v-type green plaquettes, the encoded operators can be defined by

$$X^v_{\text{enc}}(1) = X^h_{\text{enc}}(2) \tag{5.31}$$
$$X^v_{\text{enc}}(2) = X^h_{\text{enc}}(1) \tag{5.32}$$
$$Z^v_{\text{enc}}(1) = Z^h_{\text{enc}}(2) \tag{5.33}$$
$$Z^v_{\text{enc}}(2) = Z^h_{\text{enc}}(1) \tag{5.34}$$

That is, on v-type plaquettes, the definitions of the first and second encoded qubits are exchanged.

Note that these definitions are not unique. In particular, because the codespace is the +1 eigenspace of S^X_{green} and S^Z_{green}, multiplying any operator by $\begin{smallmatrix} X & X \\ X & X \end{smallmatrix}$ or $\begin{smallmatrix} Z & Z \\ Z & Z \end{smallmatrix}$ is a trivial operation, and so the encoded operators are invariant under 180° rotations.

One could more rigorously define the unitary enacting this encoding as a function from operators on the 4 qubits of each green plaquette to the 2 encoded (toric code) qubits, as well as 2 ancilla qubits. Notably, this transformation would take green color code stabilizers to an action on the ancilla space, and so they become "trivial" in the sense of Ref. [BDCP12].

In terms of the encoded toric code qubits, the action of the color code stabilizers for blue and red plaquettes is

$$S^X_{\text{red}} \to K^X(1) \tag{5.35}$$
$$S^Z_{\text{red}} \to K^Z(2) \tag{5.36}$$
$$S^X_{\text{blue}} \to K^X(2) \tag{5.37}$$
$$S^Z_{\text{blue}} \to K^Z(1) \tag{5.38}$$

if we interpret the lattices of the two toric codes as in Fig. 5.3. Thus the unitary we have described maps all the stabilizers of the original color code model to stabilizers of the toric code model, or operators on uncoupled ancilla qubits. This completes the demonstration of equivalence.

5.3.2 G-color code ↔ quantum double model equivalence

The equivalence between the qubit color code and the toric code on the 4.8.8 lattice shown above can be generalized to an equivalence between the G-color code and 2 quantum double models. However, as compared to the qubit case (which corresponds to $G = \mathbb{Z}_2$), the two quantum double models will in general be different. One will be based on the group G, while the other will be based on the Abelianization of the group $G/[G,G]$.

Before we continue, we briefly review the quantum double models [Kit03]. Conventionally, these models are defined on a directed lattice, with edge direction playing a similar role to

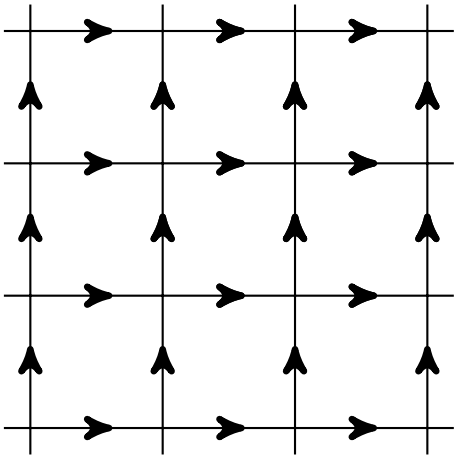

(a)

Figure 5.4 – A directed square lattice, consistent with the quantum double stabilizers defined in Eqns. (5.39) - (5.41).

our parity function. We will define a quantum double model for a group G on an particular directed square lattice (Fig. 5.4), with qudits of dimension $|G|$ placed at every edge, noting that transforming the qudit on an edge by $g \to g^{-1}$ is equivalent to reversing the direction of the edge (qudits have a natural basis labelled by $g \in G$).

At each vertex v and plaquette p of the lattice, the stabilizers of the quantum double model can be written as

$$K_v^X = \sum_g A_v(g) \tag{5.39}$$

$$A_v(g) = X^g_{-,U} X^g_{-,R} X^g_{+,D} X^g_{+,L} \tag{5.40}$$

$$K_p^Z = \sum_{g_1 g_2 g_3 g_4 = e} \prod_{i \in p} T_U^{g_1} T_R^{g_2^{-1}} T_D^{g_3^{-1}} T_L^{g_4} \tag{5.41}$$

where the subscript of the X operators in (5.40) and the T operators in (5.41) denote whether they act on the qubit Up, Right, Down, or Left from the center of the plaquette or vertex under consideration.

As was the case for the qubit color code $\leftrightarrow$ toric code mapping (the $\mathbb{Z}_2$ case), we will explicitly consider only the 4.8.8 lattice, where the square plaquettes are colored green, and the octagonal plaquettes are colored red and blue (Fig. 5.1b). The intuition for our construction is much the same, in that we will encode the quantum double degrees of freedom in the qudits at the vertices of the green plaquette. However, particularly in the case of non-Abelian group G, the mapping will be less straightforward.

As before, green plaquettes are labelled h- or v-type depending on whether red plaquettes are at their sides or above and below them. Given this, define the codespace for h-type green

plaquettes via the stabilizers of the plaquette

$$S^{Z,h}_{\text{green}} = \sum_{g_1 g_2 g_3 g_4 = e} \begin{matrix} T^{g_1} & T^{g_2} \\ T^{g_4} & T^{g_3} \end{matrix} \tag{5.42}$$

$$S^{C,h}_{l_1,\text{green}} = \sum_{n \in [G,G]} C^h_{l_1,\text{green}}(n) \tag{5.43}$$

$$S^{C,h}_{l_2,\text{green}} = \sum_{n \in [G,G]} C^h_{l_2,\text{green}}(n) \tag{5.44}$$

$$\tilde{S}^{X,h}_{\text{green}} = S^{C,h}_{l_1,\text{green}} S^{C,h}_{l_2,\text{green}} \sum_g A^h_{\text{green}}(g) \tag{5.45}$$

with

$$A^h_{\text{green}}(g) = \begin{matrix} X^g_+ & X^g_- \\ X^g_- & X^g_+ \end{matrix} \tag{5.46}$$

$$C^h_{l_1,\text{green}}(n) = \begin{matrix} X^n_+ & I \\ X^n_- & I \end{matrix} \tag{5.47}$$

$$C^h_{l_2,\text{green}}(n) = \begin{matrix} I & X^n_- \\ I & X^n_+ \end{matrix} \tag{5.48}$$

On v-type green plaquettes, the stabilizers can be found by rotating the h-type stabilizers by 90°. These definitions can be seen to be invariant under 180° rotations.

Given this codespace at each h-type green plaquette, we can write encoded operators on this space as

$$X^g_+(1) \equiv \begin{matrix} X^g_- & X^g_+ \\ I & I \end{matrix} \qquad T^g(1) \equiv \sum_{g_2 g_3 = g} \begin{matrix} I & T^{g_2} \\ I & T^{g_3} \end{matrix} \tag{5.49}$$

$$X^g_-(2) \equiv \sum_{k \in g[G,G]} \begin{matrix} I & X^k_- \\ I & X^k_+ \end{matrix} \qquad T^g(2) \equiv \sum_{g_1 g_2 \in g[G,G]} \begin{matrix} T^{g_1} & T^{g_2} \\ I & I \end{matrix} \tag{5.50}$$

$$X^g_-(1) \equiv \begin{matrix} I & I \\ X^g_+ & X^g_- \end{matrix} \qquad T^g(1) \equiv \sum_{g_4 g_1 = g^{-1}} \begin{matrix} T^{g_1} & I \\ T^{g_4} & I \end{matrix} \tag{5.51}$$

$$X^g_+(2) \equiv \sum_{k \in g[G,G]} \begin{matrix} X^k_+ & I \\ X^k_- & I \end{matrix} \qquad T^g(2) \equiv \sum_{g_3 g_4 \in g^{-1}[G,G]} \begin{matrix} I & I \\ T^{g_4} & T^{g_3} \end{matrix} \tag{5.52}$$

As in the $\mathbb{Z}_2$ case, we can define logical operators for the encoded qudits in multiple equivalent ways within the codespace. We have written two particularly useful sets of logical operators for each of the encoded qudits here. These encoded operators can be seen to commute with the stabilizers defined above. The encoded operators acting on the v-type green plaquettes can again be found by rotating the h-type operators 90° clockwise.

In the $\mathbb{Z}_2$ case, the two encoded systems (labelled 1 and 2) were both of the same dimension

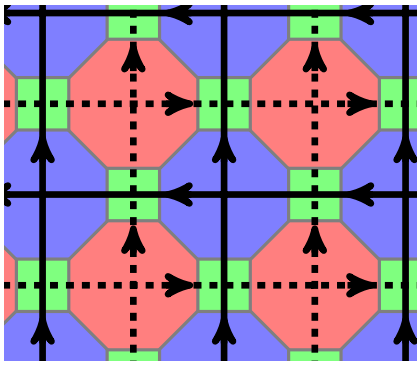

Figure 5.5 – Overlaid on the 4.8.8 G-color code lattice, the solid lines correspond to the edges of the first quantum double lattice, while the dashed lines constitute the second quantum double lattice.

(they were both encoded qubits). In general, however, this is not the case. Examining the encoded operators on qudit 2 (5.50) or (5.52), we can see that states in this space are labelled only by $k \in G/[G,G]$, and thus this qudit is $|G/[G,G]|$ dimensional. This can be seen by noting that $g[G,G]$ is the coset of G corresponding to a particular element of $G/[G,G]$, and in particular $g[G,G] = ng[G,G]$ for any $n \in [G,G]$. In contrast, qudit 1 can be seen to have basis labelled by $g \in G$, and is thus $|G|$ dimensional.

In terms of this encoding, it is clear that once again, the X-type stabilizers of the G-color code corresponding to green plaquettes can be thought of as acting only on some ancilla space (they have no action on the encoded space by construction). Similarly, the C-type stabilizers corresponding to red links of the G-color code act only within a green plaquette, and commute with the encoded operators, so they can also be interpreted as acting on an ancilla space. In contrast, the G-color code stabilizers for blue and red plaquettes can be rewritten in terms of the encoded qudits. Their action under the encoding map can be written as

$$S^X_{\text{red}} \to K^X(1) \tag{5.53}$$
$$S^Z_{\text{red}} \to K'^Z(2) \tag{5.54}$$
$$\tilde{S}^X_{\text{blue}} \to K'^X(2) \tag{5.55}$$
$$S^Z_{\text{blue}} \to K^Z(1) \tag{5.56}$$

where K' are defined by Eqs. (5.39) and (5.41) over the group $G/[G,G]$, as opposed to the K which are defined over G. The $K'(2)$ and $K(1)$ operators act on the quantum double lattices depicted in Fig. 5.5.

Thus the unitary we have described maps all the stabilizers of the G-color code model to stabilizers of the quantum double model, or operators on uncoupled ancilla qubits, in analogy to the qubit color code $\leftrightarrow$ toric code mapping. Thus we have demonstrated an equivalence between a G-color code and a G quantum double model together with a $G/[G,G]$ quantum double model (equivalently, a single $G \times G/[G,G]$ quantum double model).

5.4 Properties of Generalized Color Codes

The qubit color codes have a number of properties that make them of interest to the topological quantum information community. Here we will take a brief survey of some of the most important properties of the G-color codes. Where relevant, we will discuss the connection to the properties of the qubit color codes. Note that some properties of these models for Abelian groups G are explored in some depth in [Sar10].

5.4.1 Anyon spectrum

The correspondence between the G-color codes and the quantum double models developed in Sec. 5.3 allows us to immediately import results from the study of the quantum double models and interpret them in the context of the G-color codes.

Ref. [Bom14] shows that so-called topological stabilizer groups are equivalent iff they have isomorphic topological charges. This result does not apply directly to the equivalence that we have established between quantum double models and G-color codes because they are not Pauli stabilizer models. However, even without the level of rigor available for Pauli stabilizer models, we can still use the intuition behind this theorem to draw a correspondence between the anyonic content of the quantum double models and the G-color codes.

It is easy to see that all local operations on the qudits of the quantum double models in Sec. 5.3.2 can be mapped to some local operations on the qudits of the G-color code (though the converse is not so straightforward due to the presence of the ancillae in the mapping). Similarly, anyonic charges of the quantum double models can be mapped to charges living on the red and blue plaquettes of the G-color code. This allows us to state that the G-color code is supporting the anyons of both the G and $G/[G,G]$ quantum double models. Notably, this includes non-Abelian anyons for non-Abelian G.

In general, since the anyons of a quantum double model for group G are given by the irreducible representations of the Drinfeld double of G, $\mathrm{Irrep}(\mathcal{D}(G))$, we would expect from this line of reasoning that the anyonic content of a G-color code is given by $\mathrm{Irrep}(\mathcal{D}(G \times G/[G,G]))$.

Anyonic charges of the quantum double models can be created and moved by ribbon operators [Kit03]. Each of these ribbon operators must have a corresponding ribbon operator creating or moving the analogous charges on the G-color code. Given these operators, we could imagine braiding charges in the G-color code corresponding to any desired braiding in a quantum double model. In particular, we could perform braiding of non-Abelian anyons that implements universal quantum computation in G-color codes for G non-nilpotent [Moc03, Moc04] (see also Ref. [CHW15]).

5.4.2 Further implications of equivalence

A concrete motivation for demonstrating equivalence between two topological models is that it allows decoding or error correcting routines for one model to apply to a broader class of models [BDCP12]. In our case, this amounts to the observation that a G-color code can be decoded if an equivalent procedure for decoding the quantum double model for group G is known. Although decoding for these non-Abelian anyon models has yet to be explicitly demonstrated (though related work has been shown [WBIL14, BBD$^+$14b]), by equating our G-color codes to the well established quantum double models, we can exploit any results in terms of decoding that are available for them.

Ref. [Bom14] shows that all Pauli stabilizer codes are equivalent to copies of the toric code. The fact that we are able to demonstrate equivalence between quantum double models and our G-color codes suggests that a more general equivalence may hold whenever the models are constructed from commuting projectors based on the X and T operator algebra for a group G. This may also point to a useful restriction of the monomial stabilizer formalism [VdN11] when the desired algebra structure is related to a particular group.

Note that we have technically not demonstrated equivalence between an arbitrary G-color code and quantum double models, as our mapping is specifically tailored to the 4.8.8 lattice. This was sufficient to prove that the G-color codes are capable in principle of supporting quantum double anyons, but we have not shown that this is true for a general lattice. However, the general principles of topologically ordered systems suggest that the microscopic lattice details should not affect global properties of the system such as its anyon spectrum, and so we feel confident in taking this correspondence to hold in general.

5.4.3 Degeneracy and Boundaries

As is generic for topological codes, the degeneracy of a particular code is highly dependent on the topology of the surface in which it is embedded, or, in the planar case, the particular choice of boundary conditions. On closed (orientable) manifolds, this degeneracy is independent of the microscopic details and can be derived from the anyon spectrum [NSS$^+$08]. This means that the degeneracy of the G-color codes on closed manifold can directly be calculated as the degeneracy of the quantum double model for $G \times G/[G,G]$.

Similarly, characterization of the possible gapped boundaries for topologically ordered models is based on the anyon spectrum rather than microscopic details. Possible boundary types and their properties can thus be found by appealing to the known results for the quantum double models [BSW11, KK12, HW15]. Since this theory is already well established in general, there is no reason to delve into it here. However, before moving on we will briefly discuss some special boundary types that are natural in the context of the color codes, and planar codes that can be constructed from them.

The most common planar qubit color codes are triangular [BMD06] (Fig. 5.6a). Each side

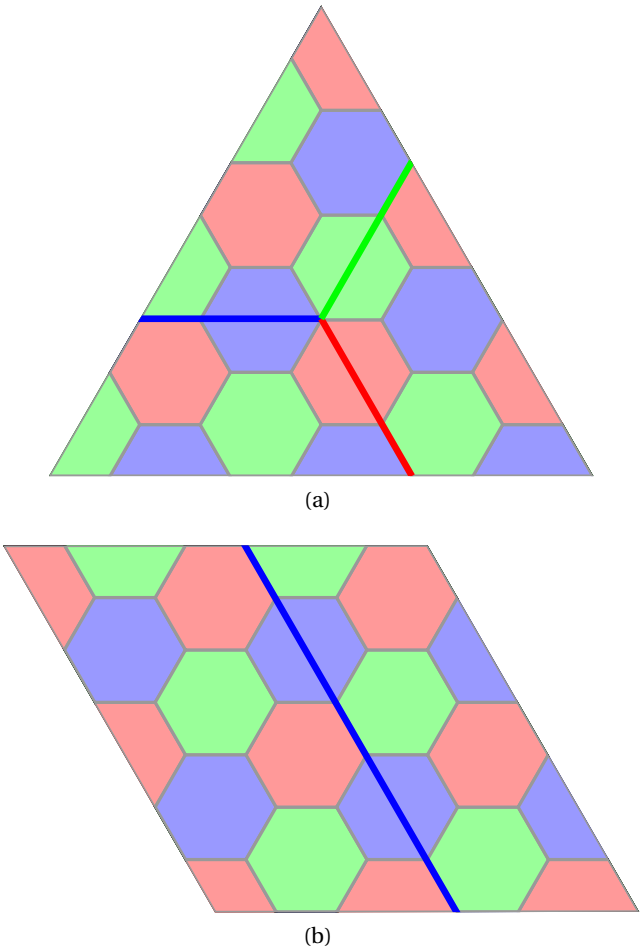

(a)

(b)

Figure 5.6 – Two examples of planar code boundaries, together with examples of logical operator strings on these lattices. (a) A triangular boundary. (b) A rectangular boundary.

of the triangle is associated with the color not appearing in plaquettes on that boundary. These triangular color codes encode one qubit. Small triangular color codes have been experimentally prepared and manipulated [NMM+14]. Another common form of planar color code is rectangular, as in Fig. 5.6b. In this case, two logical qubits are encoded. More generally, a natural boundary for the color code is labelled by a color according to the color not appearing on plaquettes at that boundary. Degeneracy is introduced to the system when the lattice boundary consists of several different colored segments. Although these boundaries arise naturally in the study of color codes, they are not the only boundary types that can occur. In particular, note that the number of boundary types we have just described is 3 (labelled by colors), while a topologically ordered model equivalent to two copies of the toric code can give rise to 6 types of boundary [BK98, BSW11, KK12, BJQ13b, BJQ13a, Lev13]). The reason that the boundaries we described are particularly natural is that they require no special modification to the stabilizer operators (only the 2-colex on which the model is defined).

In the general case of a G-color code, the effect of boundaries is a little more complicated due

to the asymmetry between the three colors (and of course the more complicated algebraic structure). As before, degeneracy is introduced to the codespace when more than two distinct boundaries exist, but the counting of this degeneracy depends on the color (or type) of the boundaries. Since the general case can be determined by appealing to results for the quantum double models, we will simply describe the logical operators and degeneracy of three distinct planar G-color codes: the blue-green rectangular codes (i.e. one with alternating blue and green boundaries as shown in Fig. 5.6b), the blue-red rectangular codes, and the triangular codes. Up to the equivalence between the blue-red rectangular code and a green-red rectangular code, this exhausts all possible rectangular and triangular codes.

In order to describe the logical operators in these codes explicitly, it would be necessary to construct ribbon operators as in the quantum double models [Kit03, BMD08a], which is straightforward but tedious. Instead, we will simply state the types of logical operators that arise and their relationships in order to calculate the degeneracy of these codes.

Blue-green rectangular code

Before discussing the logical operators of these codes, we should quickly note a subtlety in their definition. At each corner between a blue and green edge, there is a red plaquette with one qudit that touches neither green nor blue plaquettes. This qudit should be understood to have a C-type stabilizer associated with it, as would be the case if there were an edge emanating from this qudit.

Between the two blue boundaries of this code, it is possible to construct a set of X-type operators labelled by group elements in G that we call $X^g_{\text{log,blue}}$. These would (largely) run along blue links of the lattice. However, note that along a green boundary, the distinction between blue links and red links disappears. Thus along this boundary, we can construct a family of operators from C-type stabilizers, each labelled by $n \in [G,G]$ that runs along blue links connecting the blue boundaries. After accounting for equivalence up to these operators, only blue X-type logical operators labelled by $k \in G/[G,G]$ are independent. Similarly we can construct a set of independent green logical X operators labelled by $k \in G/[G,G]$, $X^k_{\text{log,green}}$. These operators will commute pairwise.

We can also construct Z- (or T)-type logical operators between the blue boundaries. However, if we were to construct an entire set $Z^g_{\text{log,blue}}$ labelled by each $g \in G$, these would not commute with the stabilizers. Instead, we can only construct independent representatives labelled by each $k \in G/[G,G]$. Similar considerations apply to the $Z^k_{\text{log,green}}$.

We can then form two pairs of logical qudit algebras generated by $X^k_{\text{log,green}}$ with $Z^k_{\text{log,blue}}$ and $X^k_{\text{log,blue}}$ with $Z^k_{\text{log,green}}$ for $k \in G/[G,G]$. We thus say the logical qudits associated with each of these sets of operators are Abelianized. The total degeneracy is $|G/[G,G]|^2$.

Blue-red rectangular code

As in the blue-green rectangular code, we can define $X^g_{\text{log,blue}}$. However, since there is no green boundary, these are now independent for all $g \in G$. In contrast, red X-type logical operators are only defined for each $k \in G/[G,G]$ (again due to equivalence under C-type stabilizers).

Conversely, the red Z-type operators are defined for each $g \in G$, while the blue Z-type operators are only independently defined for each $k \in G/[G,G]$. This leads to logical qudit algebras generated by $X^g_{\text{log,blue}}$ with $Z^g_{\text{log,red}}$ for each $g \in G$ and $X^k_{\text{log,red}}$ with $Z^k_{\text{log,blue}}$ for each $k \in G/[G,G]$. In this case only one of the logical qudits has been Abelianized, and the total degeneracy is $|G| \cdot |G/[G,G]|$.

Triangular codes

For the triangular code, it is not so straightforward to assign a color type to each logical operator because they may branch. Despite this, by constructing logical operators that run entirely along one side of the triangle, it can be seen that only independent X^k_{log} and Z^k_{log} for each $k \in G/[G,G]$ may be defined, and so determine the degeneracy of these codes to be $|G/[G,G]|$.

5.4.4 Topological defects

Topological defects can play an important role in topological systems. In particular, braiding of certain types of defects can implement quantum computation (through code deformation) in much the same way as braiding of anyons. Particular types of topological defects such as holes [BMD09] and twists [Bom10a, Bom11] have been developed for this purpose in simple models such as the toric codes or qubit color codes. As with our discussion of the anyon spectrum of G-color codes, we can import many known results from quantum double models into our study of topological defects in these models, taking the equivalence between quantum doubles and G-color codes to be general (i.e. independent of the details of the lattice).

The theory of topological defects is closely related to the theory of boundaries. The study of domain walls (general boundaries) between two topological phases can be used to explore all the topological defects we will consider here. This theory is developed for the quantum double models in [BSW11] (see also [KK12] for related work). By making use of the correspondence between the G-color codes and the quantum double models, we can import the characterization of the domain walls possible between two phases of G-color codes.

Twists are topological defects at which domain walls terminate [KK12]. They induce an automorphism of the set of anyons, such that an anyon braiding around a twist will return as a different species (as dictated by the automorphism). Twists have well-defined fusion and braiding amongst themselves, and can be used for topological quantum computation [Bom10a, Bom11]. Possible twists for quantum double models (and hence G-color codes)

are studied in Refs. [BSW11, KK12].

The second type of defects we consider are holes (or punctures). These are closed boundaries between the G-color code and vacuum (the topologically trivial phase) within a planar topological code. They can also have well-defined fusion and braiding relations, and can be used for topological quantum computation [BMD09]. Again, the characterization of such hole types can be imported from the boundary theory of quantum double models, as discussed in Sec. 5.4.3.

Finally, condensation is a mechanism via which the topological order in an anyonic model can be changed. In a condensed phase, the anyon density for a particular species is given a non-trivial value in the ground space, and this can lead to interesting effects, e.g. confinement of other anyon species. Condensation amounts to a deformation in the bulk of the model under consideration and again an analogy can be drawn to equivalent processes in quantum double models as studied in [BMD08a] (see also [Eli03, KK12, Kon14]). These kinds of effects may also be used to perform quantum computation by manipulating the regions of condensed phases [BMD11].

5.4.5 Transversality properties

One feature of the qubit color codes that is particularly appealing is its large set of transversal gates [BMD06] (in comparison to the toric code, for example). In fact, this feature is inherited for the color codes based on Abelian groups [Sar10]. The most important transversal gate that these Abelian color codes possess is the Hadamard gate. However, as discussed in [Bre15a], operator algebras based on finite non-Abelian groups will not have a counterpart to the Hadamard gate, due to the inequivalence of the group algebra and the corresponding representation algebra.

In a similar vein, logical operators for codes with similar algebraic structure to the G-color codes (significantly the quantum double models) do not generally have large transversal gate sets. The transversal "string"-like logical operators that appear for Abelian groups generally become non-transversal "ribbon" operators in this context [Kit03, BMD08a] when the topological charges of the model become non-Abelian (and thus able to perform quantum computation by braiding). For these reasons, we do not expect the G-color codes to have particularly interesting transversal gate sets.

5.4.6 Construction from cluster state

The qubit color code can be constructed in a straightforward way from a suitable cluster state [BMD08b]. We can view this relationship (appropriately generalized) as one way to define the G-cluster states.

The qubit color code can be produced by beginning with a cluster state on the lattice shown in

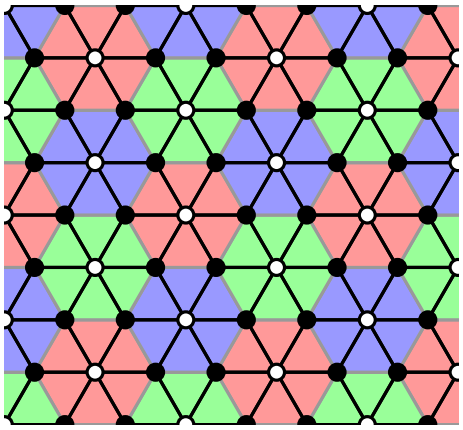

Figure 5.7 – By preparing a generalized cluster state on the lattice shown with black edges, and projecting a subset of the qudits (those represented by open circles) into particular states, we can prepare a G-color code.

Fig. 5.7, and projecting a subset of the qubits (corresponding to each plaquette of the color code) into the $|0\rangle$ state [BMD08b]. This procedure can directly be generalized to produce G-color codes from generalized cluster states [Bre15a] based on the group G. Given a suitably prepared generalized cluster state, the analogue of the $|0\rangle$ state projections would naively be expected to be a projection to $|e\rangle$. However, performing these projections would not give rise to the G-cluster states we have defined (the resulting states would not have local stabilizers).

Instead, the projection on the qudits corresponding to red plaquettes must be generalized to projections to $\sum_{n\in[G,G]}|n\rangle$, while those on blue and green plaquettes would remain as projections to $|e\rangle$. This will result in the desired G-color code state. Of course for any Abelian group G, $[G,G]=\{e\}$, and so we recover the standard qubit procedure for $G=\mathbb{Z}_2$.

As discussed in Ref. [Bre15a] for the similar case of the toric code, if we were to physically use measurements of a suitable basis in lieu of projections to the $|e\rangle$ or $\sum_{n\in[G,G]}|n\rangle$ states in an attempt to prepare G-color code states from generalized cluster states in the laboratory, the resulting state could be interpreted as an excited state of the G-color code with excitations determined by measurement outcomes.

5.5 Discussion

We have defined a generalization of the color codes to a finite group G, and explored many of their basic properties. Some of the useful features of the qubit color codes do not carry over to the general case; most notably a large set of transversal gates is not expected to be present in a general G-color code. Nonetheless, we do not have many exactly-solvable models of topologically ordered systems and so this new family may be of interest as a testbed for topological phenomena, or may have properties that are difficult to find in existing models. Furthermore, the relationship between the color codes and many other interesting systems

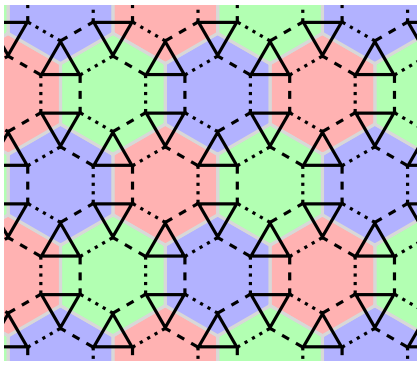

Figure 5.8 – The topological subsystem code is defined on an an expanded 2-colex lattice. In this example, we have expanded the 6.6.6 honeycomb lattice. The links of the expanded lattice come in three types, shown as dashed, dotted, and solid, corresponding to the three possible interaction types: X, Y, or Z.

may allow for further extension of this work. We briefly discuss a few of the most obvious extensions below.

5.5.1 Extensions of the model

Topological Subsystem Codes

Topological subsystem codes are a family of models that are related to color codes, but whose Hamiltonians require only 2-body interactions [BKMD09, Bom10b]. They are defined on 2-colexes whose links and sites have been expanded to create a new lattice, as in Fig. 5.8. Each edge of the expanded lattice carries an operator of the form $X \otimes X$, $Y \otimes Y$, or $Z \otimes Z$.

We will not go into details about these models, but we would not expect them to be generalizable to an arbitrary finite group G as we have done for color codes for the following reason. In our generalization, we have treated the X operator as if it were a group multiplication operator. We could also have generalized the Z operator as $Z^{\Gamma}_{ij} = \sum_g [\Gamma(g)]_{ij} T_g$, for $[\Gamma(\cdot)]_{ij}$ the $(i,j)^{\text{th}}$ matrix element of a representation Γ. In particular, for the group $\mathbb{Z}_2$ this gives $Z^{\text{triv}} = I$ and $Z^{\text{alt}} = \sigma_z$ for the trivial and alternating representations, respectively. In this way, we can interpret the Z operators as acting like representations (see Ref. [Bre15a] for a more detailed discussion).

Given these interpretations of X and Z, we can attempt to generalize a given CSS model. However, when presented with a non-CSS model such as the topological subsystem codes, the immediate problem of how to interpret a Y operator in terms of group structure has no obvious answer. For the $\mathbb{Z}_2$ case (and indeed any cyclic group), there is a natural correspondence between the group elements and the representations of the group. This allows us to unambiguously define products of $X^g Z^g$ that can serve as a generalization of Y (up to constants). For this reason, we would not expect significant obstacles to generalizing the

topological subsystem codes to Abelian groups. In contrast, for non-Abelian groups we cannot generally rely on a natural correspondence between group elements and representations, and for this reason it seems unlikely that our strategy will provide a sensible generalization of the topological subsystem codes for these groups. We refer the interested reader to Ref. [Bre15a] for a more comprehensive discussion of similar issues.

Higher dimensional models and gauge color codes

The 3D qubit color codes are introduced in [BMD07b], and D-dimensional qubit color codes can also be defined [BCHMD13] and generalized to gauge color codes [Bom13]. They are based on the notion of a D-colex in analogy to the 2-colex of the 2D model. We anticipate that the same algebraic structure used here to define the 2-dimensional G-color codes (such as the commutator subgroup) may be used to define generalizations of the higher-dimensional color codes in some cases.

The gauge color codes are the most general setting for these higher-dimensional color codes, and are defined for spatial dimension D by a D-colex and two positive integers d, e such that $d + e \leq D$. These two integers specify the geometry of the generators of the stabilizer group (or more generally the gauge group in the language of subsystem codes [KLP05, KLPL06]). In particular, the Z-type interactions in the Hamiltonian are associated with $(d+1)$-dimensional objects, while the X-type interactions are associated with $(e+1)$-dimensional objects. When generalizing these models to an arbitrary finite group G in the most naive way, it seems necessary to restrict to $d = 1$, since the definition of the S^Z stabilizers (5.14-5.16) requires these operators to be associated to an object with a notion of cycles, i.e. a 2-dimensional face. The same considerations restrict the kinds of higher-dimensional generalizations that are possible for e.g. the quantum double models and string net models, though more complex higher dimensional analogues can be defined [WW12]. However, the fact that the gauge color codes allow more general structures than the quantum double models (the analogous construction for quantum double models would not allow $d + e < D$) suggests that there may be novel ways to implement non-Abelian topological orders in higher dimension with these methods.

Extension to more general algebras

Our model is very similar in construction to the quantum double models, as can be seen by the mapping of Sec. 5.3, which makes this correspondence explicit. Given that more general quantum double models can be defined based on Hopf algebras (and potentially more general algebraic structures) [BCKA13, BMCA13], a natural question arises whether these models, too, have color code counterparts. We expect that this may be possible using similar methods to those used here, and that the resulting models would have an analogous relationship to the corresponding quantum double models.

It may also be possible to pursue a similar generalization of the color codes based on fusion categories rather than finite groups, in the spirit of the string-net models [LW05], of which the quantum double models are examples [BA09].

Chapter Review

We define a family of generalized color codes based on an arbitrary finite group that can have non-Abelian anyonic excitations.

- These generalized color codes may be derived using a similar generalization scheme to that outlined in Chapter 4.
- In contrast to the standard qubit color code, the symmetry between the three colors must in general be broken to allow for locality of the stabilizers.
- The relationship between the color code and toric code is extended to a relationship between the generalized color codes and the quantum double models. Notably, this gives the anyonic particle content of the generalized color code for group G as equivalent to a copy of the quantum double of G and a copy of the quantum double model of the Abelianization of G.
- The mapping between the generalized color codes and quantum double models allows us to determine properties of the system such as degeneracy, allowed boundary types, posssible topological defects, etc.
- We also show how the generalized color codes are related to the generalized cluster states discussed in Chapter 4.

6 Conclusion

In this thesis we have presented several new many-body models that may be of interest for quantum information processing or storage protocols. The first models presented were designed as a step towards realistic implementation of some theoretically interesting many-body Hamiltonians. We gave perturbative Hamiltonians consisting of only 2-local interactions that reproduced the quantum double models or PEPS parent Hamiltonians as their low energy limit. Following this we introduced a programme of generalizing known interesting states to give more complicated and interesting phenomenology. Specifically, we defined generalizations of the cluster states and color codes based on arbitrary finite groups, in analogy to the generalization of the toric code to the quantum double models.

We do not claim that the models we present are intended to be realistic enough to allow for direct implementation in the laboratory as written (though this may be possible for some cases). The 2-body Hamiltonians we gave for quantum doubles and PEPS should be regarded as a demonstration that it is possible to produce interesting states as the ground states of 2-body Hamiltonians, and as a stepping stone to further, increasingly realistic, models that have these desirable properties. Apart from the fact of their being 2-body, it is also of interest to find relatively natural interactions that give rise to these interesting states. Exactly what is meant by natural of course depends very much on context. In some cases, it may be desirable to attempt to engineer in the laboratory the kinds of interactions that give rise to these interesting states. If possible, this may allow for the kind of flexibility and precision that would be needed to generate the kinds of interactions we have already proposed (though again depending on implementation it may be desirable to find alternative interactions that are more easily produced). In other cases, it may be of interest to find materials that naturally have the kinds of interactions that give rise to interesting topologically ordered states. In this case a given many-body model may be a good model for the interactions of the system, even though it does not capture some features that the theoretician may deem irrelevant for the phenomena at hand. Again, in this case it would be desirable to find Hamiltonians that model the system as closely as possible while still retaining analytic or numerical tractability.

In developing our 2-body Hamiltonians we made use of a general type of perturbation gadget -

the code gadget - that may be applicable in similar attempts to find 2-body Hamiltonians to approximate other kinds of many-body models. This approach was first used to construct a 2-local parent Hamiltonian for the cluster state, but we have generalized it significantly here to the point that it is now a reasonably general approach to perturbation gadgets for quantum many-body spin systems. In analysing our construction of 2-body parent Hamiltonians for PEPS, it was convenient to introduce the notion of quasi-injectivity. Although the properties of quasi-injective PEPS are not immediately obvious (apart from those used in our analysis), this class may also be of more general interest. The related classes of injective, G-injective, (G,ω)-injective, H-injective, and MPO-injective PEPS have been very useful in understanding the relationship between symmetries of PEPS and their properties (particularly their topological properties). We conjectured that the correct definition of quasi-injectivity is in fact equivalent to a topological order condition, though we were unable to prove this. It may be the case that quasi-injectivity is a useful blanket class to describe PEPS with desirable properties for describing quantum many-body systems, particularly those with topological order.

The generalized cluster states and color codes that we defined should also not be understood as obviously realistic proposals for quantum information systems. They do, however, give new test-beds for theoretical ideas about many-body states and topological quantum computation protocols. The generalization program we outlined may also be more applicable to other interesting states, similarly allowing the definition of new families of tractable models with interesting properties. This generalization program may also lend itself to extension, for example attempting to define families of states given by members of a Hopf algebra (as is possible for the quantum double states), weak Hopf algebra (as is conjectured to be possible for the quantum double states), or by fusion categories (in analogy to the string net models). Of course, the more general the framework, the less structure is available to assist in analysis of such families, and so it may be desirable to only extend this kind of construction as far as is necessary for some fundamentally new phenomenology or to define a specific desirable state or model.

Although we only briefly sketched a protocol for adiabatic topological cluster state computation using the generalized cluster states, it may be possible to find a particular example of these generalized cluster states (or a related state) that allows for measurement-based universal topological cluster state computation. This would very much depend on the interplay between topological defects (which are simulated by choice of measurement settings) and anyons (whose world lines are specified by the random measurement outcomes). Although the standard qubit measurement-based topological cluster state computation scheme simulates the braiding of punctures in the toric code, it may be possible to simulate other topological defects such as twists. This would provide other possible avenues to construct topological cluster state computation schemes with different properties.

Generally, we hope that the general models, concepts and tools introduced in this thesis may find use beyond their immediate application. The programmes of generating more realistic many-body Hamiltonians with desired properties, as well as finding new tractable models

with interesting phenomenology, are both of central importance to the continued vitality of topological quantum systems research. That they may find application in either condensed matter physics or quantum information science, or indeed in one of several other fields, is even more reason that these kinds of systems should be carefully studied to find new methods of analysis and new models of interest.

The young field of topological quantum information has already produced some significant results, and it is clear that it is a powerful complementary way of viewing quantum information processing. It has also given many insights into the structure of condensed matter systems and how we understand macroscopic quantum behaviour in realistic systems. The study of topologically ordered systems is still discovering and refining fundamentally new concepts by looking at toy models of various degrees of realism. We have provided several such new models that we hope enable the study of topologically ordered phenomena both analytically and numerically, as well as pushing towards experimental realization of some of the more exotic topological phenomena that may enable robust quantum information processing in the real world.

Bibliography

[AAV13] D. Aharonov, I. Arad, and T. Vidick, "The quantum PCP conjecture," *SIGACT News*, vol. 44, no. 2, p. 47, 2013.

[AB09] J. Anders and D. E. Browne, "Computational power of correlations," *Phys. Rev. Lett.*, vol. 102, p. 050502, 2009.

[Agu11] M. Aguado, "From entanglement renormalisation to the disentanglement of quantum double models," *Ann. Phys.*, vol. 326, no. 9, p. 2444, 2011.

[AHHH10] R. Alicki, M. Horodecki, P. Horodecki, and R. Horodecki, "On thermal stability of topological qubit in Kitaev's 4D model," *Open Syst. Inf. Dyn.*, vol. 17, no. 01, p. 1, 2010.

[AJL09] D. Aharonov, V. Jones, and Z. Landau, "A polynomial quantum algorithm for approximating the Jones polynomial," *Algorithmica*, vol. 55, no. 3, p. 395, 2009.

[AKLT88] I. Affleck, T. Kennedy, E. H. Lieb, and H. Tasaki, "Valence bond ground states in isotropic quantum antiferromagnets," *Commun. Math. Phys.*, vol. 115, no. 3, p. 477, 1988.

[AMA14] B. Antonio, D. Markham, and J. Anders, "Adiabatic graph-state quantum computation," *New J. Phys.*, vol. 16, no. 11, p. 113070, 2014.

[Aue94] A. Auerbach, *Interacting electrons and quantum magnetism*. Springer, 1994.

[AvDK+07] D. Aharonov, W. van Dam, J. Kempe, Z. Landau, S. Lloyd, and O. Regev, "Adiabatic quantum computation is equivalent to standard quantum computation," *SIAM J. Comput.*, vol. 37, no. 1, p. 166, 2007.

[BA09] O. Buerschaper and M. Aguado, "Mapping Kitaev's quantum double lattice models to Levin and Wen's string-net models," *Phys. Rev. B*, vol. 80, p. 155136, 2009.

[Bac01] D. Bacon, "Decoherence, control, and symmetry in quantum computers," Ph.D. dissertation, University of California, Berkeley, 2001.

[Bal05] R. C. Ball, "Fermions without fermion fields," *Phys. Rev. Lett.*, vol. 95, p. 176407, 2005.

[BASP14] B. J. Brown, A. Al-Shimary, and J. K. Pachos, "Entropic barriers for two-dimensional quantum memories," *Phys. Rev. Lett.*, vol. 112, p. 120503, 2014.

[BAV09] O. Buerschaper, M. Aguado, and G. Vidal, "Explicit tensor network representation for the ground states of string-net models," *Phys. Rev. B*, vol. 79, no. 8, p. 085119, 2009.

[BBD+09] H. Briegel, D. Browne, W. Dür, R. Raussendorf, and M. Van den Nest, "Measurement-based quantum computation," *Nat. Phys.*, vol. 5, no. 1, p. 19, 2009.

[BBD14a] C. G. Brell, S. D. Bartlett, and A. C. Doherty, "Perturbative 2-body parent hamiltonians for projected entangled pair states," *New J. Phys.*, vol. 16, no. 12, p. 123056, 2014.

[BBD+14b] C. G. Brell, S. Burton, G. Dauphinais, S. T. Flammia, and D. Poulin, "Thermalization, error correction, and memory lifetime for ising anyon systems," *Phys. Rev. X*, vol. 4, p. 031058, 2014.

[BCHMD13] H. Bombin, R. W. Chhajlany, M. Horodecki, and M. A. Martin-Delgado, "Self-correcting quantum computers," *New J. Phys.*, vol. 15, no. 5, p. 055023, 2013.

[BCKA13] O. Buerschaper, M. Christandl, L. Kong, and M. Aguado, "Electric-magnetic duality of lattice systems with topological order," *Nucl. Phys. B*, vol. 876, no. 2, p. 619, 2013.

[BDCP12] H. Bombin, G. Duclos-Cianci, and D. Poulin, "Universal topological phase of two-dimensional stabilizer codes," *New J. Phys.*, vol. 14, no. 7, p. 073048, 2012.

[BDL11] S. Bravyi, D. P. DiVincenzo, and D. Loss, "Schrieffer-Wolff transformation for quantum many-body systems," *Ann. Phys.*, vol. 326, no. 10, p. 2793, 2011.

[BDLT08] S. Bravyi, D. P. DiVincenzo, D. Loss, and B. M. Terhal, "Quantum simulation of many-body Hamiltonians using perturbation theory with bounded-strength interactions," *Phys. Rev. Lett.*, vol. 101, no. 7, p. 070503, 2008.

[BF10] D. Bacon and S. T. Flammia, "Adiabatic cluster-state quantum computing," *Phys. Rev. A*, vol. 82, p. 030303, 2010.

[BFBD11] C. G. Brell, S. T. Flammia, S. D. Bartlett, and A. C. Doherty, "Toric codes and quantum doubles from two-body Hamiltonians," *New J. Phys.*, vol. 13, no. 5, p. 053039, 2011.

[BFC13] D. Bacon, S. T. Flammia, and G. M. Crosswhite, "Adiabatic quantum transistors," *Phys. Rev. X*, vol. 3, p. 021015, 2013.

[BH11a] S. Bravyi and J. Haah, "Energy landscape of 3D spin Hamiltonians with topological order," *Phys. Rev. Lett.*, vol. 107, p. 150504, 2011.

[BH11b] S. Bravyi and M. B. Hastings, "A short proof of stability of topological order under local perturbations," *Commun. Math. Phys.*, vol. 307, no. 3, p. 609, 2011.

[BHM10] S. Bravyi, M. B. Hastings, and S. Michalakis, "Topological quantum order: Stability under local perturbations," *J. Math. Phys.*, vol. 51, no. 9, p. 093512, 2010.

[BHV06] S. Bravyi, M. B. Hastings, and F. Verstraete, "Lieb-robinson bounds and the generation of correlations and topological quantum order," *Phys. Rev. Lett.*, vol. 97, p. 050401, 2006.

[BJQ13a] M. Barkeshli, C.-M. Jian, and X.-L. Qi, "Classification of topological defects in Abelian topological states," *Phys. Rev. B*, vol. 88, p. 241103, 2013.

[BJQ13b] M. Barkeshli, C.-M. Jian, and X.-L. Qi, "Theory of defects in Abelian topological states," *Phys. Rev. B*, vol. 88, p. 235103, 2013.

[BJQ13c] M. Barkeshli, C.-M. Jian, and X.-L. Qi, "Twist defects and projective non-Abelian braiding statistics," *Phys. Rev. B*, vol. 87, p. 045130, 2013.

[BK98] S. B. Bravyi and A. Y. Kitaev, "Quantum codes on a lattice with boundary," *arXiv:quant-ph/9811052*, 1998.

[BK02] S. B. Bravyi and A. Y. Kitaev, "Fermionic quantum computation," *Ann. Phys.*, vol. 298, no. 1, p. 210, 2002.

[BK05] S. Bravyi and A. Kitaev, "Universal quantum computation with ideal Clifford gates and noisy ancillas," *Phys. Rev. A*, vol. 71, p. 022316, 2005.

[BK13] S. Bravyi and R. Koenig, R.nig, "Classification of topologically protected gates for local stabilizer codes," *Phys. Rev. Lett.*, vol. 110, p. 170503, 2013.

[BKMD09] H. Bombin, M. Kargarian, and M. A. Martin-Delgado, "Quantum 2-body Hamiltonian for topological color codes," *Fortschr. Phys.*, vol. 57, p. 1103, 2009.

[Blo05] I. Bloch, "Ultracold quantum gases in optical lattices," *Nat. Phys.*, vol. 1, no. 1, p. 23, 2005.

[BM] C. G. Brell and N. C. Menicucci, *in preparation.*

[BMCA13] O. Buerschaper, J. M. Mombelli, M. Christandl, and M. Aguado, "A hierarchy of topological tensor network states," *J. Math. Phys.*, vol. 54, no. 1, p. 012201, 2013.

[BMD06] H. Bombin and M. A. Martin-Delgado, "Topological quantum distillation," *Phys. Rev. Lett.*, vol. 97, p. 180501, 2006.

[BMD07a] H. Bombin and M. A. Martin-Delgado, "Exact topological quantum order in $d = 3$ and beyond: Branyons and brane-net condensates," *Phys. Rev. B*, vol. 75, p. 075103, 2007.

[BMD07b] H. Bombin and M. A. Martin-Delgado, "Topological computation without braiding," *Phys. Rev. Lett.*, vol. 98, p. 160502, 2007.

[BMD08a] H. Bombin and M. A. Martin-Delgado, "Family of non-Abelian Kitaev models on a lattice: Topological condensation and confinement," *Phys. Rev. B*, vol. 78, p. 115421, 2008.

[BMD08b] H. Bombin and M. A. Martin-Delgado, "Statistical mechanical models and topological color codes," *Phys. Rev. A*, vol. 77, p. 042322, 2008.

[BMD09] H. Bombin and M. A. Martin-Delgado, "Quantum measurements and gates by code deformation," *J. Phys. A*, vol. 42, no. 9, p. 095302, 2009.

[BMD11] H. Bombin and M. A. Martin-Delgado, "Nested topological order," *New J. Phys.*, vol. 13, no. 12, p. 125001, 2011.

[Bom10a] H. Bombin, "Topological order with a twist: Ising anyons from an Abelian model," *Phys. Rev. Lett.*, vol. 105, p. 030403, 2010.

[Bom10b] H. Bombin, "Topological subsystem codes," *Phys. Rev. A*, vol. 81, no. 3, p. 032301, 2010.

[Bom11] H. Bombin, "Clifford gates by code deformation," *New J. Phys.*, vol. 13, no. 4, p. 043005, 2011.

[Bom13] H. Bombin, "Gauge color codes," *arXiv:1311.0879*, 2013.

[Bom14] H. Bombin, "Structure of 2d topological stabilizer codes," *Commun. Math. Phys.*, vol. 327, no. 2, p. 387, 2014.

[BP08] G. K. Brennen and J. K. Pachos, "Why should anyone care about computing with anyons?" *Proce. R. Soc. A*, vol. 464, no. 2089, p. 1, 2008.

[BR06] S. D. Bartlett and T. Rudolph, "Simple nearest-neighbor two-body Hamiltonian system for which the ground state is a universal resource for quantum computation," *Phys. Rev. A*, vol. 74, p. 040302, 2006.

[Bra06] S. Bravyi, "Universal quantum computation with the $\nu = 5/2$ fractional quantum Hall state," *Phys. Rev. A*, vol. 73, p. 042313, 2006.

[Bre15a] C. G. Brell, "Generalized cluster states based on finite groups," *New J. Phys.*, vol. 17, no. 2, p. 023029, 2015.

[Bre15b] C. G. Brell, "Generalized color codes supporting non-Abelian anyons," *Phys. Rev. A*, vol. 91, p. 042333, 2015.

[BSFB07] D. L. Bergman, R. Shindou, G. A. Fiete, and L. Balents, "Degenerate perturbation theory of quantum fluctuations in a pyrochlore antiferromagnet," *Phys. Rev. B*, vol. 75, no. 9, p. 094403, 2007.

[BSK+11] B. J. Brown, W. Son, C. V. Kraus, R. Fazio, and V. Vedral, "Generating topological order from a two-dimensional cluster state using a duality mapping," *New J. Phys.*, vol. 13, no. 6, p. 065010, 2011.

[BSW11] S. Beigi, P. Shor, and D. Whalen, "The quantum double model with boundary: Condensations and symmetries," *Commun. Math. Phys.*, vol. 306, p. 663, 2011.

[BTH+13] D. Becker, T. Tanamoto, A. Hutter, F. L. Pedrocchi, and D. Loss, "Dynamic generation of topologically protected self-correcting quantum memory," *Phys. Rev. A*, vol. 87, p. 042340, 2013.

[Bue14] O. Buerschaper, "Twisted injectivity in projected entangled pair states and the classification of quantum phases," *Ann. Phys.*, vol. 351, no. 0, p. 447, 2014.

[BVLVdN14] J. Bermejo-Vega, C. Y.-Y. Lin, and M. Van den Nest, "Normalizer circuits and a gottesman-knill theorem for infinite-dimensional systems," *arXiv:1409.3208*, 2014.

[BVVdN14] J. Bermejo-Vega and M. Van den Nest, "Classical simulations of Abelian-group normalizer circuits with intermediate measurements," *Quant. Inf. Comp.*, vol. 14, no. 3-4, p. 0181, 2014.

[CC07] C. Castelnovo and C. Chamon, "Entanglement and topological entropy of the toric code at finite temperature," *Phys. Rev. B*, vol. 76, no. 18, p. 184442, 2007.

[CGW10] X. Chen, Z.-C. Gu, and X.-G. Wen, "Local unitary transformation, long-range quantum entanglement, wave function renormalization, and topological order," *Phys. Rev. B*, vol. 82, p. 155138, 2010.

[CGW11] X. Chen, Z.-C. Gu, and X.-G. Wen, "Classification of gapped symmetric phases in one-dimensional spin systems," *Phys. Rev. B*, vol. 83, p. 035107, 2011.

[CHW15] S. Cui, S.-M. Hong, and Z. Wang, "Universal quantum computation with weakly integral anyons," *Quant. Inf. Process.*, p. 1, 2015.

[CLB+14] C. Cesare, A. J. Landahl, D. Bacon, S. T. Flammia, and A. Neels, "Adiabatic topological quantum computing," *arXiv:1406.2690*, 2014.

[CMPGS13] J. I. Cirac, S. Michalakis, D. Pérez-García, and N. Schuch, "Robustness in projected entangled pair states," *Phys. Rev. B*, vol. 88, p. 115108, 2013.

[CS96] A. R. Calderbank and P. W. Shor, "Good quantum error-correcting codes exist," *Phys. Rev. A*, vol. 54, p. 1098, 1996.

[DBB12] A. S. Darmawan, G. K. Brennen, and S. D. Bartlett, "Measurement-based quantum computation in a two-dimensional phase of matter," *New J. Phys.*, vol. 14, no. 1, p. 013023, 2012.

[DCP10] G. Duclos-Cianci and D. Poulin, "Fast decoders for topological quantum codes," *Phys. Rev. Lett.*, vol. 104, no. 5, p. 050504, 2010.

[Deu89] D. Deutsch, "Quantum computational networks," *Proc. R. Soc. A*, vol. 425, no. 1868, p. 73, 1989.

[DFRBF96] N. Datta, J. Frohlich, L. Rey-Bellet, and R. Fernandez, "Low-temperature phase diagrams of quantum lattice systems. II. convergent perturbation expansions and stability in systems with infinite degeneracy," *Helv. Phys. Acta*, vol. 69, p. 752, 1996.

[DIV04] B. Doucot, L. B. Ioffe, and J. Vidal, "Discrete non-Abelian gauge theories in Josephson-junction arrays and quantum computation," *Phys. Rev. B*, vol. 69, p. 214501, 2004.

[DKLP02] E. Dennis, A. Kitaev, A. Landahl, and J. Preskill, "Topological quantum memory," *J. Math. Phys.*, vol. 43, no. 9, p. 4452, 2002.

[DSV08] S. Dusuel, K. P. Schmidt, and J. Vidal, "Creation and manipulation of anyons in the Kitaev model," *Phys. Rev. Lett.*, vol. 100, p. 177204, 2008.

[EBD12] D. V. Else, S. D. Bartlett, and A. C. Doherty, "Symmetry protection of measurement-based quantum computation in ground states," *New J. Phys.*, vol. 14, no. 11, p. 113016, 2012.

[Eli03] S. Eliens, "Anyon condensation: Topological symmetry breaking phase transitions and commutative algebra objects in braided tensor categories," Master's thesis, Universiteit van Amsterdam, 2003.

[ESBD12] D. V. Else, I. Schwarz, S. D. Bartlett, and A. C. Doherty, "Symmetry-protected phases for measurement-based quantum computation," *Phys. Rev. Lett.*, vol. 108, p. 240505, 2012.

[FGGS00] E. Farhi, J. Goldstone, S. Gutmann, and M. Sipser, "Quantum computation by adiabatic evolution," *arXiv:quant-ph/0001106*, 2000.

[FHHW09] S. T. Flammia, A. Hamma, T. L. Hughes, and X.-G. Wen, "Topological entanglement Rényi entropy and reduced density matrix structure," *Phys. Rev. Lett.*, vol. 103, no. 26, p. 261601, 2009.

[FKW02] M. H. Freedman, A. Kitaev, and Z. Wang, "Simulation of topological field theories by quantum computers," *Commun. Math. Phys.*, vol. 227, no. 3, p. 587, 2002.

[FNW92] M. Fannes, B. Nachtergaele, and R. F. Werner, "Finitely correlated states on quantum spin chains," *Commun. Math. Phys.*, vol. 144, no. 3, p. 443, 1992.

[GB08] T. Griffin and S. D. Bartlett, "Spin lattices with two-body Hamiltonians for which the ground state encodes a cluster state," *Phys. Rev. A*, vol. 78, p. 062306, 2008.

[GESPG07] D. Gross, J. Eisert, N. Schuch, and D. Pérez-García, "Measurement-based quantum computation beyond the one-way model," *Phys. Rev. A*, vol. 76, p. 052315, 2007.

[GLSW09] Z.-C. Gu, M. Levin, B. Swingle, and X.-G. Wen, "Tensor-product representations for string-net condensed states," *Phys. Rev. B*, vol. 79, no. 8, p. 085118, 2009.

[GLW08] Z.-C. Gu, M. Levin, and X.-G. Wen, "Tensor-entanglement renormalization group approach as a unified method for symmetry breaking and topological phase transitions," *Phys. Rev. B*, vol. 78, p. 205116, 2008.

[Got97] D. Gottesman, "Stabilizer codes and quantum error correction," Ph.D. dissertation, Caltech, quant-ph/9705052, 1997.

[Got99a] D. Gottesman, "Fault-tolerant quantum computation with higher-dimensional systems," in *Quantum Computing and Quantum Communications*, ser. Lecture Notes in Computer Science, C. Williams, Ed. Springer Berlin Heidelberg, 1999, vol. 1509, p. 302.

[Got99b] D. Gottesman, "The Heisenberg representation of quantum computers," in *International Conference on Group Theoretic Methods in Physics*, S. P. Corney, R. Delbourgo, and P. D. Jarvis, Eds. International Press, 1999, p. 32.

[GTK+09] C. Gils, S. Trebst, A. Kitaev, A. W. W. Ludwig, M. Troyer, and Z. Wang, "Topology-driven quantum phase transitions in time-reversal-invariant anyonic quantum liquids," *Nat. Phys.*, vol. 5, no. 11, p. 834, 2009.

[GW09] Z.-C. Gu and X.-G. Wen, "Tensor-entanglement-filtering renormalization approach and symmetry-protected topological order," *Phys. Rev. B*, vol. 80, p. 155131, 2009.

[Haa13] J. Haah, "Commuting Pauli Hamiltonians as maps between free modules," *Commun. Math. Phys.*, vol. 324, no. 2, p. 351, 2013.

[Hal07] W. Hall, "Cluster state quantum computation for many-level systems," *Quant. Inf. Comp.*, vol. 7, no. 3, p. 0184, 2007.

[Has06] M. B. Hastings, "Solving gapped Hamiltonians locally," *Phys. Rev. B*, vol. 73, no. 8, p. 085115, 2006.

[Has07] M. B. Hastings, "An area law for one-dimensional quantum systems," *J. Stat. Mech.*, vol. 08, p. P08024, 2007.

[HIZ05] A. Hamma, R. Ionicioiu, and P. Zanardi, "Bipartite entanglement and entropic boundary law in lattice spin systems," *Phys. Rev. A*, vol. 71, no. 2, p. 022315, 2005.

[HL08] A. Hamma and D. A. Lidar, "Adiabatic preparation of topological order," *Phys. Rev. Lett.*, vol. 100, p. 030502, 2008.

[HRD07] Y.-J. Han, R. Raussendorf, and L.-M. Duan, "Scheme for demonstration of fractional statistics of anyons in an exactly solvable model," *Phys. Rev. Lett.*, vol. 98, p. 150404, 2007.

[Hub63] J. Hubbard, "Electron correlations in narrow energy bands," *Proc. R. Soc. A*, vol. 276, no. 1365, p. 238, 1963.

[HW05] M. B. Hastings and X.-G. Wen, "Quasiadiabatic continuation of quantum states: The stability of topological ground-state degeneracy and emergent gauge invariance," *Phys. Rev. B*, vol. 72, p. 045141, 2005.

[HW15] L.-Y. Hung and Y. Wan, "Ground-state degeneracy of topological phases on open surfaces," *Phys. Rev. Lett.*, vol. 114, p. 076401, 2015.

[HWW13] Y. Hu, Y. Wan, and Y.-S. Wu, "Twisted quantum double model of topological phases in two dimensions," *Phys. Rev. B*, vol. 87, p. 125114, 2013.

[JF08] S. P. Jordan and E. Farhi, "Perturbative gadgets at arbitrary orders," *Phys. Rev. A*, vol. 77, no. 6, p. 062329, 2008.

[JW28] P. Jordan and E. Wigner, "Über das Paulische Äquivalenzverbot," *Z. Physik*, vol. 47, no. 9-10, p. 631, 1928.

[KBMD10] M. Kargarian, H. Bombin, and M. A. Martin-Delgado, "Topological color codes and two-body quantum lattice Hamiltonians," *New J. Phys.*, vol. 12, no. 2, p. 025018, 2010.

[Kit03] A. Kitaev, "Fault-tolerant quantum computation by anyons," *Ann. Phys.*, vol. 303, no. 1, p. 2, 2003.

[Kit06] A. Kitaev, "Anyons in an exactly solved model and beyond," *Ann. Phys.*, vol. 321, no. 1, p. 2, 2006.

[KK12] A. Kitaev and L. Kong, "Models for gapped boundaries and domain walls," *Commun. Math. Phys.*, vol. 313, no. 2, p. 351, 2012.

[KKR06] J. Kempe, A. Kitaev, and O. Regev, "The complexity of the local Hamiltonian problem," *SIAM J. Comput.*, vol. 35, no. 5, p. 1070, 2006.

[Kle74] D. J. Klein, "Degenerate perturbation theory," *J. Chem. Phys.*, vol. 61, no. 3, p. 786, 1974.

[KLP05] D. Kribs, R. Laflamme, and D. Poulin, "Unified and generalized approach to quantum error correction," *Phys. Rev. Lett.*, vol. 94, no. 18, p. 180501, 2005.

[KLPL06] D. W. Kribs, R. Laflamme, D. Poulin, and M. Lesosky, "Operator quantum error correction," *Quant. Inf. Comp.*, vol. 6, p. 0383, 2006.

[KMS06] T. Konopka, F. Markopoulou, and L. Smolin, "Quantum graphity," *arXiv:hep-th/0611197*, 2006.

[Koe10] R. Koenig, "Simplifying quantum double Hamitonians using perturbative gadgets," *Quant. Inf. Comp.*, vol. 10, no. 3, p. 0292, 2010.

[Kog79] J. B. Kogut, "An introduction to lattice gauge theory and spin systems," *Rev. Mod. Phys.*, vol. 51, p. 659, 1979.

[Kon14] L. Kong, "Anyon condensation and tensor categories," *Nucl. Phys. B*, vol. 886, p. 436, 2014.

[KP06] A. Kitaev and J. Preskill, "Topological entanglement entropy," *Phys. Rev. Lett.*, vol. 96, no. 11, p. 110404, 2006.

[KP14] R. Koenig and F. Pastawski, "Generating topological order: No speedup by dissipation," *Phys. Rev. B*, vol. 90, p. 045101, 2014.

[KS75] J. Kogut and L. Susskind, "Hamiltonian formulation of Wilson's lattice gauge theories," *Phys. Rev. D*, vol. 11, p. 395, 1975.

[LAR11] A. J. Landahl, J. T. Anderson, and P. R. Rice, "Fault-tolerant quantum computing with color codes," *arXiv:1108.5738*, 2011.

[Lev13] M. Levin, "Protected edge modes without symmetry," *Phys. Rev. X*, vol. 3, p. 021009, 2013.

[LP09] V. Lahtinen and J. K. Pachos, "Non-abelian statistics as a berry phase in exactly solvable models," *New J. Phys.*, vol. 11, no. 9, p. 093027, 2009.

[LR72] E. H. Lieb and D. W. Robinson, "The finite group velocity of quantum spin systems," *Commun. Math. Phys.*, vol. 28, no. 3, p. 251, 1972.

[LW03] M. Levin and X.-G. Wen, "Fermions, strings, and gauge fields in lattice spin models," *Phys. Rev. B*, vol. 67, p. 245316, 2003.

[LW05] M. A. Levin and X.-G. Wen, "String-net condensation: A physical mechanism for topological phases," *Phys. Rev. B*, vol. 71, p. 045110, 2005.

[LW06] M. Levin and X.-G. Wen, "Detecting topological order in a ground state wave function," *Phys. Rev. Lett.*, vol. 96, no. 11, p. 110405, 2006.

[Mic14] K. P. Michnicki, "3d topological quantum memory with a power-law energy barrier," *Phys. Rev. Lett.*, vol. 113, p. 130501, 2014.

[Miy11] A. Miyake, "Quantum computational capability of a 2D valence bond solid phase," *Ann. Phys.*, vol. 326, no. 7, p. 1656, 2011.

[Moc03] C. Mochon, "Anyons from nonsolvable finite groups are sufficient for universal quantum computation," *Phys. Rev. A*, vol. 67, no. 2, p. 022315, 2003.

[Moc04] C. Mochon, "Anyon computers with smaller groups," *Phys. Rev. A*, vol. 69, no. 3, p. 032306, 2004.

[MvLG+06] N. C. Menicucci, P. van Loock, M. Gu, C. Weedbrook, T. C. Ralph, and M. A. Nielsen, "Universal quantum computation with continuous-variable cluster states," *Phys. Rev. Lett.*, vol. 97, p. 110501, 2006.

[MZ13] S. Michalakis and J. P. Zwolak, "Stability of frustration-free Hamiltonians," *Commun. Math. Phys.*, vol. 322, no. 2, p. 277, 2013.

[NBVdN15] X. Ni, O. Buerschaper, and M. Van den Nest, "A non-commuting stabilizer formalism," *J. Math. Phys.*, vol. 56, no. 5, p. 052201, 2015.

[NC10] M. A. Nielsen and I. L. Chuang, *Quantum computation and quantum information*. Cambridge university press, 2010.

[NMM+14] D. Nigg, M. Müller, E. A. Martinez, P. Schindler, M. Hennrich, T. Monz, M. A. Martin-Delgado, and R. Blatt, "Quantum computations on a topologically encoded qubit," *Science*, vol. 345, no. 6194, p. 302, 2014.

[NO08] Z. Nussinov and G. Ortiz, "Autocorrelations and thermal fragility of anyonic loops in topologically quantum ordered systems," *Phys. Rev. B*, vol. 77, no. 6, p. 064302, 2008.

[NSS+08] C. Nayak, S. H. Simon, A. Stern, M. Freedman, and S. Das Sarma, "Non-Abelian anyons and topological quantum computation," *Rev. Mod. Phys.*, vol. 80, no. 3, p. 1083, 2008.

[OT08] R. Oliveira and B. M. Terhal, "The complexity of quantum spin systems on a two-dimensional square lattice," *Quant. Inf. Comp.*, vol. 8, no. 10, p. 0900, 2008.

[Pac12] J. K. Pachos, *Introduction to topological quantum computation*. Cambridge University Press, 2012.

[PGVCW08] D. Perez-Garcia, F. Verstraete, J. I. Cirac, and M. M. Wolf, "PEPS as unique ground states of local Hamiltonians," *Quant. Inf. Comp.*, vol. 8, p. 0650, 2008.

[PGVWC07] D. Perez-Garcia, F. Verstraete, M. M. Wolf, and J. I. Cirac, "Matrix product state representations," *Quant. Inf. Comp.*, vol. 7, p. 0401, 2007.

[PHWL13] F. L. Pedrocchi, A. Hutter, J. R. Wootton, and D. Loss, "Enhanced thermal stability of the toric code through coupling to a bosonic bath," *Phys. Rev. A*, vol. 88, p. 062313, 2013.

[Pre98] J. Preskill, *Fault-tolerant Quantum Computation*. World Scientific, 1998.

[PVMDC05] M. Popp, F. Verstraete, M. A. Martín-Delgado, and J. I. Cirac, "Localizable entanglement," *Phys. Rev. A*, vol. 71, p. 042306, 2005.

[Rau13] R. Raussendorf, "Contextuality in measurement-based quantum computation," *Phys. Rev. A*, vol. 88, p. 022322, 2013.

[RB01] R. Raussendorf and H. J. Briegel, "A one-way quantum computer," *Phys. Rev. Lett.*, vol. 86, no. 22, p. 5188, 2001.

[RBB03] R. Raussendorf, D. E. Browne, and H. J. Briegel, "Measurement-based quantum computation on cluster states," *Phys. Rev. A*, vol. 68, p. 022312, 2003.

[RBH05] R. Raussendorf, S. Bravyi, and J. Harrington, "Long-range quantum entanglement in noisy cluster states," *Phys. Rev. A*, vol. 71, p. 062313, 2005.

[RH07] R. Raussendorf and J. Harrington, "Fault-tolerant quantum computation with high threshold in two dimensions," *Phys. Rev. Lett.*, vol. 98, no. 19, p. 190504, 2007.

[RHG06] R. Raussendorf, J. Harrington, and K. Goyal, "A fault-tolerant one-way quantum computer," *Ann. Phys.*, vol. 321, no. 9, p. 2242, 2006.

[RHG07] R. Raussendorf, J. Harrington, and K. Goyal, "Topological fault-tolerance in cluster state quantum computation," *New J. Phys.*, vol. 9, no. 6, p. 199, 2007.

[Rov08] C. Rovelli, "Loop quantum gravity," *Living Rev. Relat.*, vol. 11, no. 5, 2008.

[SAF+11] W. Son, L. Amico, R. Fazio, A. Hamma, S. Pascazio, and V. Vedral, "Quantum phase transition between cluster and antiferromagnetic states," *Europhys. Lett.*, vol. 95, no. 5, p. 50001, 2011.

[Sar10] P. Sarvepalli, "Topological color codes over higher alphabet," *2010 IEEE Information Theory Workshop*, p. 1, 2010.

[SAV12] W. Son, L. Amico, and V. Vedral, "Topological order in 1D cluster state protected by symmetry," *Quant. Inf. Process.*, vol. 11, no. 6, p. 1961, 2012.

[SBT11] M. Suchara, S. Bravyi, and B. Terhal, "Constructions and noise threshold of topological subsystem codes," *J. Phys. A*, vol. 44, no. 15, p. 155301, 2011.

[SCPG10] N. Schuch, I. Cirac, and D. Pérez-García, "PEPS as ground states: Degeneracy and topology," *Ann. Phys.*, vol. 325, no. 10, p. 2153, 2010.

[SDV08] K. Schmidt, S. Dusuel, and J. Vidal, "Emergent fermions and anyons in the Kitaev model," *Phys. Rev. Lett.*, vol. 100, no. 5, p. 057208, 2008.

[Sei09] A. Seidel, "Linear independence of nearest-neighbor valence-bond states on the kagome lattice and construction of $su(2)$-invariant spin-$\frac{1}{2}$ Hamiltonian with a Sutherland-Rokhsar-Kivelson quantum liquid ground state," *Phys. Rev. B*, vol. 80, p. 165131, 2009.

[Sho95] P. W. Shor, "Scheme for reducing decoherence in quantum computer memory," *Phys. Rev. A*, vol. 52, no. 4, pp. R2493–R2496, 1995.

[SPCPG12] N. Schuch, D. Poilblanc, J. I. Cirac, and D. Pérez-García, "Resonating valence bond states in the PEPS formalism," *Phys. Rev. B*, vol. 86, p. 115108, 2012.

[SPGC11] N. Schuch, D. Pérez-García, and I. Cirac, "Classifying quantum phases using matrix product states and projected entangled pair states," *Phys. Rev. B*, vol. 84, p. 165139, 2011.

[Ste96] A. M. Steane, "Error correcting codes in quantum theory," *Phys. Rev. Lett.*, vol. 77, no. 5, p. 793, 1996.

[SW66] J. R. Schrieffer and P. A. Wolff, "Relation between the Anderson and Kondo Hamiltonians," *Phys. Rev.*, vol. 149, p. 491, 1966.

[SW15] O. Szehr and M. Wolf, "Perturbation theory for parent hamiltonians of matrix product states," *J. Stat. Phys.*, vol. 159, no. 4, p. 752, 2015.

[SWB+14] M. B. Sahinoglu, D. Williamson, N. Bultinck, M. Marien, J. Haegeman, N. Schuch, and F. Verstraete, "Characterizing topological order with matrix product operators," *arXiv:1409.2150*, 2014.

[VC04] F. Verstraete and J. I. Cirac, "Valence-bond states for quantum computation," *Phys. Rev. A*, vol. 70, p. 060302, 2004.

[VC05] F. Verstraete and J. I. Cirac, "Mapping local Hamiltonians of fermions to local Hamiltonians of spins," *J. Stat. Mech.*, vol. 2005, no. 09, p. P09012, 2005.

[VdN11] M. Van den Nest, "A monomial matrix formalism to describe quantum many-body states," *New J. Phys.*, vol. 13, no. 12, p. 123004, 2011.

[VdN13] M. Van den Nest, "Efficient classical simulations of quantum fourier transforms and normalizer circuits over abelian groups," *Quant. Inf. Comp.*, vol. 13, no. 11-12, p. 1007, 2013.

[VdNDDM04] M. Van den Nest, J. Dehaene, and B. De Moor, "Graphical description of the action of local Clifford transformations on graph states," *Phys. Rev. A*, vol. 69, p. 022316, 2004.

[VdNLDB08] M. Van den Nest, K. Luttmer, W. Dür, and H. J. Briegel, "Graph states as ground states of many-body spin-1/2 Hamiltonians," *Phys. Rev. A*, vol. 77, no. 1, p. 012301, 2008.

[Vid03] G. Vidal, "Efficient classical simulation of slightly entangled quantum computations," *Phys. Rev. Lett.*, vol. 91, no. 14, p. 147902, 2003.

[Vid08] G. Vidal, "Class of quantum many-body states that can be efficiently simulated," *Phys. Rev. Lett.*, vol. 101, p. 110501, 2008.

[VSD08] J. Vidal, K. Schmidt, and S. Dusuel, "Perturbative approach to an exactly solved problem: Kitaev honeycomb model," *Phys. Rev. B*, vol. 78, no. 24, p. 245121, 2008.

[VWPGC06a] F. Verstraete, M. Wolf, D. Pérez-García, and J. I. Cirac, "Projected entangled states: Properties and applications," *Int. J. Mod. Phys. B*, vol. 20, p. 5142, 2006.

[VWPGC06b] F. Verstraete, M. M. Wolf, D. Pérez-García, and J. I. Cirac, "Criticality, the area law, and the computational power of projected entangled pair states," *Phys. Rev. Lett.*, vol. 96, no. 22, p. 220601, 2006.

[Wan10] Z. Wang, *Topological quantum computation*. American Mathematical Soc., 2010, no. 112.

[WAR11] T.-C. Wei, I. Affleck, and R. Raussendorf, "Affleck-Kennedy-Lieb-Tasaki state on a honeycomb lattice is a universal quantum computational resource," *Phys. Rev. Lett.*, vol. 106, p. 070501, 2011.

[WBIL14] J. R. Wootton, J. Burri, S. Iblisdir, and D. Loss, "Error correction for non-Abelian topological quantum computation," *Phys. Rev. X*, vol. 4, p. 011051, 2014.

[Wen07] X.-G. Wen, *Quantum field theory of many-body systems*. Oxford University Press, 2007.

[WHP03] C. Wang, J. Harrington, and J. Preskill, "Confinement-Higgs transition in a disordered gauge theory and the accuracy threshold for quantum memory," *Ann. Phys.*, vol. 303, no. 1, p. 31, 2003.

[WOP99] R. Walter Ogburn and J. Preskill, "Topological quantum computation," in *Quantum Computing and Quantum Communications*, ser. Lecture Notes in Computer Science, C. Williams, Ed. Springer Berlin / Heidelberg, 1999, vol. 1509, p. 341.

[WW12] K. Walker and Z. Wang, "(3+1)-TQFTs and topological insulators," *Front. Phys.*, vol. 7, no. 2, p. 150, 2012.

[YZS07] S. Yang, D. L. Zhou, and C. P. Sun, "Mosaic spin models with topological order," *Phys. Rev. B*, vol. 76, no. 18, p. 180404, 2007.

[ZB06] J. Zhang and S. L. Braunstein, "Continuous-variable Gaussian analog of cluster states," *Phys. Rev. A*, vol. 73, p. 032318, 2006.

[ZZ14] B. Zeng and D.-L. Zhou, "Topological and error-correcting properties for symmetry-protected topological order," *arXiv:1407.3413*, 2014.

[ZZXS03] D. L. Zhou, B. Zeng, Z. Xu, and C. P. Sun, "Quantum computation based on d-level cluster state," *Phys. Rev. A*, vol. 68, p. 062303, 2003.